

Vrije Universiteit Brussel
Faculty of Applied Science
Department Electrical Engineering



“Simulation software for comparison and design of electric,
hybrid electric and internal combustion vehicles with
respect to energy, emissions and performances”

Joeri Van Mierlo

Thesis submitted for the degree of
DOCTOR IN APPLIED SCIENCES

Promotor: Prof. Dr. ir. G. MAGGETTO

June 2000

© Vrije Universiteit Brussel – Faculty of Applied Science
Pleinlaan 2, 1050 Brussels, Belgium
2000

All rights reserved. No parts of this publication may be reproduced, stored in a retrieval system, or transmitted in any form by any means, electronic, mechanical, photocopying, recording or otherwise, without prior written permission of the publisher.

ACKNOWLEDGEMENTS

At this occasion I would like fore mostly to express my sincere thanks for Professor Gaston Maggetto, for his continuous support towards the achievement of this work. In particular, I want to praise his contribution to the creation of an exciting and stimulating environment at the Electrical Engineering Department (ETEC), which he enthusiastically leads.

The synergies established at ETEC, more particularly within its “electric vehicle team”, have permitted a mutual sharing of opinions, thus allowing the formation of a global view of the different aspects of electric and hybrid vehicles. Therefore I wish to express my thanks to the whole team, above all to Peter Van den Bossche, with whom, despite opinions sometimes diametrically opposed to mine, fruitful discussions could always take place within a hearty friendship. Furthermore I would like to draw attention to the special friendship with my ex-colleague Wim Deloof. Especially his perseverance and critical sense are essential qualities.

I would also like to thank all those who assisted me in correcting my text: Tania Van Mierlo, Gitte Otten, Peter Van den Bossche, Wim Deloof and Prof. Gaston Maggetto, for all the time they spent in tedious proofreading page after page.

I have to mention in particular the continuous moral support of my wife, Els Grielens, who made it possible to achieve this work through its final rush. She always succeeded to give me the courage to proceed, even in the hardest times.

Finally, the interest my parents have shown for my research was also very heartening.

Jury

Prof. Dr. ir. A. Barel, Chairman, Vrije Universiteit Brussel, Belgium

Prof. Dr. ir. J. Vereecken, Vice-Chairman, Vrije Universiteit Brussel, Belgium

Prof. Dr. ir. G. Maggetto, Promotor, Vrije Universiteit Brussel, Belgium

Prof. Dr. ir. Ph. Lataire, Secretary, Vrije Universiteit Brussel, Belgium

Prof. Dr. ir. M. Van Overmeire, Vrije Universiteit Brussel, Belgium

Prof. Dr.-Ing. H. Kahlen, Universität Kaiserslautern, Germany

Prof. Dr. ir. R. Belmans, Katholieke Universiteit Leuven, Belgium

Mr. M. J. Beretta; Manager Research and Advanced Projects "Electric and Electronic Systems"; PSA Peugeot-Citroen; France

“In urban traffic, due to their beneficial effect on environment, electric vehicles are an important factor for improvement of traffic and more particularly for a healthier living environment.”

(Van den Bossche Peter)

Dit werk draag ik graag op aan mijn dochter Hanne. Geboren in de laatste maanden van het doctoraatswerk. Haar lieve lach en gelukkige aanblik gaven mij steeds weer de energie om verder te zetten. Voor haar, haar toekomst, een mooie toekomst, een gezondere toekomst met elektrische en hybride wagens.

Je papa

Table of contents

0	FOREWORD	1
0.1	Introduction	1
0.2	Objective	1
0.3	Content	2
<i>PART I THEORETICAL INTRODUCTION</i>		<i>1</i>
1	INTRODUCTION TO PART I	7
1.1	Electric and Hybrid Vehicles	7
1.2	Why Electric Vehicles ?	10
1.2.1	Exhaust Gas Emissions	11
1.2.2	Effects on Nature	13
1.3	The Market	14
1.3.1	Cost	14
1.3.2	Electric Vehicle Deployment Potential	15
1.3.3	Legislation and Incentives	16
2	ELECTRIC VEHICLES	23
2.1	Requirements for Electric Vehicles	23
2.2	Traction Motors	26
2.2.1	Different Types of Motors	26
2.2.2	DC-Motors	26
2.2.3	AC-Motors	27
2.2.4	Permanent Magnet Motors	28
2.2.5	Comparison of Drives for Electric Vehicles	29
2.3	Power Convertors	30
2.3.1	Chopper Circuits for DC Motors	30
2.3.2	Inverter for AC Motors	31
2.4	Batteries and Energy Storage	33
2.4.1	Lead-Acid Batteries	34
2.4.2	Nickel Batteries	35
2.4.3	Redox Batteries	36
2.4.4	Sodium Batteries	37
2.4.5	Lithium Batteries	37
2.4.6	Super-Capacitors	38
2.4.7	Flywheels	39
2.4.8	Fuel Cells	39
2.5	Chargers and Infrastructure	42
3	HYBRID ELECTRIC VEHICLES	47
3.1	Hybrid Drivetrain Configurations	47
3.1.1	Parallel Hybrid	48
3.1.2	Series Hybrid	50
3.1.3	Combined Hybrid	51
3.1.4	Some Examples	52
3.2	Definitions Used to Characterise Hybrid Systems	54

3.3	Classification	57
3.4	Powerflow Control Algorithms	58
3.4.1	Series Hybrid Electric Vehicle Control Algorithms	59
3.4.2	Parallel Hybrid Electric Vehicle Control Algorithms	63
3.4.3	Combined Hybrid Electric Vehicle Control Algorithms	65
3.4.4	Some Examples	68
3.5	The Need for Simulation Tools	69
4	THE SIMULATION PROGRAMME	71
4.1	Other Programmes	71
4.2	VSP Main Features	74
4.3	Main User Interface	76
4.4	Programme Language	78
4.5	Calculation Methodology	81
4.5.1	Different Approaches	81
4.5.2	Longitudinal Dynamics Simulation	82
4.5.3	How to Describe the Forces Acting on the Vehicle ?	84
4.5.4	Component Characteristics Modelling	85
4.6	Programming Structure	90
4.7	Different Levels of Accessibility	92
	PART II SOFTWARE DESCRIPTION	71
5	INTRODUCTION TO PART II	97
6	VSP	99
6.1	VSP .vi	99
6.1.1	Frame 1: Initialisation	100
6.1.2	Frame 2: Main Loop	101
6.1.3	Frame 3: End Results	102
6.1.4	Frame 4: Storing and Visualisation	104
6.2	Speed Cycle .vi	104
6.2.1	How to Define a Speed Cycle: Speed (Time) or Speed (Distance)	107
6.2.2	How Does VSP Manage this Problem ?	108
6.2.3	Example	108
6.3	Electricity Production .vi	109
6.4	Fuel Refinery .vi	112
6.5	Heater .vi	113
6.6	Error Message .vi	113
7	VEHICLE DRIVETRAINS	115
7.1	Battery Electric Vehicle .vi	115
7.2	Flywheel Electric Vehicle .vi	117
7.3	Fuel Cell Electric Vehicle .vi	118
7.4	Diesel Electric Vehicle .vi	118
7.5	Thermal Vehicle .vi	119
7.6	Series Hybrid Vehicle .vi	120

7.7	Parallel Hybrid Vehicle .vi	123
7.8	Combined Hybrid Vehicle .vi	124
7.9	Fuel Cell Hybrid Electric Vehicle .vi	126
8	ITERATION ALGORITHM	127
8.1	Philosophy	127
8.2	The Reduction Parameters	128
8.3	Acceleration Reduction Calculation	129
8.3.1	AR, PR (T) Calculation .vi	133
8.3.2	AR, PR (ω) Calculation	135
8.3.3	AR, PR (P) Calculation	137
8.4	Some Examples	140
8.5	Summary of AR, PR Calculation	142
8.6	Iteration Order	142
8.6.1	1 st order system	142
8.6.2	2 nd order system	143
8.6.3	3 rd order system	144
8.7	End of Iteration	146
8.8	Flow Chart and Front Panel of the “Iteration Algorithm .vi”	147
9	POWER CONTROL DEVICES FOR HYBRID VEHICLES	149
9.1	DC-Bus Controller .vi	149
9.2	Torque Splitter .vi	152
9.3	Planetary Gear .vi	157
10	FORCE AND TORQUE CALCULATION: FROM WHEELS TO TRANSMISSION	161
10.1	Body & Weight .vi	161
10.2	Wheels .vi	162
10.3	Differential .vi	166
10.4	Gear .vi	167
11	POWERFLOW TRANSFORMATION	171
11.1	Motor .vi	171
11.1.1	Working Boundaries	171
11.1.2	Different Motor Models	172
11.1.3	Separate excited DC-motors	174
11.1.4	Series excited DC-motors	175
11.1.5	Asynchronous motors	176
11.1.6	Permanent magnet motor	179
11.2	Convertor .vi	179
11.3	Battery .vi	181
11.4	Ultra-capacitor .vi	187
11.5	Charger .vi	188
11.6	Generator .vi	190
11.7	Clutch .vi	192
11.8	Engine .vi	194
11.9	Fuel Cell .vi	199

11.10	Flywheel .vi	201
11.11	Auxiliaries .vi	203

PART III EXPERIMENTS, RESULTS AND COMPARATIVE ASSESSMENTS **171**

12	INTRODUCTION TO PART III	209
13	MEASUREMENT EQUIPMENT	211
13.1	Measurement System Requirements	211
13.2	Measuring Points on Roll Bench and Laboratory Test Bench	212
13.3	“ON ROAD” Measurement Equipment	214
13.3.1	First Measurement System (only DC)	214
13.3.2	AC and DC Measurement System	215
14	THE COMPONENT LIBRARY	219
14.1	Examples	220
14.2	Database	222
15	SOFTWARE VALIDATION	225
15.1	Error Analysis	225
15.2	Simulation Time vs. Accuracy	226
15.3	Parameter Sensitivity	227
15.4	Calibration and Validation	230
15.4.1	Speed Cycles	230
15.4.2	Acceleration Test	230
15.5	Software Validation Conclusions	232
16	SIMULATION RESULTS	233
16.1	Engine Start-up, Clutch and Gear Shifting	233
16.2	Electric & Internal Combustion Vehicle	234
16.3	Series Hybrid Vehicle	236
16.4	Parallel Hybrid Vehicle	239
16.5	Combined Hybrid Vehicle	241
17	COMPARISON	245
17.1	Hypothesis	245
17.2	Internal Combustion Vehicles	247
17.3	Battery Electric Vehicles	248
17.4	Hybrid Electric Vehicles	251
17.4.1	Series Hybrid Vehicle	251
17.4.2	Parallel Hybrid Vehicle	254
17.4.3	Combined Hybrid Vehicle	255
17.5	Comparison of Drivetrain Topologies	256
17.5.1	Energy Consumption	256
17.5.2	NOx and CO-emissions	258
17.5.3	Acceleration Performance	259
17.6	Comparison of Commercial Passenger Cars	261

PART IV CONCLUSIONS _____ **245**

18	CONCLUSIONS	265
18.1	Overview of The Research	265
18.1.1	Overview of Part I	265
18.1.2	Overview of Part II	265
18.1.3	Overview of Part III	266
18.2	General Achievements	266
18.3	Concluding Comparative Assessment of Energy Consumptions and Emissions	268
18.3.1	General Hybrid Power Management Optimization Criteria	268
18.3.2	Parallel Hybrid Electric Vehicles Conclusions	269
18.3.3	Series Hybrid Electric Vehicles Conclusions	269
18.3.4	Combined Hybrid Electric Vehicles Conclusions	270
18.3.5	Electric Vehicles Conclusions	271
18.3.6	General Comparison	271

List of figures

Fig. 1.1:	ICE vehicle	8
Fig. 1.2:	Electric vehicle	8
Fig. 1.3:	Series hybrid electric vehicle	9
Fig. 1.4:	Parallel Hybrid Electric vehicle	9
Fig. 2.1:	Driving torque curve	25
Fig. 2.2:	Smart flux optimisation []	32
Fig. 3.1:	Series hybrid	47
Fig. 3.2:	Parallel hybrid	47
Fig. 3.3:	Combined hybrid	47
Fig. 3.4:	Series hybrid with peak power unit	47
Fig. 3.5:	Parallel drivetrain with torque addition	48
Fig. 3.6:	Planetary gear	49
Fig. 3.7:	Combined hybrid drivetrain	52
Fig. 3.8:	Different hybrid electric vehicles classification	57
Fig. 3.9:	State of charge deviation criterion	62
Fig. 3.10:	Power Distribution Factor of an optimized combined hybrid drivetrain power control algorithm	67
Fig. 4.1:	The front panel of the Vehicle Simulation Programme	76
Fig. 4.2:	Example of 'While loop' in text based language and LabVIEW graphical language	80
Fig. 4.3:	Frequency distribution of working points	82
Fig. 4.4:	Direction of calculation: cause-effect method	83
Fig. 4.5:	Direction of calculation: effect cause method	83
Fig. 4.6:	Longitudinal dynamics simulation (e.g. Japan 15 reference cycle)	84
Fig. 4.7:	Forces acting on the vehicle	84
Fig. 4.8:	Bilinear interpolation of a two-dimensional efficiency curve	86
Fig. 4.9:	System boundary	87
Fig. 4.10:	Possible speed calculation	87
Fig. 4.11:	Demonstration of the controller algorithm	88
Fig. 4.12:	Flow chart of Vehicle Simulation Programme	91
Fig. 4.13:	Different accessibility levels of the simulation programme	93
Fig. 6.1:	The main programme	99
Fig. 6.2:	ECE-15 speed cycle	105
Fig. 6.3:	Speed and slope profile of the on-road measured Brussels urban bus line 71	105
Fig. 6.4:	Comparison between route profile definitions	108
Fig. 7.1:	Front panel of Battery Electric Vehicle .vi	115
Fig. 7.2:	Block diagramme of second frame of Battery Electric Vehicle .vi	116
Fig. 7.3:	Block diagramme of second frame of Flywheel Electric Vehicle .vi	117
Fig. 7.4:	Block diagramme of second frame of Flywheel Electric Vehicle .vi	118
Fig. 7.5:	Block diagramme of second frame of Diesel Electric Vehicle .vi	118
Fig. 7.6:	Block diagramme of second frame of Internal combustion vehicle .vi	119
Fig. 7.7:	Front panel of Series Hybrid Electric Vehicle .vi	121
Fig. 7.8:	Block diagramme of second frame of Series Hybrid Electric Vehicle.vi	122

Fig. 7.9:	<i>Block diagramme of second frame of Parallel Hybrid Electric Vehicle .vi</i>	124
Fig. 7.10:	<i>Block diagramme of second frame of Combined Hybrid Electric Vehicle .vi</i>	125
Fig. 7.11:	<i>Block diagramme of second frame of Fuel Cell Hybrid Electric Vehicle .vi</i>	126
Fig. 8.1:	<i>AR and PR of acceleration subsystem or power subsystem</i>	129
Fig. 8.2:	<i>Example of an AR calculation</i>	130
Fig. 8.3:	<i>Example of Acceleration Reduction multiplication</i>	132
Fig. 8.4:	<i>Six examples of acceleration and resistive torque combinations</i>	140
Fig. 8.5:	<i>Iteration order and end of iteration flow chart</i>	147
Fig. 8.6:	<i>Front panel of "Iteration Algorithm .vi"</i>	148
Fig. 9.1:	<i>SoC deviation APU power criterion</i>	150
Fig. 9.2:	<i>Front panel of DC-bus controller .vi</i>	151
Fig. 9.3:	<i>Front panel of Torque Splitter .vi</i>	156
Fig. 9.4:	<i>Front panel of Planetary gear .vi</i>	157
Fig. 9.5:	<i>Planetary gear</i>	158
Fig. 10.1:	<i>Front panel of gear model</i>	169
Fig. 11.1:	<i>Front panel of theoretical asynchronous motor model</i>	176
Fig. 11.2:	<i>The battery capacity versus discharge current</i>	184
Fig. 11.3:	<i>Equivalent scheme of a simple battery model</i>	185
Fig. 11.4:	<i>Dynamic battery model</i>	185
Fig. 11.5:	<i>Equivalent circuit for the NiCd Battery</i>	185
Fig. 11.6:	<i>Ultra-capacitor equivalent circuit</i>	188
Fig. 11.7:	<i>Charge profiles: I-U (left) and I-U-I (right)</i>	189
Fig. 11.8:	<i>Front panel of the Auxiliary .vi</i>	203
Fig. 13.1:	<i>Series hybrid drivetrain characterisation</i>	213
Fig. 13.2:	<i>Roll bench</i>	213
Fig. 13.3:	<i>Laboratory test bench</i>	213
Fig. 13.4:	<i>Component characterisation</i>	213
Fig. 13.5:	<i>Principal outline of the measurement system</i>	214
Fig. 13.6:	<i>Speed measurement</i>	215
Fig. 13.7:	<i>On road DC-measuring system</i>	215
Fig. 13.8:	<i>Principle outline of the second measurement system</i>	216
Fig. 13.9:	<i>On road AC and DC-measuring system</i>	217
Fig. 14.1:	<i>Step-by-step working procedure, covering the whole operating range</i>	219
Fig. 14.2:	<i>Motor current model</i>	221
Fig. 14.3:	<i>Chopper efficiency model</i>	222
Fig. 15.1:	<i>Effect of time increment on simulation accuracy</i>	227
Fig. 15.2:	<i>Output deviation in function of 10% deviation of input parameters</i>	228
Fig. 15.3:	<i>Output deviation in function of head wind and road inclination</i>	229
Fig. 15.4:	<i>Acceleration simulation vs. measurement</i>	231
Fig. 15.5:	<i>Deceleration simulation vs. measurement</i>	231
Fig. 15.6:	<i>Motor current and voltage comparison</i>	232
Fig. 15.7:	<i>Battery voltage and current</i>	232

Fig. 16.1:	ICV – Gearshifts at fixed differential speed	233
Fig. 16.2:	ICV – Gearshifts keeping the ICE within speed limits	233
Fig. 16.3:	SHEV – Engine start	234
Fig. 16.4:	ICV – ECE – Power	234
Fig. 16.5:	BEV – ECE – Power	235
Fig. 16.6:	BEV – ECE – Current and voltage	235
Fig. 16.7:	SHEV – ECE – Maximum regeneration – Power	236
Fig. 16.8:	SHEV – ECE – Less regeneration – Power	237
Fig. 16.9:	SHEV – ECE – Constant battery charging – Power	237
Fig. 16.10:	SHEV – ECE – APU power in function of SoC – Power	237
Fig. 16.11:	SHEV – ECE – Relative power distribution – Power	238
Fig. 16.12:	SHEV – ECE – With flywheel. – Power	238
Fig. 16.13:	SoC in thermostat SHEV	239
Fig. 16.14:	PHEV – ECE – P_{ICE} in function of SoC – Power	239
Fig. 16.15:	PHEV – Acceleration – P_{ICE} in function of SoC (2) – Power	240
Fig. 16.16:	PHEV – ECE – Electric-assist – Power	240
Fig. 16.17:	PHEV – Acceleration test – Electric-assist – Power	240
Fig. 16.18:	CHEV – ECE – Constant working point – Speed	241
Fig. 16.19:	CHEV – ECE – Constant working point – Torque	241
Fig. 16.20:	CHEV – ECE – Constant working point – Power	242
Fig. 16.21:	CHEV – ECE – Minimum losses – Power	243
Fig. 16.22:	CHEV – ECE – Minimum losses – Torque	243
Fig. 16.23:	CHEV – ECE – Relative power distribution – Power	243
Fig. 16.24:	CHEV – ECE – Relative power distribution – Torque	244
Fig. 17.1:	Comparison of fuel consumption	247
Fig. 17.2:	Evolution in energy consumption of battery electric vehicles	248
Fig. 17.3:	Energy consumption in function of drive cycle and SoC start value (VI2)	248
Fig. 17.4:	Energy consumption of an electric passenger car and electric van	249
Fig. 17.5:	Primary energy consumption in function of electricity production plant	249
Fig. 17.6:	Background emissions of EV driving ECE cycle	250
Fig. 17.7:	Comparison of fuel consumption of different power control strategies in SHEV	252
Fig. 17.8:	Comparison of NOx emissions for the different power control strategies in SHEV	253
Fig. 17.9:	Fuel consumption and NOx emissions for different SoC start values (case 7)	253
Fig. 17.10:	Comparison of fuel consumption for different power control strategies in PHEV	254
Fig. 17.11:	Comparison of fuel consumption of different power control strategies in CHEV	255
Fig. 17.12:	Global comparison of primary energy consumption	257
Fig. 17.13:	Global comparison of primary energy consumption of a 1,7 and a 2,7 light duty van with different drivetrain topologies	258
Fig. 17.14:	Global comparison of NOx-emissions	258

<i>Fig. 17.15: Global comparison of CO emissions</i>	259
<i>Fig. 17.16: Acceleration comparison</i>	260
<i>Fig. 17.17: Power in CHEV – acceleration test</i>	260
<i>Fig. 17.18: Primary energy comparison of an electric (V12) and an ICE (V16) passenger car</i>	261
<i>Fig. 17.19: Acceleration of electric (V12) and ICE (V16) passenger car</i>	262
<i>Fig. 18.1: Primary energy consumption of different types of drivetrains with a total static weight ranging from 1,7 to 2,7 ton</i>	272

List of tables

Table 1.1:	Comparison of emissions for electric and thermal vehicles []	11
Table 1.2:	Share of consumption and emissions by the transport sector for Europe []	11
Table 1.3:	Proposed LEV II exhaust emission standards [] and EURO gasoline limits	18
Table 2.1:	Comparison of different motor types	29
Table 2.2:	Battery characteristics [5,,,,,,,,]	34
Table 3.1:	Overview of different APU powerflow control algorithms	60
Table 4.1:	Possible interchangeable components with the same 'function'	89
Table 6.1:	The ECE-15 speed cycle	104
Table 6.2:	Implemented speed cycles	106
Table 6.3:	Percentage of total electricity production by fuel type and country [110]	110
Table 6.4:	Emissions from electricity production [154]	111
Table 6.5:	Efficiency values for fuel preparation	112
Table 6.6:	Emission for fuel preparation [154]	113
Table 6.7:	List of error messages implemented up-to-now	114
Table 8.1:	Acceleration and power subsystem	128
Table 8.2:	Possible AR and PR implementation for ω -max	142
Table 8.3:	Possible AR and PR implementation for T-max and P-max	142
Table 11.1:	Possible AR en PR implementation for engine operating limits	195
Table 14.1:	Example of look-up table	220
Table 15.1:	Speed cycle: simulation vs. measurements	230
Table 17.1:	Background emissions of EV driving ECE cycle	250
Table 17.2:	Simulated power strategies for a SHEV	251
Table 17.3:	Simulated power strategies for a PHEV	254
Table 17.4:	Simulated power strategies for a CHEV	255

List of symbols

α	road inclination ($^{\circ}$)
a	rotational acceleration (rad/s^2)
a_{\max}	maximum acceleration before wheel slip (m/s^2)
a, b, c,	constant values
a_C	carrier angular acceleration (rad/s^2)
Ah_t^+	new charged capacity (Ah)
Ah_{t-1}^+	previous charged capacity (Ah)
Ah_t^-	new charged capacity (Ah)
Ah_{t-1}^-	previous charged capacity (Ah)
a_i	acceleration at wheel side (rad/s^2)
α_i	conduction loss coefficient
a_{\max}	maximum acceleration (rad/s^2)
a_o	acceleration at motor side (rad/s^2)
a_{o1}	output shaft 1 acceleration (rad/s^2)
a_{o2}	output shaft 2 acceleration (rad/s^2)
a_{pos}	possible acceleration (rad/s^2)
AR	acceleration reduction
a_R	ring angular acceleration (rad/s^2)
AR _{att}	attenuated acceleration reduction
a_{req}	required acceleration (rad/s^2)
AR _{prev}	acceleration reduction due to a limit of a previous component
a_S	sun angular acceleration (rad/s^2)
a_{start}	start-up acceleration (rad/s^2)
a_v	linear vehicle acceleration (m/s^2)
ASM	asynchronous motor
β_1	commutation loss coefficient
BE	background emissions (g/km)
BEV	battery electric vehicle
C_5	capacity at five hour rate (Ah)
C_{aux}	auxiliary battery capacity (Ah)
CHEV	combined hybrid electric vehicle
CO	Carbon monoxide
CO ₂	Carbon dioxide
Cons	fuel consumption (L/s)
C_{tot}	total available battery capacity (Ah)
C_x	aerodynamic drag coefficient
D	fuel density (kg/L)
DCM	direct current motor
d_{\max}	maximum deceleration before wheel slip (m/s^2)
DE	direct emissions (g/km)
DSoC	state of charge increment
D_t	previous distance value (km)
D_{t+1}	distance (km)
E_{bat}	energy to battery (kWh)
eci	exponent for normalised field current
ecn	exponent for normalised rotational speed
E_{cons}	energy consumption (Wh)
ef	exponent for friction losses calculation
E_{fuel}	specific energy (MJ/L)

E_{fw}^t	flywheel energy (Wh)
E_{fw}^{t-1}	previous flywheel energy (Wh)
E_{grid}	energy from the grid (kWh)
E_{H2}	specific energy of hydrogen (MJ/kg)
E_{max}	maximum energy content (Wh)
E_{emis}	emissions (g)
EV	electric vehicle
F_a	acceleration force
f_c	commutation frequency (Hz)
f_c	fuel consumption (g/s)
FC	fuel consumption (L/100km)
f_c	fuel consumption per cell (L/s)
F_c	climbing resistance (n)
f_f	synchronous frequency (Hz)
f_r	friction coefficient
F_r	rolling resistance (n)
f_r	rated frequency (Hz)
F_t	fuel content (L)
F_{t-1}	previous fuel content (L)
F_v	aerodynamic force (n)
g	gravity constant (9.81 m/s^2)
HC	Hydrocarbons
HEV	hybrid electric vehicle
η	efficiency (%)
η_c	compressor efficiency (%)
η_{conv}	convertor efficiency (%)
η_{grid}	electricity transportation and distribution efficiency (%)
η_{ref}	reformer efficiency loss (%)
η_{slip}	additional slip efficiency (%)
i	completed repetitions of the while loop
I_{ar}	armature current (A)
I_{bat}	battery current (A)
I_c	compressor current (A)
I_{cap}	capacity current (A)
ICE	internal combustion engine
I_{cell}	cell current (A)
I_{ch}	charging current (A)
I_{max}^{ch}	maximum charge current (A)
ICV	internal combustion vehicle
I_{ex}	excitation current (A)
I_{dis}^{max}	maximum discharge current (A)
i_f	normalised field current ($= i_f/i_{f,nom}$)
I_f	field current (A)
i_f	normalised field current ($= i_f/i_{f,nom}$)
I_{max}	maximum current (A)
I_{mot}	motor current (A)
i_p	pressure ratio (p.u./Ws)
i_{pd}	pressure drop ratio (%)
I_{regen}^{max}	maximum regeneration current (A)
I_{tot}	total current (A)
J	inertia seen at wheel side (kg.m^2)

k	Peukert's constant
K_c	constant for core losses calculation
K_f	constant for friction losses calculation
k_r	1 for four wheel drive; 1/2 for two wheel drive; 1/4 for one wheel drive
L_{end}	end value of contents in fuel tank (L)
L_{start}	begin value of contents in fuel tank (L)
M	total weight (kg)
m	number of phases
M_f	mass of remaining fuel (kg)
m_r	static friction coefficient
n	attenuation factor
NOx	Nitrogen oxides
$N_{r_{cells}}$	number of cells
N_r^p	number of serie-cells in parallel
N_r^s	number of cells in serie
p	brake pressure level (p.u.)
P	power at motor side (W)
p	number of pole pares
P_a	acceleration power (W)
P_a^i	acceleration power at wheel side (W)
P_{alt}	alternator power (W)
P_{ar}	armature losses (W)
P_a^o	acceleration power at energy source side (W)
P_{aux}	auxiliary power (W)
P_b	brake pressure drop (W) (£ 0)
P_{bat}	battery power (W)
P_C	carrier power (W)
P_{ch}	battery charging power (W)
P_{core}	core losses due to eddy current and hysteresis (W)
PD	pressure drop (W)
P_{DC}	electric dc generator power (W)
PDF	power distribution factor
PDF_1	power distribution factor 1
PDF_2	power distribution factor 2
PDF_{eff}	effective power distribution factor
PDF_{pos}	possible power distribution factor
PDF_{req}	required power distribution factor
P_{elec}	electrical motor input power (W)
P_f	field losses (W)
P_{FC}	convertor power to dc-bus (W)
P_{fric}	friction losses (W)
P_{fc}	fuel cell power (W)
P_{fuel}	fuel power (W)
P_{fw}	flywheel delivered dc-power
P_{gen}	mechanical generator power (W)
$P_{gen}^{setpoint}$	generator set point power (W)
P_{grid}	grid power (W)
$P_{heating}$	heating power (W)
PHEV	parallel hybrid electric vehicle

P_i	input power (W)
P_{ice}	mechanical engine shaft power (W)
P_{inv}	inverter power (W)
P_{inv2}	second inverter power (W)
P_{inv}^{max}	maximum inverter regeneration power (W)
P_{lcore}	core losses due to eddy current and hysteresis (W)
P_{le}	electrical armature losses (W)
P_{lfri}	friction losses (W)
P_{Loss}	losses (W)
P_{lrot}	losses due to rotation (W)
PM	permanent magnet motor
P_m	mechanical power (W)
P_{max}	maximum power (W)
$P_{max}(I_{max})$	maximum power corresponding to maximum battery current (A)
$P_{max}(U_{max})$	maximum charge power corresponding to maximum cell voltage (W)
$P_{max}(U_{min})$	maximum discharge power corresponding to minimum cell voltage (W)
P_{mi}	inertia mechanical power (W)
P_{mot}	mechanical motor power (W)
P_{o1}	output 1 power (W)
P_{o2}	output 2 power (W)
P_p	pump produced power (W)
P_{pos}	possible power (W)
P_{pu}	power unit (flywheel) power (W)
PR	power reduction
P_r	resistive power (W)
P_R	ring power (W)
P_{ref}	reformer power (W)
P_{req}	required power (W)
PR_{prev}	power reduction due to a limit of a previous component
P_S	sun power (W)
P_{sp}	power setpoint (W)
P_{sp}^{pos}	possible acceleration power (W)
P_{stack}	fuel cell stack power (W)
P_w	wheel power
ρ	air density (kg/m^3)
R	wheel radius (m)
R_{ar}	armature resistance (W)
RC_{pp}	relative contribution of a power plant to the electricity production
Regen	regeneration percentage (%)
R_f	field resistance (W)
R_i	internal resistance (W)
RoH	rate of hybridisation
RoH_{el}	electric rate of hybridisation
RoH_{th}	thermal rate of hybridisation
R_r	rotor resistance (W)
R_s	stator resistance (W)
S	frontal surface (m^2)
s	slip
s	road slope (%)
SE_{pp}	specific emissions of a power plant
SHEV	series hybrid electric vehicle

SO ₂	Sulphur dioxide
SoC	state of charge (%)
SoC _{end}	end value of (°C)
SoC _{min}	minimum allowed (°C)
SoC _{start}	begin value of (°C)
SoC _t	new state of charge (%)
SoC _{t-1}	previous state of charge (%)
SoE	state of energy (%)
SoE _{min}	minimum allowed SoE
SRM	switch reluctance motor
SYN	synchronous motor
T	torque (Nm)
t ^o	temperature (°C)
T _a	acceleration torque (Nm)
t _a ^o	ambient temperature (°C)
T _a ^C	carrier acceleration torque (Nm)
T _a ⁱ	acceleration torque at wheel side (Nm)
T _a ^o	acceleration torque at motor side (Nm)
T _a ^{o1}	output acceleration torque 1 (Nm)
T _a ^{o2}	output acceleration torque 2 (Nm)
T _a ^R	ring acceleration torque (Nm)
T _a ^S	sun acceleration torque (Nm)
T _{req} ^{AS}	total required torque of the acceleration subsystem
T _b	brake torque (Nm)
TCI _t	previous time correction increment (s)
TCI _{t+1}	new time correction increment (s)
T _{em}	electromagnetic torque (Nm)
T _{fr}	friction moment (Nm)
T _{ice}	total engine torque (Nm)
Time	time reference (s)
T _{inertia}	inertia torque (Nm)
T _{inertia1}	inertia torque of component 1 (Nm)
T _{inertia2}	inertia torque of component 2 (Nm)
T _{inertia3}	inertia torque of component 3 (Nm)
T _{max}	maximum torque (Nm)
T _{mot}	motor torque (Nm)
TP	tyre pressure (bar)
T _{req} ^{PS}	required torque of power subsystem
T _r	resistive torque (Nm)
T _r ^C	carrier resistive torque (Nm)
T _{req}	required torque (Nm)
T _r ⁱ	resistive torque at wheel side (Nm)
T _r ^o	resistive torque at motor side (Nm)
T _r ^{o1}	output 1 resistive torque (Nm)
T _r ^{o2}	output 2 resistive torque (Nm)
T _r ^R	ring resistive torque (Nm)
T _r ^S	sun resistive torque (Nm)
T _s	simulation time increment (s)
T _{sp}	torque setpoint (Nm)
T _{sp} ^{pos}	possible acceleration torque (Nm)
T _{start}	required start-up time (s)

U_{ar}	armature voltage (V)
U_{aux}	auxiliary battery voltage (V)
U_b	brush voltage (V)
U_{bat}	battery voltage (V)
U_c	capacity cell voltage (V)
U_{cap}	capacity voltage (V)
U_{cell}^{max}	maximum cell voltage (V)
U_{cell}^{min}	minimum cell voltage (V)
U_{ex}	excitation voltage (V)
U_{mot}	motor voltage (V)
U_{nom}	nominal motor voltage (V)
U_o	open loop voltage (V)
v	velocity (km/h)
v_{av}	average velocity (km/h)
v_{cur}	current velocity (km/h)
VOC	Volatile Organic Compounds
v_{pos}	possible velocity (km/h)
v_{req}	required velocity (km/h)
VSP	Vehicle Simulation programme
v_w	average head wind velocity (km/h)
ω	angular velocity (rad/s)
ω_C	carrier angular velocity (rad/s)
ω_{fw}	flywheel velocity (rad/s)
ω_i	velocity at wheel side (rad/s)
ω_{ice}	engine angular velocity (rad/s)
ω_{idle}	idle velocity (rad/s)
ω_{max}	maximum angular velocity (rad/s)
ω_{nom}	nominal rotational speed (rad/s)
ω_o	velocity at motor side (rad/s)
ω_{o1}	output shaft velocity 1 (rad/s)
ω_{o2}	output shaft velocity 2 (rad/s)
ω_R	ring angular velocity (rad/s)
ω_S	sun angular velocity (rad/s)
ω_s	synchronous speed (rad/s)
ω_{start}	start-up velocity (rad/s)
ω_{gen}^{t-1}	previous generator velocity (rad/s)
ω_{ice}^{t-1}	previous engine velocity (rad/s)
ω_{gen}^t	generator velocity (rad/s)
ω_{ice}^t	engine velocity (rad/s)
X	transmission ratio (x:1)
X_1	transmission ratio (x:1) corresponding to output 1
X_2	transmission ratio (x:1) corresponding to output 2
$X_{C/R}$	carrier to ring transmission ratio
X_{fr1}	friction constant
X_{fr2}	friction speed coefficient
X_i	transmission ratio (x:1) corresponding to gear i
X_m	magnetisation reactance
X_{rr}	rotor reactance
X_{ss}	stator reactance

0 FOREWORD

0.1 Introduction

The requirements for improved environmental conditions, particularly in urban areas, together with an increasing demand for mobility, make it essential to optimize energy-environmentally efficient transport systems. One technology that can meet this challenge is the use of electric traction in electric and hybrid vehicles. Electric vehicles are totally emission-free at their point of use, and the overall pollution balance remains in favour of the electric vehicle even when taking into account electricity production. Hence electrically propelled vehicles are likely to become the mainstay of urban transport in the 21st century. Local authorities deploying them will find exciting new opportunities to solve the environmental problems they are facing today [1]. Hybrid vehicles have a large potential to minimise fuel consumption and drastically reduce tail pipe emissions.

Electric and hybrid vehicles have become increasingly popular as components design and performance improve and prototypes continue to demonstrate system feasibility. Electric and hybrid electric vehicles are energy efficient and should have low running cost. Unfortunately, the cost of development and testing of these vehicles, dictated by the level of complexity, flexibility and performance, is high. A software tool can help in selecting and matching of energy storage devices, hybrid powertrain layouts and vehicle energy management, depending on the total energy spent and environmental impact of the transport systems over specific or generalised routes and hence can help minimizing both common testing, time and cost. Such models can also enable the investigation of future, more advanced technologies to optimize overall system efficiency, range, performance and emissions. A simulation programme will therefore be useful for system developers, engineers and vehicle manufacturers and even for policy makers and transport planners in their common goal of producing more environmentally sustainable and energy efficient transport solutions [2].

0.2 Objective

The scope of this Ph.D. research is the comparative assessment to the real environmental impact of different traction systems based on available technologies. Therefore a computer simulation has been developed. This simulation tool is a modular, interactive programme, which is flexible in use, has a database structure allowing different types of data formats and is based on a powerful algorithm

capable to simulate acceleration tests and a wide range of hybrid powerflow control strategies.

The programme enables the simulation of electric, hybrid and internal combustion vehicles. The comparison is realized at the level of consumption (fuel and electricity) and emissions (CO₂, HC, NO_x, CO, particles, etc.) as well as at the level of performances (acceleration, range, maximum slope, etc.).

The simulation tool is useful for a wide variety of users with different expertise, like: engineers, transport operators and suppliers, energy utilities and decision-makers. But mainly it is an engineering tool to evaluate different drivetrains and to optimize power management in hybrid vehicles in particular. It is a powerful tool to develop new concepts. The programme has a high degree of flexibility to be able to model any driveline structure and to allow the use of different data sources.

Based on experimental results, different components have been modelled, calibrated and validated. Finally a comparative assessment of the energy consumption and emissions of different vehicles as well as a comparative evaluation of different hybrid drivetrain topologies and powerflow algorithms have been carried out.

0.3 Content

This work (thesis) consists of 4 parts. The first part will describe the background theory. The second part contains the technical description of the software tool, including component models. The third part describes the experiments for retrieving the required data, software calibration and validation. It also contains the comparative assessment. Final conclusions are formulated in the last part.

Part One: Theoretical introduction

The purpose of this theoretical introduction is to have a good summary and overview of the electric and hybrid electric vehicle technology. What are electric and hybrid electric vehicles ? Which infrastructures do they require ? What is their potential market and which incentives can be used to stimulate this market ? This introduction is mainly based on recent publications [1,3] of G. Maggetto¹, H. Kahlen² and P. Van den Bossche³, all experts in the field of electric and hybrid electric vehicles.

¹ Prof. Dr. ir. G. Maggetto is President of AVERE, the European Association of Road Electric Vehicles; general secretary of CITELEC, the European association of cities interested in the use and promotion of electric and hybrid vehicles and professor of the Vrije Universiteit Brussel. He is also the promotor of this PhD.

² Prof. Dr.-Ing. H. Kahlen, professor at the Institute for Power Electronics and Electronics of the University of Kaiserslautern, Germany, was formerly President of AVERE and is current Vice-President.

³ ir. P. Van den Bossche is Director of CITELEC.

Those who are familiar with the non-technical aspects of electric vehicles can skip the first chapter. The second chapter contains a summary of the technical characteristics of the most important components of the electric vehicle: traction motor, convertor, battery and charger. The third chapter, concerning hybrid drivetrains, is recommended to better understand the model description given in the second part of this thesis. The different drivetrain topologies as well as power control algorithms of hybrid electric vehicles will be described.

Finally the different features of the simulation programme itself are described: the fundamental calculation algorithms of the software and the component modelling; the characteristics and benefits of the language environment and the different levels of accessibility for potential software distribution.

Part two: Software description

A detailed system identification was required to develop a data structure for electric and hybrid vehicle parameters and route profiles. Different drivetrain components like chassis, body, power units, transmissions, auxiliaries, electrical power systems and energy storage had to be modelled. Besides the conventional systems, with diesel and petrol powertrains, it was necessary to implement other drivetrains based on battery technology, fuel cells, etc and controlled with different powerflow strategies. A design tool was developed which integrates the control algorithms required for the various hybrid operational performance and for energy storage. The control of the powerflow is an added complexity not found in conventional vehicles that requires specific software tools.

This second part is a very technical part describing the models of the different subprogrammes of the simulation software. The different equations on which the models are based are given. The fact that the models are related to each other in sometimes a rather complex manner, makes it necessary to refer in the description of one model to that of another. Especially the iteration algorithm, that defines the possible drivetrain acceleration and powerflow, is a process that interferes with a lot of subprogrammes.

The main programme and related subprogrammes (electricity production, speed cycle definition, etc.) will be presented first. Afterwards the implemented drivetrains of the different vehicles are explained. Closely related to these drivetrains are the mechanical and electric power control devices for hybrid vehicles. In these subprogrammes the different hybrid drivetrain control strategies are mainly implemented. They are following the specification of the iteration algorithm. This iteration process is an intelligent algorithm to define, among other things, the maximum vehicle performance. Afterwards one can find the models for the different components of the drivetrain, starting from the wheels and going to the energy source(s). The first components are related to the forces acting on the vehicle body and wheels and the mechanical transmission. Finally the drivetrain components, figuring as powerflow transformation are detailed.

Part three: Experiments and results and comparative assessment

Having a powerful simulation tool, with detailed models of different components does not mean that realistic and accurate simulation results are obtained. The accuracy and reliability of the input data are very important. Due to the fact that the simulation tool has been used in different research programmes for several years, the software could be debugged, the programme structure could be made flexible to allow different kinds of data and the minimum data requirements could be well defined. Furthermore a good test protocol has been developed and fine-tuned.

The Electrical Engineering Department of the VUB has measurement equipment available to characterize electrical and mechanical components, as well as entire vehicles. In this third part the equipment is briefly described as well as the different types of measurements that can be performed. Furthermore the transformation of the measured data into useful input for the simulation is explained. Additionally the approach of the calibration and validation of the simulation programme are described. A sensitivity analysis is performed to illustrate how sensitive the output (e.g. energy consumption) is to changes in the input parameters (e.g. vehicle weight).

In this part different vehicles are compared as well as different powerflow control strategies of hybrid electric vehicles. How is the loss distribution in the drivetrain ? What is an optimization of the power distribution in hybrid electric vehicles ?

Part four: Conclusions

The last part is the shortest but very important part containing the final conclusions. The most important features of VSP are highlighted. A summary is given of the comparative assessment of the different drivetrains and corresponding power management strategies.

PART I
THEORETICAL
INTRODUCTION

1 INTRODUCTION TO PART I

The main parts of the electric vehicle were invented during the 19th century. The electric parts: battery, motor and electromechanical controller were also used for general purpose and the mechanical transmission was used in common machinery applications. A century ago electric vehicles were already driving the road. Moreover the first car exceeding the 100km/h was an electric vehicle, designed in 1899 by a Belgian engineer, Camille Jénatzy. He called it the “Jamais Contente”. The event took place at the race track of Achère (France) where a speed of 105,85 Km/h on a 1 km long track was reached [4].



Today's technology includes modern electric motor design influenced by power electronics and automotive views and energy sources performing better and better to match acceptable vehicle performances [3]. Electric traction has already demonstrated its merits in other applications like trams, trolley busses, trains (high speed trains) and internal-transport vehicles (industrial trucks, forklifts). More than half of all internal transport vehicles rely on electric drive units [5]. Due to environmental concern a new market is created for electric road vehicles.

While conventional thermal vehicles, also called internal-combustion engine (ICE) vehicles, use a fossil fuel like petroleum, the electric vehicle (EV) uses electricity. Electricity can be considered as the ideal energy source for traction purposes: electric motors are powerful, have a large torque range and have a high efficiency [1]. But electricity is only a secondary energy source and it has to be produced using a number of primary sources. Fortunately it seems that this number is large and can be used with efficiency. Due to battery limitations the range of an electric vehicle is restricted in comparison with ICE-vehicles (ICV). The range can be extended by an additional energy source. This type of vehicles is called hybrid electric vehicles (HEV).

This chapter will give a brief introduction to these vehicles concepts. Furthermore, their benefits on the environment and their potential market are described, as well as the possible incentives to stimulate this market. A detailed description of the electric and hybrid drives can be found in the succeeding chapters.

1.1 Electric and Hybrid Vehicles

Fig. 1.1 illustrates the drivetrain of an internal combustion vehicle (ICV). The drive system is composed of an engine (2) connected to the wheels (6) via a speed gear (4)

and a differential (5). An internal combustion engine is not able to deliver torque below a certain engine rotational velocity. To start the vehicle at zero speed a clutch (3) is necessary. The energy is contained in a fuel tank (1).

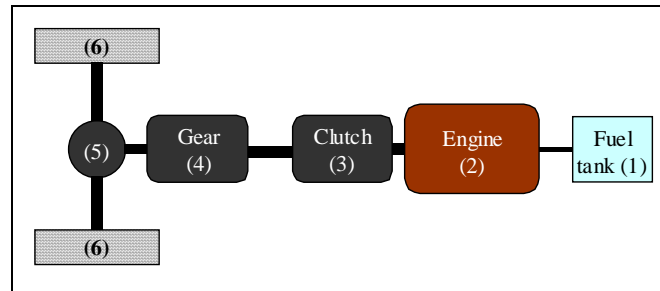


Fig. 1.1: ICE vehicle

The electric drive system (Fig. 1.2) consists in the simplest case in a battery (1), a convertor (2), a motor (3), a gear (changeable or fixed) (4) and a differential gear (5). Besides the torque splitting by means of the differential gear, a two-motor propulsion is also possible [6].

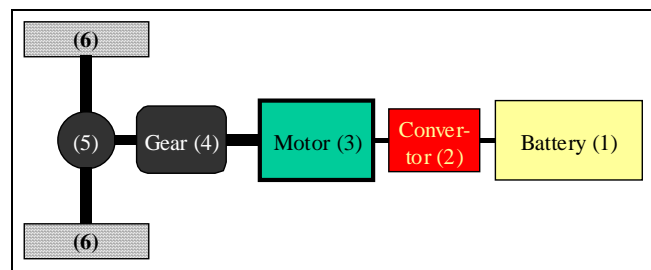


Fig. 1.2: Electric vehicle

Hybrid electric vehicles (HEV) combine different energy sources and/or drive systems, such as internal combustion engines, gas turbines and fuel cells. In general they have a longer range than battery electric vehicles, and still have the option of running on electricity alone in urban environments. The integration of power-producing components with electrical energy storage components allows many different types of hybrid electric vehicle designs. A power control strategy is needed to control the flow of power. This results in different morphologies. The most important are:

- The series hybrid electric vehicle (SHEV) (Fig. 1.3) is a combination or hybridisation of energy sources [7]. “A series electric hybrid vehicle is an electric hybrid vehicle for which its movement comes only from an electric powertrain and which contains an additional other form of on board energy source supplying power electrically to the electric traction system” (standard of reference [8]). One or more electric traction motors can drive the wheels

exclusively. The electricity is generated by an on-board energy source (e.g. engine-generator group), commonly called the auxiliary power unit (APU). This APU is connected to a battery that is acting as an energy buffer. In the future, the engine group could be replaced by fuel cells resulting in potential zero emissions or very low emissions.

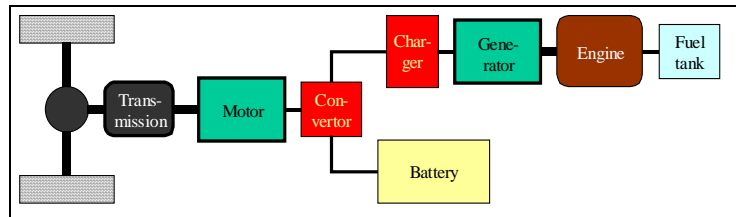


Fig. 1.3: Series hybrid electric vehicle

- The parallel hybrid electric vehicle (PHEV) (Fig. 1.4) is a combination of drive-systems. “A parallel electric hybrid vehicle is an electric hybrid vehicle for which its movement comes from an electric drivetrain and/or from a thermal machine through a transmission which can be common or individual” [8]. Either an electric motor or an internal combustion engine can drive the wheels.

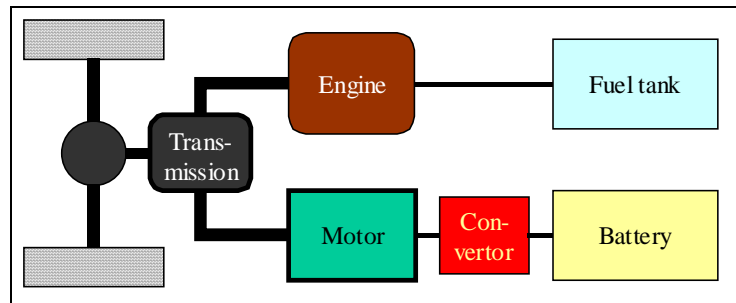


Fig. 1.4: Parallel Hybrid Electric vehicle

- All topologies different from the series and parallel hybrid electric vehicle will be called in this research ‘complex hybrid vehicles’. The complex hybrid electric vehicle encompasses three or more energy sources and/or drive-systems. The possible options are manifold. Complex hybrid vehicles include series hybrids with peak power units, parallel hybrids with a flywheel mechanically connected via e.g. a continuous variable transmission (CVT) or combined hybrid vehicles (please do not confuse the names). A combined hybrid (CHEV) is defined as a combination of a series and a parallel hybrid drivetrain (see subchapter 3.1.3).

In the “CEN prEN 13447” standard [8] one can find a distinction between *electric hybrid vehicle* and *thermal electric hybrid vehicle*. The electric hybrid vehicle is an electrically propelled road vehicle integrating an electric traction system, which permits a pure electric driving mode, and having at least one additional other form of on board energy source (for traction purpose). This means that this standard does not consider vehicles integrating an electric machine for functional assistance to the

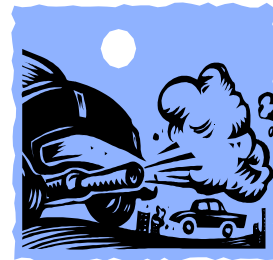
engine such as a load-leveling device, a starter, an electrically driven auxiliary unit, etc., as electric hybrid vehicles, because they do not allow a pure electric mode. The thermal electric hybrid vehicle is an electric hybrid vehicle in which the additional other form of energy source includes a thermal (internal combustion, gas, etc.) engine.

The “SAE J1711” [9] considers the hybrid electric vehicle as a road vehicle that can draw propulsion energy from two on-vehicle sources of stored energy: a consumable fuel and a rechargeable energy storage system, which is recharged by an electric motor-generator system, an off-vehicle electrical energy source, or both.

1.2 Why Electric Vehicles ?

The finite oil resources and its political and economical impact lead to the elaboration of alternative energy sources and the need to diminishing the dependency on imported oil. These problems will force us to change our economy completely where the question is not if but when, and which problem may trigger new technologies first.

Besides these economic and political aspects, there are important environmental reasons to change our transport systems. In comparison with internal combustion vehicles, electric vehicles consume less energy for the same performance and have better ecological characteristics. Electric motors do not require a minimum motor speed (idle working point). They do not consume energy while the car is standing before traffic lights or in traffic jams. They also have the possibility of regenerative braking, i.e. of recharging the battery while decelerating the vehicle. Regenerative braking is one of the special attributes of electric and hybrid electric vehicles.



The ecological characteristics are related to chemical and noise pollution. Sound emission of electric vehicles or hybrid electric vehicles driving in electric mode can be considered to be limited to the rolling and aerodynamic noise of the vehicle, which results in considerable reduction of noise pollution in urban areas. Chemical pollution in these areas can obviously be considered zero. Even taking into account the pollution due to electricity production necessary to recharge the battery, the advantage of electric vehicles is extremely high. Table 1.1 demonstrates the background emissions in case of electric vehicles and direct emissions in case of thermal vehicles. When driving hybrid, the emissions of a hybrid vehicle are easier to control and less than an ICE-vehicle, since hybrid vehicles allow a better engine operation. A more detailed comparison can be found in Part III, in which different

hybrid drivetrain topologies and strategies will be compared mutually and with electric and internal combustion vehicles.

Table 1.1: Comparison of emissions for electric and thermal vehicles [10]

(g/km)	Background emissions of BEV	Direct emissions of Diesel vehicle	Direct emissions of Petrol vehicle
CO ₂	100	209	222
CO	0,020	1,050	6,320
HC	0,010	0,220	0,865
NO _x	0,200	1,120	0,820
SO ₂	0,450	0,215	0,085

City traffic without exhausting gas and low noise is already partly realised by trams, undergrounds, railways, trolleybuses and other recently developed automatic and light rail systems (e.g. airport shuttles). But cars, vans, buses and lorries are route independent vehicles for low and high speed, for city traffic and long distances [3].

At the present the transport sector is responsible for a considerable share of the total emissions. The following tables give an overview of the share of primary energy use and emissions compared to other sectors in Europe.

Table 1.2: Share of consumption and emissions by the transport sector for Europe [11]

	prim energy	CO ₂	SO ₂	NO _x	VOC	CO
Transport	22%	22%	4%	57%	87%	87%
Buildings	28%	25%	10%	5%	10%	10%
Energy industry	29%	35%	67%	27%	2%	1%
Industry	21%	18%	19%	11%	1%	2%

These air pollutants affect human health, damage the ecosystems, and attack (historical) buildings. Carbon dioxide (CO₂) is a major greenhouse gas. Nitrogen oxides (NO_x) and volatile organic compounds (VOC) contribute to photochemical air pollution (tropospheric ozone formation). Sulphur dioxide and nitrogen oxide play a role in the acidification of ecosystems. Exhaust gases contain furthermore carcinogenic hydrocarbons like benzene. It is not the scope of this research to describe the environmental effect. However, since electric vehicles can contribute to an improvement of air quality, especially in cities, some major effects of traffic pollution will be highlighted.

1.2.1 Exhaust Gas Emissions

The most important agents in these exhaust gases and their effect are the following [12,13,14,15]:

a) Carbon monoxide (CO)

Carbon monoxide is a colourless and odourless gas, resulting from an incomplete burning process of carbon. CO is highly toxic. It reacts with the haemoglobin in the blood, reducing oxygen supply to the human cells. Only 0,3 % CO can be mortal in 30 minutes [16]. It causes headaches, dizziness and unconsciousness.

b) Nitrogen oxides (NO_x)

Nitrogen oxides consist mainly of nitric oxide with some nitrogen dioxide. It is produced during the combustion at high temperatures, mostly at high loads of the engine. These gases are colourless and odourless at normal concentrations. Nitrogen oxides affect the bronchial tubes, causing breathing problems. Besides adversely affecting the respiratory system, these gases are considered responsible for photochemical smog and acid rain.

c) Sulphur dioxide (SO₂)

Sulphur dioxide is formed by oxidation of the fuel sulphur. It is an irritant gas that affects the bronchial tubes and contributes also to acid rain formation.

d) Hydrocarbons (HC)

Hydrocarbons just contain hydrogen and carbon, both of which are fuel molecules that can be burned to form water or carbon dioxide. The non-burned hydrocarbons are a mixture of a large number of compounds. Hydrocarbons can be emitted by evaporations of gasoline during distribution and vehicle refuelling. These products are sometimes referred to as 'NMVOC' (non-methane volatile organic compounds). Hydrocarbons are colourless; some have an odour. Some hydrocarbons are toxic or can be carcinogenic (benzene). Volatile organic compounds are major contributors to photochemical air pollution.

e) Particles (soot, dust)

Particles usually refer to the dark particles emitted from exhaust. There is a large variation in particle size and composition. Particles are usually associated with diesel engines. Particulate matter and soot are formed when the combustion is incomplete. Particles obscure vision. They adsorb other components like polyaromatic hydrocarbons, which can be carcinogenic. Small particles stay longer in the lungs, which increases the absorption of harmful components. Particles also affect the bronchial tubes.

f) Carbon dioxide (CO₂)

Carbon dioxide has no colour and no smell. It is the result of the burning process of hydrocarbon and oxygen. Carbon dioxide emission is directly related to fuel

consumption. Reducing fuel consumption will reduce CO₂ emissions. Carbon dioxide is considered as the main cause of the 'greenhouse effect'.

g) Lead (Pb)

Lead is a particle emission found only with petrol engine vehicles since added as an anti-knock additive. Lead impairs the formation of blood and may cause mental disorder. Lead is also an element in some of the electric vehicle batteries.

1.2.2 Effects on Nature

As can be seen from the characteristics of the exhaust gases, they can have an impact on human health. Health effects include cancer, leukaemia and respiratory problems such as asthma. Furthermore they contribute to some environmental aspects, like the greenhouse effect, acidification and photochemical pollution. A brief overview is given of these problems [17,18,19,20].

a) Photochemical Air Pollution

Nitrogen oxides (NO_x) and volatile organic compounds (VOC) contribute to photochemical air pollution (tropospheric ozone formation). NO is a precursor to ozone formation in the troposphere and a direct contributor to ozone destruction in the stratosphere. NO is the most important NO_x pollutant and is highly reactive. It converts within minutes to NO₂ in ambient air. Photolysis of NO₂ and VOC by the sun's radiation produces atomic oxygen, which forms ozone when reacting with molecular oxygen [18]. Ozone concentration increases in polluted cities, which leads to irritations of the eyes, nose, mucous membranes, etc. Photochemical air pollution also causes damage to forests and ecosystems.

b) Greenhouse Effect and Global Warming:

Most of the infrared radiation given off by the earth escapes back into space. However, as gases such as carbon dioxide and methane build up in the atmosphere, more and more of this radiation is reflected back, as the gases act as a greenhouse and raise the earth's temperature. The main greenhouse gases are carbon dioxide (CO₂), methane (CH₄), nitrous oxide (N₂O), ozone (O₃), chlorofluorocarbons (CFCs). The first three components are exhaust gases from road traffic.

The equilibrium concentration of greenhouse gases in the atmosphere is governed by photosynthesis and respiration of the earth's biosphere and physical and chemical interaction with the oceans. The natural CO₂ exchange between earth's surface and

the atmosphere is approximately 200 GtC¹/year. Men additionally produce 8 GtC/year, 6 GtC from combustion and 2 from deforestation [18].

The mean surface temperature of the earth has increased by over 0,5°C in the last century. Although the temperature of the earth's surface has been increasing since the last ice age, the current higher rate of increase is most likely due to the greenhouse effect. This has been brought about due to rapid industrial development, deforestation and the vast use of fossil fuels. It has been predicted that before the year 2050, a further 1,5°C to 4,5°C increase could occur. This may not sound like a significant change until you put it into context. Even a small change in temperature can have a significant effect on an area's natural ecosystem and the ability to grow crops. The phenomenon could entail many consequences, like a rise in the sea level, the drying up of certain zones and even disappearance of certain coastal areas and islands.

c) Acid Rain

Acid rain is caused by sulphur and nitrogen emissions. Fuels contain sulphur and nitrogen, producing sulphur dioxide and nitrogen oxides through the combustion process. Sulphur dioxide (SO₂) is expelled into the atmosphere where it reacts with oxygen to form sulphur trioxide (SO₃). When this mixes with water, sulphuric acid is formed, and hence, acid rain. Nitrogen oxides are converted to acid HNO₃.

Acid rain causes a string of problems as it contaminates lakes and ponds, making it impossible for water-life to develop there. It also damages crops and vegetation, and erodes buildings making them unsightly and unsafe.

1.3 The Market

If electric vehicles represent such benefit on environment and human health, why are there only a few electric vehicles running on our streets ? In this chapter the potential market, the market introduction hindrances and the different incentives to stimulate the market are described. This non-technical chapter will highlight the importance of cost-efficient research tools like simulation programmes.

1.3.1 Cost

Possible alternative solutions for road transportation have to offer a considerable advantage on the environment. Furthermore, the cost of these solutions should imply a positive economic balance, particularly if we take into account the total

¹ GtC = Gigatons carbon

benefit for the society as a consequence of environmental improvement. The traditional cost of a vehicle can be subdivided into purchase cost, exploitation cost and maintenance cost. The overall cost should also include external costs.

The *purchase cost* of electric vehicles is usually higher than for diesel or petrol vehicles. This is mainly due to the small production volume of electric vehicles on one hand: electric vehicles do not benefit from economy of scale the way thermal vehicles do. On the other hand it is due to the presence of a traction battery that represents an important share of the vehicle's price. When investment decisions are only based on initial costs, the electric vehicle is clearly disadvantaged.

The *exploitation costs* however are substantially lower. Electricity cost (per km) is very low, particularly when battery charging can be done during night time. In most countries the cost is less than 50 % of the fuel cost for a diesel vehicle [1]. For hybrid electric vehicles important fuel savings (30 to 50 %) can be realized. The insurance and taxation rate, furthermore, will be lower in the case of electric vehicles due to the fact that the power value on which these costs are calculated are differently classified.

The simplicity of the electric traction system and the reliability of the components also lead to substantially lower *maintenance costs*.

The *external costs* are costs caused around the vehicle due to its presents, its use and elimination.

The overall balance of costs should be made for each different vehicle market segment. It is clear, that electric vehicles can offer operational cost benefits, provided that they are offered on the market at a realistic price level compared with diesel or petrol vehicles. This will be the case when they are manufactured in larger numbers. Nowadays however, electric (and hybrid) vehicles are still in a phase of small-scale or prototype production, and government support schemes are advisable. In fact, it should be taken into account that electric vehicles offer other, non-accountable benefits for the environment (i.e. less external costs) and thus contribute to the quality of life in urban areas. In the European Union, the total cost of the adverse environmental and health effects of transport, including congestion, is estimated to be up to 260 billion EURO per year [21].

1.3.2 Electric Vehicle Deployment Potential

In collaboration with the European Union RTD Programs, studies have been performed by CITELEC about the opportunities for electric and hybrid vehicle introduction in European cities. These studies have reinforced the results obtained in the COST 302 study [22] and in the EDS study for the European Parliament [23] and performed by AVERE. The studies all concluded there is a market between

10 to 30 % for EV. The Californian market imposed by law for 2003 provides 10 % selling for EV and 25 % for HEV [3].

The COST 302 study stated a potential of 7 % for passenger cars and 12 % for light goods vehicles in the European Union (12 countries). According to this study, this market could be realized in 10 years time, with a production of 600 000 cars per year and 100 000 vans, which corresponds to 12 manufacturing plants. In 1992, the MIP consortium (Politecnico di Milano) made a study about the number of thermal vehicles, which could be replaced by electric ones, particularly in Milan. This feasibility study took into account traffic and pollution problems in Milan. According to MIP, the EV potential in Milan is 18,2 % for cars and 21,7 % for vans.

The present-day car fleet is conceived for trip-lengths (more than 100 km), which number only represent less than 10 % of the total number of trips. In France only 16 % of the daily trips are longer than 10 km and in Europe 2 % of all travel distances are between 50 and 100 km; only 1% is longer than 100 km. In the city of La Rochelle 90 % of all daily drive range is less than 100 km [24]. Investigations of passenger car owners in Germany show that only 2 % of the cars drive more than 50 km in one trip. About 75 % of the trips cover distances that do not exceed 10 km [25]. Identical conclusion can be found in the MEET-COST 319 study [26], which carried out a broad survey of driving statistics travel data gathered from several European sources and countries.

The short length of the trips is connected with a long parking period of the vehicles. Indeed, the average daily driving time in Germany is only 40 minutes per day, which corresponds to a parking average of more than 23 hours. Therefore, the time needed for recharging the batteries of electric and hybrid vehicles is more than enough.

1.3.3 Legislation and Incentives

The introduction of electric and hybrid vehicles will clearly cover all the needs if economically justified [1].

A first possibility is of course the improvement of electric vehicle performances. Higher speeds and longer ranges could make the electric vehicle a viable alternative to the internal-combustion engine one. But one should consider that the advent of the high-speed, high-performance electric vehicle is mainly depending on the development of the high-energy, high-power battery. Such batteries are nowadays available, but not really as market products; furthermore they are very expensive. Taking the characteristics of available technology as a starting point, one could take several other actions to increase the market share of electric vehicles. Most of these actions can be taken by the public authorities and policy makers not only for environmental and health reasons but also to diminish the dependency on imported oil.

a) Legislative actions - Traffic restrictions

Traffic-related problems are generally the worst in city centres. In several cities measures are being taken to reduce traffic in the most affected areas. Many cities have a mediaeval city centre which is not at all suited for modern automotive traffic. The renewed interest in the importance of the historical centres lead to a general refurbishment of these sites; in the field of traffic, following measures apply:

- The heart of the city is completely closed to private cars, with the exception of residents and deliveries.
- Parking in the centre streets is heavily restricted or even completely suppressed; only residents having access to a garage may enter the centre.
- Only buses, taxis and two-wheelers are allowed in the centre.
- A new scheme of one-way streets makes it impossible to cross the centre: a car entering the centre is directed to the same place of the ring road (“traffic loop system”). It is however still possible to reach the centre by car. This scheme does not apply to buses, taxis and bicycles: these vehicles can still circulate unimpeded. The public transport service is enhanced and improved.
- Parking in the centre is restricted and in some areas it is reserved to residents.
- Large vehicles such as heavy goods vehicles, full-size buses and coaches are largely banned.

Similar actions could be taken to promote the use of electric vehicles. By allowing only electric vehicles in the limited areas, or by giving them special access and parking privileges, several objectives could be achieved. On one hand, the traffic in the city centre would be limited to environment-friendly electric vehicles, enhancing quality of life, on the other hand, these electric vehicles would operate in a nearly ideal environment.

b) Legislative actions - The American initiatives – Emission regulations

A completely other approach to legislative actions for promoting electric vehicles is found in the state of California. The city of Los Angeles, California, is one of the most “motorised” in the world. Automotive traffic is laying a heavy burden on the city and its surroundings (“the L.A. basin”): road vehicles cause more than 75 % of the air pollution in the L.A. basin. Electricity generation only accounts for 0,7 % of total emissions [1].

The State of California has passed a law on vehicle emissions, which defines that certain percentages of manufacturers’ sales are to be “cleaner” vehicles. In 2003, 10 % of the vehicle sale must be zero-emission (ZEV) and 15 % must be ultra-low-emission (ULEV) and the rest low-emission (LEV) (see Table 1.3). Measures of this kind are likely to create a market. Note that a reasonable time scale must be foreseen to allow manufacturers to develop new and reliable products meeting the new requirements.

Table 1.3: Proposed LEV II exhaust emission standards [27] and EURO gasoline limits

Emission in g/km	CO	HC+NOx	HC	NMOG	NOx
LEV	2,11	-	-	0,05	0,12
ULEV	1,06	-	-	0,02	0,12
EURO I	2,72	0,97	-	-	-
EURO II	2,2	0,5	-	-	-
EURO III	2,3	-	0,2	-	0,15
EURO IV	1,0	-	0,1	-	0,08

c) Direct financial incentives

Direct financial support to organizations willing to introduce electric vehicles might be a good initiative to compensate the higher purchase price of electric vehicles. A direct support scheme, publicly funded, should benefit public corporations such as city administrations. Such actions are very positive and are exemplary for public initiatives needed for the wholesale deployment of electric vehicles in our cities. It is recommended however to extend such support schemes also to the electric vehicle infrastructures, which represent an additional investment cost.

d) Indirect fiscal incentives

Whereas direct financial supports are more suitable for the promotion of electric vehicle use by public authorities, all potential users can benefit from an indirect financial support, through fiscal measures. Several fiscal measures can be taken:

- The exemption of purchase taxes and the relief of VAT on purchasing the vehicle. This is done in some countries, for example Denmark. The effect of this measure is more important when the existing tax for thermal vehicles is high (in Denmark, it exceeds 100 %!). This way, the difference in purchase price between thermal and electric vehicles is reduced, and the electrics can actually become cheaper! A reduced VAT rate can also be applied for the purchase of traction batteries.
- The exemption of electric vehicles from road tax. This has already been done in a number of countries, for example in the United Kingdom.
- The introduction of accelerated depreciation rates for electric vehicles. This measure is particularly useful for corporate users. It has been applied in France, where electric vehicles can now be depreciated in one year, against five years for thermal vehicles.
- The adoption of tax benefits for private owners of electric vehicles. When purchasing an electric vehicle, they could for example be allowed to deduct an amount representing the extra cost of the vehicle from their taxable income; also, the tax deductions for car expenses could be made more generous for electric vehicle owners.

e) Public charging stations

Even when you take into account that most electric vehicles can be charged at home garages, the provision of public charging stations (e.g. Berlin (D), Erlangen (D), La Rochelle (F), Paris (F), Stockholm (S), Göteborg (S), Mendrisio (CH), network of charging stations in Germany and Switzerland) [28] may be a necessity, for the following reasons [3]:

- Some users, particularly in densely built urban areas, do not have a private garage available. They must rely on street-side parking or on public car parks.
- The availability of public charging stations may be an interesting point taking into account the possibility of opportunity charging.
- Today's electric vehicles are mostly able to cover distances of 100 km or more on a single charge. Like stated above daily covered distances for urban vehicle users are often only half of this or even less. However, in some cases an extra long distance might be covered in one day, and in these cases the availability of opportunity charging may be an interesting option. Moreover, the knowledge of the fact that extra charging is available "wherever" will greatly enhance the confidence of the user in the electric vehicle and in its ability to cover his or her transportation needs.
- The highly visible implantation of electric vehicle charging infrastructure on public roads greatly enhances the awareness of the public concerning this infrastructure and the environmental image of the city concerned.

f) Promoting niche markets and fleet application

Fleet applications are characterised by the use of a number of identical vehicles, which allows a more rational management of resources and use of the infrastructure. Some typical examples are given hereunder [3].

An *automatic rent-a-car system* allows a user to travel with public transport for long journeys and taking an electric vehicle from an automatic rent-a-car parking station. From the station he can freely drive around, probably to a destination that is difficult to reach with other public transport means. He can leave the car at another designated parking station or bring it back to the original location. He will be billed for the time of use. The manipulations to be done by the driver are as simple as possible: ideally, only identifying himself to the system (e.g. with a credit card), board the vehicle and drive away (the credit card could serve as "ignition key"). Any additional activities, such as unplugging and storing a cable are clearly unwanted. In this viewpoint, inductive charging systems are particularly attractive for these applications.

A first prototype system was developed in Amsterdam (Witcar system) in 1976 [29]. The "Brussels electric vehicle experiment" (EV Brussels) was developed in 1979-1982 at the Vrije Universiteit Brussel. At that time it was still an automatic rent a car system without inductive charger. At the moment the VUB is in charge of an important EU research project to develop inductive charging systems.

The Praxitèle [30] self-service electric vehicle demonstration in St Quentin-en-Yvelines (F), 20km from Paris yielded promising results and the Liselec [31] system in La Rochelle (F) has been inaugurated in 24 September 1999 and is now running very well. In these systems, electric vehicles are stationed in parking lots near busy areas, where they can be charged with the help of inductive chargers or by connecting them with a charging column. Customers can use the cars for their private needs as long as they return them to one of the designated parking stations within a relatively short period of time. Use of the car is billed through a special card that also gives access to the urban transport network [32].

Car sharing systems as those pretty successful nowadays in Switzerland, the Netherlands and Germany could also be a means to popularise EV's, especially the new coming generation with range extender.

City centres are the usual operation theatres for *taxi fleets*, which makes them particularly attractive for electric traction. The daily mileage of taxis in big cities however can be quite important (150-200 km) and may exceed the range of a typical electric vehicle. This problem may be countered through the use of opportunity charging, which can easily be implemented taking into account that taxis usually spend an important lot of time waiting at taxi ranks. Here too EV's with range extender could be attractive.

Commercial vehicles (i.e. light goods vehicles) are one of the most obvious potential applications for electric vehicles in urban areas. The ubiquitous British milk floats are a well-known example; furthermore, advanced electric vehicles are used in a growing number of European cities for goods distribution and service applications.

Last but not least the European project EVD-post [33] is demonstrating successfully the good matching of EV's for postal services. In this project CITELEC works together with the Post Offices of Belgium, Finland, France, Germany, Sweden.

g) Other actions

A number of additional actions can be taken to improve the operation conditions of electric vehicles in cities. Some examples:

- The electricity distribution companies can support the introduction of electric vehicles by means of supplying the necessary distribution and charging infrastructure. Also, they can offer electricity at a reduced price for vehicle charging. For public, on-street charging stations, the cost of electricity can be included in the parking fee. This way, electric energy is offered "free" to electric vehicle users. The cost of the energy used during charging is much lower than normal downtown parking fees. Offering special (off-peak) rates for electric vehicle charging, using designated power outlets can support private or corporate users of electric vehicles.
- Insurance premiums for electric vehicles can be kept at a low level.

- In parking lots for the use of shopping centres, businesses or public authorities, a number of spaces could be reserved for electric vehicles, with charging facilities offered.

2 ELECTRIC VEHICLES

In the previous introduction the drivetrain layout of the electric vehicle was clarified (see Fig. 1.2). In this chapter some features, fundamental characteristics and developments of the most important components (motor, convertor, batteries and charger) are highlighted. These characteristics are closely related to the requirements of the electric vehicle driveline.

The electric motor is well suited for traction purpose. Starting from zero speed the motor is able to deliver torque and accelerate the vehicle without the obligation to have a gearbox and clutch, like it is required for internal combustion vehicles. Furthermore an electric motor has the capability to be overcharged which is not the case with an engine. During a certain period the motor can deliver a higher power, sometimes 2 to 4 times higher, than its rated power. Internal combustion engines are characterised by idling consumption and cannot regenerate the braking energy like electric motors do. Intermittent service as is necessarily for a vehicle is a natural working situation for the electric motor.

2.1 Requirements for Electric Vehicles

An electric vehicle has to fulfil all demands of the urban and suburban traffic. These demands are different and depending on the vehicle kind and size. It is not possible to assess and conduct evaluations on one type of vehicle and utilisation pattern representing all together the different segments of the automobile population. As in the case of an ICE vehicle, a specification sheet must be drawn up for each segment. This will define a (hybrid) electric vehicle with performance levels comparable to the ICE-driven vehicle in the segment one wishes to penetrate. The basic criterion is the price, which is justified by technical performance and equipment [3]. The different market segments can be: small passenger cars or second family car, the family car or intermediate car segment, high class segment, commercial delivery vans, trucks, minibuses and urban buses; but also electric bicycles and scooters.

Generally the vehicle characteristics are described by the maximum and continuous velocity, gradeability, acceleration and range.

A high gradeability is not only necessary to move the vehicle on streets with a certain inclination but also higher demands are required for driving on ramps of parking houses or getting out of a hole or a kerbstone. This gradeability is closely related to the maximum available torque, which also defines the maximum acceleration of the vehicle.

High acceleration performance mostly conflicts with energy consumption requirements.

The driving range of a pure electric vehicle is defined by the battery energy content. For hybrid electric vehicle two ranges can be defined: pure electric mode and combined with the thermal mode. A high range requires a high overall efficiency for different operating points.

The wished continuous speed on a flat road is used to design the battery and the components of the drive system for the continuous or 1/2 hour power rating [34].

The maximum rotational speed of the motor mainly defines the maximum vehicle velocity. A protection of the motor speed is mostly realised by an automatic decrease of allowed battery current. Possibly, when driving downhill, the motor will automatically switch to generator working to decelerate the vehicle. For this a sufficient high enough brake torque and battery recharging current must be available to fulfil this requirement.

Fig. 2.1 shows the throttle pedal characteristics of an electric vehicle. One can recognise the maximum torque and velocity when the vehicle is in forward driving mode.

Note that a braking torque is available at a higher speed than normal driving and this in order to be able to protect the motor against overspeed.

Two possible solutions exist for starting from standstill. The one illustrated in the figure corresponds to an automatic gearbox way of driving in which the vehicle will automatic start when leaving the brake pedal without pushing the accelerator pedal. The other approach consists in starting the vehicle only when the accelerator pedal is pushed down. When the accelerator pedal is released the motor will automatically decelerate the vehicle.

Some vehicles allow regenerative braking when pushing the brake pedal or manually with a handle at the steering wheel (typically for buses).

The left side of the vertical axle illustrates the forward acceleration while rolling backwards e.g. on a slope. A similar characteristic can be set-up for backwards driving, but the maximum speed shall be lower.

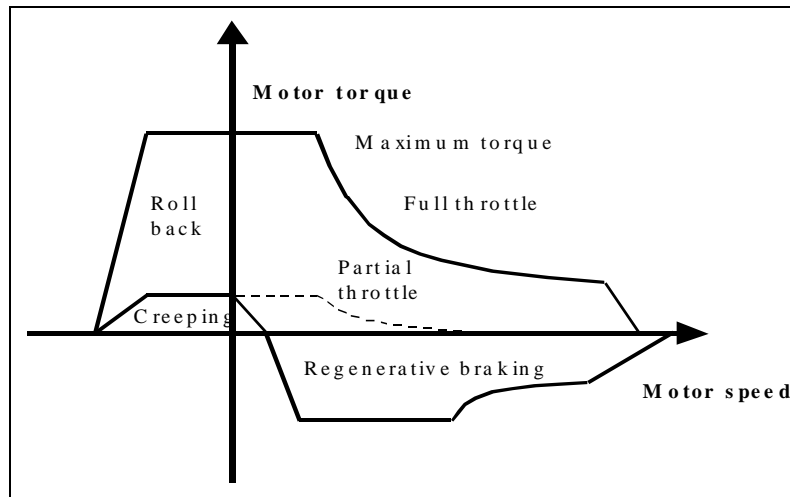


Fig. 2.1: Driving torque curve

All these performance characteristics (maximum velocity, gradeability, etc.) are to be seen in the scope of vehicle acceptance by the customer. Hence the vehicle must be characterised by an acceptable mass production cost.

Electric drives have the advantage of a very low maintenance cost (no engine oil, oil or air filters). Furthermore electric motors in industrial applications have a very long lifetime, longer than required in vehicle application. To limit the production cost the application should be lifetime oriented and as much as possible standardised to be able to install the component in different types vehicles.

The driveability is very important, which requires a high starting torque at standstill, a quick and stable response of the motor and an efficient controllable regenerative braking. To have a smooth gentle start the rate of power increase of the motor should be limited.

Additional to the performance and driveability needs there are important safety requirements. Battery under and over voltage protection is required as well as maximum battery current limitation. Thermal protection of motor and inverter by temperature and over current control is essential. To prevent starting the drive system when the vehicle acceleration pedal is already depressed the controller should remain off [35]. In vehicle applications a high reliability and high robustness is essential and when a fault occurs the vehicle must be stopped in a safe manner.

The electric vehicle drivetrain requirements, corresponding to the market needs, can be summarised as follows:

- Low losses (driving range)
- Low weight
- Low manufacturing cost
- Good control capacity (driveability)
- High overload capacity (acceleration)
- High torque range (gradeability, acceleration)
- Speed range (vehicle velocity)
- Reversibility of torque direction (regenerative braking)
- Application oriented lifetime
- Poor noise emission
- Little maintenance
- Universal installation

2.2 Traction Motors

2.2.1 *Different Types of Motors*

This section will briefly introduce different motor types in connotation with their use in electric vehicle designs:

1. Direct current motors (DCM):
 - Separated excited motor
 - Series excited motor
 - Compound motor
 - Permanent magnet motor
2. Alternating current motors (ACM):
 - Asynchronous motor
 - (Permanent magnet) Synchronous motor
 - Reluctance motor

2.2.2 *DC-Motors*

The magnetic field in a *separated excited DC motor* is created by a small convertor, which delivers the excitation current. This results in a magnetic field developed by the stator poles. Independent from this convertor, the main convertor delivers the rotor current to build up the torque.

The structure of the *series excited DC motor* is basically the same as the structure of a separated excited DC motor. In series excited motor the armature current also

flows through the excitation windings, which results in a torque depending quadratically from the armature current and creates consequently a high starting torque. Since the motor field and armature currents are in series exceeding the rated motor speed results in a decrease in output torque proportional to the square of the motor rotational velocity. This means that a transmission with several conversion ratios is almost always required.

Due to the fact that the series DC machines requires a very simple power convertor they were preferred for traction motors first. The easy field weakening and regenerative braking have made the separated excited motor increasingly popular. Investigations in the early 70s have shown that drives with separately excited motors are more efficient [36]. DC motors are limited in speed and have a lower power density than AC motors. The DC motor maximum speed is less than 7,000 rpm [37], due to the mechanical commutator. They have brushes and a collector, which requires maintenance and can be a point of weakness. Most DC motors uses forced cooling by a separate fan.

2.2.3 AC-Motors

a) Asynchronous Motor

The *asynchronous motor* (ASM) does not carry any field winding. It relies on induction to create a rotor current. Asynchronous motors can be of two types: squirrel cage and wound rotor. Wound rotor machines as their name indicates, carry a three phase symmetrical winding on their rotor [38]. The asynchronous motor has (mostly) a squirrel cage rotor and is fed by a multiphase alternating voltage source to create a rotating field. The difference of rotating speed between the air-gap field and the rotor results in torque production. More and more AC motors are designed with water-cooling. Asynchronous motors are compact, light and are brushless. The asynchronous motor has the advantage of its high robustness. They are less expensive than DC, synchronous and switched reluctance motors. Reference [39] mentions a higher efficiency than permanent magnet motors, but this is a point of discussion, and there is obviously no demagnetisation of magnets possible. Asynchronous motors have a higher power capacity at high speed than synchronous motors [40]. Furthermore they have a good durability at high rotation speed.

b) Switched Reluctance Motor

The *switched reluctance motor* (SRM) makes use of torque generated by the salient polarity (salient poles on stator and rotor). DC excitation is not needed. It needs a large excitation current from the stator side and is characterised by a small rotor gap, maintenance free and a high starting torque. The torque is proportional to the square of the current. Switched reluctance motors are simple and reliable [41]. Corresponding [42] they have a lower manufacturing cost than induction machines

and show a superior thermal and mechanical robustness. Switched reluctance motors can accept high rotation speeds and high temperatures. They have a good torque/weight ration, but they are noisy and give large torque ripple, resulting in bad driveability (shudder). The equivalent circuit is complex and a detection of rotational angle is necessary. By using an observer that controls the phase currents avoid the necessity of a position sensor and by a proper control of current pulse shape reduce noise and vibrations. Both solutions are proposed in reference [43].

c) Synchronous Motor

The *synchronous machine* (SYM) is fed by a multiphase alternating voltage source, mostly three phases. DC current flows in field winding to control the flux of rotor poles. Brushes and slip rings are necessary (maintenance), unless a more complex brushless excitor is used. Synchronous machines can have higher efficiencies at low speed than asynchronous motors [40]. Instead of using a field winding the synchronous machine can also be equipped with permanent magnets.

d) Permanent Magnet Motors

The *permanent magnet motor* (PM) is a kind of synchronous motor, in which permanent magnets (e.g. NdFeB) are fitted in the rotor. Magnetic poles are created that rotate synchronously [44]. Next to the asynchronous motor, it is one of the most important research areas in the field of electric vehicles. Probably it is the solution to be implemented in case of integration of the motors into the wheels.

Permanent magnet motors do not have rotor copper losses. They are characterised by a constant magnetic flux, no excitation, brushless, natural commutation, simple structure and high power density. Mostly they have a higher efficiency than asynchronous motors [45], but extra currents for field weakening control, even at no loads, are necessary as well as a position sensor.

The *surface type* permanent magnet motor is characterised by a large equivalent air gap. The armature reactance can be made small, which results in an improvement in torque linearity and responsiveness to the current. It is unsuitable for field weakening control due to equal q-axis and d-axis reactance. The construction of the *inset type* permanent magnet motor looks like something between a surface type and the imbedded type. There is an iron core between one magnet and another. In the case of an *imbedded type* permanent magnet motor an iron core faces the air gap surface and reduces the air gap. The construction results in a difference between q-axis and d-axis reactance. Large armature reaction and field weakening control is easy to perform, with maximum torque and/or efficiency control. Furthermore there is high mechanical strength and low iron loss.

The permanent magnet *hybrid motor* has a permanent magnet field and a field winding, to control the air gap magnetic flux, with independent magnetic paths. A back yoke mechanically and magnetically couples the two armature cores. It can be

constructed at the same size as a permanent magnet motor, but it needs an extra controller for the DC magnetic field. It is less efficient than the permanent magnet motor, but more efficient than synchronous machine, due to the negligible field loss at low load [46]. Major disadvantages are the high costs of the rotor construction and the required maintenance for the brushes [47].

Permanent magnet motors are usually referred to as synchronous motors but often also as “brushless DC” motors even when it is basically the same type of motor. The vocabulary is in this respect not very strict, but the most widely accepted definition is that the PM synchronous motor is fed with sinusoidal stator currents while the PM “brushless DC” motor is fed with square wave currents [48]. This type of permanent magnet motor should not be confused with the direct current motors where the field is build up with magnets and the armature fed by a DC current. The magnetic field of the “brushless DC” motor has a rectangular form, which results in a high power density but low speed range. The advantage of the square wave currents is a somewhat larger integrated current resulting in a larger maximum torque. The disadvantage is a larger amount of harmonics resulting in higher losses, more noise and a risk for torque pulsation.

2.2.4 Comparison of Drives for Electric Vehicles

Table 2.1 gives a comparison of different motor types [49]. Motors should always be evaluated in function of the needs of the application. E.g. each of the different motors can be less efficient than the others in some regions of operation, and it can be more efficient than the others in some other regions. To make a good comparison, one must not compare maximum efficiencies, but relate the efficiency map to a certain speed cycle.

Table 2.1: Comparison of different motor types

	ASM	PM	SRM	DCM	SYM
Motor size, mass	0	+	0	-	0
High speed	+	+	+	-	-
Endurance, maintenance	+	0	+	-	-
Efficiency	0	+	0	-	0
Controller size, mass	0	0	0	+	0
Controllability	+	+	-	+	0
Nr power devices	0	0	+	+	0
Reliability	0	0	0	0	0
TOTAL	+++	++++	++	--	--

The table shows an advantage for the permanent magnet motor as traction motor for electric vehicles. Indeed, on the level of performance the permanent magnet motor has a lot of interesting features. But considering the production cost, one must take into account the high price of the magnets and the more complex construction of the

motor. As long as this price is too high, the global result will probably be in the advantage of the asynchronous motor.

2.3 Power Convertors

2.3.1 *Chopper Circuits for DC Motors*

The series wound motor needs only one DC/DC convertor unit. This type of drive unit employs the most basic convertor design. A power switch directs the battery current to the motor at a variable pulse-duty frequency adjusting the voltage at the motor to provide the desired current (step down chopper). When a series motor is used the specific torque-speed curve is used rather than the classical constant torque - constant power characteristics. For braking and reverse driving, additional elements are necessary in the circuit, because the field or the armature connections have to be changed.

The separately excited DC motor requires an additional controller compared with the series wound motor. The field current is independent of the armature current. Mostly a transistorised field current chopper will control this low current. In this case the constant torque - constant power working field is mostly exploited with a speed ratio approaching 1:4.

For braking there are two relevant implementations: in a circuit with a two-quadrant chopper the armature current is reversed or, as a second interesting solution, the field current is controlled [50].

The choice of semiconductor technology is based on criteria of power capability, switching frequency, switching and conduction losses, additional elements and finally the costs. MOSFETs allow very fast switching rates (100-800kHz) but are limited in power capability [47]. From today's view, the IGBT will be the common switching device for EVs. Only convertors for low battery voltages (< 100V) and convertors with very high frequencies (DC/DC convertor, charger) will be equipped with MOSFETs [51].

In a drive system with DC motor and chopper, the battery will be stressed by current pulses in the armature control range if no additional filter capacitors are used. The current root mean square (rms) value is much higher in chopper mode than the mean value. This causes higher losses in the battery or in the filter.

2.3.2 Inverter for AC Motors

Today's sophisticated microprocessors and micro-controllers form the foundation stone for the activation of switches according to the wished waveforms and are essential for the implementation of efficient control algorithms. Today's inverters for electric vehicles will be designed with modules of bipolar transistors, MOSFETs or IGBTs. Three-phase full bridges low current modules are available at reasonable prices. AC drives need to be fed by a sinusoidal voltage or in some applications a trapezoidal voltage. This is realized by a DC source connected to a three-phase inverter working in pulse width modulation (PWM) mode. The load filters the current. Harmonic currents should be low compared to the fundamental current to keep the additional losses small. Compared to DC chopper circuits with relatively low frequency, inverters need a big filter capacitor to reduce the current pulses in the battery.

In the case of *asynchronous or synchronous motors*, the control modes used are scalar and vector control.

The scalar mode performs an action on the slip in case of an asynchronous motor or in case of a synchronous motor on the amplitude of the stator current while maintaining the angle between the current and the rotor flux. This mode therefore takes into account the natural characteristics of the motor.

The basic principle of vector control is a mathematically splitting up of the motor current into torque current and excitation current. In this way the torque and the field can be controlled separately, making the control of an AC motor similar to that of the separately excited DC motor. This makes it possible to attain very high levels of dynamic performance [52]. For this methodology it is necessary to know the motor parameters, but these parameters can change due to temperature variations for instance. The rotor resistance can be evaluated by the use of a thermistor on the stator or an estimation algorithm.

If the field forming current value is maintained constant to achieve a constant flux level (conventional vector control systems), the ratio of core loss to total losses increases in the light load torque region [53]. Therefore a lot of researchers are developing an adaptive or smart rotor flux observer. The magnitudes of torque and magnetic flux current are adapted in function of speed and load to maximise motor efficiency (see Fig. 2.2). The magnetic saturation and control stability cause problems with this control strategy [54]. Combining a fast rotor flux control for transient behaviour and a maximum efficiency flux control for steady state, can solve these problems [55].

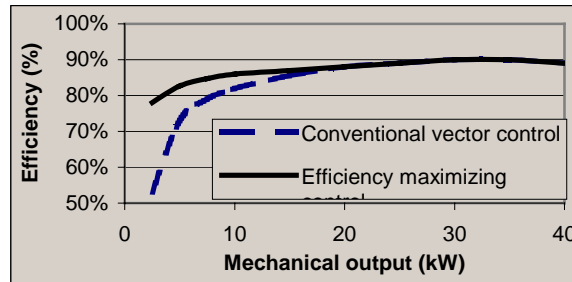


Fig. 2.2: Smart flux optimisation [56]

The operating principle of the converter of the *switched reluctance motor* is as follows: when one of the rotor pole tips get very close to a stator pole tip, the phase winding associated with this stator pole is energized pulling the rotor pole into alignment with it. In the aligned position the reluctance of the path is switched to its minimum value (hence the name switched reluctance). At the moment a rotor pole and a stator pole (or a set of poles) are getting aligned, another rotor pole is getting very close to another stator pole, and the switches associated with the phase winding of this last stator pole are turned on while the switches associated with the phase winding of the poles that were getting aligned are turned off, and so forth; thus generating torque and causing the rotor to rotate.

The timing at which the phase current pulse is applied (firing angle) and the time duration of the pulse (dwell) determine the torque, the efficiency, and other parameters of the motor. For that reason, it is essential for the inverter to know the exact rotor position at all times. An encoder or a resolver is used to provide the necessary position information to the controller circuitry [57].

The power part of the inverter of a “*brushless DC*” motor is similar to the inverter for asynchronous motors. The pole position has to be detected by a sensor system or by the motor voltage. In comparison with the asynchronous motors or the separately excited DC motor, operation in the range above base speed is less simple. Control can be achieved here with a reactive current and a greater pole angle. The ratio between constant torque and constant power working field will be quite different from the case with asynchronous motor (1:2 to compare with 1:4) [58]. By advancing the conduction angle ϕ (between phase voltage and rotational electromagnetic force (EMF)) the rotational EMF can be made higher than the phase voltage [59,60,61], which results in an equivalent field weakening effect.

With flux weakening control, the currents will generate a field in opposite direction to the flux due to permanent magnets and hence may cause irreversible demagnetisation. Due to eddy current losses, temperature increases which results also in demagnetisation [62]. Flux weakening techniques sacrifice the power factor and the efficiency is degraded [63]. Using permanent magnet *hybrid motor* can

possibly solve this problem, because they combine a permanent magnet with a field winding.

2.4 Batteries and Energy Storage

The traction battery is the most critical component of the vehicle and in most cases it will also be the most expensive component. Through the years, several battery types have been developed. Only a small number however, can be considered for use in electric vehicles. Different types of batteries are being presented on the market; the most important ones are presented here as well as some other energy storage devices like flywheels, super capacitors and fuel cells.

Batteries are characterised by their life cycle, energy and power density and energy efficiency. The life cycle represents the number of charging and discharging cycles possible before it loses its ability to hold a useful charge (mostly when the available capacity drops under 80% of the initial capacity). Life cycle typically depends on the depth of discharge. Life cycle multiplied by the energy content corresponds with the calendar life, which gives an idea how many times the battery is to be replaced during the lifetime of the vehicle.

When charging and discharging a battery not all energy, stored in the battery, will be available due to battery losses, which are characterised by the battery efficiency.

The energy and power density describes the energy content (vehicle range) respectively the possible power (vehicle performance) in function of the weight of the battery.

The maximum power is often defined for a full charged system and a terminal voltage equals 50% the initial open circuit voltage [64]. In the draft standard out of reference [65] the maximum deliverable battery power is defined as the power at which the battery terminal voltage would fall to $2/3$ of the open circuit voltage.

A battery can be optimised to have a high-energy contents or it can be optimised to have a high power capability. The first optimisation is important for battery electric vehicles, while the second is required for hybrid drivetrains.

The State of Charge (SoC) of a battery is the amount of electrical charge in the battery, expressed as a percentage of the difference between the fully charged and fully discharged states.

A battery of an electric vehicle consists of a combination in series, and possibly connected parallel, of individual battery modules. Minor differences in module characteristics can be present. A battery management system is a key point for battery reliability.

A specific energy of at least 50 Wh/kg and a specific power ranging from 100 W/kg, continuous, up to 200 or 300 W/kg is a must for an good electric vehicle design. Ideally 150 Wh/kg and/or 500 W/kg up to 1000 W/kg (in the case of super-capacitor) would be better, especially for hybrid vehicles [3]. The US Advanced Battery Consortium (USABC) mid term goals are 150 W/kg and 135 Wh/kg and long term goals 400 W/kg and 300 Wh/kg for respectively battery power and energy density.

Table 2.2 shows some characteristics of the most important electric vehicle batteries as reported in the literature. The life cycle is the most doubtful data since it requires a lot of practical experiments. Data on energy and power density can vary in function of if one battery cell or a whole battery pack is characterised.

Table 2.2: Battery characteristics [5,66,67,68,69,70,71,72,73]

	Lead based	Nickel based	Zinc based	Sodium based	Lithium based
<i>Cell voltage</i>	2 V	1,2 V	1,4...1,6 V	2...2,5 V	3,5 V
<i>Energy density</i>	30...35 Wh/kg	50...80 Wh/kg	70...80 Wh/kg	90...130 Wh/kg	80...200 Wh/kg
<i>Power density</i>	70...130 W/kg	175...700 W/kg	100...125 W/kg	100...160 W/kg	140...1000 W/kg
<i>Energy efficiency¹</i>	70...85 %	60...85 %	65...85 %	80...90 %	85...95 %
<i>Life cycle</i>	600...1000	1500...2000	500...2000	600...1000	>1000
<i>Cost</i>	100...150 ECU/kWh	300...500 ECU/kWh	125...250 ECU/kWh	150...400 ECU/kWh	100...200 ECU/kWh

2.4.1 Lead-Acid Batteries

The lead-acid battery is the best known. The battery energy efficiency can exceed 80 %. Its major drawback however is its low energy density: 30 to 35 Wh/kg for current traction cells. A lead-acid fitted electric vehicle will thus have a limited range. The development of the lead-acid battery is still going on. Batteries with extra capacities of 15 % and 25 % over standard cells are now available. However, these high-capacity cells do not yet achieve the same life cycle as standard cells.

For traction purposes two types exist. The first type, the *Vented battery with liquid electrolyte*, needs regular maintenance, namely topping up the electrolyte with distilled water. This operation is essential for the good keeping of the battery. Vented batteries emit hydrogen gas during charging, which may cause explosion hazards. Several electrode structures exists: the "traction battery", with tubular

¹ without heating

positive plates and the “semi-traction battery”, with flat positive plates. Flat-plate batteries are less expensive to make, but tubular-plate batteries have a longer life.

The second type is the *Maintenance-free battery*, also called the Valve Regulated Lead Acid (VRLA) battery, where the electrolyte is immobilised in a gel or in a glass fibre mat and water consumption is avoided through hydrogen/oxygen recombination. This battery is completely maintenance-free, and during normal operation, emits no gases. This advantage is offset by their higher price. They are also more sensitive to deep discharges and overcharges and they may only be used with specially designed chargers. The use of a temperature balancing system is important for the service life [70]. Their ease of use and lack of maintenance however makes them very popular with electric vehicle manufacturers.

2.4.2 Nickel Batteries

The *nickel-iron battery* was developed especially for electric vehicles. Because of a high water decomposition, this system has an inefficient charging factor and needs good and frequent water refilling. A maintenance-free battery is not feasible.

In the *nickel-cadmium battery* the iron is replaced by cadmium. Nickel based batteries are currently in widespread use in general-purpose electrical equipment. While appliance batteries employ sealed designs, open nickel cadmium cells are common in tractive application [5].

The battery has a high power density and fast charging possibilities. Its energy density is higher than that of a Lead-Acid battery. But its energy efficiency is limited. Nickel-Cadmium batteries also emit hydrogen gases when charging.

For traction purposes, nickel-cadmium batteries come in two versions according to the electrode design (sintered or fibrous electrodes). Maintenance-free Nickel-Cadmium batteries have been developed recently.

Long term continuous overcharging produces an artificially induced drop in capacity and decrease the overall life of the cell. This capacity loss is caused by loss of contact of the cadmium hydroxide particles with the negative cadmium plate. A deep discharge / charge cycle restores the hydroxide particles to their normal smaller size and increases surface contact. Repeated precise charge cycles affects the ability of the cell's active chemicals to charge fully, after which the positive nickel plate begins to produce oxygen. Overcharging reverses the memory effect [74].

The high cost associated with the use of relatively expensive materials and complicated production could be amortised by a service life, which is substantially longer than that of the lead-acid battery. The limited resources of cadmium could prevent the large-scale use of this type of battery. Cadmium can cause objections if

it is not completely recycled [70]. The nickel can be reused to manufacture stainless steel and one hundred percent of the cadmium can be reprocessed for use in new batteries [75].

In *nickel-metal-hydride batteries* [76,77] an alloy storing hydrogen will be used for the negative electrode, instead of cadmium. Energy density and power density increase, compared to the nickel cadmium battery [78]. High power prismatic cells (higher than 600 W/kg) [79] as well as bipolar pack designs, reducing fabrication cost, [80] are under development. Because nickel-based batteries also have higher power density ratios, they are particularly interesting for hybrid vehicles. However one should find a good compromise between power density and energy efficiency.

2.4.3 Redox Batteries

The *zinc-bromine battery* uses soluble active material and liquid electrolyte. This battery is in fact a complex electrochemical system with a battery flow stack and two external tanks of electrolyte. It is a so-called “redox” battery. It uses bipolar cells, which are connected to a stack. A bromine complex is pumped through on one side of the cell and a zinc-bromine on the other. Its characteristics made it promising for electric vehicle applications. At the moment it exists as pre-commercial prototype. Like all systems with circulating electrolyte, the expenditure for the zinc-bromine battery is higher in order to cover the current losses in the line system, pump energy and recharge the auxiliary battery. The auxiliary battery guarantees secondary vehicle functions and restarting when the zinc-bromine battery is empty.

Considering the toxicity of bromine, the safety aspects of this battery and its behaviour in case of accidents are viewed more or less critically [70,81].

Another zinc-based battery is the *zinc-air battery*. It has an extensively enlarged surface and it probably will have an energy density up to 8 times higher than that of a lead-acid battery. For recharging however the electrodes have to be removed from the system and regenerated in a chemical plant.

The *Vanadium Redox Battery* stores energy in the vanadium pentoxide electrolyte and uses conduction polymer plates with a graphite felt surface to collect the current. This current is generated by the transfer of electrons from the electrolyte in the positive half-cell to the electrolyte in the negative half-cell and is supported by the flow of hydrogen ions across a membrane separating the electrolytes [82].

The characteristics of the battery permit considerable latitude in designing systems for specific storage applications. One of the most important features is that the use of solutions for energy storage allows independent sizing of system power (determined by the number of cells in the stack and the size of the electrodes) and

the energy storage capacity. Cycle data indicates up to 5000 cycles without performance degradation [82].

The battery can be recharged in a few minutes by exchanging discharged electrolyte with charged electrolyte.

The electrolyte that flows through the cell stack removes waste heat and all cells remain in the same state of charge. Individual cells do not require monitoring or balancing. Overcharging for cell equalisation is not required and explosion hazard is minimised. The electrolyte has indefinite life and low cost. Reused electrolyte ensures low environmental impact. Deep cycling does not affect battery life [82].

2.4.4 Sodium Batteries

The *sodium-sulphur battery* essentially differs from batteries with liquid electrolyte. It is a so-called “high temperature” battery: the electrodes (sodium and sulphur) are present in molten state at a working temperature of around 300°C, separated by a ceramic solid electrolyte. The whole battery, containing a large number of small individual cells, is enclosed in a thermal envelope and fitted with a thermal management system.

The chemical components of the battery are completely sealed and there are no gas emissions. Its main advantage is its high energy density (100 Wh/kg, three times more than for the lead-acid battery). However the failure to realise batteries with adequate life cycle has led to the abandonment of this technology.

The *sodium-nickel chloride battery* is very promising. It has cells similar to the sodium-sulphur cells and operates also at high temperatures. The active ingredients are sodium and nickel chloride. It is also known as the ZEBRA battery and exists in a pre-commercial prototype state. From the point of view of safety, it is easier to handle and the battery does not react sensitively to overcharging and over discharging. A disadvantage is the higher internal resistance, which can change due to the electrochemical reactions [70]. It offers also the main advantages of a high energy density (100 Wh/kg). This battery could come on the market if an efficient marketing action is operated.

2.4.5 Lithium Batteries

An advanced battery is the lithium battery. Lithium is the lightest metal with highest electrochemical potential. Small cells are established in the portable electronic market. Batteries for electric vehicles are under development [83,84]. Lithium based batteries concepts furnish higher energy density (100 – 150 Wh/kg), than sodium units in a package suitable for the use at normal ambient temperatures.

Lithium secondary batteries using nickel-cobalt composite oxide as the positive electrode material and a mixture of graphite and coke (hybrid carbon) as the negative electrode material have been examined to develop long life and large-scale batteries [85].

A *Lithium polymer* elementary cell is made by laminating together five thin materials including an insulator, a lithium foil anode, a solid conductive polymer electrolyte, a metal oxide cathode and a current collector [86]. Lithium polymer batteries have high tolerance to abuse conditions such as overcharging and overheating. Optimal performance for EV applications is achieved when operating the battery between 60°C and 80°C. They have low heat capacity and thus can be rapidly heated-up with a small amount of energy [84], but the application for EV will necessitate a performant thermal management system.

The working principle of a *lithium-ion* intercalation cell is different from most current systems. It is not based on a chemical reconstitution reaction, i.e. a chemical phase change in the active materials. Lithium atoms are rather stored in the respective host structures of the active materials. The insertion process is called intercalation. During charge lithium is oxidized at the negative electrode. The lithium ions are then transferred through the electrolyte to the positive electrode. Here they are again stored in the respective intercalation material. During discharging the reverse process is taking place [87].

Lithium-ion cells achieve coulomb efficiencies of nearly 100 %. A few internal effects could increase the capacity imbalance between the cells [88]. This is the reason why a battery management system must control very tightly the balance cell by cell. The open circuit voltage, after a sufficient relaxation time (a few minutes) gives a clear indication of the cell's state of charge [72].

2.4.6 Super-Capacitors

Super or ultra-capacitors (800-1500 F) behave, like very high-power, low-capacity batteries but store electric energy by accumulating and separating unlike-charges physically, as opposed to batteries, which store energy chemically in reversible chemical reactions. One key aspect of super-capacitors is that they have excellent life cycle. When fully developed for vehicles, they could be expected to last as long as the car. This is because it is possible to cycle super-capacitors very quickly and deeply without having the large decrease in life cycle that most chemical batteries experience. They also have a high cycle efficiency (up to 90 % [89]) compared with chemical batteries. The primary obstacles with super-capacitors at this point are their low specific energy, which are in the range of 5-10 Wh/kg and the large possible voltage dispersion between individual cells. Super-capacitors also have the unique feature that their voltage is directly proportional to their state-of-charge. Therefore, either their operating range must be limited to high state-of-charge regions, or control electronics must be used to compensate for the widely varying

voltage. The fact that super-capacitors can provide high power for accelerations and can accept high power during regenerative braking makes them ideally suited for the load levelling required in electric and hybrid electric vehicle. Power densities of 2000 to 4000 W/kg have been demonstrated by ultra-capacitors in the laboratory [90].

2.4.7 Flywheels

Flywheels store energy mechanically in the form of kinetic energy. One can distinguish mechanical and electrical flywheels. The mechanical flywheel is connected to the drive system via an axle. The electrical flywheel takes an electrical input to accelerate the rotor by using a built-in motor, and returns the electrical energy by using this same motor as a generator.

The most significant factor affecting flywheel design is the materials used to construct the flywheel rim. A flywheel rim needs to be made of a high tensile strength to density ratio material to maximize the kinetic energy stored (thanks to a high rotational speed) while minimizing the chance of failure. Flywheels show technical promise as a potential load-levelling device for hybrid electric vehicles; however, they are still under development and are not yet commercially available. Flywheels could become an excellent high power density storage devices, with one optimistic estimate for specific power ranging between 2000 W/kg (short-term) and 8000 W/kg (long-term) [91]. The corresponding specific energy is ranging from 4 to 50 Wh/kg [92].

2.4.8 Fuel Cells

The development of fuel cells goes back to the last century. The fuel cell electrochemically combines air with fuel and converts it into other elements with a production of electricity. The conversion is similar to a conventional battery, except that the reductant and oxidant are continuously supplied to the cell instead of being contained in the cell. In addition, fuel cells are 'recharged' by filling up the fuel supply.

Fuel cells are electric generators, basically fed with hydrogen as a fuel. This hydrogen can either be stored as such in the vehicle, or be generated in the vehicle by means of reformers. Hydrocarbon fuels such as methanol, natural gas or synthesis gas can be used by employing a chemical reactor prior to entering the fuel cell. The hydrocarbon fuel is converted into hydrogen rich synthesis gas via water vapour reformer or a partial oxidizing burner and then is purified in a gas purification stage to clean hydrogen. Emissions of these processes usually are CO and CO₂ [93].

When hydrogen is stored as such this can be as a compressed gas in vessels, as a cryogenically liquid at a temperature of minus 253 °C or hydrogen atoms adsorbed in reversible metal hydrides, as obtained by applying hydrogen gas under pressure on suitable metal alloys. The low temperature and pressure at which the reaction occurs and the stability of the hydrides, preventing leakage flows in case of damage, make this form of storage particularly attractive for road transportation applications. Compared to lead acid batteries this storage contains up to 10 times more energy [94].

The fuel cell has the potential to be more efficient than a gasoline or diesel engine. Fuel cells are at the opposite of most electrical devices in that peak efficiency occurs at minimum load. Efficiency is 60% at no load and 40% at full load at the current state of development and the theoretical maximum is 83% [95]. A fuel cell has very few moving parts (reactant pumps and valves), which produce very little friction. The fuel is oxidised at low temperature instead of being combusted at very high temperatures as in an internal combustion engine. Low emissions are a result of low temperature oxidation and appropriate fuel selection when a reformer is used with hydrocarbon fuels. If methanol is used to generate hydrogen with a reformer, 25 volume percent of the gas output is CO₂ [96]. In the case of hydrogen (the ideal fuel), the only by-product is water.

The fuel cell is still under development. Fuel cell systems are still relatively large and heavy compared to conventional engines. Cost is still very high, mainly because fuel cells are constructed from expensive materials and are produced in low volumes. As manufacturing issues are tackled, lower cost materials and lower precision tolerances should considerably bring the cost down.

The fuel distribution infrastructure for hydrogen is very limited. A reformer based vehicle system has the advantage of using existing hydrocarbon fuels that are more readily available than hydrogen.

- Methanol is the simplest hydrocarbon, making it relatively easy to reform and it is liquid, so it fits more easily into the existing motor fuel distribution infrastructure.
- When using gasoline reformers the existing fuel infrastructure can be used, but their additional emissions are still being examined.
- Hydrogen can also be produced out of natural gas at existing refuelling stations [97].

The fuel cell is in principle very simple, however the chemic reactions do not readily take place, and unless special materials are used for the electrodes and the electrolyte, the current produced per cm² is small and the electrical power losses in the electrolyte are large. To overcome these problems, different types of fuel cells have been developed. The different varieties are distinguished by the electrolyte used though the construction of the electrodes is also different in each case. However, in all types there are separate reactions at the anode and the cathode, and

charged ions move through the electrolyte, while electrons move round an external circuit. Another common feature is that the electrodes should be porous, because the gasses have to be in contact with the electrode and the electrolyte at the same time [98].

a) Phosphoric Acid Fuel Cell

The Phosphoric Acid fuel cell is already being used stationary in such diverse applications as hospitals, nursing homes, hotels, office buildings, schools, utility power plants, and airport terminals. Phosphoric acid fuel cells generate electricity at more than 40% efficiency and the steam this fuel cell produces can be used for co-generation. Operating temperatures are in the range of 200°C. These fuel cells also can be used in larger vehicles, such as buses and locomotives.

b) Alkaline Fuel Cell

The Alkaline fuel cells (AFC) can achieve power generating efficiencies of up to 70%. It uses liquid alkaline potassium hydroxide as the electrolyte. Until recently it was too costly for commercial applications, but several companies are examining ways to reduce costs and improve operating flexibility. The operating temperature is about 70 °C [96].

c) Proton Exchange Membrane Fuel Cell

The proton exchange membrane fuel cell (PEM) has a solid electrolyte. The power density of PEM fuel cells is significantly higher than that of alkaline fuel. The PEM fuel cell is currently more complex than the AFC. Nevertheless, though the performance of the cells seems to be different, they have to be compared to both the whole system and to the different applications in vehicle use (starting period, stop time, idle time, etc.). Motion sensitivity and the origin of the hydrogen are also relevant issues. If the hydrogen is not obtained from fossil fuels, alkaline cells will be favoured, whereas a production of methanol from coal will favour the PEM fuel cell [99]. The Proton Exchange Membrane cells operate at relatively low temperatures (about 90 degrees C°), have high power density, can vary their output quickly to meet shifts in power demand, and are suited for applications – such as in automobiles – where quick start-up is required [98].

d) Molten Carbonate Fuel Cell

The Molten carbonate fuel cell promises high fuel-to-electricity efficiencies and the ability to consume coal-based fuels. This cell operates at about 650°C. The first full-scale molten carbonate stacks have been tested.

e) Solid Oxide Fuel Cell

The Solid Oxide fuel cell could be used in big, high-power applications including industrial and large-scale central electricity generating stations. Some developers also consider that solid oxide can be used in motor vehicles. A solid oxide system usually uses hard ceramic material instead of a liquid electrolyte, allowing operation temperatures to reach 900°C. Power generating efficiencies could reach 60%.

f) Direct Methanol Fuel Cell

The Direct methanol fuel cell is a relatively new member of the fuel cell family. This cell is similar to the PEM cell since they both use a polymer membrane as the electrolyte. However, in the direct methanol fuel cell the anode catalyst itself draws the hydrogen from the liquid methanol, eliminating the need for a reformer. Hence they are very attractive since no gaseous fuel is needed. Efficiencies about 40% are expected. It would typically operate at a temperature between 50 and 90°C. Higher efficiencies are achieved at higher temperatures [98].

2.5 Chargers and Infrastructure

The introduction of large numbers of electric vehicles will require the development of charging infrastructure. Electric vehicles using batteries require access to an electricity distribution network in order to recharge their energy source. The charger itself may be located on-board, off-board or partially on-board the vehicle. For vehicles used in public transport, and used on fixed routes, off-board chargers are mostly used. The use of partially on-board chargers offers interesting possibilities, particularly for opportunity charging. These devices are based on inductive energy transfer (see below).

a) The battery charger

Electric vehicles are largely independent of the charging place if they are equipped with an on-board charger connectable with any AC outlet. A 230 V / 16 A outlet can supply an apparent power of more than 3,5 kVA. A battery of 15 kWh can be charged in less than five hours (main charge). In Europe, three-phase feeding is generally used for powers higher than 3,5 kW. High power is available from the three-phase AC 400 V-grid. High power fast charging techniques add weight and size to the charger convertor and hence will be mostly used as off-board charger. Stationary chargers should be able to provide 20 to 200 Amps at output voltages from 60 to 200 V. This means a 40 kW connection to the mains has to be provided [102] allowing charging an almost empty 15 kWh-battery in 20 minutes. Adaptive process controlled charging technology are on the market for 25 kW to 150 kW fast chargers [100] and even up to 300 kW chargers for buses [101] are available.

The electric vehicle has to be connected to the AC electric vehicle supply equipment so that in normal conditions the charging function operates safely, indoors or outdoors, causing no danger to persons or surroundings, even in the event of carelessness that may occur in normal use.

Electromagnetic compatibility is considered particularly important; both the immunity against external disturbances and the generated electromagnetic disturbances are treated. Lack of immunity against electromagnetic disturbances may in fact have consequences on other electric vehicle equipment. Electric utilities in Europe are nowadays demanding more and more consumers with low distortion and reactive power requirements.

The charging techniques are quite important since they have great influence on the lifetime of the battery, energy efficiency and maintenance. The purpose is to control the chargers in such a way that they optimally fit the electro-chemical process inside the battery [102]. When fast chargers are used for different kind of vehicle with different batteries, an information transfer is required to adapt the charging process at the characteristics of the battery.

b) Inductive charging

The basic idea of the inductive charging system is quite straightforward: the main transformer of the battery charger is split in two parts. The primary is mounted fixed on the ground, the secondary is mounted on the vehicle. It is then sufficient to place the primary adjacent to the secondary to "re-assemble" the transformer and to allow energy transfer from the grid to the battery. The present state of the art of inductive charging system shows several approaches, which have led or may lead to industrial developments.

Systems using the grid frequency (50 Hz) are available for industrial vehicle applications. The control of the charging procedure can be based on a ferro-resonant working point of the transformer [103].

A system using intermediate frequencies (400 Hz) retains some interesting features of the mains-frequency systems while considerably reducing weight and size. It can be integrated with 400 Hz generating equipment which is an industry standard. The control of the charging procedure can be based on classical 400 Hz PWM convertors existing in the aircraft sector [104].

Systems using high frequencies, between 25 and 100 kHz, have been developed in the USA for power ranges up to 120 kW. They offer exceptional power transfer capability in a small and light unit, but mostly they have to be manipulated by hand.

In Europe, high-frequency systems, which require no manipulation, are being developed in the framework of automatic rent-a-car systems. The charging procedure is automatically initiated when parking the vehicle, through the matching

of the primary inductor (mounted in the road surface or in a box on the road side) with the secondary inductor (mounted on the underside of the vehicle or on the front side of the vehicle protected by the bumper) [104].

Due to its particular characteristics of user-friendliness and safety, inductive charging is well suited for a large number of electric vehicle applications. Because of the infrastructure needed, it seems likely however that, in a first period, fleet applications will be the most important. Considering the substantial cost savings associated with large-scale production, it may be feasible to offer *private electric cars* fitted with standardised provisions for inductive charging at a limited extra cost. This would give the private electric vehicle owner access to public inductive charging stations for cable-free opportunity charging and overnight charging, to be performed at on-street or off-street car parks. To allow home charging, it still seems advisable to provide the possibility for conductive charging however, except when small portable units can be provided [3].

c) Electricity production and distribution

According to a study by CITELEC [105], the extra demand of electric energy can be covered without problems by the existing base power stations, when a penetration of 30 % of electric vehicles in Europe is assumed. Battery charging largely takes place overnight and there still is an important excess generating capacity during off-peak hours. The extra consumption could be covered without major additions to the electricity production park. According to reference [106] an introduction of 10 % electric vehicles in the Netherlands would require an additional power of 700 MW to be installed if these vehicles would be charged during the day. If these vehicles are charged at night the cost to produce the electricity would decrease and no additional installed power would probably be needed. Ten million electric vehicles in Germany would represent less than 5 % of the electricity generated in Germany [5]. One million electric vehicles in France require less than 1 % of their electricity production [107].

The electric energy needed to recharge the electric vehicles can thus be delivered by existing power stations; however, the impact on the local, medium and low-voltage distribution network has to be considered, in particular for heavily populated areas. When assuming slow (five-hour or more) charging, the existing low-voltage distribution network can mostly cope with the 30 % electric vehicles penetration potential [1].

Fast opportunity charging adds to the range and operational flexibility of electric vehicles, but lays a heavy burden on the electricity distribution. Fast charging would occur at moments of the day at which the distribution network is already highly loaded. The marginal cost per kWh is then excessively high. Furthermore, the demanded power could be extremely high. The super-fast charging techniques presented by some manufacturers would require expensive high-current connections. Therefore slow overnight charging is preferred wherever possible.

Another interesting way to explore is the possibility to provide fast charging points fed by independent electricity production units such as fuel cells, windmills, solar plants, etc, associated or not with an accumulation system (stationary battery or redox battery). This way, electric vehicles can add to the peak-shaving strategy of electricity producers. The use of multiple tariffication can be an important incentive for users to make a good choice.

How to assign a type of power plant (renewal (sun, wind, etc), coal, nuclear, etc)) to the consumption of electricity by the vehicle is described in Part II subchapter 6.3

3 HYBRID ELECTRIC VEHICLES

'Hybrid electric vehicles' is the name of a large group of different kinds of vehicles. A hybrid drive system is resulting from the combination of two or more simple systems, which can operate simultaneously [7]. Hybrid electric vehicles combine electric and other drive or generating systems, such as internal combustion engines, gas turbines and fuel cells. Hybrid electric vehicles combine the zero pollution and high efficiency benefits of electric traction with the high fuel energy density benefits of an energy source or thermal engine.

Different concepts of the hybrid drivetrain topology can be examined. Furthermore the relative contribution of each energy source to the traction effort, expressed in the rate of hybridisation, has an important impact on the final drivetrain. In the next paragraphs these different solutions will be described.

3.1 Hybrid Drivetrain Configurations

The number of different topologies for the configuration of hybrid drivetrain is enormous. In reference [108] one can find 23 different solutions. The most important four can be found in Fig. 3.2 to Fig. 3.4. The basic designs are series and parallel hybrid drives.

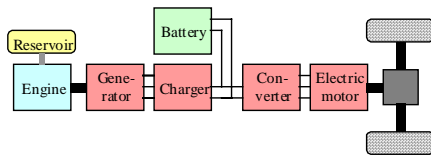


Fig. 3.1: Series hybrid

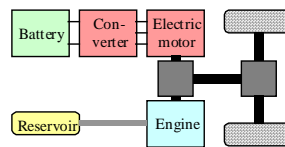


Fig. 3.2: Parallel hybrid

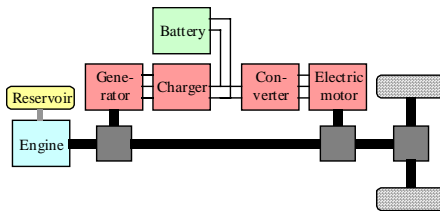


Fig. 3.3: Combined hybrid

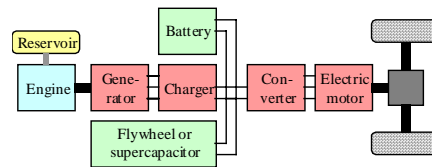


Fig. 3.4: Series hybrid with peak power unit

3.1.1 Parallel Hybrid

The parallel hybrid (Fig. 3.2) is a combination of traction systems [7]. Several electric motors or internal combustion engines, being part of two or more driveshafts perform the traction. Each driveshaft has to be associated with an energy source [7]. The parallel hybrid drive shows a purely mechanical power addition. In a parallel hybrid an internal combustion engine and an electric motor can be coupled directly or via a gearbox. Clutches can disconnect each motor. This way, it is possible to drive only with the electric motor, only with the internal combustion engine, with both motors or with the internal combustion engine driving only the electric machine to charge the battery. Both motors will be coupled on the same shaft, which is driving the wheels [7]. Solutions with completely disconnected motors driving each one axle are called *dual mode hybrids* [53].

Parallel drives can be divided into torque and speed addition designs. In the torque addition configuration the speed values of both motors have always the same relation to each other. The speed addition can only be realised by planetary gears in which the torque values of all the shafts have a constant relation to each other.

To modulate the torque of the engine (2) in a *torque addition parallel hybrid* drive (Fig. 3.5), an electric motor (6) is mechanically coupled to the wheels (3). In function of the load (speed cycle) the electric motor torque can be controlled e.g. in such a way that the engine torque remains constant. In this case the engine speed is still depending on the vehicle speed. A toothed wheel (7) performs this coupling.

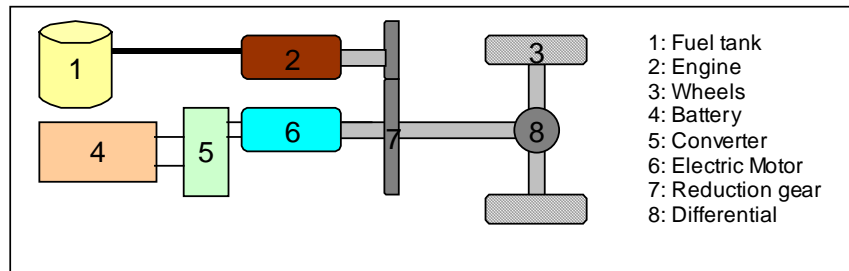


Fig. 3.5: Parallel drivetrain with torque addition

The linear relation between the velocities, as well as the torque addition can be described with the following equations:

$$T_8 = \frac{T_6}{\eta_6} + \frac{x_2 \cdot T_2}{\eta_2} \quad (3.1)$$

$$\omega_8 = \omega_6 = \omega_2 / x_2 \quad (3.2)$$

With :

- T: torque
- η_6 : efficiency of toothed wheel connecting motor with differential
- η_2 : efficiency of toothed wheel connecting engine with differential
- ω : rotational speed
- x: transmission ratio

Instead of adding the delivered torques one can also add the rotational speed of different components by the use of a planetary gear, which is the case in the speed addition parallel hybrid drive. The planetary gear set is often used in an automatic transmission [109]. Such a gear set can supply one or two gear reductions and reverse, depending on the design, by simultaneously engaging or locking various elements of the planetary systems. In hybrid drives the speed of the elements can be controlled with electric motors, instead of locking the elements.

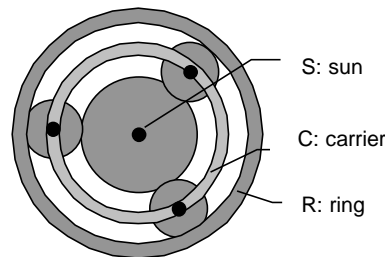


Fig. 3.6: Planetary gear

The next equations demonstrate the possibility to regulate the speed of the carrier (C) by changing the sun (S) speed independently of the ring (R) speed [110]. A detailed description of the functionality of this planetary gear in a combined hybrid drivetrain can be found in Part II.

$$(1 + \rho) \cdot \omega_C = \rho \cdot \omega_S + \omega_R \quad (3.3)$$

$$T_C = \frac{(1 + \rho)}{\eta_S \cdot \rho} \cdot T_S = \frac{(1 + \rho)}{\eta_R} \cdot T_R \quad (3.4)$$

With :

- T: torque
- η_S : efficiency from sun to carrier
- η_R : efficiency from ring to carrier
- ω : rotational speed
- ρ : planetary gear ratio (= nr. of sun gear teeth / nr. of ring gear teeth)

3.1.2 Series Hybrid

The series hybrid is a combination of energy sources [7]. The traction is obtained by only one central electric motor or by wheelhub motors. The on-board total energy source results from the combination of two or more energy sources. In series hybrid drives there are no mechanical connections (Fig. 3.1) between the internal combustion engine (or other energy source) and the wheels. All thermal energy is converted first into mechanical energy in a thermal engine and further in electrical energy by a generator driven by the thermal engine. Hence a decoupling of the operation of the energy source from the required traction power is possible. Mostly the energy source, also called auxiliary power unit (APU), will act as base power unit delivering the average traction power while the battery acts as peak power unit or energy buffer. The series hybrid has the advantage of operating a thermal engine in a chosen optimal operating field, for instance with low specific fuel consumption in the torque-speed operating area.

The series electric hybrid concept can also be chosen for a *two-motor propulsion* (four motor or multi-motor propulsion) in the same way as for pure electric vehicles. In this case, each motor needs a separate convertor with speed and torque control, which guarantees the necessary torque splitting in each condition (electronic differential) [111]. This can give interesting solutions for low floor buses, because there is no need to have an axle under the floor going to the wheels.

In the case there is no battery used one finds the classical *diesel-electric traction* system back, which doesn't allow the recuperation of braking energy and the diesel engine will not operate in a constant working point.

Thermal engines are usually petrol or diesel motors, but the use of turbines and Stirling motors is investigated too. Turbines have the advantage of a high power/volume ratio compared to reciprocating engines [112]. But for this type of use a *gas turbine* is hardly appropriate. The low level of power demand in comparison with other turbine applications makes it at the moment difficult to reach a sufficient energetic efficiency (about 20 %) [51]. As a result of its very high speed and low dynamic behaviour a gas turbine is only usable in a series hybrid system. Passenger cars equipped with gas turbines are today experimental cars.

The *Stirling motor* is often described as the external combustion engine. Similar to the gasoline engine a working medium (gas) is first compressed at low temperature; subsequently it is heated and finally expanded. At the contrary to the internal combustion engine, this gas is heated via a heat exchanger [113]. Different fuels can be used to heat-up this gas. Their engine efficiency should approach 30 %. These engines have a low dynamic behaviour. Due to their complicated design they have a high manufacturing cost.

The *fuel cell hybrid* structure is a series structure in which the engine and the generator are replaced by a fuel cell system producing electric energy starting from

stored hydrogen or from a fuel tank feeding a reformer to produce hydrogen [3]. The excess of electricity produced by the fuel cell can be stored in a buffer battery. When the battery is left out one has no longer a hybrid vehicle but a *fuel cell electric vehicle*. Hence the fuel cell has to have enough dynamics to meet shifts in power demand.

Fig. 3.4 illustrates an example of a *series hybrid with peak power* unit, in which the generator set provides a constant average power, the battery functions as an energy buffer and the flywheel (or super capacitor) caters for the brake and acceleration power peaks. In this configuration the battery dimension can be smaller or it can possibly be omitted. The efficiency and reliability of the flywheel or super capacitor are an important factor for the development of these drivetrains.

3.1.3 Combined Hybrid

All topologies different from the series and parallel hybrid electric vehicle shall be called *complex hybrid vehicles*. Hence complex hybrid vehicles include series hybrid with peak power units, parallel hybrids with flywheel mechanically connected via e.g. a continuous variable transmission (CVT) or combined hybrid vehicles.

A *combined hybrid* is a combination of a series and a parallel hybrid drivetrain. The latter will be described in this subchapter. By adding a mechanical connection in a series hybrid between the internal combustion engine and the electric motor a combination of series and parallel hybrid working mode can be realised (Fig. 3.3 and Fig. 3.7). This solution allows benefiting from the parallel as well as from the series hybrid concepts. In Fig. 3.7 the transmission consists of a single planetary gear set coupled to the engine and a generator. The planetary gear set (7) divides the engine's (2) driving force into two forces: one that is transmitted via the ring gear to drive the wheels (8) and the other that drives the generator (9) through the sun gear. The electrical energy, produced in the generator, is re-converted into mechanical energy through the motor (6) via the convertor (5). Since the motor is also directly connected to the ring gear, this force is transmitted to the wheels. In addition, batteries (4) provide supplementary driving force to the motor as needed. The batteries also recover and reuse the braking energy transformed into electrical energy by the motor (6) [110].

This drivetrain topology allows controlling the engine speed and torque and this way minimizing the fuel consumption of the engine. For any given steady-state vehicle speed, the speed of the engine can be adjusted simply by varying the speed of the generator (9), as shown in equation (3.3) [114]. The generator is also used to start the engine.

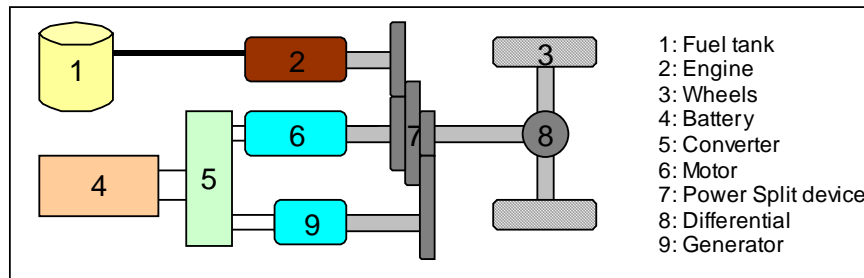


Fig. 3.7: Combined hybrid drivetrain

3.1.4 Some Examples

To give the reader an impression on the dynamics in the development of the car manufacturers some examples are highlighted in this paragraph. One can notice different approaches. Series, parallel, combined as well as fuel cell vehicles are under development.

- The Audi Duo was first developed as a dual mode hybrid concept where front wheels were driven by the engine and rear wheels by a small electric motor. The 1996 version is based on the A4 Avant. The front axle is powered by a four-cylinder 1,9l TDI engine with automated clutch system. The front-axle can also be powered by a 21,6 kW permanent magnet three-phase synchronous motor. The change of operating mode is automatic [115]. The electric motor has to be integrated into the gear tunnel, the inverter is integrated below the rear seat and the batteries are located below the luggage compartment [116]. The latter are 22 maintenance free lead-acid batteries with a maximum voltage of 264 V [118]
- The hybrid Golf VW includes a 44 kW diesel engine with catalyst and a 7 kW AC motor, placed in the clutch housing with two clutches. The AC motor integrates the function of engine flywheel, generator and starter. The clutches are operated by a microprocessor to switch from electric drive mode to combustion drive mode depending on the driving condition [108].
- The Toyota Prius is a combined hybrid vehicle that comprises three key elements: a highly efficient 1,5 litre engine that enables 5 L/100 km in city driving conditions, a nickel metal hydride batteries and a planetary gear as mechanical splitter device [118]. An 30 kW permanent magnet motor and 15 kW permanent magnet generator control the power flow in the drive train.
- The Honda Insight is a two-seat hybrid vehicle, weighting less than one ton. Honda's new integrated motor assist system combines a one-litre, three-cylinder gasoline engine with an electric motor powered by nickel metal hydride batteries. It consumes 3,9 L/100km in city driving conditions and 3,4 L/100km

on the highway. The Insight meets California's strict ultra-low emission vehicle standard [117].

- The Renault VERT is essentially a series hybrid composed of a diesel-turbine and two 45 kW asynchronous motors [118].
- Renault also has developed the electric Kangoo with range extender. This consists of a small, direct-injection engine (500 cc), which increases the electric model's range significantly to between 200 and 300 kilometres.
- Mercedes-Benz C Class series hybrid vehicle has a combustion engine of 65 kW, a generator of 60 kW and two electric motors of 35 kW each. The acceleration is around 16 seconds from 1-100 km/h and the maximum speed is 170 km/h. This vehicle is equipped with 34 kW NiMH battery [119].
- The natural gas/electric series hybrid Altrobus, has a 105 kW asynchronous motor driving the wheels and connected to a 100 Ah / 600 V lead acid battery pack. The vehicle's permanent magnet generator group delivers 30 kW and is powered by a 2,5 litre natural gas engine running at constant speed. It gives a better efficiency than a conventional configuration. The whole bus's HC+NOx and CO emissions are even within the California's ULEV and EURO II passenger car limits [120].
- NEBUS is the fuel cell version of Daimler-Benz's O-405 N model, a 12-meter, low-floor city bus with 34 seats plus standing room for 24 persons. The Ballard-designed PEM fuel cell consists of ten 25 kW stacks of 150 individual cells each, providing a total output of about 250 kW [98]. The hydrogen is stored in bottles.
- The FEVER (Fuel Cell Electric Vehicle for Efficiency and Range") is powered by a PEM fuel system and runs on stored liquid hydrogen. It has a nickel-metal hydride 2,8 kWh battery for energy buffer storage. The expected range is 500 km, with a top speed of 120km/h [98].

Next to the two fuel cell vehicles illustrated above, also other car manufacturers are investing in fuel cell technology and are building fuel cell vehicles. Some examples: Daimler-Chrysler Commander (methanol); Merced-Benz A class (methanol); Opel Zaffira (50 kW PEM); Ford P2000 Prodigy (pure hydrogen); PSA (PEM); Renault Laguna Estate; BMW 7 series Sedans (hydrogen combustion engine with a small fuel cell for the auxiliaries); Volkswagen/Volvo Golf (methanol PEM fuel cell); Zevco London Taxi (Alkaline Fuel Cell); Toyota RAV4 (Methanol and Hydrogen PEM); Mazda Demio (hydrogen). Up to now the PEM fuel cell with a methanol reformer seems to gain the most interest by the car manufacturers.

3.2 Definitions Used to Characterise Hybrid Systems

To better understand the hybrid concepts some definitions are given.

a) Order of hybridisation

The order of a hybrid system is the number of different systems necessary to build the drivetrain [7].

In the case of an electric or thermal vehicle there is only one motor or engine driving the vehicle. These drivetrains are from the first order. Also fuel cell vehicles without a battery are first order systems.

A parallel hybrid built up with one engine and one motor is a second order hybridisation as well as a series hybrid electric vehicle containing a battery and another energy source.

When a peak power unit, like a flywheel or super-capacitor, is added next to the APU and battery, the vehicle is from the third order. All complex hybrid drivetrains are third or higher order systems.

A combined hybrid drivetrain like Fig. 3.3 can also be seen as a third order hybridisation. Although there are only two energy sources, there are three shafts: one connected to the engine, one to the generator and one to the electric motor. All three are mechanically connected to the wheels.

b) Electric Hybridisation Rate (EHR)

The Electric Hybridisation Rate (EHR) gives an indication of the performance, and above all, the range in protected areas. This means the 'more battery', the longer one can drive without generator or engine, the higher the electric hybridisation rate. It is the ratio between the electric power and the total traction power (equation (3.5)), and it is expressed as a percentage [3]. The higher this rate, the more the vehicle tends to a pure electric vehicle.

In the case of a series hybrid electric vehicle the traction power corresponds with the nominal electric motor power, since this motor is in charge of all traction effort. The electric power is the maximum battery power. This maximum power is difficult to be defined (see subchapter 2.4). The difference between nominal motor power and nominal generator power can also be used. Consequently the EHR for a series hybrid is given by equation (3.6).

For a parallel hybrid electric vehicle, the EHR is equal to the ratio of the electric motor power to the overall power (equation (3.7)). This overall power is the sum of the engine power and motor power, since both are in charge of the traction exertion.

Be aware that it is difficult to compare the power of an electric motor to the power of an internal combustion engine. The power of an engine corresponds to its maximum deliverable power. At the contrary the power of an electric motor mostly expresses its continuous or one-hour rated power. Its maximum power can be more than double the continuous power.

$$EHR = \frac{\text{electric power}}{\text{traction power}} \quad (3.5)$$

Electric Hybridisation Rate

$$EHR = \frac{P_{bat}}{P_{mot}} = \frac{P_{mot} - P_{gen}}{P_{bat} + P_{gen}} \quad (3.6)$$

E.g. series HEV

$$EHR = \frac{P_{mot}}{P_{ICE} + P_{mot}} \quad (3.7)$$

E.g. parallel HEV

A 12 m series hybrid bus, with a 2,5 L engine of 40 kW is taken as example. This power is sufficient to drive a 30 kW generator feeding a 125 kW electric motor. The battery delivers the acceleration power [3]. The Electric Hybridisation Rate is in this case 76 %. The importance of the electric contribution is relatively high.

A second example is a parallel hybrid passenger car with a 15 kW electric motor mechanically connected to a small 30 kW engine. It has an EHR of 33 %. In this case the EHR is relatively low and hence the electric contribution is modest.

c) Combustion Hybridisation Rate (CHR)

To have an idea of the relative contribution of the internal combustion engine a complementary definition to the Electric Hybridisation Rate can be introduced: Combustion Hybridisation Rate (CHR). It is the ratio between the thermal power and the total traction power (equation (3.8)), expressed as a percentage. The higher the rate, the more the vehicle tends to a pure thermal vehicle.

In the case of a series hybrid electric vehicle, the thermal power is defined equal to the rated generator power and hence the CHR is defined by equation (3.9).

For a parallel hybrid electric vehicle, the CHR is equal to the ratio of the engine motor power to the overall power [7] (see equation (3.10)).

$$CHR = \frac{\text{thermal power}}{\text{traction power}} \quad (3.8)$$

Combustion Hybridisation Rate

$$CHR = \frac{P_{gen}}{P_{mot}} = \frac{P_{mot} - P_{bat}}{P_{bat} + P_{gen}} \quad (3.9)$$

E.g. series HEV

$$CHR = \frac{P_{ICE}}{P_{ICE} + P_{mot}} \quad (3.10)$$

E.g. parallel HEV

For the example of the 12 m series hybrid bus, the Combustion Hybridisation Rate is 24 %. For the parallel hybrid passenger car it is 67 %, which means a high contribution of the combustion engine.

Notice that the sum of the CHR and EHR is always equal one.

d) Rate of Hybridisation (RoH)

Neither the Electric Hybridisation Rate nor the Combustion Hybridisation Rate express the degree of hybridisation itself, but how much a vehicle leans against the electric vehicle side or respectively to the thermal vehicle side. The Rate of Hybridisation (RoH) describes the relative contribution of each energy source (in the case of series hybrid electric vehicles) or traction system (in the case of parallel hybrids). If both systems have an equal contribution to the traction effort, the Rate of Hybridisation is defined equal to one (the maximum). If the contribution of the thermal system is higher then the electric system, the rate of hybridisation (RoH_{th}) equals the ratio of the electric power to the thermal power and vice-versa (RoH_{el}) (equation (3.11)). Hence first order systems always have a rate of hybridisation that equals zero.

In the case of the series hybrid vehicle the RoH is consequently defined by (3.12) and in the case of the parallel hybrid vehicle equation (3.13) gives the RoH.

$$\begin{aligned} \text{If } P_{el} < P_{th} & \quad RoH_{th} = \frac{P_{el}}{P_{th}} \\ \text{If } P_{th} < P_{el} & \quad RoH_{el} = \frac{P_{th}}{P_{el}} \end{aligned} \quad (3.11)$$

Rate of Hybridisation

$$RoH_{th} = \frac{P_{mot} - P_{gen}}{P_{gen}}$$

$$RoH_{el} = \frac{P_{gen}}{P_{mot} - P_{gen}}$$

(3.12)

E.g. series HEV

$$RoH_{th} = \frac{P_{mot}}{P_{ICE}}$$

$$RoH_{el} = \frac{P_{ICE}}{P_{mot}}$$

(3.13)

E.g. parallel HEV

One gets for the given example of the series hybrid electric bus 32 % and for the parallel hybrid electric car 50 %.

These definitions are valid for second order hybrid electric vehicles only. When the hybrid electric vehicle become more complex the definition of the Rate of Hybridisation is not straightforward anymore and cannot be used.

3.3 Classification

Armed with these definitions, a table, representing a panorama of second order hybrids can be constructed. This user-friendly diagramme will point out the different possibilities of hybridisation in terms of power by varying progressively the electric and combustion hybridisation rate. The diagramme is based on reference [7].

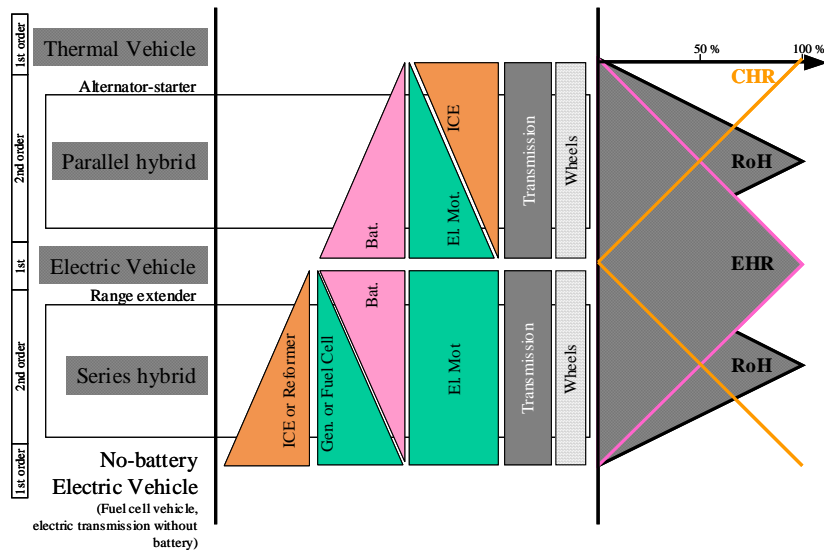


Fig. 3.8: Different hybrid electric vehicles classification

When the size of the alternator of a thermal vehicles is increased in such a way that it can be used as starter motor too, one gets a kind of hybrid electric vehicle where the engine can be switched off at e.g. traffic lights. Increasing this motor dimension even more leads to a full parallel hybrid electric vehicle, where the engine as well as the electric motor can drive the vehicle.

Excluding the engine results in a pure electric vehicle.

Starting from the thermal vehicle and going down in Fig. 3.8 to the electric vehicle the combustion hybridisation rate (CHR) decreases and the electric hybridisation rate increases (EHR).

Some electric vehicles are equipped with a small auxiliary power unit (a small engine connected to a generator) to extend the driving range of the vehicle (in the middle of Fig. 3.8). The range is still mainly depending on the battery capacity.

The dimension of the generator can be enlarged until the range is primarily function of the fuel content, i.e. the battery never gets discharged. The CHR rises and the EHR reduces (from the middle of Fig. 3.8 downwards).

When the APU is large enough to deliver the whole traction power the battery can even be left out, which corresponds with the 'classical' diesel-electric solution. This can result in a poor efficiency of the entire drivetrain. When the engine-generator group is replaced by an efficient fuel cell however, this can lead to a promising environmentally friendly vehicle.

The gross evaluation and classification does not stop there, as more complexity will appear in the evaluation as one passes from simple to more complex hybrids. There exists no single optimal solution. The selection must be based on the required application (a bus is not a cab), the performance and the comfort, the controllability and state of the art, the environment and the cost. Once the selection of the drivetrain topology (physical lay-out) is done the work has just to begin: how to tune the ICE, how to control battery state of charge, when is zero emission drive required, etc ?

3.4 Powerflow Control Algorithms

A HEV is not simply an assembly of hardware components hooked up electrically and mechanically, with nothing telling them what to do or when to do it. A control strategy brings the components together as a system and provides the intelligence that makes the components work together. The flexibility in design of hybrid vehicles comes from the ability of the powerflow strategy to control how much power is flowing to or from each component. This way, the components can be integrated with a control strategy to achieve the optimal design for a given set of

design constraints. There are many, often conflicting, objectives desirable for hybrid electric vehicles.

The primary being [121]:

- Maximised fuel economy;
- Minimised emissions;
- Minimised propulsion system cost;
- Acceptable performance (acceleration, noise, range, handling, etc.).

A hybrid drivetrain is a complex system in which APU power set-point, battery charging/discharging profile, DC-bus voltage, etc, will influence the consumption and emissions of the vehicle. The combination of the effect of all these parameters can best be evaluated with the help of a powerful simulation tool. To minimise the consumption and emissions it is not only important to select an appropriate drivetrain topology, but next to the individual component efficiency, the development of the powerflow control algorithm is mainly decisive to optimise the global drivetrain energy efficiency. This furthermore closely relates to the vehicle application (type of drive cycle).

The following sections will describe different possible control strategies implementable in hybrid electric drivetrains. A non-exhaustive list is established of possibilities applicable on series, parallel and combined hybrid vehicles. Part II describes the implementation in the software programme of these control algorithms. Finally to understand them better simulation results can be found in Part III.

3.4.1 Series Hybrid Electric Vehicle Control Algorithms

Table 3.1 summarises different possible APU powerflow control algorithms applicable in series hybrid electric vehicles. At one end the energy source (APU) will be forced to track the car load demand (continuously variable*) at the other end the batteries will take care of all traction dynamics and the APU will operate only at one working point corresponding to the average required power (Constant**).

The “Goal” describes the moment in a drive cycle when operating the APU. It is closely related to the rate of hybridisation.

Once the APU is working it can deliver a constant power or its output power can fluctuate. This is described by the “Delivered power”.

The APU power can be delivered on different manners, this means that different speed-torque working points can provide the same output power; this is summarised under “Set point”.

Finally some parameters are discussed which influence the drivetrain “Strategy”.

Table 3.1: Overview of different APU powerflow control algorithms

Goal - range extender - continuous mode - intermittent mode	Delivered power - none - constant** - discrete - continuously variable *
Set point - optimal operating point - optimal operating line - deviation allowed between limits - maximum deviation speed - constant speed, variable torque	Strategy - APU power as a function of: - battery voltage - location : city or country - State of Charge (SoC) - vehicle speed - SoC deviation in time - SoC and vehicle speed combination - minimum ON time - relative distribution - required traction power - history

a) Goal

- *Range extender.* With a small rate of hybridisation the APU is used to extend the range of the electric vehicle. However the autonomy is still depending on the capacity of the battery. The battery will discharge less quickly than without a range extender; nevertheless the APU power is not sufficient to maintain the battery state of charge. This type is also called a ‘battery depleting hybrid’ [122] where the state of charge of the traction battery at the end of a service day or driving cycle is lower than at the beginning. The batteries thus have to be recharged from an external source (electricity grid). The normal battery charger of around 3 kW is mostly used as convertor for the APU power as well.
- *Continuous mode.* With this implementation the APU will have a bigger rated power compared to the APU of the range extender. It is the purpose to operate the APU continuously. The state of charge of the traction battery at the end of the service day or trip is mostly equal to that at the beginning. (The state of charge of the battery at any given time will of course be variable.) This drivetrain is mostly of the ‘non-depleting’ or ‘charge-sustaining’ hybrid type. The solution allows a smaller energy content of the battery due to the fact that this battery is only in charge of the peak power requirements.
- *Intermittent mode.* In this category the vehicle is able to drive pure electric in certain parts of the drive cycle, e.g. in urban city centres. The APU must be powerful designed to be able to charge the battery in the episode in which it is operating. The battery must be sufficiently large to secure the pure electric driving phase. Several APU-operating strategies for this working mode can be taken under consideration.

b) Delivered power

- *Constant.* When the APU is in use it will deliver a constant power corresponding to a certain setpoint (see further).
- *Discrete* (manual or automatic). In this case the APU power can only be set on beforehand defined values. The selection can be carried out by either the driver (who can have an idea of the type of driving trip he will perform) or automatically by a microprocessor. This working mode allows selecting the APU power in function of the demanded battery power without having much dynamic fluctuations of the engine.
- *Continue variable.* This option allows changing the APU power continuously. E.g. the generator-engine group can charge the battery at its maximum charging power and at the same time deliver the required traction power. The dynamic operation of the engine however is a serious drawback of this solution (higher emission and fuel consumption).

c) Set point

The necessity to choose a setpoint is a typical action needed for an engine-generator group.

- *Optimal operating point.* One can choose to operate the engine in an optimal working point. The torque and rotational velocity corresponding to the lowest fuel consumption (in g/kWh) can be chosen to define this point. It can also correspond to the lowest NO_x-emission or SO₂-emission. The optimal emission point can be different from the optimal consumption operating point. This optimal operating point can also be a compromise between fuel consumption and emissions.
- *Optimal operating line.* When a generator has to deliver different power levels, the engine rotational velocity can be chosen for each power level corresponding to the lowest emissions or fuel consumption or a combination of both.
- *Deviation allowed between limits.* One can choose to operate the engine only in a certain velocity span. Most engines have an operating area (in torque and velocity plane) in which the fuel efficiency remains rather good.
- *Maximum deviation speed.* When the engine's working point has to change, the deviation in function of time can be restricted, to avoid fast engine fluctuations and hence to minimise engine dynamics.
- *Constant speed, variable torque.* Another approach consists in keeping the engine speed constant (no additional inertia torque) and allowing to change its output torque in function of the required generator power.

d) Strategy

The APU power can be selected in function of different parameters and requirements, like:

- *Battery voltage.* Independently of what strategy is used the battery voltage should be kept within its safety operating limits. Otherwise the battery can be damaged (inversion of polarisation, abundant gassing, etc).
- *Location* (city or country). One of the main advantages of hybrid electric vehicles is the ability to drive pure electric in certain (historical) city centres. This can be manually selected or automatically. With the help of the rising telematics technology radio beacons can be installed at the entrances of protected areas. These can disengage the APU, with the due safety and warning, while driving into such a neighbourhood.
- *Vehicle speed.* Internal combustion engines produce an important amount of noise. This can be agitating when an internal combustion engine is delivering full power while the vehicle itself is standing still. One can organise the decrease of the APU power or even the complete cutting off of the engine when the vehicle's velocity decreases beneath a certain value.
- *State of Charge (SoC).* The state of charge of the battery can be an important parameter to regulate the generator. The state of charge may not be too low to have enough battery power left for acceleration. To allow maximum regeneration of braking energy the battery should not be completely charged. When the SoC reaches a maximum level the APU should be switched off or operated in idle mode. The APU should be switched on when exceeding a low SoC limit. Additionally when a critical SoC low limit is reached the APU power can be increased to its maximum level to charge the battery as fast as possible.
- *State of Charge deviation* [112]. In the same philosophy of previous paragraph the engine power setpoint can be chosen in function of a desired SoC deviation. Two deviation levels can be chosen. A recommended level (Fig. 3.9) that describes how fast the SoC may decrease. This value is closely related to the maximum range of the hybrid electric vehicle. If this is chosen equal zero, the range is defined by the content of the fuel tank. Otherwise the SoC will decrease until the battery is empty (battery depleting type). A second maximum deviation level can be chosen. If the SoC deviation is higher than this maximum limit (Fig. 3.9) the APU power level should be as high as possible. If the SoC deviation is between the recommended and the maximum limit the engine power can be selected according its lowest consumption. Furthermore if the SoC deviation is slower than the recommended level than the engine can be switched off or set to idle mode.

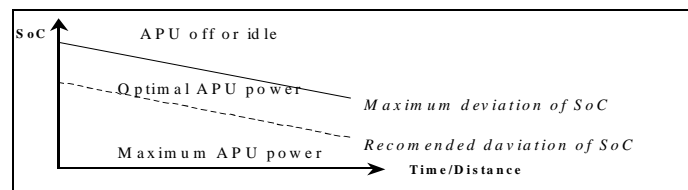


Fig. 3.9: State of charge deviation criterion

- *State of charge and vehicle velocity combination.* The APU should be switched on when the vehicle speed exceeds a certain limit. This vehicle speed

corresponds with a certain required power and hence energy consumption. This speed level can be adjustable in function of the state of charge described with the equation (3.14).

$$v = v_s \left(1 - \alpha \frac{SoC_{high} - SoC}{SoC_{high} - SoC_{low}} \right) \quad (3.14)$$

- *Minimum ON time.* Frequent switching on and off the engine will result in additional consumption and emissions. To avoid this, a minimum APU on-time can be imposed.
- *Relative distribution.* The previous strategies describe whenever the APU should be switched ON or OFF. One can also chose to relatively split-up the required traction power between the APU and the battery. E.g. the first delivers 70 % of the power and the latter 30 %. The APU can only provide power and hence all braking power can only be recuperated by the battery.
- *Required traction power.* The maximum allowed charging power of a battery is in most cases much lower than the maximum discharge power. If the APU is only allowed to deliver a constant power, this power will be used for driving and battery charging together. In this case the maximum value of the APU power must be limited to the maximum battery charging power (at standstill all APU power goes to the battery). Another solution is modulating the APU power in function of the required traction power. Hence the battery can be charged at its maximum charging power level. The battery does not act as peak power unit anymore; the APU will deliver them. Power requirements are an important design parameter for the battery of a hybrid electric vehicle opposite to energy requirements.
- *History.* Previous discussion clearly shows that the pros and contras of a certain strategy should be evaluated. Operating the engine in its working point corresponding to its lowest fuel consumption can be at first site very promising. This can be conflicting with battery charging constraints (charging/discharging losses). On the contrary, allowing a fluctuation of APU power will lead to additional inertia torques and fuel consumption. However one can choose to allow a slow changing of the APU operating point in function of the delivered energy. While driving at constant speed a lower APU power should be required. When driving a very demanding drive cycle the APU power should increase slowly. A microprocessor can integrate the required traction power and modulate the APU power in function of this parameter or similar one can establish a linear relation between APU power and SoC.

3.4.2 Parallel Hybrid Electric Vehicle Control Algorithms

The parallel hybrid electric vehicle can operate in several modes: electric only, engine only and dual power source or hybrid mode [123]. The electric motor can also operate as a generator during braking. Compared to a conventional vehicle the parallel electric drivetrain has the main advantage that it is able to regenerate the

braking energy. This implies that during braking all braking torque will be delivered by the electric motor and the engine needs to be disengaged.

Moreover the parallel solution allows using the electric motor as starter motor. Even the alternator can be omitted and a DC/DC convertor can be used to charge the auxiliary battery via the main traction battery.

The same approach of the powerflow strategy for the series hybrid drivetrain as described above (3.4.1) in 'Goal, 'Delivered power' and 'Strategy' is applicable for the parallel hybrid drivetrain too. Only the 'Set point' is different due to the fact that the engine is mechanically connected to the wheels. There is one degree of freedom less compared to the series hybrid vehicle. Indeed in most parallel hybrid vehicles the engine is mechanically connected to the wheels via a toothed wheel, resulting in an engine speed proportional to the vehicle velocity. The number of power control algorithms in parallel hybrid vehicles is thus much smaller than one can find for the series hybrid vehicle, where engine speed and torque can be controlled independently from the traction effort.

Equation (3.1) on page 48 shows the possibility to control the engine torque via the electric motor, independent from the required traction torque. Several approaches are possible. Five of them are explained below:

- a. *Relative distribution.* The required driving torque is proportionally split up; e.g. the engine could deliver 70 % of the traction torque and the electric motor 30 %. This relative contribution of each motor can be kept constant during the whole drive cycle. This approach in itself has little benefits.
- b. *Constant torque.* One could consider keeping the torque value of the engine constant. This torque value can be chosen in function of the engine's highest efficiency and/or lowest emissions. The electric motor must deliver the remaining part of the required torque. Hence the motor is in charge of the vehicle dynamics. It will deliver the acceleration torque (see '4.5 Calculation Methodology'). The engine will deliver a constant base torque. Furthermore the engine can be declutched when its velocity drops under a certain limits or exceeds a maximum value. In this way the engine working point can be kept within an operating range corresponding with low fuel consumption. When declutching the engine one has the possibility to completely switch off the engine or to operate it at idle speed.
- c. *Minimum Efficiency loss.* This third approach is a more intelligent one. Hence it is possible to operate the engine on its optimal working line corresponding with low fuel consumption. The transmission ratio and the input velocity define indeed the engine velocity. One can define a power division to minimise the efficiency loss for the entire vehicle. This covers the total efficiency loss for all of the individual vehicle components. The most dominant loss will be the engine loss. The total efficiency loss can depend on the respective driving

condition [124]. Calculating for each time step of a reference speed cycle the best operating point, with the lowest drivetrain losses, will not necessarily result in the lowest total fuel consumption, because battery charging and discharging are not taken into account. This charging-discharging profile is time and speed cycle dependent. Time integration can partially solve this problem, but provides only a solution for the considered reference speed cycle.

- d. *In function of $SoC(P_{APU}(SoC))$.* This criterion takes the state of charge into account. Hence the influence of the driving cycle is considered in an indirect way. When the speed cycle is a very demanding one, which means that the battery SoC is decreasing very fast, the engine power level should be enlarged to compensate this energy consumption. At the contrary, when driving a very moderate cycle, e.g. cruising at 50km/h, the engine will provide the traction power and probably it will charge the battery at the same time. At this moment the engine power level can be decreased.
- e. *In function of SoC bis ($Switch_{APU}(SoC)$).* The use of the state of charge as control parameter can be slightly different than in the case of the series hybrid vehicle. When the battery SoC is low, the engine can provide the driving torque and an additional torque to recharge the battery via the electric motor. When the SoC is high the electric motor only launches the vehicle [125].

Combining some of these considerations can result in an example where the control strategy uses the electric motor for additional power when needed. This can be done in a variety of ways [126]:

- a. The electric motor can be used for all driving torque below a certain minimum vehicle speed.
- b. The electric motor is used for torque assist if the required torque is greater than the maximum producible by the engine at the engine's operating speed.
- c. The electric motor charges the batteries by regenerative braking.
- d. When the engine is running inefficiently at the required engine torque at a given speed, the engine is shut off and the electric motor will produce the required torque.
- e. When the battery SOC is low, the engine will provide excess torque, which will be used by the electric motor to charge the battery.

3.4.3 Combined Hybrid Electric Vehicle Control Algorithms

By introducing a planetary gear connected to a generator in the parallel hybrid configuration one gets a combined drivetrain with one degree of freedom more. This drivetrain has consequently a lot of possibilities to control the powerflow and to minimise this way the energy consumption. The drivetrain has a planetary gear and a torque splitter (toothed wheel), which allow us to control the speed as well as the torque of the engine.

- a. *Constant working point.* One could consider keeping the torque value of the engine constant, like it is described in the previous paragraph. Furthermore due to the planetary gear the engine velocity can be modulated with the help of the generator (see equation (3.3) in subchapter '3.1 Hybrid Drivetrain Configurations'). Consequently both torque and speed of the engine can be freely chosen independently from the driving requirements. The engine working point can be selected corresponding to its lowest consumption. Hence the drivetrain is controlled like it is generally done in a series hybrid vehicle: the engine delivers the average driving power; the acceleration peaks are covered by the electric motor; the battery is used as the energy buffer. Different to the series configuration is the fact that the engine power is mechanically coupled to the wheels. If this average power is higher than the required value, the remaining part is transmitted through the generator and possibly through the motor to recharge the battery.

Although the engine operates in its most efficient working point, this control strategy does not automatically imply a low energy consumption of the total drivetrain. Indeed, a constant engine power results in frequent charging and discharging the battery, with high power levels. Moreover, in the drivetrain the power from the engine can flow via the planetary gear, through the generator and back through the motor to finally reach the differential, instead of going directly to the differential (see Fig. 3.7). This strategy can also imply the necessity of a larger generator nominal power and battery capacity.

- b. *Overall lowest power loss minimalisation.* Another approach considers operating the engine on its optimal working line, which describes the relation between engine torque and speed corresponding with the lowest fuel consumption. The speed of the engine can be adjusted in correlation with the required torque, by varying the generator speed (see (3.3)). The torque can be controlled corresponding equation (3.1). The power distribution can be defined in function of the overall lowest power losses. This covers the total efficiency loss for all vehicle components. The total efficiency loss depends on the respective driving condition [124]. To define this power distribution a simulation programme is required. With the help of this simulation programme one has to find, for each required wheel torque and speed value of the considered reference cycle, the best power distribution according to the lowest total efficiency loss (power to battery and wheels compared to engine power).

An example is illustrated by Fig. 3.10. The power distribution is here described as a Power Distribution factor (PDF) used in the simulation model of the Torque Splitter (see Part II). One can recognize at low torque levels a very high PDF to impose a high enough torque at engine side. At this moment a part of the engine power is used to drive the vehicle and another part to charge the battery. For medium torque levels this PDF equals one. This means that the engine directly delivers all the traction power. At higher torque levels the engine as well as the electric motor is contributing in the power demand.

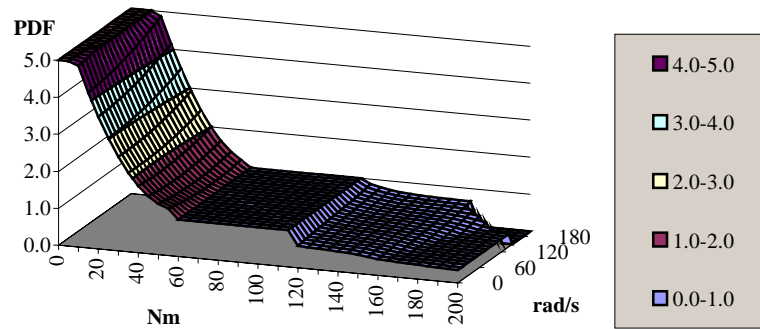


Fig. 3.10: Power Distribution Factor of an optimized combined hybrid drivetrain power control algorithm

For the operating points which require a low power level (e.g. at low constant speed), the engine efficiency will be in any case unfavourable. This can be solved by

- Operating the engine only above a certain engine power level.
- Locking the generator at low required power (all engine power flows directly to the differential).

During braking no torque should go to the planetary gear, but all braking energy should be regenerated directly via the motor to the battery.

Calculating for each time step of a reference speed cycle the best operating point, with the lowest drivetrain losses, will not necessarily result in the lowest total fuel consumption, because battery charging and discharging is still not taken into account. This charging-discharging profile is time and speed cycle dependent.

- c. *Maintaining battery SoC.* If the battery size is chosen rather small, to minimise vehicle weight, previous strategies cannot be implemented completely. Indeed, the battery SoC can decrease very fast in function of the drive cycle. To maintain the battery SoC level, it can be required to impose a power demand for battery charging. In this strategy the battery will provide energy when high vehicle acceleration is necessary or when a very low driving power is required. In the first case engine and motor will drive the wheels together. In the second case the engine is switched off and the electric motor is in charge of the driving force. When a moderate driving power is required, the engine will drive the wheels and will also charge the battery via the generator with a charging power in function of the SoC. This control strategy is implemented in the Toyota Prius [127].

3.4.4 Some Examples

Some example showing combinations of some of the above-described criteria are illustrated hereafter:

The *diesel-electric vehicle* has no battery and hence is not able to regenerate braking energy and regulate engines operating point. It is a kind of series hybrid where the APU is working continuously. Neither optimal setpoint, nor powerflow strategy can be implemented. It allows using wheel motors in low-floor buses where engine and wheels are not mechanically connected. However the fact there is no battery for energy buffering imposes the engine to follow the required traction power, thus with the same dynamics as in a conventional vehicle, with that difference that the mechanical decoupling of the internal combustion engine from the wheels yields higher losses due to the multiple energy conversion. Hence the overall efficiency can even be worth than that of a conventional vehicle.

The *electric-assist parallel* uses the engine as the primary propulsion component, which is mechanically connected to the wheels. The electric motor and batteries provide the peaking power (in the form of additional torque to the wheels) to increase the total power available while decreasing the power required from the engine. This keeps the engine in a more efficient region of operation and helps reducing emissions from “full throttle” conditions. The electric motor and batteries are also available to capture regenerative braking energy from decelerations, an added efficiency boost during urban-type driving. This control strategy is sometimes called a “power-assist”.

The *APU-assist parallel* uses the electric motor and batteries as the primary propulsion components while the APU is only turned on for higher speeds, hill climbing, or hard accelerations. The advantage of this control strategy is that most of the energy used is electrical energy, which would tend to reduce overall emissions and the amount of fuel used. It also allows the electric engine starter to be eliminated because the vehicle is moving when the APU is turned on. The APU should be designed for an optimal operating at high power load.

The objective of a *thermostat series* [121,128] vehicle is to operate entirely on electrical energy, with the batteries being discharged until a low state of charge (SOC) is reached. The APU is then turned on to recharge the batteries until a “full” SOC is reached and the APU is turned off. This continues indefinitely if the APU is adequately sized, in which case it would be a charge sustaining thermostat series hybrid. The word thermostat is used because the SOC of the batteries is allowed to fluctuate between a high and low set-point in the same way that a building’s temperature is allowed to fluctuate between the set-points regulated by the thermostat. Advantages of this type of hybrid are that the APU can be set to operate at one point of torque and speed at which it is most efficient and least polluting. This prevents the APU from experiencing any transient loads, which also should reduce the emissions. Another potential reduction of emissions can come from the

addition of an electrically heated catalyst, which can easily be implemented to reduce cold-start emissions since there is ample knowledge of when the APU will come on.

Load-leveller series: The goal of a *load-leveller series* hybrid is to match the average power requirement of the vehicle with the electrical power that is produced from the APU. The batteries provide the power peaks, while during the low power periods, the batteries are recharged such that the state of charge of the batteries hovers around a mid-level SOC. The advantage of this type of hybrid is that the battery pack energy can be relatively small and has instead a high power capability. In general, this allows the weight of the propulsion system to be lower. It does, however, force the APU to change its power output as the load changes. Changing its throttle slowly can minimise the transients that the engine sees, but the engine still has to operate at multiple points in its efficiency and emissions maps.

3.5 The Need for Simulation Tools

Due to their more complex structure, hybrid solutions will be more expensive than the conventional solution; so their lower fuel consumption alone may not be enough to make the increased investment worthwhile. This additional cost depends on the complexity of the solution and the component design. Lower fuel consumption is not the main and only benefit: the reduction of CO₂ emissions may range from 30-50 %.

It is clear that a considerable development effort is necessary to determine the most appropriate solutions. The analysis of road vehicle use in Europe shows that hybrid electric vehicles must fulfil different missions, and must satisfy acceleration, maximum speed, high range, gross weight and payload criteria [1]. The energy management systems of all hybrid structures will play a fundamental role because of their influence on the global energy efficiency and the emissions [3].

To minimising both common testing, time and development cost, a software tool can facilitate engineers in evaluating current vehicle technologies and can support them in the selection and matching of energy storage devices, hybrid powertrain layouts and vehicle energy management.

4 THE SIMULATION PROGRAMME

4.1 Other Programmes

Before ‘inventing the wheel a second time’, it is always interesting to evaluate what other researcher have already done. In this chapter other simulation programmes will be briefly described.

The last ten years simulation programmes dedicated for the evaluation of vehicles has known an important progress. Most simulation tools were originally designed to evaluate specific drivetrains and each model has been implemented for its own particular scenario. They were mostly written in text-based languages, with data structures that were difficult to access. Admission to many of these programmes is limited by commercial considerations. Multimedia technology allows now relatively rapid development of highly graphical and interactive user interfaces.

In the following paragraphs examples of some important and recently developed programmes are described. These descriptions are based on the corresponding publications, but most of them could not be verified. All the programmes use the same fundamental principle, based on longitudinal upstream-looking quasi steady state time stepping algorithm. This algorithm has already proven its validity and will be described further on.

While reading the literature of the above-described simulation programmes the same remark systematically came back: ‘due to lack of information’, ‘data is hard to find’, ‘the availability of the required information to implement is not a trivial point’, ‘parameters will not be easily at disposal’. Its is clear that one of the problems of vehicle simulation software is the availability of data.

The Vehicle Simulation Programme (VSP) differs fundamentally from these examples:

- *It has a unique iteration algorithm dedicated for the flexible implantation of different kind of hybrid drivetrain topologies and powerflow control algorithms taking into account the component operating boundaries or desired operating conditions.*
- *It has an in-depth worked out programme modularity in which almost all parameters are only accessible in the module of the component itself.*
- *It has a flexible database structure, integrated in the component models, allowing an easy implementation of different kind of component data in the form of look-up table, maps, theoretical equations, and empirical formula; in function of the available data.*

a) Drivetrain Simulator (DTS)

Our first major experience with vehicle simulation software was in the framework of a JOULE II programme, funded by the Commission of the European Communities, as collaborator of the University of Kaiserslautern in Germany. Within this project a transparent simulation for electric and hybrid vehicles, called Drivetrain Simulator (DTS) was developed [129,130].

Thanks to the main user interface, the user does not have to deal with the source code of the main programme. This user interface shows a modular structure of the drivetrain. For each object the user has to decide which variables will be drawn during and at the end of a simulation, as well as how often tracing occurs. Every component is described thanks to an integrated programming language called DTS [131]. The DTS-source code looks in some regards like the PASCAL language. Simulation source code can be modified to create new components and to change the structure of the studied system. For some components, such as the drive cycle, data and characteristic curves are stored in tables, which can be changed. Thanks to a "diagram viewer" the tables of results can be converted into graphs. Limitations in components can be introduced in modules so that the demanded power is reduced if one or more components are overloaded.

b) SIMPLEV[®]

SIMPLEV[®] is an Electric and Hybrid Vehicle simulation program developed by the Idaho National Engineering and Environmental Laboratory (INEEL). The INEEL is a multi-program engineering and environmental laboratory doing research and solving national problems for the U.S. Department of Energy (DOE). The software is available free of charge. SIMPLEV[®] is written in a traditional text based programming language, QuickBasic 4.5, which runs under DOS. Its main use is as a vehicle performance simulation tool which capable of simulating vehicles having conventional, all electric, series hybrid, and parallel hybrid propulsion systems. SIMPLEV[®] provides second-by-second predictions of powertrain component performance parameters over any user specified speed-time or speed-distance driving regime. Vehicle propulsion system components are modelled by user-written ASCII data files of component performance [132].

c) EHVSP

The Electric and Hybrid Vehicle Simulation Programme is developed at the Department of Electrical Engineering at the University of Hawaii at Manoa, USA [133]. The software is developed using MATLAB[®] 4.2a and SIMULINK[®] 1.3a. The software has a user interface and a simulation toolbox. The toolbox currently uses statistical data and look-up tables to simulate several parts of the simulator. A friendly user interface has been added to the program in order to facilitate the user. The simulation toolbox was prepared for the Advanced Research Program Agency (ARPA). The first version of the programme is currently available for the ARPA

coalitions. The inputs to the programme can be given by double clicking the appropriate input data module buttons. This feature enables the user to test different configurations. Several combinations can be structured. Finally, the output module facilitates the output of the data. The user by pressing the appropriate button can see dozens of graphs and results [134,135].

d) ELVIS

The Series Electric and Hybrid Vehicle Simulator (ELVIS) was developed at the Southwest Research Institute (SwRI) [136]. It has been developed using MATLAB/SIMULINK[®] as well as in LabVIEW[™], both graphical languages. They also had experience with SIPMPLEV[®], but it was found not very flexible due to the text based programming language [137]. The simulator uses statistical data and look-up tables to simulate several parts of the simulator. Using this model, engineers helped the Advanced Research Projects Agency (ARPA) select and optimise auxiliary power units for series hybrid cars and buses. ELVIS calculates varying operations of pure electric vehicles, series and parallel hybrid electric vehicles and conventional mechanical drive vehicles [138], but only predefined drivetrain topologies can be simulated.

e) ADVISOR

The ADVanced VehIcle SimulatOR (ADVISOR) is developed by the National Renewable Energy Laboratory (NREL), Golden, CO, USA. The model was created in support of the hybrid vehicle subcontracts with auto industry for the U.S. Department of Energy. It contains a set of models, data, and script text files for use with MATLAB[®] and SIMULINK[®]. It is suited for doing parametric studies to map out the design space of potential high fuel economic vehicles consistent with the goals of the Partnership for New Generation of vehicles (PNGV).

ADVISOR also provides a backbone for the detailed simulation and analysis of user defined drivetrain components [139]. It has been applied to many different systems analysis problems, such as helping develop the SAE J1711 test procedure for hybrid vehicles and helping evaluating new technologies as part of the PNGV technology selection process [140]. ADVISOR contains 'autosize' function to scale component data and 'optimiser' functions to adapt the size of components one to each other. Five vehicle configurations have been modelled [125]. The software can be free downloaded from the Internet, but MATLAB[®] and SIMULINK should be purchased anyway.

f) HYGIEA

HYGEIA is a vehicle mission tool for thermal, electric and hybrid vehicles developed in the framework of the FLEETS-ENERGY project. The Commission of the European Communities has sponsored this JOULE project. Our experience in the field of vehicle simulation could give some interesting inputs to this project via

the collaboration of CITELEC, which was one of the main project partners. HYGEIA is a piece of software written at the Motor Industry Research Association (MIRA), Nuneaton, UK, which enables the modelling of a wide range of vehicles. Within the program, various vehicles can be designed including ICE, Electric, Fuel Cell and Hybrid vehicles [12]. The software has been coded using Borland-Dephi. This language provides a visual programming system for developing the graphical user interface, includes the Borland Database Engine for development of the required data tables and has Object PASCAL for coding the modelling and calculation routines [141]. The database is a passive component that is used purely for data storage. An advanced development version is for sale at a price of 5000 Euro.

Dedicated mainly for the transport sector, where engineering skills are less required to evaluate the vehicles, it enables fleet operators and policy makers to predict cost of operating these vehicles in service, thus providing an analysis and decision making tool which can be used by different groups [142]. It uses generic control strategy for each type of hybrid, which limits the variation in hybrid layouts that can be modelled [143]. The software has achieved the compromise between allowing flexible vehicle design and operating hybrid vehicles [118]. It allows the implementation of external control through telematics to improve vehicle and energy utilisation. Both forward and backward calculation methodologies are implemented (see further). It includes also models for thermal control, airco, heat transfer characteristics, etc.

4.2 VSP Main Features

VSP, Vehicle Simulation Programme, is used in several European and national research programmes. In each project a special problem and drivetrain layout was studied resulting in a different system modelling. These models had to be uniformed to come finally to one model that was applicable for all types of drivetrains and power algorithms. To be able to leave out, change or introduce components in the simulated drivetrain it was required to have a uniform definition of the different components.

The development of a standardized iteration process applicable on all kind of hybrid vehicles was harder than originally expected. While simulating on-road measured drive cycles different combinations of component operating limits in very exceptional cases occurred, which had lead the iteration process to an infinitive loop.

Due to the utilisation in different research project it was possible to debug the software and validate it based on real vehicle problems. Hence it was possible to develop a modular user-friendly interactive programme that allows simulating the behaviour of electric, hybrid and internal combustion vehicles. Nowadays VSP is a powerful tool to develop new concepts of different drivetrains. Existing vehicles

can be compared or, due to the large library, components of the drivetrain can be substituted to improve the performance of the vehicle.

The flexible design of the software and the rather unique iteration algorithm allows the use of different simulation methodologies (cause-effect or semi-effect-cause) as well as of different database structures (mathematics formulae or statistical data based on measurements in equation form or look-up table) and of route profile types (standardised, measured or maximum allowed speeds).

The goal of the simulation programme is to study powerflows in drivetrains and corresponding component losses, as well as to compare different drivetrain topologies. This comparison can be realised at the level of consumption (fuel and electricity) and emissions (CO₂, HC, NO_x, CO, particles, ...) as well as at the level of performances (acceleration, range, maximum slope, ...). The general aim of the simulation programme is to know the energy consumption of a vehicle while driving a certain reference cycle. For thermal vehicle this energy consumption corresponds to fuel consumption and in the case of electric vehicles this is the energy drawn out of the battery. For hybrid electric vehicles fuel consumption as well as energy out of the battery are required. Based on models for battery charging, electricity production and fuel refinery, the primary energy consumption can be simulated.

To verify the models, input - output interfaces are developed as well as parameters tracers. During the simulation run the progress in vehicle status is displayed and can be controlled by the user. It is possible to compare measured values with simulated ones for exactly the same speed cycle. Hence it is possible to calibrate the models resulting in accuracy's within 5 %. Most of the components models are based on experimental results and curve fitting, instead of mathematical models based on equivalent circuits. For this purpose a large amount of measurements was done with a self-developed "On road measurement system".

VSP can be used by a wide variety of users with different expertise like: engineers, transport operators and suppliers, energy utilities and decision-makers. It is mainly an engineering tool to evaluate different drivetrains, but due to the large database it can be used by all kind of people to compare different vehicles. Furthermore VSP has the possibility to be coupled to traffic simulation programmes allowing traffic planners to examine congestion and related emission problems.

The simulation programme is able to model any driveline structure without programme modifications. This degree of flexibility can be achieved only by formulating generally applicable program modules, which can be linked via defined interfaces. The interface, between the different components of this drivetrain, is very strictly structured. This allows the user to define and select the powertrain layout and the control strategy in an easy way. The modelling of the component itself is on the contrary very flexible to allow the use of different data sources.

It is not the scope of the simulation tool to simulate e.g. speed control algorithms (PID-controller, etc). Also transient phenomena in the time domain of milliseconds are not relevant in this simulation tool.

In the following chapters user interface, programme language, calculation methodology and the main features are described. In Part II the software is described in detail.

4.3 Main User Interface

Fig. 4.1 shows the main user interface of VSP. How to perform a simulation will be described below.

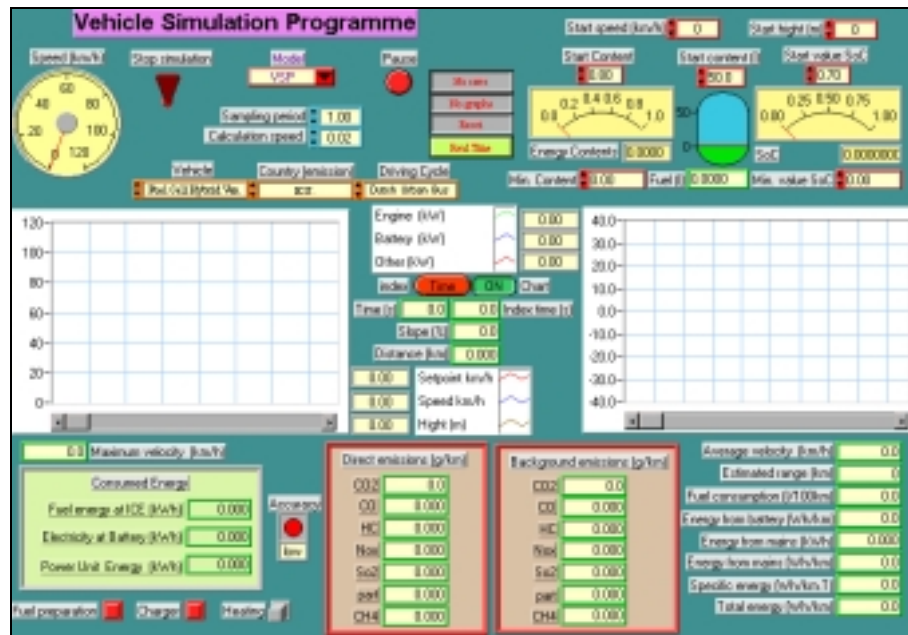


Fig. 4.1: The front panel of the Vehicle Simulation Programme

Before starting a simulation run the user has to select the desired vehicle, the imposed cycle it has to run and the country in which the background emissions, due to the production of electricity, have to be calculated.

The user can select if the speed cycle is defined in function of time or in function of distance (see Part II 'Drive cycle'). Furthermore the user can select the sampling period or better named the speed cycle time increment. The time increment is fixed during a run and should be chosen in relation with the chosen cycle. Indeed for

range determination a time step of 10 s can be sufficient, whilst the ECE 15 cycle is best evaluated every second. The acceleration from zero to a constant speed requires a 0,1 s time increment if you want to determine the vehicle dynamics precisely.

The user has the possibility to select whether or not the results should be saved. If he is interested in the detailed values of the different parameters (speed, torque, power, current and voltage) in function of time of the different components, he has to enable the 'Graph' button.

During the simulation some error messages can occur when a component is not able to follow the imposed speed cycle. When in a next run this should not be displayed a second time the user should chose to disengage the 'Reset' button.

Some computers can be equipped with very fast processors; even so fast that the intermediate results changes to fast on the screen. The user can slow down the programme by selecting the 'Real time' button and the corresponding 'Calculation speed'. On the other hand when the user is only interested in the end results he can disengage the graphs, showing the speed and corresponding power levels on the main user interface.

Additionally some start and minimum values should be chosen before starting the simulation. These start value are the start value of the: fuel tank content, the battery state of charge, the Sate of Energy content of an optional additional power unit, vehicle velocity and level (height) of the road. The minimum values are these for the minimum state of charge and state of energy. Finally the user can select whether or not fuel preparation (refinery), battery charging and cabin heating should be taken into account and simulated.

Once this is selected one can start the simulation. At the left top of the panel a gauge indicator gives the momentary value of the actual speed.

At the right the state of charge of the battery is indicated as well as the contents of the fuel tank and the state of energy of an additional power unit.

A strip chart in the left middle displays the imposed speed and possible speed as well as the height of the road. The power level of the battery, engine and possibly of an other unit is displayed in a other strip chart besides. Between both graphs the interface shows the covered distance and actual slope.

Furthermore the actual time as well as the index used to define the next required speed out of the speed cycle is displayed.

The cluster at the left bottom corner contains the total energy consumption: the energy contents of the consumed fuel, the electricity out of the battery and out of another unit.

All indicators described up to now have their value changed once every sampling period. The following indicators have their value changed only after execution of a run, i.e. when, either the cycle is over, the battery is empty or the run is stopped with the toggle switch.

At the right bottom corner one can find the average velocity (km/h), fuel consumption (l/100 km), the energy from the battery (Wh/km) and the energy from the mains in kWh as well as in kWh/km. This is the total energy required at the mains to load the battery after the run to a state of charge (SoC) equal to its start value. Dividing this energy by the average vehicle weight gives us a figure that is often used to characterise the performance of a drivetrain; it is called the specific energy (Wh/Tkm).

For hybrid electric vehicles the primary energy consumptions corresponding to electricity production (battery charging) and fuel refinery (fuel consumption) are added to have an idea of the total energy consumption (Wh/km). Based on the consumed fuel and/or battery energy and the corresponding covered distance the total possible range is estimated.

In the middle of the bottom the direct emissions (g/km) cluster gives the CO₂, CO, NO_x, CH₄, SO₂, hydrocarbon (HC) and particles emissions provoked by the vehicle at the place of operation. They are of course related to the use of ICE in a classic car or hydride vehicle. The heater of an EV can also emit direct emissions.

The background emissions (g/km) cluster gives the same kind of emissions provoked by the vehicle but not at the place of operation. They are related to the charging of the batteries from the mains and are depending of the composition of the electricity production park. Additional emissions can also be related to fuel refinery.

4.4 Programme Language

The programme runs in a LabVIEW™ environment. Different other programming languages could also be used like C++, Matlab/Simulink®, Delphi, etc. Traditional text based programming languages like FORTRAN, BASIC, C++, etc are not flexible to use for a modular simulation programme. Modifications, other than changing parameter values, in this type of model will usually lead to a major reprogramming effort and reformatting of input files. Both LabVIEW™ from National Instruments as Matlab/Simulink® from Math Works have developed a graphical user interface (GUI) and corresponding programming language. Programme experience and cost were the decisive parameters to choose for LabVIEW™. Furthermore programming in C can be required when one wants to implement new functions in Simulink®[137].

This paragraph will describe the advantage and drawbacks of LabVIEW™ used as a simulation tool. In the same time the specific LabVIEW™ terminology will be explained. Hence the user could understand better the simulation models.

LabVIEW™ is a general-purpose programming system, but it also includes libraries of functions and development tools designed specifically for data acquisition and instrument control. Most users do utilise it for measurement purposes. To programme the data-acquisition systems used to measure different components of the database LabVIEW™ is also used (see Part III).

LabVIEW™ is a high-level programming tool, with the advantage of being a user-friendly interface with a high graphical performance. LabVIEW™ is easy to learn and does not mandate special training. Within one week one can already develop simple programmes. LabVIEW™ programmes are called **virtual instruments (VIs)** because their appearance and operation can imitate actual instruments. However, VIs are similar to the functions of conventional programmes. A VI consists of an interactive user interface, a data-flow diagramme that serves as the source code, and icon connections that set up the VI so that it can be called from higher level VIs.

More specifically, VIs are structured as follows [144]:

- The interactive user interface of a VI is called the **front panel**. The front panel can contain knobs, pushbuttons, graphs, and other controls and indicators. Using a mouse and keyboard one can enter data and then view the results on the computer screen.
- The VI receives instructions from a **block diagramme** construct in LabVIEW™. The block diagramme is a pictorial solution to a programming problem. Such a diagramme allows having a good overview of the structure of the programme. The block diagramme is also the source code for the VI.

Contrary to text based languages like C or BASIC, LabVIEW™ uses a graphical programming language, like illustrated in Fig. 4.2. This figure is a very simple example of a straightforward programme. Left one can see a traditional text based programme of a While loop in which several subprogrammes, simulating the components of an electrical drivetrain, are executed successively. The right part illustrates the same programme written in LabVIEW™. When more complex structures should be written with several loops, one into another, and different parameters are used at different levels, the graphical programme will give a better overview of the programme structure than a text based programming language.

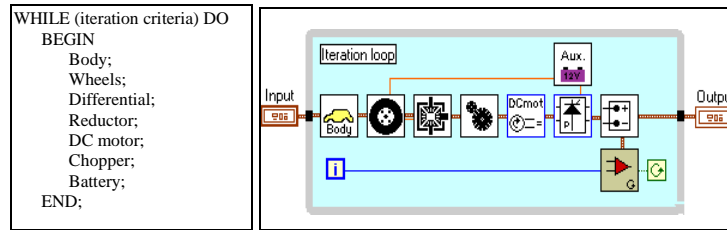


Fig. 4.2: Example of ‘While loop’ in text based language and LabVIEW graphical language

VIs are hierarchical and modular. They can be used as top-level program, or as subprograms within other programs or subprograms. A VI, when used within another VI, is called a subVI. The **icon** and connector of a VI work like a graphical parameter list so that other VIs can pass data to a subVI.

With these features, LabVIEW™ makes the best use of the concept of modular programming. An application is to be divided into a series of tasks, which can be divided again until a complicated application becomes a series of simple subtasks. A VI is build to accomplish each subtask and then these VIs are combined on another block diagramme to accomplish the larger task. Finally, the top-level VI contains a collection of subVIs that represent application functions. In our case this top-level VI is the Vehicle Simulation Programme, “**VSP .vi**”, that contains as subVIs among other things the models of the different drivetrains and the different drive cycles.

Because each subVI can be executed by itself, separate from the rest of the application, debugging is much easier. Furthermore, many low-level subVIs often perform tasks common to several applications, so one can develop a specialised set of subVIs well-suited to future applications [144]. Graphical debugging tools enable the programmer to visualise the data flow and interpret problems. Simulation parameters can be changed while the program is running.

One of the big advantages of LabVIEW, but also a specific difficulty is the fixed in- and outputs of each sub programme. Each component is modelled as a black box. It allows the construction of a very modular drivetrain. This means that every component can be replaced by another component of the component library. E.g. in the same drivetrain a lead acid battery can be replaced by a nickel cadmium battery just by clicking with the mouse on it, without influencing the in- and output parameters.

The definition of these in- and output parameters is a very important issue of the development of the simulation tool, because once defined they should not change anymore. The use of global variable should be avoided to preserve the modularity of the programme.

Within each component of the drivetrain at the contrary the user has a large flexibility to implement the component's data. It is very difficult to find good component data. These data that could be found in literature are usually from different shapes and forms. A fixed predefined database does not allow an easy implementation of different data structures. This is why is chosen for a flexible database, integrated in the component model itself (see Part II). A drawback of this approach is that there is no distinction between component model and component data.

Additional LabVIEW™ terminology:

- **Frame:** The sequence structure, which looks like a frame of a film, consists of one or more subdiagrammes, or frames that execute sequentially. The sequence structure is used to control the order of execution.
- **Global:** Global variables store data used by several VIs. Global variables have to be used judiciously because they hide the data flow of the diagram.
- **Cluster:** A cluster is an ordered collection of one or more elements, similar to structures in C and other languages. Clusters can be used to group related data elements that appear in multiple places on the diagram, which reduces wire clutter and the number of connector terminals subVIs need.

4.5 Calculation Methodology

4.5.1 Different Approaches

In literature one can find different approaches to simulate the behaviour of a vehicle. One can try to describe the whole problem into *matrices*, where the solution is found using matrix linearisation and calculation. This is a very mathematical approach and requires rather simple models. The matrix approach can be interesting as an optimisation technique for a dedicated problem. However for every new problem (e.g. drivetrain topology) one needs to start almost from scratch again.

Another approach is based on the comparison of *frequency distribution* of operating point with efficiency curves. The calculation of the time independent frequency distribution for a given driving cycle requires that wheel speed and torque are known for the complete cycle. Since both quantities depend on different vehicle parameters, frequency distribution can only be applied to a specific vehicle. Integrating the product of frequency distribution and losses characteristics gives the average power losses. The energy losses result from the product of average power losses and cycle time [124]. Fig. 4.3 (left) illustrates an on-road measured driving pattern [145] (distribution of wheel torque in function of wheel velocity), which has to be correlated with the overall drivetrain efficiency, as illustrated in the example at the right side with the motor efficiency map (in the motor torque - speed plane) [47].

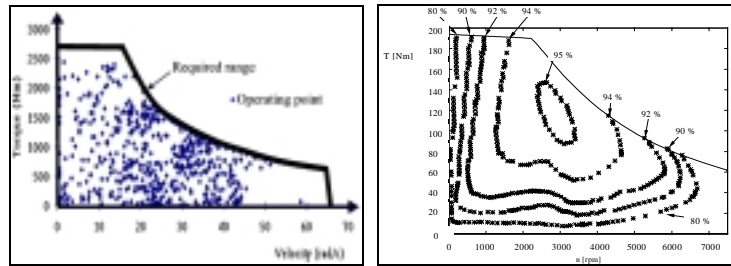


Fig. 4.3: Frequency distribution of working points

Another approach is the *longitudinal dynamics simulation*, on which VSP is based and which is described in 4.5.2.

4.5.2 Longitudinal Dynamics Simulation

The basic modelling strategy is the well tried and trusted method of dividing the drive cycle into a number of time steps and calculating the characteristics of the vehicle at the end of each time interval.

Longitudinal dynamics simulation serves to calculate the time characteristics of several quantities in a vehicle. Therefore it is a good tool to detect the weak points in the drivetrain and moreover to assess further improvements of single drive components [146]. The simulator approximates the behaviour of a vehicle as a series of discrete steps during each of which the components are assumed to be in steady state. The smaller this step, called time increment, the higher the accuracy. At each step the transient effects of changing current, voltage, torque, etc. are neglected. This allows the use of efficiency or other look-up tables, which are generated by testing a drivetrain component at fixed working points.

In handling the modelling process it is important that the direct energy flow can have a forward as well as reverse direction, corresponding with driving or braking the vehicle [112]. The energy flow direction will be called “physical direction”. The calculation direction of this energy flow can be different from this physical direction. Two main groups can be distinguished the forward calculation (cause-effect) and the reverse (effect-cause) method [147].

- *The first one starts at the setpoint set by a driver (acceleration pedal) or controller. With this setpoint one can calculate the force acting on the wheels (Fig. 4.4). The speed profile of the vehicle is thus depending on the setpoint. This method is interesting to test control algorithms (for example PID-controller). Also the effect of the driver can be evaluated. Reproduction of exactly the same speed profile is not possible without a speed controller.*

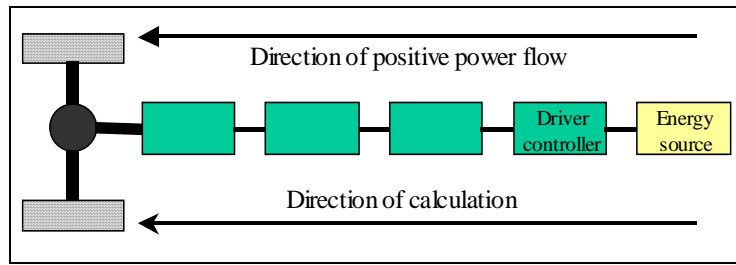


Fig. 4.4: Direction of calculation: cause-effect method

- *The other method simulates backwards (Fig. 4.5). With an imposed speed cycle one calculates the forces acting on the wheels and simulate backwards through the drivetrain up to the primary energy sources, which is either fuel or electricity. The driver's behaviour is not taken into account, since the cycles are followed precisely, gear switching occurs at fixed moments, etc.*

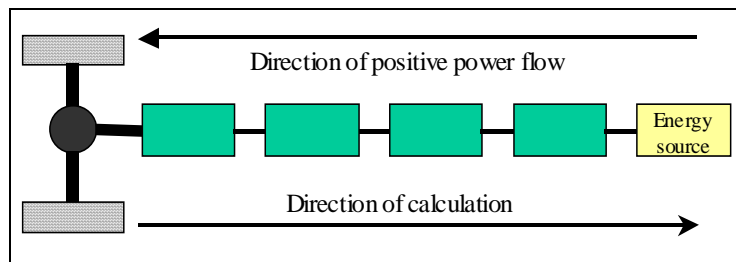


Fig. 4.5: Direction of calculation: effect-cause method

In VSP the calculation is performed using the procedure working backwards from the demand imposed by a required drive cycle, to calculate the properties of the powertrain components as they attempt to meet this demand. For a vehicle simulation typically the following steps are carried out [148].

- The tractive effort required from the vehicle is calculated from the required acceleration and resistive forces such as aerodynamic and gravitational drag.
- This tractive effort is converted by the wheels into the required torque and speed.
- The torque and speed are transformed through the powertrain by the successively intervening system components (such as differential or gearbox) until a prime mover such as an engine or electric motor is reached.
- The prime mover typically uses an efficiency map to predict its energy requirements (f.i. in terms of fuel consumption for an IC engine or power to be drawn from a battery).

This calculation is repeated at each time step during the vehicle cycle.

Fig. 4.6 illustrates the longitudinal calculation algorithm. The left part represents a drive cycle and the right part is the resulting power drawn out the energy source.

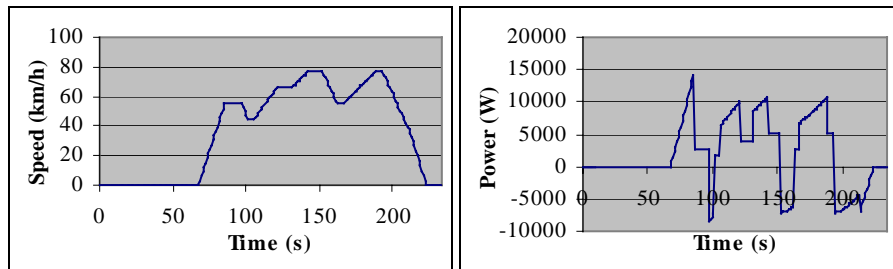


Fig. 4.6: Longitudinal dynamics simulation (e.g. Japan 15 reference cycle)

4.5.3 How to Describe the Forces Acting on the Vehicle ?

Using primary parameters for vehicle's body shell and chassis (e.g. cumulative mass of powertrain components, payload, body design characteristics, etc.) and route parameters (gradient, wind velocity, etc.), the programme calculates the forces acting on the vehicle.

The tractive force (F_{trac}) acting via the tyre contact surface of the driven wheels is determined by the engine or motor torque and by the gear ratios and inertias of the driveline. For level driving, the resistive forces acting in the direction of motion are the components rolling resistance (F_r) and air resistance (F_v). If the propulsion forces are not in equilibrium with the driving resistance at the considered steady speed, vehicle acceleration (a) or braking occurs, producing an inertial force (F_a), which acts at the vehicle centre of gravity [147].

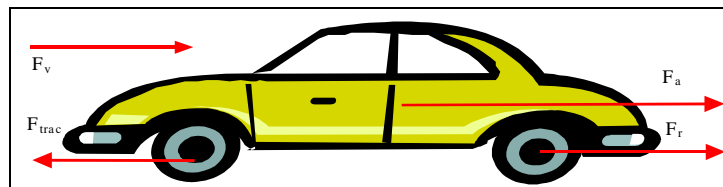


Fig. 4.7: Forces acting on the vehicle

When driving uphill (road inclination α) or when there is a head wind (velocity v_w) additional forces are acting on the vehicle. The total resistive force can be expressed with equation (4.1) [16,130]. This equation will be described in detail in Part II and the description of the different symbols can be found in the list of symbols.

$$F_R = \frac{I}{2} \cdot \rho \cdot S \cdot C_x \left(\frac{v_{\text{cur}} + v_w}{3,6} \right)^2 + M \cdot g \cdot f_r \cdot \cos(\alpha) + M \cdot g \cdot \sin(\alpha) \quad (4.1)$$

For accelerating the vehicle an additional force corresponding to Newton's 3rd law of motion (4.2) has to be delivered by the traction system.

$$F_a = M \cdot a_v \quad (4.2)$$

The supplementary force corresponding to the inertia of the different components is taken into account within the components themselves.

4.5.4 Component Characteristics Modelling

A component model can be as sophisticated or simple as the programmer's time and budget permits. Different parameters and even different modelling methods can be used to describe a component. Although there may be different types of models, the subprogrammes have the same interface, return predefined outputs and use the same predefined inputs.

Since the general aim of the simulation programme is to know the energy consumption of a vehicle, all parameters, which have an influence on this energy consumption, have to be defined. With the forces acting on the vehicle corresponds a certain power level. The battery or fuel does not only need to deliver this power, but also the losses of the different components of the drivetrain. A good description of these losses is thus required. The different parameters defining these losses should be calculated. The accuracy of the model will define the accuracy of the overall energy consumption.

a) Efficiency covering the whole working field

A lot of publications use a constant value for the efficiency of a component, generally corresponding to its maximum value. They multiply the different efficiencies to describe the overall efficiency. This approach is a very rough estimation and corresponds mostly to a very optimistic energy consumption. This is also the reason why one can find in literature so many different results on the energy comparison of different drivetrain. A more accurate solution would be to simulate the behaviour taking into account the whole map of working points.

b) Analytical models

The components (electric motor, chopper, charger, etc) can be defined by *physical equations* and equivalent circuit (analytical models) or by measured efficiency characteristics (statistical models).

Physical laws and equivalent circuits can describe the characteristics of a component. Such theoretical models can be used for different motors or inverters, only the component parameters are to be changed. However the component parameters are not always available. If they are received from the manufacturer, they are generally measured under laboratory conditions (sinusoidal voltage, standard measuring points, etc). They can be fine-tuned while calibrating the entire vehicle model.

c) Statistical models

On the basis of numerous measurements one can calculate statistical models for the components. These measured data can be stored in one or two dimensional *look-up tables* or arrays. Parameters can be calculated by bilinear interpolations on a network of two dimensional efficiency curves. The precision depends on the density of the points of the map. This approach is explained by example of Fig. 4.8. The considered parameters can be emissions, fuel consumption, voltage, efficiency, etc.

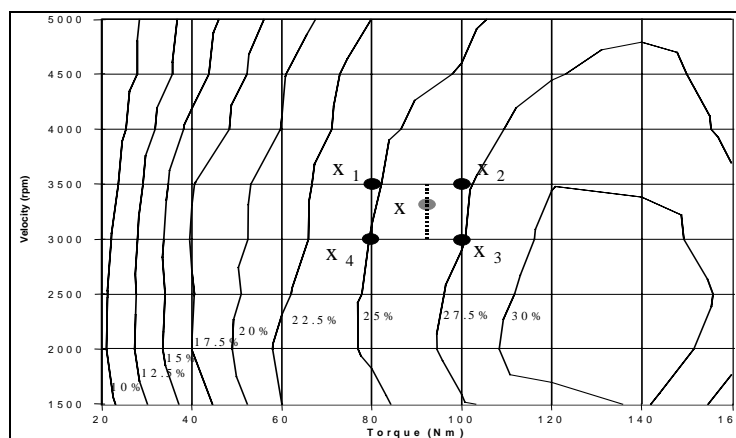


Fig. 4.8: Bilinear interpolation of a two-dimensional efficiency curve

In the simulation programme a two dimensional model is mostly used. A parameter (efficiency, power, etc) can be defined e.g. in function of torque and speed, or current and voltage. Other models can be a one-dimensional table of only one parameter, e.g. the maximum torque in function of speed. In some cases it can be necessary to have a multiple dimensional function. In this later case a interpolation in a look-up table will become very complex. The use of *statistical formulae* will be required. Using statistical equations has the benefit to use less memory and to allow a faster simulation. It is thus recommended to transform the look-up table into statistical formulae. This can be done with the help of mathematical programmes like Matlab[®] or spreadsheet programmes like Excel.

Statistical piecewise models, derived out of the measurements data, have the advantage of being closer to the reality, and thus are mainly used, as an accurate input, in the database of the Vehicle Simulation Programme.

The more parameters used to define these statistical equations or look-up tables, the more complicate the simulation programme becomes and the slower the programme will run. It is thus advisable to determine those parameters, which have an important influence on the required end-result (the energy consumption). A parameter sensitivity analysis is performed in Part III.

d) Components boundaries modellisation

Each system is identified by its operating limits (Fig. 4.9). While simulating the behaviour of a drivetrain performing a chosen cycle, it is possible that one of the components cannot satisfy the demanded requirements. For instance a motor can reach its maximum torque or can come in overspeed, a battery or inverter can be overloaded. In that case it is interesting to reduce the required acceleration and hence to evaluate the maximum performance (possible speed) of the drivetrain. To ensure that all components operate within defined boundaries, corresponding to loading limitations, acceleration reductions are introduced. This *acceleration reduction* (AR) is used to iterate towards the possible vehicle speed domain. The limiting values can be either properties of the specific part or defined by the user.

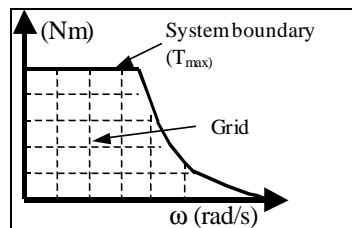


Fig. 4.9: System boundary

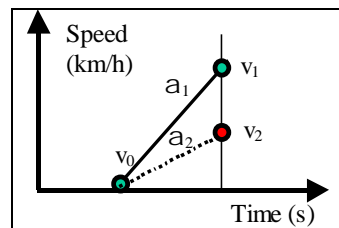


Fig. 4.10: Possible speed calculation

Fig. 4.10 illustrates the reduction of the required acceleration a_1 , corresponding to a desired velocity v_1 into the possible acceleration a_2 , resulting in a possible velocity v_2 . This complex iteration algorithm is extensively described in Part II. By means of this higher simulation level it is also possible to simulate acceleration and maximum speed performance tests.

e) The iteration algorithm also allows a kind of semi ‘cause-effect’ calculation

Due to the use of this iteration algorithm it is also possible to simulate the influence of the driver or controller. Normally the *cause-effect* method or forward calculation method (see above) is used to simulate the effect of the driver. Nevertheless VSP uses the effect-cause method, which means that during the simulation the desired

speed can be set to a maximum value that never will be reached by the drivetrain. In this way an acceleration reduction is always calculated. In a special model for the driver the acceleration reduction (AR) is implemented in the same way as it is done in all other components of the drivetrain. In the driver model a setpoint for power, speed or torque is evaluated as if it would be a maximum limit or boundary. Due to the iteration process the programme will calculate the speed corresponding with this setpoint.

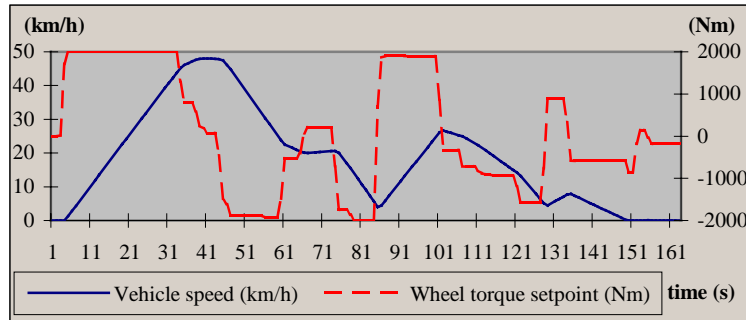


Fig. 4.11: Demonstration of the controller algorithm

In the graph, Fig. 4.11, the controller algorithm is demonstrated. Normally out of the speed cycle the torque acting on the wheels is calculated. In this case, with same programme using its special iteration algorithm, one can change in real time a setpoint for the torque (dashed line). This setting is coming for instance from an acceleration pedal. The actual speed is following this setpoint (straight line).

f) Powerflow control algorithm

The powerflow control strategy of hybrid drivetrains is implemented with the same iteration process as for calculating the vehicles performance. The power distribution between the several mechanical shafts or energy sources is controlled with the help of a *Power Distribution Factor* (PDF).

When exceeding the operating boundaries, instead of using an acceleration reduction, a *Power Reduction* (PR) will be introduced to regulate the power split (the PDF) in the different components that are in charge of the power division in the hybrid drivetrain (e.g. toothed wheel and DC-bus controller).

Opposite to the Acceleration Reduction the Power Reduction is not used to change the vehicle acceleration performance, but to control the powerflow in the hybrid drivetrain.

In more complex hybrid structures a *second PDF* and *Power Reduction* can be necessary: for instance in a series hybrid vehicle with a traction battery (AR), a generator (PR₁) and a Flywheel (PR₂). Until now the software is build up to

simulate maximally third order hybrid systems. The software can easily be extended to higher order systems if necessary. Consequently additional Power Reduction factors have to be introduced.

In the case of hybrid vehicles the iteration process is much more complex: the PR can change the power split or the AR can reduce the acceleration. Due to the fact that several reductions can occur within one drivetrain an intelligent *iteration order* is required. This methodology is described in Part II. Hence a *hierarchy* of different hybrid control strategies is developed and inherently implemented in the software. This means that the control algorithm is not a separate block of the simulation programme, but makes part of the different components on which it has an influence. This is necessary because there is a high degree of interaction between components models, particularly with respect to operation limits, and powerflow control strategy.

The difficult challenge was to develop this iteration algorithm in such a way that it was applicable on all kind of vehicles: electric, thermal, series and parallel and even complex hybrid vehicles. For this reason it was necessary to develop a *uniform* approach to introduce the Acceleration and Power Reduction for each type of operating limit (speed, torque, power, etc.) and to develop an iteration control module to tackle all these reductions.

g) Interchangeable component library

One of the purposes of the simulation programme is the ability to calculate the performance of a vehicle comprising any set of components that have been connected together in a physically sensible manner.

Table 4.1: Possible interchangeable components with the same ‘function’

Transmission	Power transformation	Energy source
Differential	AC motor + inverter	Battery (all types)
Gear	DC-motor + chopper	APU
Reductor	Engine	Electric Flywheel
	Mechanical flywheel	Super capacitor
		Fuel cell

Components of the same type can be exchanged, e.g. a lead acid battery by a NiCd battery, but also components with the same function, e.g. a battery by a fuel cell. Table 4.1 illustrates the possible interchangeable components. Components that do not have an equivalent counterpart are the body, wheels, torque splitter, planetary gear, DC-bus controller and the auxiliaries. They can only be replaced by other components out of the database of the same type.

The model of the engine is developed in such a way that it can be used in an APU for a series hybrid vehicle as well as traction unit in an ICE-vehicle.

4.6 Programming Structure

The programming structure of LabVIEW™ lends itself to a top down approach. The programme, VSP, therefore can be seen as a three level structure.

- The top level is the main programme of which the user interface is described in a previous chapter and the technical description can be found in Part II. This level contains the icons of the subprogrammes for the different vehicles and also for drive cycles, electricity production, etc.
- The second level is consequently the level of the different drivetrains. Each drivetrain is composed of different vehicle components. The manner these components are connected together will represent the topology of the drivetrain. This second level represents in fact the energy flow and conversion through the vehicle drivetrain. Each component is modelled as a separate subprogramme.
- The third level is the level of the different component models.

The flow chart of Fig. 4.12 gives an overview of the software. One can recognise two different simulation loops: one that defines each step a new required velocity in function of the chosen speed cycle and another that contains an iteration algorithm to define the possible vehicle performance in the case the vehicle is not able to follow the imposed speed cycle. Additionally there is a very small loop that is used to pause the simulation process.

After the initialisation phase the required velocity of the vehicle is defined by the speed cycle that the user has selected on the main user interface. The model of this speed cycle contains also the load of the vehicle, the slope of the road and whether or not the vehicle is driving in the city (centre). Based on these parameters and the characteristics and weight of the selected vehicle body and of the wheels, the forces acting on the vehicle can be calculated. In function of the powerflow in the drivetrain (the hybrid drivetrain power strategy), the component losses and the energy consumption from the battery, fuel tank or other energy source is processed. In the case of non-pure electric vehicles the direct emissions are simulated too.

When the end of the drivetrain is reached, this means one has processed all calculations from the wheels to the energy sources, the iteration algorithm checks if all components were able to deliver the required torque, speed, power, current, etc. If one or more components were out of data range, the required acceleration is adapted (via the acceleration reduction) and the drivetrain is simulated again until all components are within limits. Hence the imposed speed cycle is only exactly followed when all components are able to do so.

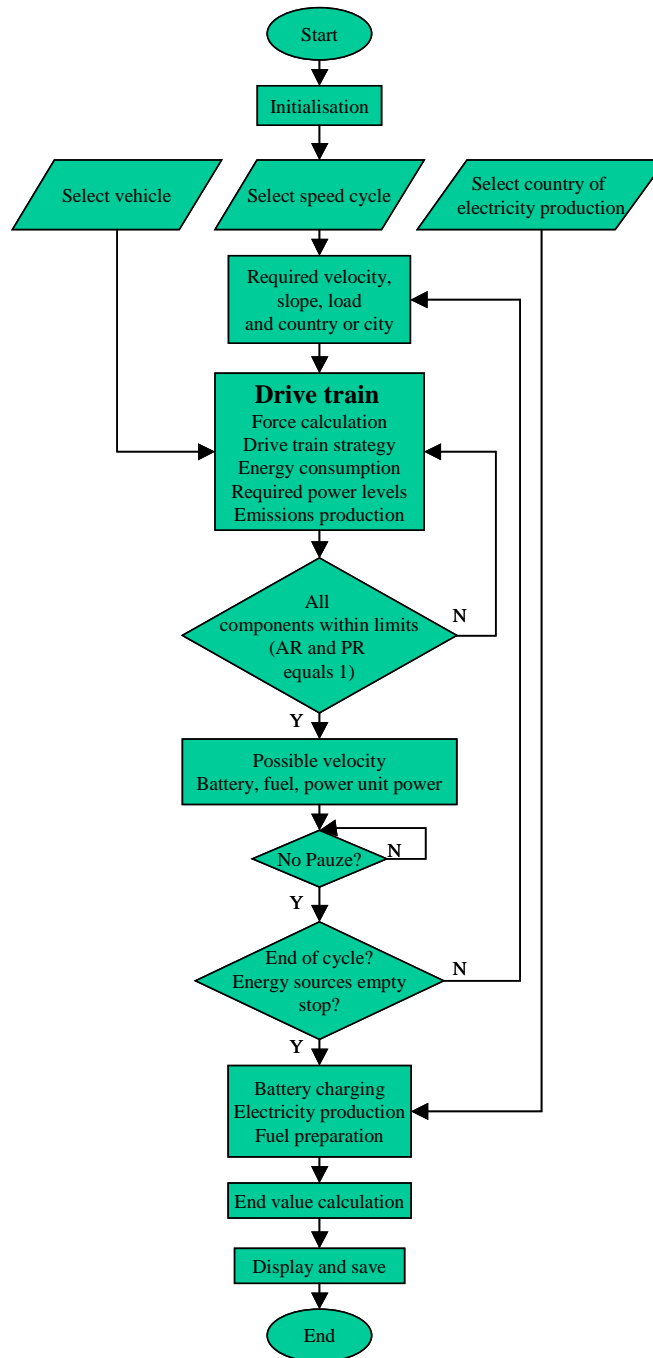


Fig. 4.12: Flow chart of Vehicle Simulation Programme

The power levels of the energy sources are visualised in the main user interface and the next required speed step is used to calculate the forces acting on the vehicle. If the speed cycle is completely simulated or all energy sources are empty or the user stops the simulation, the programme will go to the last part. In this part the battery will be recharged, the corresponding background emissions are calculated and possibly the additional energy consumption due to fuel refinery is defined. The end results are displayed and if wanted saved on hard disc.

All different aspects will be described in detail in Part II.

4.7 Different Levels of Accessibility

To conclude this first part the different accessibility levels are described. VSP is a software tool that can be used by a large range of different customers, with different skills and desires. Different password protected accessibility levels are foreseen and allow the user to have admission to a certain level of information.

The *first level* corresponds with the front panel of the main programme, like described in paragraph 4.3 “Main User Interface”. At this level the user can select a vehicle of the database, a to be driven speed cycle and some other features. At the end of the simulation the energy consumption and emissions are the most important results. This level is dedicated to novice users.

Level two give access to the front panels of the vehicle and electricity production models. Especially for hybrid electric vehicles this gives the opportunity to define some general drivetrain power strategies, like whether or not the generator should be engaged and in function of which criteria. By choosing a certain country one select the way the electricity is produced to recharge the battery. The relative contribution of the different types of power plants in each country can be different. By having access to the front panel of this electricity production model one can change the pollution and energy losses of the considered country.

Level three is related to the vehicle components. Each drivetrain consists of different components. The major parameters describing the working of such a component can be found on its front panel. While having access to level three the user can change the parameters on the front panel of the different components of the drivetrain. Furthermore this level allows replacing a component of the drivetrain by another out of the component library or database. For this level some technical skills are required. Sometimes it can be difficult to get access to data. In this case standard values are proposed.

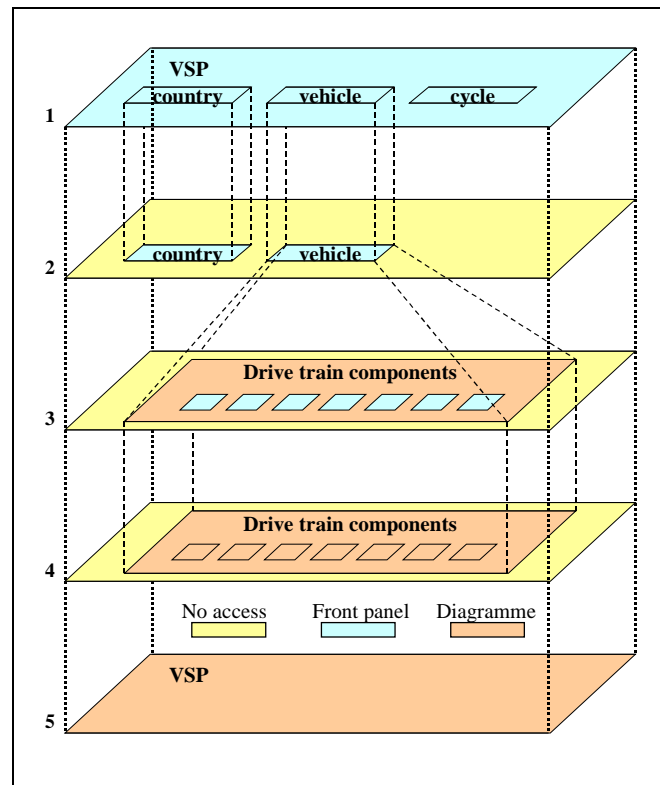


Fig. 4.13: Different accessibility levels of the simulation programme

The *fourth level* is related to the creation of new component models. Most component data can be found within the diagramme of the component model. This diagramme contains submodels, equations, case structures, etc. When one wants to make models of new components one should have access to this fourth level. Some engineering skills are required concerning characteristics and modelling of motors, engines, convertors, batteries, etc. The user must also be familiar with LabVIEW. This level is more dedicated to expert users.

The last and *fifth accessibility level* gives admission to the whole software tool. At this moment the user can change any part of the software from main programme to detailed subprogramme. An in-depth knowledge and understanding of the simulation programme is required. How are all programmes related to each other? Which parameters will influence another and via which process? Only when fundamental changes have to be made access to this level is obligatory. This most in-depth level is dedicated to users with engineering expertise.

PART II

SOFTWARE DESCRIPTION

5 INTRODUCTION TO PART II

This second part is a technical part describing the models of the subprogrammes of the simulation software. The different equations on which the models are based will be explained. The fact that the models are related to each other in sometimes a rather complex structure makes it necessary to refer in the description of one model to that of another. Especially the iteration algorithm interferes with a lot of subprogrammes.

First the *main programme* and related subprogrammes (electricity production, speed cycle definition, etc.) will be described. Afterwards the implemented *drivetrains* of the different vehicles are explained. Closely related to these drivetrains are the *mechanical and electric power control devices* for hybrid vehicles. In these subprogrammes the different hybrid drivetrain control strategies are mainly implemented.

They are described after the specification of the iteration algorithm. As already mentioned in Part I this *iteration process* is an intelligent algorithm to define the maximum vehicle performance and to control the powerflow of hybrid drivetrains.

Afterwards one can find the models for the different components of the drivetrain, starting from the wheels and going to the energy source(s). The first components are related to the *forces acting on the vehicle* body and wheels and the *mechanical transmission*. Finally in this Part II the drivetrain components, figuring as *powerflow transformation* are described.

To understand the different models it is required to read the fundamental principles of Part I. All chapters are entitled with the corresponding name of the subprogramme of the simulation tool. In LabVIEW the file extension is named (*.vi).

6 VSP

This first chapter of Part II will describe the model of the main programme and some specific subprogrammes defining the speed cycle and handling the error messages. Furthermore the calculation of the background emissions due to electricity production as well as the additional emissions and energy consumption due to fuel refinery is explained in this chapter.

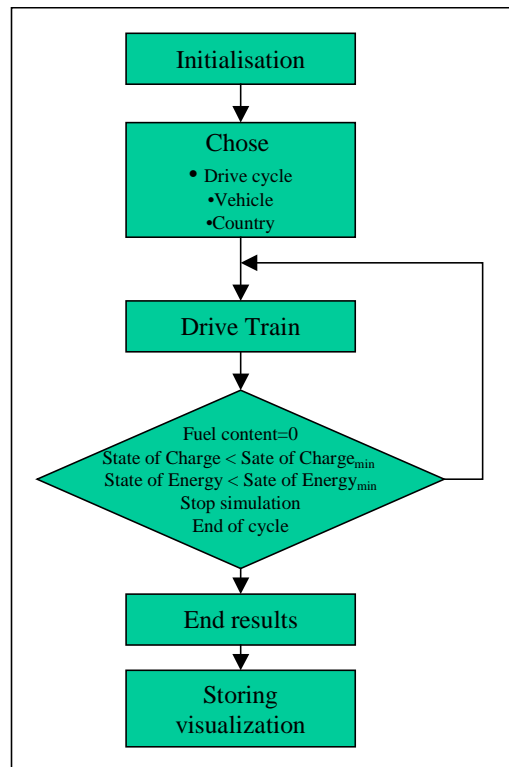


Fig. 6.1: The main programme

6.1 VSP .vi

The main programme, “VSP .vi” is build up out of 4 different parts, called frames:

- Initialisation
- Main loop
- End calculations
- Storing results

The first frame executes the initialisations. The selection of the drive cycle is performed in a ‘case’ instruction that gets its selection variable from the driving cycle ring control.

The second frame contains the actual repetitive execution of the process simulation. This is implemented in a ‘while loop’.

In the third frame the specific end results are calculated. It contains also the models of the battery chargers and the models for electricity production and fuel preparation..

The last frame stores all traced parameters and presents this in a graphical user interface.

6.1.1 *Frame 1: Initialisation*

All tracers used to store results during the simulation process, are initialised to zero. These tracers are part of the “**Tracer .vi**”. These tracers are arrays containing for each step of the speed cycle the value of the velocity, torque, power, current and voltage and this for every component of the drivetrain. Additionally tracers are used to store the mass of each component.

The “**VSP global .vi**” is as well initialised. It contains the only global parameters used in VSP:

- *The battery voltage (V)*: Due to the fact that this battery parameter is required for different components to simulate their behaviour, it is impossible to define it as a local variable and hence this parameter is used as a global.
- *State of Charge*: This global contains the state of charge of the battery.
- *State of Energy*: In case of a power unit, like a flywheel, an additional filling indicator is required which is called Sate of Energy.
- *Fuel content*: When a fuel tank is used its content is stored in the fuel content global.
- *Time increment (s)*: This global is the speed cycle time step. The smaller this value the higher the accuracy of the simulation results, but the slower the programme.
- *Time (s)*: This global accumulates the time during the simulation.
- *Accuracy selector*: This global, allows to indicate the accuracy of the component’s model and especially of its data. In each component the user can give an indication of the accuracy of his data. The worst indication will be used as overall accuracy. This indication can be selected out of three levels:
 - High : measured data, calibrated and validated model;
 - Medium : measured data;
 - Low : data out of literature.

- *Initialisation boolean*: Component models of the drivetrain will be simulated several times during the iteration. Some calculation needs to be performed only once. With the help of the initialisation boolean recurrences of identical processes can be avoided (e.g. tracing of component weight).
- *No iteration boolean*: During the iterative process that defines the maximum performance of the drivetrain and controls the powerflow, some simulation processes are not to be executed (e.g. tracing and displaying of results). Only when this iterative process has found a possible solution, the no-iteration boolean will be true and some processes can be executed (see further).
- *Run boolean*: With the help of this boolean it is possible to stop the simulation process whenever required.

6.1.2 Frame 2: Main Loop

The second frame contains the actual repetitive execution of the process simulation. It is implemented in a while loop which is repeated until:

- The speed cycle is finished. This corresponds with a time smaller than the last value of the time array of the speed cycle (see subchapter 6.2 Speed Cycle .vi).
- The toggle switch 'STOP' is active or the simulation is stopped with the run boolean (see above).
- The battery (State of Charge), the fuel tank (Fuel Content) or another energy source (State of Energy) is empty. Some batteries should not be discharged completely. They are supposed to be empty when they reach their minimum allowed State of Charge (SoC_{min}), selectable on the front panel of the main user interface.

During the execution of the while loop the *Time* (s) is increased with the *Time increment* $T_s(s)$ or like described with equation (6.1) the *Time* is the number of completed repetitions (*i*) multiplied by the *Time increment*.

$$Time = i.T_s \quad (6.1)$$

The *power level of the battery, generator and power unit* is displayed on a graph. Another graph illustrates the required and possible velocity as well as the *height of the road*. The latter is calculated by integrating the road inclination. To fastener the programme these graphs can be disabled.

The level of the battery *State of Charge*, the *Fuel Tank Content* and the power unit *State of Energy* are displayed on the front panel.

Furthermore a *Pause* selector is installed in another while-loop. As long as the Pause is active (True) the small loop will be executed resulting in an interruption of the rest of the simulation programme.

The user can select to run the programme as fast as possible or the slow down the simulation process by introducing a wait function. The value of this *waiting time* can be selected on the front panel. This feature is useful to be able to closely follow the different simulation results during the simulation run. If the programmes runs as fast as possible, it can be possible that the interim results cannot be seen while using a fast computer processor.

Additional results will be stored in the “**Tracer .vi**”, to be able to visualise them at the end of the simulation. If one is not interested in these results, but only in global results, this tracer can be reset to reduce memory occupation and fastener the computation.

All indicators described in this paragraph have their value up-dated by every time repetition in the loop.

6.1.3 Frame 3: End Results

After the execution of the main loop the end results are calculated.

The *accuracy* global parameter is traced out of the data of the different components and the worst value is displayed on the front panel.

In function of the covered distance D (km) and drive time the *average velocity* v_{av} (km/h) is calculated.

$$v_{av} = \frac{D}{Time.3600} \quad (6.2)$$

The covered distance is also used to calculate the *average fuel consumption* (FC) in L/100km. In equation (6.3) the begin value of content of the fuel tank is L_{start} and the end value is L_{end} ; both expressed in litre.

$$FC = \frac{L_{start} - L_{end}}{D}.100 \quad (6.3)$$

By dividing the emissions $Emis$ (in g) stored during the simulation in the “**Tracer .vi**” one gets the *direct emissions* DE expressed in g/km (equation (6.4)).

$$DE = \frac{Emis}{D} \quad (6.4)$$

The possible *driving range* R is estimated based on the consumed fuel L and/or energy (State of Charge, SoC, and State of Energy, SoE) for driving a distance D and the total available content (see equation (6.5)). If the difference between start and end value is very small, which could be the case for very short speed cycles, this difference will not be taken into account due to the fact that at this moment the driving range would have a very low reliability.

$$R = D \cdot \left\{ \frac{L_{start}}{L_{start} - L_{end}} + \frac{1 - SoC_{min}}{SoC_{start} - SoC_{end}} + \frac{1 - SoE_{min}}{SoE_{start} - SoE_{end}} \right\} \quad (6.5)$$

With :

- SoC_{min} : minimum allowed SoC
- SoC_{start} : begin value of SoC
- SoC_{end} : end value of SoC
- SoE_{min} : minimum allowed SoE
- SoC_{start} : begin value of SoC
- SoC_{end} : end value of SoC

By dividing the battery energy with the covered distance one gets the *energy from the battery* in Wh/km. The *specific battery energy* consumption is obtained by dividing this value with the average total vehicle weight (see “**Body & weight .vi**”). This figure is often used to characterise the performance of an electric drivetrain.

In function of the selected vehicle the corresponding battery charger is chosen. With the help of the “**Charger .vi**” the battery is recharged until a state of charge corresponding with its start value. Hence one gets the required energy from the mains E_{grid}. Division with the covered distance gives the *grid energy* in Wh/km.

This energy delivered by the grid must be produced in electricity production plants. The power plants can generate at their turn additional *background emissions* and are characterised by additional losses. For each European country there is a model describing the electricity production park, which can be found in the subprogramme “**Electricity production .vi**” (see subchapter 6.3).

Some vehicles are equipped with a *burner* or heater to heat the vehicle interior during wintertime (see “**Heater .vi**”). The user can select whether or not this heater should be engaged to simulate the additional fuel consumption and direct emissions.

Finally a sub programme is foreseen to simulate the oil *refinery* to prepare the fuel. This process give additional background emissions and requires additional energy

consumption. They are defined in “**Fuel Refinery .vi**” in function of the consumed fuel.

6.1.4 Frame 4: Storing and Visualisation

Finally in the last frame of the main programme all simulation results are saved on the hard disc if desired. All these results are saved in ASCII-format allowing reading them with spreadsheet programmes for further evaluation. If the user wants to he can also visualise the simulation results of the “**Tracer .vi**” directly on a LabVIEW graph via the “**TracerGraph .vi**”.

6.2 Speed Cycle .vi

Each speed cycle is defined by a piecewise linear description of velocity, road inclination, load (passengers and luggage weight), and whether or not driving in zero emission protected area's. These parameters are defined in function of time and stored in a two dimensional array. Table 6.1 illustrates such an array for the ECE-15 cycle. This cycle is defined by European standards and is the basis for pollution and consumption homologation tests. This cycle should normally be driven four times subsequently, but since no thermal effects are considered in VSP, driving one cycle is sufficient.

Table 6.1: The ECE-15 speed cycle

Time (s)	0	11	15	23	28	49	61	85	96	117	143	155	163	176	188	195
Velocity (km/h)	0	0	15	15	0	0	32	32	0	0	50	50	35	35	0	0
Road slope (%)	0	0	0	0	0	0	0	0	0	0	0	0	0	0	0	0
Load (kg)	80	80	80	80	80	80	80	80	80	80	80	80	80	80	80	80
City/country	T	T	T	T	T	T	T	T	T	T	T	T	T	T	T	T

The road inclination is an important factor to define the rolling resistance in hilly areas. The road inclination (s) is expressed as a percentage and is function of the angle (α) between the road and the horizontal.

$$s = 100.tg(\alpha) \quad (6.6)$$

The load parameter can be used to simulate urban city buses. The number of passengers going on and of the bus during the trip will change the total bus weight, which influence again the rolling resistance but also the required acceleration force. If one is interested in simulating goods distribution, this load parameter is also helpful to take the effect of the change of the merchandise into account. Furthermore the city/country-boolean is used to define if one is driving in a city area

where it is not allowed to switch on the APU of an hybrid vehicle (see Part I). This feature can be seen as a kind of *telematics* introduced in the route profile.

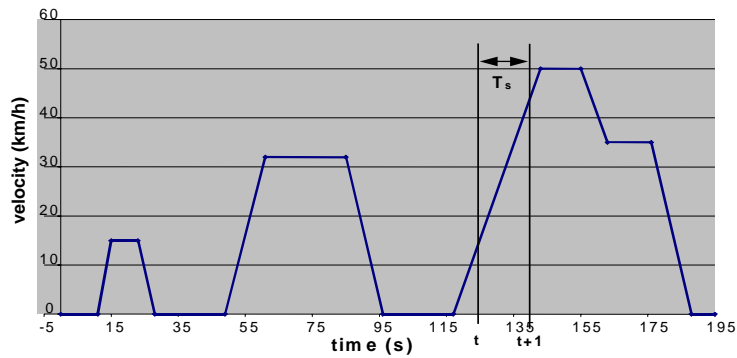


Fig. 6.2: ECE-15 speed cycle

Fig. 6.2 illustrates the ECE-15 reference cycle and the sampling of the different requested velocities based on the time increment T_s . All other cycles are defined in a similar way and new cycles can be automatically imported based on ASCII file formats.

Another example is illustrated with Fig. 6.3. This graph describes the speed and slope profile of the on-road measured Brussels urban bus line 71.

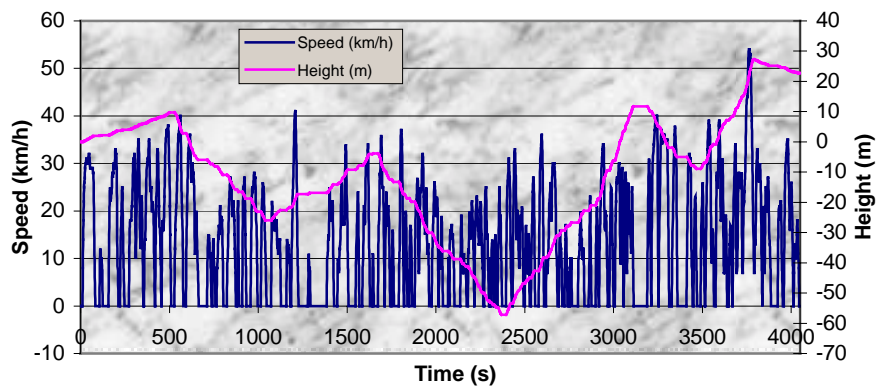
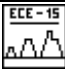





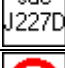













Fig. 6.3: Speed and slope profile of the on-road measured Brussels urban bus line 71

Following cycles are until now implemented:

Table 6.2: Implemented speed cycles

	Name and description	Max. velocity	Average velocity	Total time
	ECE-15 .vi A European certification cycle for vehicles [149].	50 km/h	18,7 km/h	195 sec.
	ECE 47.vi A European certification cycle for scooters.	80 km/h	–	110 sec.
	EUROPE 90 .vi A European certification cycle for vehicles [150].	90 km/h	32,4 km/h	1180 sec.
	EUROPE 120 .vi A European certification cycle for vehicles (EUDC).	120 km/h	33,6 km/h	1180 sec.
	Traffic Jam .vi First part of ECE-15 cycle.	32 km/h	11,1 km/h	117 sec.
	Japanese cycle .vi A Japanese certification cycle for vehicles [151].	70 km/h	33,6 km/h	231 sec.
	USA cycle .vi SAE J227 D test cycle.	72 km/h	43,5 km/h	122 sec.
	Aut.30km-h .vi Constant velocities at zero slope.	30 km/h	–	–
	Aut.50km-h .vi Constant velocities at zero slope.	50 km/h	–	–
	Aut.70km-h .vi Constant velocities at zero slope.	70 km/h	–	–
	Aut.85km-h .vi Constant velocities at zero slope.	85 km/h	–	–
	Aut.90km-h .vi Constant velocities at zero slope.	90 km/h	–	–
	Aut.120km-h .vi Constant velocities at zero slope.	120 km/h	–	–
	Step .vi Constant velocity steps at zero slope.	100 km/h	50 km/h	55 sec.
	Acc-Dec .vi Constant velocities at zero slope for 50 seconds then braking to standstill.	120 km/h	–	–
	110-120km-h .vi Starting from 110 km/h accelerating to 120km/h .	120 km/h	–	–
	X% slope .vi 20% grade at 10 km/h.	10 km/h	–	–
	Sudden sloop .vi A sudden slope.	90 km/h	70,6 km/h	100 sec.

line 71	Bus line 71 .vi On road measured Brussels city bus cycle (L71).	54 km/h	13,2 km/h	4048 sec.
VLIET	VLIET cycle .vi On road measured cycle combining city and sub-urban traffic.	72,1 km/h	22,3 km/h	2700 sec.
Jumper	Jumper cycle .vi On road measured sub-urban cycle.	69,9 km/h	26,9 km/h	4374 sec.
DUB cycle	Dutch Urban Bus cycle .vi On-road measured data that is put together in such a way that the sum of all data is a reference cycle representative for average Dutch urban bus use [152].	63,4 km/h	21,4 km/h	881 sec.
III →	New cycle .vi Other cycles can easily be imported from any ASCII-table.	-	-	-

6.2.1 How to Define a Speed Cycle: Speed (Time) or Speed (Distance)

As explained in Part I VSP starts from the effect-cause method, using pre-defined (or on-road measured) driving patterns to calculate the forces acting on the vehicle. Is the desired speed a function of time (like it is done in most simulation programmes) or a function of distance ?

When considering the ECE-cycle or a city bus route profile the stop times are important whereby the route has to be defined in time. But the topography of the route is depending on the covered distance. Also to know if one is in a city centre, where one should switch off the APU in the case of hybrid vehicles, it is necessary to know the real distance. The same can be said when one wants to take into account the maximum allowed speed of a certain street.

As long as the desired speed is equal to the possible vehicle speed v_{pos} (km/h) (all components can deliver the desired power) one can calculate the distance D (km) out of the speed and the time increment (see equation (6.7)).

$$D_{t+1} = D_t + v_{pos} \cdot \frac{T_s}{3600} \quad (6.7)$$

But when a car is not able to follow the speed profile, due to lack of power, the possible speed is different from the desired speed. The real distance will be different from the theoretical distance corresponding to the pre-defined cycle.

6.2.2 How Does VSP Manage this Problem ?

Considering the relative difference between the possible speed, v_{pos} , and the required speed, v_{req} , a time correction increment (TCI) is calculated (see equation (6.8)). In this way the 'Index Time' is corresponding with the covered distance and is used to define the new desired speed (see equation (6.9)). The 'Index Time' can thus be different from the real 'Time'. The user can select which index he will use to simulate the speed cycle. When simulating on road measured cycles one should use the 'Index Time'. While simulating an acceleration test the real 'Time' should be used.

$$TCI_{t+1} = TCI_t + \frac{v_{pos} - v_{req}}{v_{req}} \cdot T_s \quad (6.8)$$

$$IndexTime = Time + TCI_{t+1} \quad (6.9)$$

Based on this time index the next required velocity, road inclination, load and city/country-boolean are selected with the help of interpolation function.

6.2.3 Example

In the next two graphs (Fig. 6.4) a comparison is made between the classical route definition, which is defined with speed as a function of time, and the VSP approach whereby the time index for the speed cycle is corrected in function of the real possible speed. The test vehicle performance is decreased in such a way that a clear visible difference occurs between required speed and possible speed.

One can see in the right graph a longer covered time, due to the fact that the vehicle is driving slower than supposed.

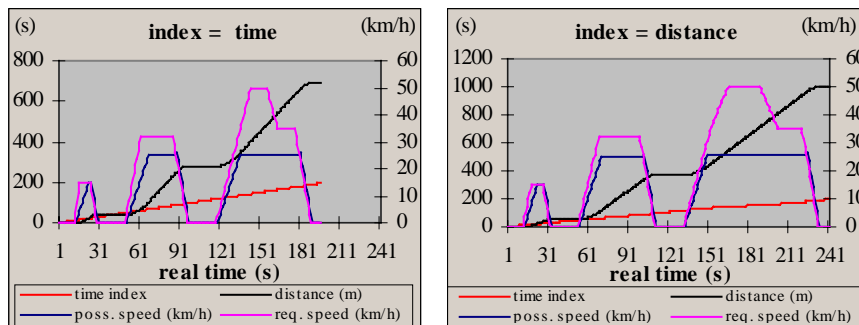


Fig. 6.4: Comparison between route profile definitions

6.3 Electricity Production .vi

The electricity production will cause background emissions. At the contrary of direct emissions these background emissions are not produced at the place of vehicle operation. These values are function of the type of power plant (nuclear, coal, gas, wind, water, ...) and the relative contribution of each power plant to the consumed energy. To know the amount of emissions generated by the production of one unit (1 kWh) of electricity, one must know the exact production mix (i.e. the division of electricity production over the different power plants) in the area considered, according to the time of the day and the season. However, since the electricity grids in Europe are connected in an international mesh network, it is very difficult to attribute a particular energy flow of an appliance (i.e. an electric vehicle) to one particular power plant. It is thus necessary to consider the overall primary energy mix in Europe and to treat all consumers of electrical energy equally: all energy users are divided equally between all power plants in the system. This is a medium worst case for EV's.

Using the average electricity production mix as a basis, seems at first sight a straightforward approach, but it is not completely correct.

First of all electric vehicles will be charged mostly during the night, with a total different composition of electricity production then the average. Taking into account that night time electricity production mainly relies on the so-called "base" power stations, which have generally a better efficiency and lower relative emissions, this approximation of the average production mix will give a slightly "pessimist" image of electric vehicle emissions.

Further, the average contains also old power plants. If one wants to take into account the introduction of electric vehicles in the next ten years, then one needs to consider the investment policy of the electricity production companies. In Belgium most new power plants are of the Steam and Gas Combined Cycle (SGC) type. The SGC has an efficiency of 53% [177]. Furthermore there is a moratorium on nuclear energy. The energy shall be produced by other power plants. It has to be noticed that the introduction of electric vehicles is wrongly coupled with the promotion of nuclear power plants. This point of view can be compared with discouraging the use of trains and trams for public transportation because they use electricity that can possibly be delivered by nuclear power plants.

A third consideration is related with individual electricity production. Companies, institutes (like universities, governments administrations,...), can combine their central heating system with a high efficient electricity generator. This is called the Combined Heat Power (CHP) system. The system produces electricity (with an efficiency up to 50%) as well as heat for the heating of buildings (the overall efficiency of this system can be higher than 80%) [177]. In this case one can consider that the fleet of electric vehicles of that company is charged by their own power plant. The same can be said for a private person who installs solar cells or

Not only within one country there are differences between the types of power plant but there are also variations between diverse countries. France and Belgium for example, rely heavily on nuclear power, while in the U.K or in Denmark coal is the most important primary energy. In countries where the geographical situation permits, such as Norway or Switzerland, hydroelectric energy is predominant. If VSP would be used in Norway, the background emissions would quasi be nihil, since the entire electricity consumption is provided by hydraulic.

Taking together all European power stations, one comes to the production mix illustrated with Table 6.3. In this table the percentage of the total electricity production in function of the fuel type is given for Europe, Belgium and the best and worst European country. The best country corresponds to the lowest emissions and vice versa. The other countries are added below.

In function of this production mix an average emission level can be calculated for each pollutant in function of the energy production, as illustrated with Table 6.4. This table takes into account extraction and transportation of fuel; the processing of fuel and transport to the power plant as well as the generation, transmission and distribution of electricity.

Table 6.4: Emissions from electricity production [Error! Bookmark not defined.]

	CO ₂ g/kWh	CO mg/kWh	NO _x mg/kWh	HC mg/kWh	SO ₂ mg/kWh	CH ₄ mg/kWh	PM mg/kWh
<i>European average</i>	458,6	76,7	1173,2	81,4	2681,6	1017,4	140,8
<i>Belgium</i>	339,5	60,1	1041,8	43,9	1920,6	865,1	97,9
<i>Norway (best)</i>	6,1	2,2	10,1	0,7	13,3	2,2	0,7
<i>Denmark (worst)</i>	926,3	154,8	2921,8	88,9	3286,4	3249,7	225,7
<i>Austria</i>	226,4	52,2	333,7	57,6	267,1	289,1	24,8
<i>Finland</i>	558,4	139,0	1106,3	56,2	712,8	1119,2	84,2
<i>France</i>	63,4	11,5	219,6	11,5	662,0	130,0	28,4
<i>Germany</i>	682,9	98,3	1102,7	33,8	3353,4	1674,4	202,3
<i>Greece</i>	1067,0	139,3	1417,0	140,0	3525,1	2174,4	224,6
<i>Ireland</i>	766,4	121,7	2419,2	160,6	5902,2	1680,1	267,5
<i>Italy</i>	585,0	120,2	1986,1	379,1	3517,9	402,5	148,0
<i>Luxemburg</i>	366,8	58,3	324,4	60,8	256,0	98,3	13,3
<i>Netherlands</i>	632,5	113,8	1014,5	115,2	666,7	1413,0	68,4
<i>Portugal</i>	613,4	122,4	1825,6	193,3	4538,5	1292,4	213,8
<i>Spain</i>	456,5	69,8	1491,1	57,6	4448,9	1104,5	208,1
<i>Sweden</i>	74,2	21,6	151,9	23,8	124,9	79,9	11,2
<i>Switzerland</i>	23,8	9,0	46,4	5,0	77,4	2,5	4,0
<i>UK</i>	604,1	98,6	2274,5	72,7	5204,9	1652,0	251,6

A theoretical model can be established allowing the user to define the relative contribution of each type of electricity production plant. For each type of pollutant one can use the specific power plant emission SE_{pp} (kg/GJ), the relative contribution RC_{pp} (%) and efficiency η_{pp} of each considered power plant (PP) to calculate the total background emissions BE (g/km). Furthermore the background emissions are

function of the electricity consumption E_{grid} (Wh/km), which is required to recharge the battery, and of the efficiency of electricity transportation and distribution η_{grid} .

$$BE = 0,0036 \cdot \frac{E_{grid}}{\eta_{grid}} \left\{ \frac{RC_{pp} \cdot SE_{pp}}{\eta_{pp}} \right\} \quad (6.10)$$

This formula is used to calculate the background emissions for CO, CO₂, NO_x, HC, CH₄, SO₂ and particles.

Additionally to the selection of a desired country the user can select a theoretical model in which these contributions can be freely chosen.

Forecasts of emissions from electricity production by Sporckmann (1997) [153] suggest that electricity emissions will have decreased by 2000 due to the introduction of further emissions control technologies and the increased use of less polluting fuels. He assume that the basic technology mix remains unchanged, but that newer plants replace older ones and will be equipped with Selective Catalytic Reduction exhaust gas treatment units. The total effect in the year 2020, with respect to the year 1994, is -70% for NO_x and SO₂, and -50% for HC and particles.

6.4 Fuel Refinery .vi

Crude oil provides the raw input of most current transport fuel production. Crude oil is essentially a complex mixture of hydrocarbons with very different chemical and physical properties. The processing of crude oil is aimed at separating the mixture into groups of chemicals with similar properties for use in particular applications. The route from extraction of the crude oil to the use of the individual refined components is long and complex. Emissions result from the extraction (gas flaring, venting, gas turbines), transportation (energy used, losses), processing (different refinery types) and distribution (mainly VOC evaporation for gasoline) of crude oil [154].

Table 6.5: Efficiency values for fuel preparation

	Efficiency (%)
Fuel transport	99,7
Refinery	92,5
Oil transport	98,0
Oil mining	99,0
Total preparation	89,5

Hence, for life-cycle emissions of internal-combustion engine vehicles not only the tailpipe emissions, but also the energy loss and emissions generated during oil

transport and refining should be considered. This can be calculated out of the energy content of the consumed fuel (in kWh).

Table 6.6 shows the emissions for the fuel preparation taking into account the extraction (offshore) and transport of crude oil, the refining and the distribution (transport and evaporation) of fuel. In the case of bio fuels the agriculture, transport, processing, distribution and storage are considered. Also the extra required energy for these processes are taken into account.

Table 6.6: Emission for fuel preparation [Error! Bookmark not defined.]

	CO2 g/kWh	CO mg/kWh	Nox mg/kWh	NMHC mg/kWh	CH4 mg/kWh	SO2 mg/kWh	PM mg/kWh
<i>Gasoline</i>	33.1	18.4	151.9	761.4	62.6	236.2	8.6
<i>Diesel</i>	24.5	16.6	129.6	315.4	56.5	174.2	3.6
<i>LPG</i>	21.6	14.8	116.3	202.7	58.0	114.1	5.4
<i>Kerosene</i>	23.0	16.2	130.7	298.4	57.6	192.6	4.3
<i>Heavy fuel oil</i>	19.8	14.4	114.5	283.7	53.3	100.4	4.3
<i>CNG</i>	14.8	5.0	38.2	99.0	805.3	60.8	2.9
<i>Bio fuels - RME</i>	108.7	493.2	871.9	280.4		245.5	66.6

6.5 Heater .vi

The “**Heater .vi**” is a small subprogramme containing the data of a potential burner to heat the interior of the vehicle. These burners will produce small additional direct emissions (in g/h) and they have a specific fuel consumption (in L/h). By multiplying them with the total trip Time (in s) and dividing by the covered distance the corresponding *direct emissions* in g/km and fuel consumption in L/km are calculated. The user can select whether or not this burner is enabled. These direct emissions are added to the other direct emissions (coming from a possible engine of the vehicle drivetrain).

The implemented data are only for comparative purpose. The model does not consider any influence of the ambient temperature. Furthermore it indicates only the level of emissions for one type of heater. When the data is available this model can easily be extended to a model for each vehicle of the database, taking into account it’s specific heater emission and fuel consumption.

6.6 Error Message .vi

In case an Acceleration or Power Reduction is required, an error message will be displayed indicating which vehicle component is not able to deliver the demanded performance and the reason why. The user can continue the simulation by clicking on the OK button or by pressing RETURN.

Often the error situation lasts for several times. Nevertheless it will be displayed only one time. Furthermore when a simulation is finished and the user likes to perform another one, he can select if the error message should be reset or not. If not, the previous manifested messages will not be displayed during this second simulation.

With each error corresponds an error index. All error indexes smaller than 10 are general messages concerning the simulation process itself. The first digit, of error indexes higher than 10, corresponds to the component, the second to the physical parameter that is exceeded. Table 6.7 shows all errors messages implemented up-to-now.

Table 6.7: List of error messages implemented up-to-now

0		Iteration problem
1		Data out of range
2	Simulation Process	Impossible settings
5		Drivetrain strategy limits
8		Problem
9		Energy sources empty
12		Maximum wheel power (wheel slip)
20	Motor	You are going to overspeed your motor
21		Your motor is overloaded (torque)
22		Motor overloaded (power)
34	DC-bus	Maximum DC-bus voltage
36		Regeneration is higher than desired deceleration
42	Battery	Battery overloaded
43		Battery current too high
44		Battery voltage too high
45		Battery voltage too low
49		Battery empty!
50	Generator	You are going to overspeed your generator
52		Generator overloaded
60	Engine	You are going to overspeed your engine
62		ICE overloaded
65		Engine is starting
66		Clutch is slipping
69		Fuel tank empty
72	Fuel cell	Fuel Cell overloaded
80	Flywheel	Flywheel out of speed limits
82		Flywheel overloaded
85		Key switch Flywheel OFF
100		VSP starts

7 VEHICLE DRIVETRAINS

In this chapter the general description of the vehicle drivetrain model can be found. The description of the components is given in chapters 8, 9, and 10. Eighteen vehicles are up-to now introduced in the database. Following different types of drivetrain are implemented:

- *Battery Electric Vehicle* *BEV*
- *Flywheel Electric Vehicle* *FWEV*
- *Fuel Cell Electric vehicle* *FCEV*
- *Diesel Electric Vehicle* *DEV*
- *Internal Combustion Vehicle* *ICV*
- *Series Hybrid Electric Vehicle* *SHEV*
- *Parallel Hybrid Electric Vehicle* *PHEV*
- *Combine Hybrid Electric Vehicle* *CHEV*
- *Fuel Cell Hybrid Electric Vehicle* *FCHEV*

Other drivetrain topologies are as well possible to implement in the software tool. This can be done on a straightforward way by connecting one component to another. The different drivetrain topologies are described in the following chapters.

7.1 Battery Electric Vehicle .vi

The “**Battery Electric Vehicle .vi**” contains a model for the drivetrain of a pure electric vehicle. This model is activated each sequence of a required speed cycle (see “**VSP .vi**”). It contains the iteration process to define the possible acceleration and speed. The approach used for modelling the electric vehicle drivetrain is compatible for all kind of drivetrains. The front panel (user interface) is illustrated with Fig. 7.1

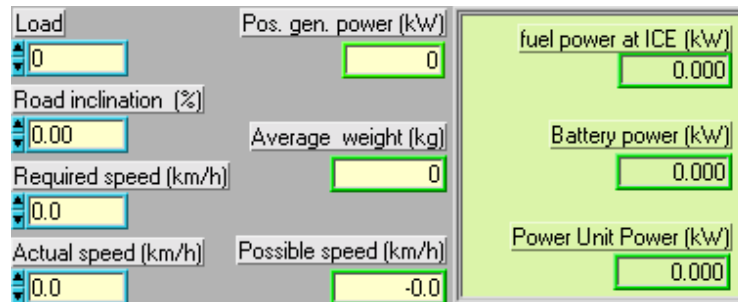


Fig. 7.1: Front panel of Battery Electric Vehicle .vi

This model is composed of a sequence structure of three frames.

In the *first frame* an initialisation for the iteration parameters is set as well as for the battery voltage. The required acceleration $a_v(\text{m/s}^2)$ corresponding to the current $v_{\text{cur}}(\text{km/h})$ and required velocity $v_{\text{req}}(\text{km/h})$ is calculated. $T_s(\text{s})$ is the selected time step.

$$a_v = \frac{v_{\text{req}} - v_{\text{cur}}}{T_s \cdot 3,6} \quad (7.1)$$

The *second frame* contains the actual iteration loop and the different components of the drivetrain. This is based on an algorithm that can be used for all different drivetrains. It simulates the state of each component backward from the body and wheels through the drivetrain up to the primary energy source.

Each component is modelled as a black box. Fig. 7.2 illustrates the second frame of the block diagramme. In the model of this electric vehicle one can recognise from left to right the sub.vi's for body (1), the wheels (2), the differential (3), the gear (or reductor) (4), the motor (5), the convertor (6) and the battery (7). One can also find the model for the auxiliaries (8).

In the right bottom corner of the diagramme the core of the iteration algorithm is located, the "**Iteration Algorithm .vi**" (9). This subprogramme controls the iteration process. When the AR is different from one, the required acceleration $a_v(\text{m/s}^2)$ is reduced in the following iteration step to the possible acceleration $a_{\text{pos}}(\text{m/s}^2)$. Once the possible acceleration is found, the iteration loop stops. A detailed description of this "**Iteration Algorithm .vi**" can be found in chapter 8.

$$a_{\text{pos}} = AR \cdot a_v \quad (7.2)$$

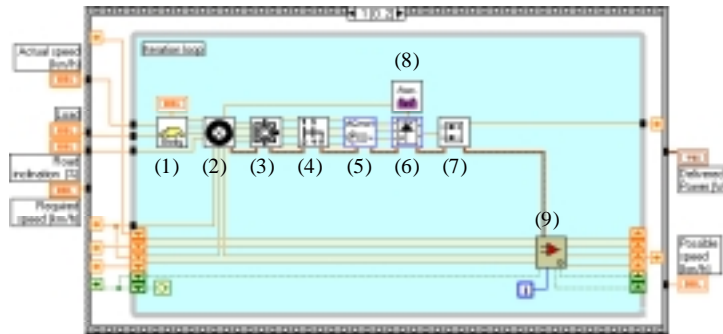


Fig. 7.2: Block diagramme of second frame of Battery Electric Vehicle .vi

In the *third frame* the possible speed $v_{\text{pos}}(\text{km/h})$ is calculated (7.3).

$$v_{\text{pos}} = v_{\text{cur}} + a_{\text{pos}} \cdot T_s \cdot 3,6 \quad (7.3)$$

The corresponding delivered power is stored in a cluster as an output of the “**Battery Electric Vehicle .vi**”. Due to the fact that this model is compatible with the models for other types of drivetrains, this cluster also contains the outputs for the delivered fuel power and the power from a third power unit like a flywheel. These values are in this case set to zero.

7.2 Flywheel Electric Vehicle .vi

The model of the flywheel electric vehicle is similar to the battery electric vehicle. Only the differences are described below.

The model for the electrical flywheel itself (“**Flywheel .vi**”) was originally developed as peak power unit that could be used in the “**Series Hybrid Vehicle .vi**”. Due to the modularity of the simulation programme and the flexible iteration process, this flywheel model can also be used instead of the battery model of the “**Battery Electric Vehicle .vi**”.

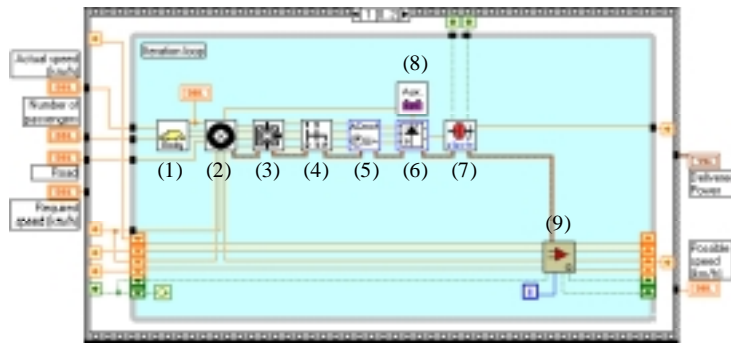


Fig. 7.3: Block diagramme of second frame of Flywheel Electric Vehicle .vi

Fig. 7.3 illustrates the block diagramme of the programme. In this figure one can recognise from left to right the sub.vi’s for the body (1), the wheels (2), the differential (3), the gear (or reductor) (4), the motor (5), the converter (6) and the flywheel (7). One can also find the model for the auxiliaries (8) and for the iteration algorithm (9).

The fundamental principles as described in the “**Battery Electric Vehicle .vi**” are still valid. The power that previous was required from the battery is now demanded to the flywheel.

7.3 Fuel Cell Electric Vehicle .vi

It is not only possible to replace the battery by a flywheel model, but with a simple 'click and replace' one can build a pure fuel cell electric vehicle as illustrated with Fig. 7.4. In this figure one can recognise from left to right the sub.vi's for the body (1), the wheels (2), the differential (3), the gear (or reductor) (4), the motor (5), the convertor (6) and the fuel cell (7). One can also find the model for the auxiliaries (8) and for the iteration algorithm (9).

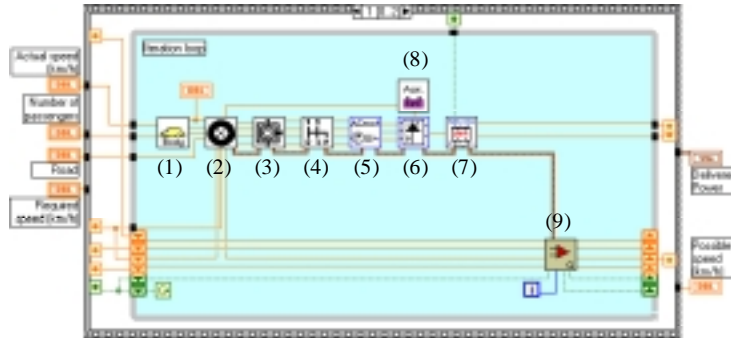


Fig. 7.4: Block diagramme of second frame of Flywheel Electric Vehicle .vi

7.4 Diesel Electric Vehicle .vi

The battery can also be replaced by an internal combustion engine as illustrated with Fig. 7.5. This type of drivetrain is not to be confused with a series hybrid electric vehicle that additionally contains a battery (see further).

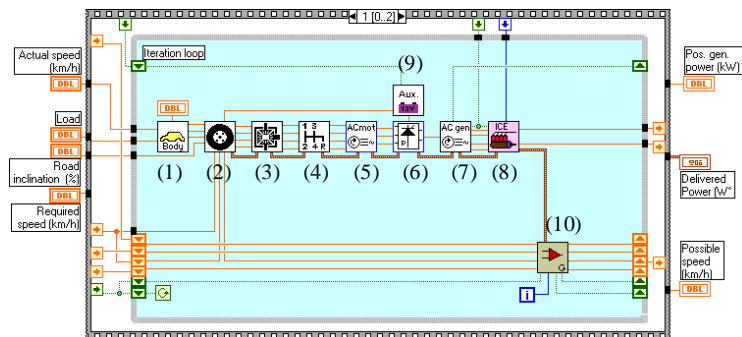


Fig. 7.5: Block diagramme of second frame of Diesel Electric Vehicle .vi

In this figure one can recognise from left to right the sub.vi's for the body (1), the wheels (2), the differential (3), the gear (or reductor) (4), the motor (5), the

converter (6), the generator (7) and the ICE (8). One can also find the model for the auxiliaries (9) and for the iteration algorithm (10).

7.5 Thermal Vehicle .vi

The same iteration algorithm is applicable on the models of internal combustion vehicles.

In the initialisation frame the function of the engine has to be selected. Due to the fact that this engine model must be relevant in different kind of drivetrain topologies (parallel, series, combined hybrid electric as well as in thermal vehicles) the iteration process should act in the appropriate manner. Indeed when the engine is used in an APU the powerflow should be adapted when e.g. the engine is overloaded. However when this engine model is used in an internal combustion vehicle the acceleration should be reduced to keep the engine operating point within its boundaries. Additional information can be found in subchapter 11.8 Engine .vi.

Furthermore in this initialisation phase the engine key switch is turned ON and although there is no battery in a thermal vehicle, the battery voltage is initialised because the programme uses the same iteration algorithm as for the other types of drivetrains.

In Fig. 7.6 one can recognise from left to right the sub.vi's for the body (1), the wheels (2), the differential (3), the gear (4), the clutch (5) and the engine (6). One can also find the model for the auxiliaries (7). This auxiliary system is also in charge of the power required for the starter motor to switch on the engine.

The delivered power corresponding to the fuel consumption is put in a cluster as an output of the **“Internal combustion vehicle .vi”**. This power is defined in the **“Engine .vi”** model (see subchapter 11.8).

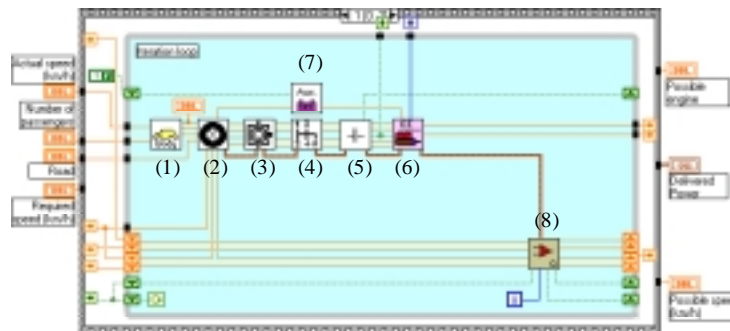


Fig. 7.6: Block diagramme of second frame of Internal combustion vehicle .vi

7.6 Series Hybrid Vehicle .vi

The model becomes somewhat more complicate in the case of hybrid drivetrains. Once again the iteration process is applicable on all kind of hybrid vehicles.

The powerflow in the drivetrain of hybrid vehicles can be controlled in different ways taking into account diverse criteria and desiderata (see Part I). The implementation of the control strategies is described below as well as in the different component description. The drivetrain strategy is implemented in two levels: the primary control algorithm and the component dedicated control algorithm. The former defines whether or not the APU operates as well as the fundamental iteration order. The latter is used to take the component proper characteristics into account. In the case of this series hybrid vehicle the main control of the powerflow can be found in the “**DC-bus controller .vi**” (see subchapter 9.1).

Like the other drivetrain models the “**Series Hybrid Vehicle .vi**” contains a sequence structure of three frames.

In the *first frame* an initialisation of the iteration parameters is done as well as of the battery voltage. The required acceleration a_v corresponding to the current speed v_{cur} and required speed v_{req} is calculated (see equation (7.1)).

The selection of the APU engagement can be done on the front panel of this vehicle (see Fig. 7.7). This selection can be based on the following criteria (described in subchapter 3.4.1):

1. In function of the vehicle velocity. If the vehicle velocity drops under a certain limit the APU can be switched off.
2. In function of whether or not the vehicle is running in a city centre defined by the speed cycle.
3. In function of the State of Charge (SoC) of the battery, which control is implemented as a hysteresis loop with the help of the “**Hysteresis .vi**” subprogramme.
4. In function of a combination of case 2 and 3, where the switching-off velocity is defined in function of the SoC of the battery.
5. Finally the user can select the minimum time the APU needs to be engaged before it can be switched off.

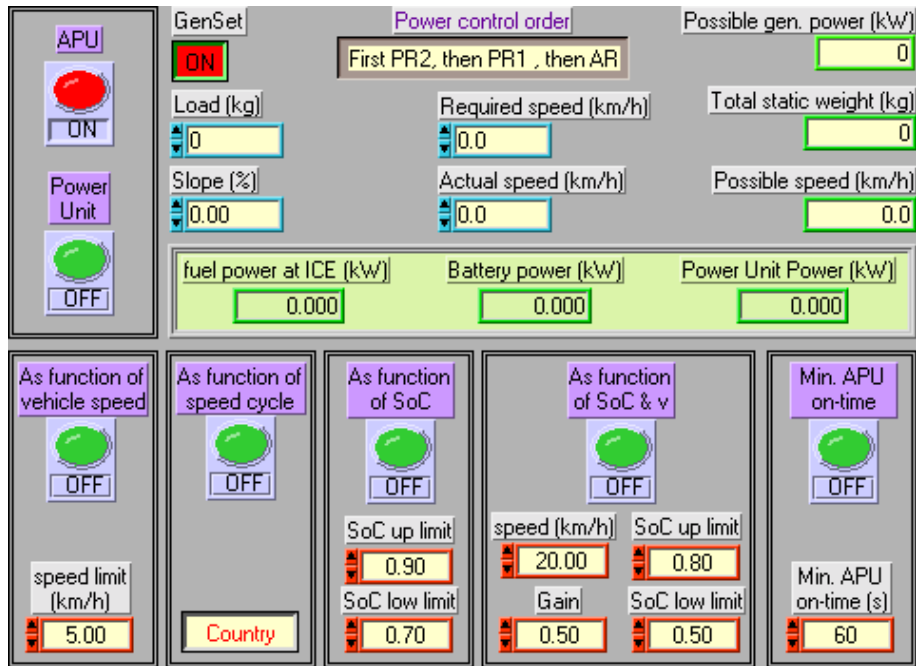


Fig. 7.7: Front panel of Series Hybrid Electric Vehicle .vi

The user has the possibility via the front panel to disengage the APU independently from the previous criteria. In any case this is also done when the fuel tank is empty.

If the series hybrid vehicle contains also a power unit, e.g. flywheel or supercapacitor, a second ON/OFF switch is foreseen to whether or not engaging this unit.

Furthermore the fundamental iteration order is selected in this front panel too. This iteration order is described in detail in subchapter 8.6. Basically it describes if the operating setpoint of the APU is dominant on the performance of the vehicle or if it is allowed to modify the powerflow in the drivetrain to improve vehicle performance. In the first case the AR will be implemented before a PR and vice versa in the second case.

The *second frame* contains the iteration loop as illustrated by Fig. 7.8. In this figure one can recognise from left to right the sub .vi 's for the body (1), the wheels (2), the differential (3), the gear (4), the motor (5), the convertor (6), the DC-bus-controller (7) and the battery (8).

At the level of the battery one sees from top to bottom the flywheel (9) and the APU consisting in a generator (10) and an engine (11).

Under the battery one can find the braking resistant (12) to possibly protect the battery against over-voltage. One can also find the model for the auxiliaries (13).

In the right bottom corner of the diagramme the core of the iteration algorithm (14) is located.

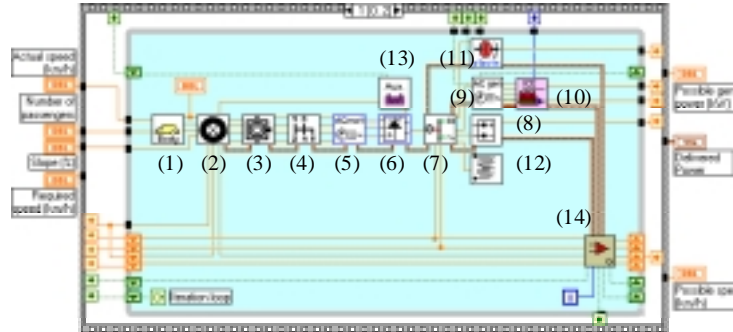


Fig. 7.8: Block diagramme of second frame of Series Hybrid Electric Vehicle.vi

In the hybrid drivetrains, next to the acceleration, this iteration process controls the Power Distribution Factors (PDF1 and PDF2) via the Power Reductions 1 and 2 (equation (7.4)). These Power Distribution Factors define the relative distribution of the power between the different parts of the drivetrain. PDF_1 will determine how much power the APU will deliver (see equation (7.5)), and PDF_2 gives the part that will be produced by the flywheel (see equation (7.6)). The remaining part of the required traction power is assigned to the battery (see equation (7.7)). All these equations are implemented and further elucidate in the “**DC bus controller .vi**” and in the “**Iteration Algorithm .vi**”. Once the possible acceleration, PDF_1 and PDF_2 are found, the iteration loop stops.

$$PDF_{pos} = PR \cdot PDF_{req} \quad (7.4)$$

$$P_{gen} = PDF_1 \cdot P_{gen}^{setpoint} \quad (7.5)$$

$$P_{pu} = PDF_2 \cdot (P_{req} - P_{gen}) \quad (7.6)$$

$$P_{bat} = P_{req} - P_{gen} - P_{pu} \quad (7.7)$$

With :

- PDF_{req} : required Power Distribution Factor
- PDF_{pos} : possible Power Distribution Factor
- PR : Power Reduction
- PDF_1 : Power Distribution Factor 1
- PDF_2 : Power Distribution Factor 2
- $P_{gen}^{setpoint}$: generator set point power (W)
- P_{gen} : generator power (W)
- P_{pu} : power unit (flywheel) power (W)
- P_{bat} : battery power (W)
- P_{req} : required power (W)

In the *third frame* the possible speed (v_{pos}) is calculated (see equation (7.3)). The delivered battery power as well as the delivered fuel power and the power from flywheel are stored in a cluster as an output of the “**Series Hybrid Vehicle .vi**”. The DC power delivered by the APU is an additional output of the programme.

7.7 Parallel Hybrid Vehicle .vi

The topology of a parallel hybrid drivetrain is rather different from the one of a series hybrid drivetrain, but the modelling is quite similar and once again the same iteration process is used.

The “**Parallel Hybrid Vehicle .vi**” model contains a sequence structure of three frames.

Switching On or OFF the engine can be selected based on the same criteria as described in the “**Series Hybrid Vehicle .vi**”. When the engine is disengaged it can be mechanically declutched from the rest of the drivetrain and operated in idle mode or it can be completely switched off. This is implemented in the clutch model (see “**Clutch .vi**”, see subchapter 11.7).

Analogue to the model of other drivetrains the iteration loop determines the possible acceleration and Power Distribution Factor (PDF). The PDF of a parallel hybrid drive defines the relative distribution of the power between the electric motor and the internal combustion engine (see (7.8) and (7.9)). This power division and the diverse definitions of the PDF are implemented in the “**Torque Splitter .vi**” (see subchapter 9.2), which is essentially a model of a toothed gear, together with a PDF controller.

$$P_{ol} = PDF.P_i \quad (7.8)$$

$$P_{o2} = (1 - PDF) \cdot P_i \quad (7.9)$$

With :

- PDF : Power Distribution Factor
- P_i : input power from wheels (W)
- P_{o1} : output 1 power to engine (W)
- P_{o2} : output 2 power to battery (W)

In the parallel hybrid vehicle model of Fig. 7.9 one can recognise from left to right the sub.vi's for the body (1), the wheels (2) and the differential (3). Beside one can find the torque splitter (4) that divides the required traction torque between the electric motor (5), inverter (6) and battery (7) on one side and gear (8), clutch (9) and engine (10) on the other side (above). One can also find the model for the auxiliaries (11). In the right bottom corner of the diagramme the core of the iteration algorithm (12) is located.

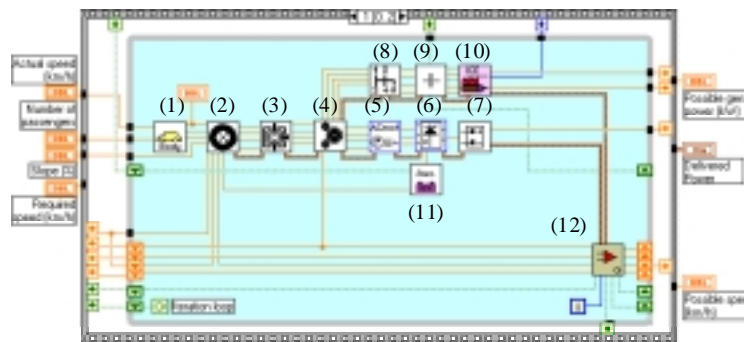


Fig. 7.9: Block diagramme of second frame of Parallel Hybrid Electric Vehicle .vi

7.8 Combined Hybrid Vehicle .vi

The combined hybrid drivetrain is one of the most complex models of the Vehicle Simulation Programme. It combines the series hybrid with the parallel hybrid drivetrain.

Switching ON or OFF the engine can be done based on the same criteria as described in the “**Series Hybrid Vehicle .vi**”. Opposed to the parallel hybrid drive when the engine is disengaged it cannot be mechanically declutched from the rest of the drivetrain. But the planetary gear, which connects the engine with the torque splitter, can be locked (see “**Planetary gear .vi**” of subchapter 9.3).

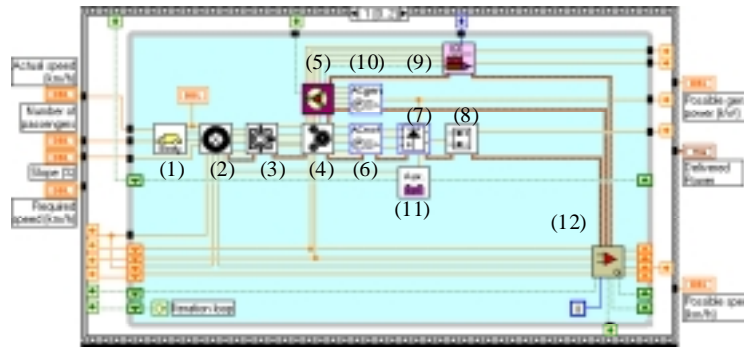


Fig. 7.10: Block diagramme of second frame of Combined Hybrid Electric Vehicle .vi

This combined hybrid vehicle is build up from left to right with the following sub.vi's: the body (1), the wheels (2) and the differential (3). Beside one can find the torque splitter (toothed gear) (4) that divides the required traction torque between the planetary gear (5) on one side and electric motor (6), inverter (7) and battery (8) on the other side. The torque division is controlled via the Power Distribution Factor 1 (PDF_1).

Until now one has the same approach as for the parallel hybrid drivetrain.

The planetary gear itself introduces a second degree of freedom in comparison with the parallel hybrid drive. The planetary gear set divides the engine (9) driving force into two forces: one that drives the wheels, via the torque splitter, and the other that drives a generator (10). The electrical energy, produced by the generator, is re-converted into mechanical energy through the electric motor or stored in the battery. Within the iteration process a second PDF_2 will control the power path of the generator. This PDF_2 is not entirely unrelated with the PDF_1 , due to the fact that the generator power is dependent from the power division in the torque splitter (see subchapter 9.2). The generator velocity setting determines the speed of the engine. This is explained in “**Planetary gear .vi**” with equation (9.26). Hence the working of the internal combustion engine can be fully controlled independently from the required traction force and vehicle velocity (see subchapter 9.3).

Furthermore one can also find the model for the auxiliaries (11).

In the right bottom corner of the diagramme the model controlling the iteration process is located (12).

The delivered battery power as well as the delivered fuel power is stored in a cluster as an output of the “**Combined Hybrid Vehicle .vi**”. The by the engine delivered mechanical power as well as the power delivered by the generator to the inverter are additional outputs of the programme.

7.9 Fuel Cell Hybrid Electric Vehicle .vi

The fuel cell hybrid electric vehicle is the last implemented drivetrain topology. Basically it is the same model as that of the series hybrid electric vehicle in which the APU is replaced by a fuel cell.

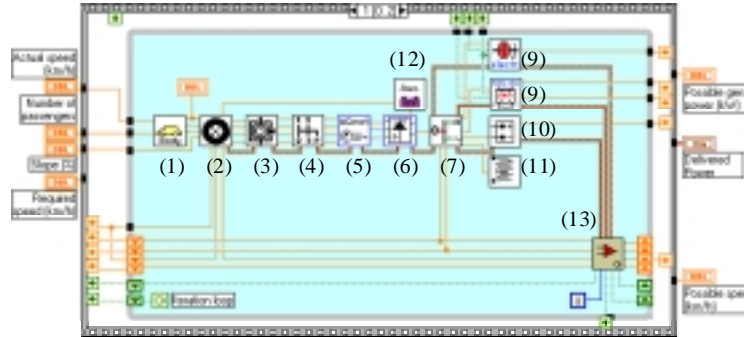


Fig. 7.11: Block diagramme of second frame of Fuel Cell Hybrid Electric Vehicle .vi

The “**Fuel Cell Hybrid Vehicle .vi**” is composed of (from left to right in Fig. 7.11) the sub .vi 's for the body (1), the wheels (2), the differential (3), the gear (4), the motor (5), the converter (6) and the DC-bus-controller (7). This DC-bus-controller regulates the powerflow of (from top to bottom) a potential flywheel (8) (can be discard), the fuel cell (9), the battery (10) and the braking resistant (11). All these components can be disengaged if required. The fuel cell plays the same role as the APU of the series hybrid drivetrain. The fundamental principles as described in the “**Series Hybrid Vehicle .vi**” are still valid.

8 ITERATION ALGORITHM

In Part I several concepts of the calculation methodology are clarified: uniform iteration process, modular programme, Acceleration reduction, Power Reduction, iteration order, inherent implemented powerflow control strategy, etc. Based on these concepts an in-depth description of the iteration algorithm is explained in this chapter.

8.1 Philosophy

In the case of an electric or thermal vehicle the AR will reduce the acceleration of the vehicle. Hence the required torque will decrease as well as the corresponding power.

In the case of hybrid vehicles different solution are possible to keep the operating points of a component within limits. The iteration process is much more complex. A PR can change the Power Distribution Factor (PDF) or the AR can reduce the acceleration. Which one has to be implemented first makes part of an intelligent iteration order (see further). An AR and a PR can be introduced at the same time. When only one of them is first implemented, the limit of the other can already have disappeared.

To be able to explain the philosophy of the iteration process some definitions should be introduced. Each hybrid drivetrain are theoretically divided in three parts: a 'common subsystem', an 'acceleration subsystem' and a 'power subsystem'.

- *The **acceleration subsystem** defines in essence, via the Acceleration Reduction factor, the mechanical quantities of the vehicle.*
- *The **power subsystem** is characterised principally by powerflow, which is controlled in the simulation programme with the help of the PDF via the Power Reduction factor.*
- *All traction effort to drive the wheels, coming from the acceleration subsystem as well as from the power subsystem, goes through the **common subsystem**.*

The name of these subsystems is related to the simulation methodology and not necessarily to the function of the components being part of that subsystem. The components can have different functions. A component of the acceleration subsystem can deliver a constant power and a component of the power drivetrain can be in charge of the acceleration of the vehicle (see further). Consequently these definitions are theoretical names to explain the iteration algorithm.

Table 8.1 defines to which part of the drivetrain the components of the different vehicle types belong to. The acceleration subsystem always contains the battery and the power subsystem the engine (or other energy source).

Table 8.1: Acceleration and power subsystem

	Common subsystem	Acceleration subsystem	Power subsystem
EV	body, wheels, differential, reductor	motor, convertor, battery	not present
ICV	body, wheels, differential, gear	clutch, engine	not present
SHEV	body, wheels, differential, reductor, motor, convertor, dc-bus-controller	battery	generator, engine, (possible flywheel)
PHEV	body, wheels, differential, torque splitter	motor, convertor, battery	gear, clutch, engine
CHEV	body, wheels, differential, torque splitter	motor, convertor, battery	planetary gear, engine, generator

As explained in the previous chapter the division of power between engine and battery in a series hybrid drivetrain is controlled in the “**DC-bus controller .vi**”. In a parallel hybrid vehicle this is implemented in the “**Torque Splitter .vi**”. From the beginning of the force calculation in the “**Wheel .vi**” the acceleration force and resistive force are two separated parameters. The resistive force is the force corresponding to the friction force, aerodynamic force and the climbing force. The acceleration force is proportional to the vehicle acceleration (for further description see chapter 7). By having the acceleration force separated from the resistive force it is possible to calculate the possible acceleration. This process is always performed in the acceleration subsystem. The power subsystem delivers ‘resistive’ power. This basic philosophy allows the control of the acceleration as well as the power distribution (PDF). The fact that the acceleration subsystem is responsible for the acceleration of the vehicle does not mean that the power delivered by the power subsystem is not used for acceleration. The power of the power subsystem will reduce the required power of the acceleration subsystem and hence it will take part in the acceleration process in an indirect way (see paragraph 8.6)

8.2 The Reduction Parameters

The iteration process is structured taking into account three types of limits:

- Speed limit (ω -max)
- Torque limit (T-max)
- Power limit (P-max)

All other limits (current and voltage) are to be transformed to power limits. Hence the iteration process could be uniformed. Also the speed and torque could be converted to a power limit, but this would decrease the iteration accuracy. Due to the straightforward relationship between the acceleration on one side and the velocity and torque on the other side, one should keep this close liaison, instead of

passing through a power limit conversion. Each type of limit can result in an AR, a PR or both. The next paragraphs will describe the different possibilities. Fig. 8.1 illustrates these possibilities.

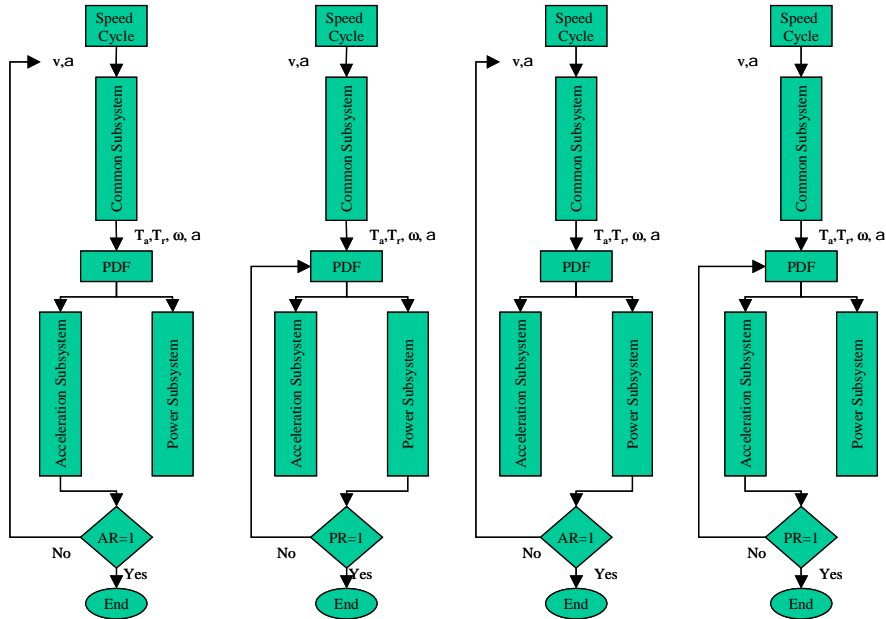


Fig. 8.1: AR and PR of acceleration subsystem or power subsystem

The AR is used as a feedback to control the vehicle acceleration. Mostly the AR will be defined in the common subsystem or the acceleration subsystem. In an exceptional case (PHEV, see 8.3.2) it can be defined in the power subsystem.

The PR controls the PDF and is hence used in the feedback loop defining the power distribution between acceleration and power subsystem. PR's will never be generated in the common subsystem, but however can either be defined in the acceleration or power subsystem.

8.3 Acceleration Reduction Calculation

In an iteration process it is necessary to have a constant reference. During the iteration process the vehicle velocity will remain constant, which corresponds to a constant resistive torque.

When the required torque is higher than the maximum torque the iteration process will act on the acceleration to reduce the acceleration torque T_a , which is

proportional to the acceleration a (see equation (10.11)). When the required torque exceeds the maximum torque T_{\max} the Acceleration Reduction will be calculated by comparing the part of maximum torque that can be assigned for acceleration to the required acceleration torque (equation (8.1)). Indeed, due to the fact that the vehicle is running at a certain velocity the resistive torque T_r should be delivered in any case. Thus the possible acceleration torque is the remaining part of the maximum torque that is not assigned to the resistive torque. Hence acceleration is only possible if the maximum torque is bigger than the resistive torque.

$$AR = \frac{T_{\max} - T_r}{T_a} \quad (8.1)$$

$$a_{pos} = a_{req} \cdot AR \quad (8.2)$$

Fig. 8.2 illustrates the calculation methodology. This is an example of a torque limit for a gear. To simplify the example the transmission ratio of the gear is equal to one and its efficiency is 100%.

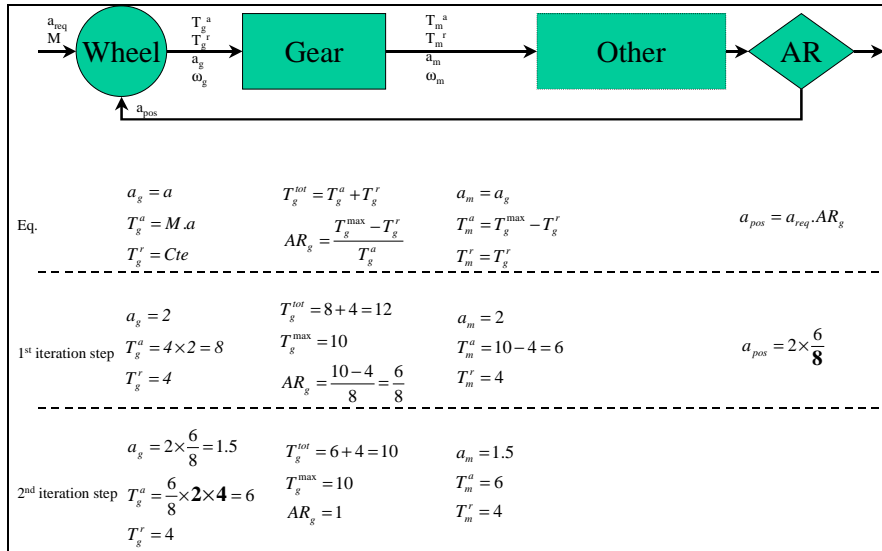


Fig. 8.2: Example of an AR calculation

The values are chosen without dimension just as numeric example: the acceleration equals 2, the weight equals 4 as well as the resistive torque. In the first iteration step the total required gear torque (12) is higher than the maximum torque (10). The AR is calculated in function of acceleration and resistive torque. The output torque of the gear is limited to the maximum value. When all components are successively simulated during this first iteration step, the required vehicle acceleration is reduced

in function of this Acceleration Reduction. Hence in the next iteration step the required acceleration gear torque is lower and the corresponding required total gear torque is equal to the allowed maximum value.

The iteration parameters are grouped in one cluster. This cluster is used in each component of the drivetrain to calculate the possible required reduction. (In LabVIEWTH a cluster defines a group of parameters.) The cluster contains the reference and the reduction parameter: respectively the resistive torque and the Acceleration Reduction. The comparison of maximum and required value, as well as the calculation of the corresponding Acceleration and/or Power Reduction and the visualization of the error message is grouped in one sub programme called. This subprogramme is used in the models of the different components of the drivetrain. In the case of a torque limit this subprogramme is called **“AR, PR (T) calculation .vi”**. For a speed and power limit these are called respectively **“AR, PR (ω) calculation .vi”** and **“AR, PR (P) calculation .vi”**. The reduction of the vehicle required acceleration and Power Distribution Factor are performed in a subprogramme that controls the iteration process and which is called **“Iteration Algorithm .vi”**.

While calculating backwards through the drivetrain the only way the resistive torque reference can change is by change of the transmission ratio of gear units and by the efficiency variation of the mechanical components. The acceleration torque itself of equation (8.1) is not used to calculate the Acceleration Reduction due to the fact that the inertia of each component will also influence this value. The acceleration torque can be obtained by subtracting the resistive torque from the required torque (equation (8.3)). This way the only inputs of the **“AR, PR (T) calculation .vi”** are the maximum torque, the required torque, the possible transmission ratio, the possible efficiency and the reduction cluster.

$$AR = \frac{T_{\max} - T_r}{T_{req} - T_r} \quad (8.3)$$

The output parameters are possible torque and the new reduction cluster. This possible torque is always lower than or equal to the maximum value. The component characteristics are only defined and valid within their operating limits. Thus by using the possible torque instead of the required torque one can be certain to remain within the component working boundaries. E.g. one could calculate the efficiency of a motor based on a fitted efficiency curve. When this curve is expressed as an equation in function of torque and the considered torque value would exceed strongly the validity domain of the function, one could get completely unrealistic extrapolated results.

What to do when in two or more components of the drivetrain the required torque exceeds the operating area ? The first component will introduce an Acceleration Reduction (AR_{prev}) and its output parameters will be limited in function of this

boundary. As the torque in a following component also exceeds the maximum limit, a second Acceleration Reduction will be calculated. Hence all encountered Acceleration Reductions have to be multiplied.

$$AR = \frac{T_{\max} - T_r}{T_{req} - T_r} \cdot AR_{prev} \quad (8.4)$$

Due to the first limit the required value is limited to the maximum value and hence the corresponding acceleration torque is also restricted. But in the “**Iteration Algorithm .vi**” the new possible acceleration will be calculated based on the desired acceleration a_{req} and corresponding desired acceleration torque (equation (8.2)). The desired acceleration is defined by the imposed speed cycle. This means that the denominator of the acceleration reduction must always corresponds with this acceleration torque. This denominator is calculated by subtracting the resistive torque from the required torque. But when this required torque is already limited due to a previous limitation one loses the correlation with the original acceleration torque. By multiplying both Acceleration Reductions one keeps the correlation with the original acceleration torque (equation (8.4)). This reasoning is illustrated with the following example.

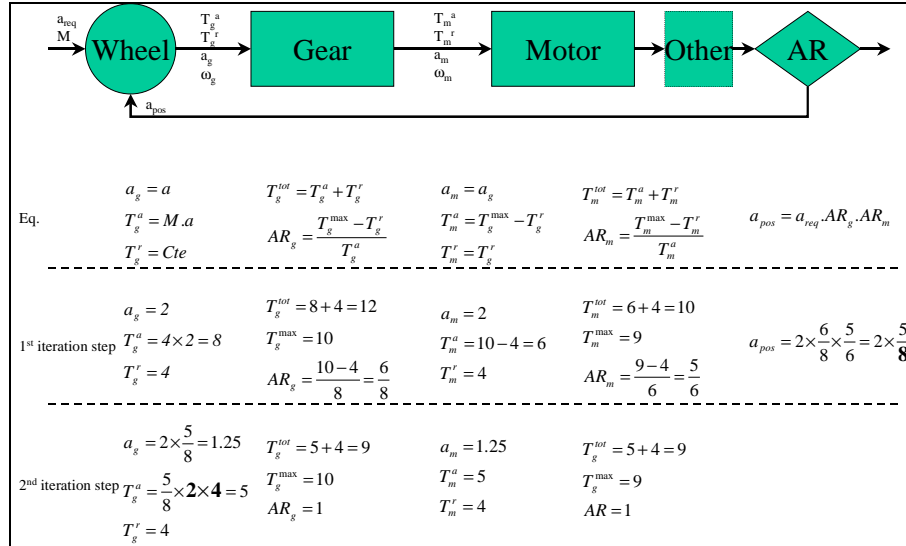


Fig. 8.3: Example of Acceleration Reduction multiplication

Fig. 8.3 shows an example of a torque limit in the gear as well as in the motor. The torque limit of the gear introduces an AR (= 6/8). Its output torque is limited corresponding the maximum value (10). But this required motor torque is still higher than the possible motor torque (9). Hence this motor brings up at its turn a second AR (=5/6). The possible acceleration is calculated by multiplying the

required acceleration with all encountered ARs. In the second iteration step the required gear torque is in this way lower than the maximum gear torque ($9 < 10$) and the total motor torque is equal to the maximum motor torque. Notice that the final denominator equals the original acceleration torque (8).

This chapter explained the fundamental approach for the calculation of the acceleration reduction in the case of a torque limit. The following chapters will give details of the other possible operating limits treatment.

8.3.1 AR, PR (T) Calculation .vi

a) Acceleration Subsystem - Acceleration Reduction

This type is described in the previous chapter.

b) Power Subsystem - Power Reduction

Once a component is used in the power subsystem, it makes no sense to limit the acceleration. At this moment the only way to get the operating point of the component within its maximum limits is by reducing the Power Distribution Factor (PDF), with the help of a Power Reduction (PR) factor. In the case of a parallel or combined hybrid drivetrain this PDF imposes a certain torque that can be seen as a pure resistive torque (see “**Torque Splitter .vi**” in subchapter 9.2). Based on the fundamental philosophy of the iteration process all torque, to accelerate the vehicle, is delivered by the acceleration subsystem. The reference to calculate the Power Reduction in this iteration process will be the torque setpoint T_{sp} defined by the PDF and the required input torque at wheel side T_{req} (equation (8.5)).

$$T_{sp} = T_{req} \cdot PDF \quad (8.5)$$

In the “**Iteration Algorithm .vi**” the calculation process can first iterate towards the possible acceleration, with the help of the Acceleration Reduction, and afterwards it iterates towards the possible PDF. Due to the mechanical connection in parallel and combined hybrid drivetrains, the acceleration of the power subsystem is related to the acceleration of the vehicle. Hence once the possible acceleration is found, the acceleration of the components in the power subsystem is defined. This acceleration leads to additional inertia torques, $T_{inertia}$, which has to be delivered in any case. Thus the possible torque setpoint is the remaining part of the maximum torque that is not assigned to the inertia torque. When the required torque is higher than the maximum torque, T_{max} , the iteration process will act on the PDF to reduce the torque setpoint T_{sp} . When the required torque exceeds the maximum torque the Power Reduction will be calculated by comparing the part of maximum torque that can be assigned to the torque setpoint with the required torque setpoint (equation (8.6)).

$$PR = \frac{T_{\max} - T_{inertia}}{T_{sp}} \quad (8.6)$$

The PR is not defined in function of power by considering the speed (multiplied by torque) since this would increase subprogramme complexity and would decrease the iteration accuracy.

All rotating components of the power subsystem will contribute to the inertia torque. Equation (8.7) defines the required torque of the power subsystem mechanical components. To reduce the number of input parameters of the “**AR, PR(T) calculation .vi**” equation (8.8) will be used to calculate the Power Reduction, in which the same parameters as for the calculation of AR are employed. Similar to the AR no parameters that changes due to inertia are chosen to define the AR and PR. These parameters are the acceleration torque (acceleration subsystem) and the inertia torque (power subsystem). Only parameters that change due to efficiency and transmission ratio are used. This way the Power and Acceleration Reduction can be calculated in a uniform way in all components.

$$T_{req}^{PS} = T_{sp} + T_{inertia1} + T_{inertia2} + T_{inertia3} + \dots \quad (8.7)$$

$$PR = \frac{T_{\max} - T_{req} + T_{sp}}{T_{sp}} \cdot PR_{prev} \quad (8.8)$$

To be able to use the torque setpoint in a possible additional torque limitation of a *succeeding* component, this torque setpoint has to be reduced in correlation with the maximum torque. Indeed, the required torque T_{req} will be limited to the maximum value T_{\max} and the corresponding torque setpoint T_{sp} equals this maximum value minus the inertia torques $T_{inertia}$.

$$T_{sp}^{pos} = T_{\max} - T_{inertia} = T_{\max} - T_{req} + T_{sp} \quad (8.9)$$

In the “**Iteration Algorithm .vi**” the new possible PDF will be calculated by multiplying the original PDF with the Power Reduction. This means that the denominator of the Power Reduction must always corresponds with this original PDF, which is proportional to the torque setpoint. Similar to the AR, when an operating limit occurs in two succeeding components, by multiplying the two Power Reductions one keeps the correlation with the original PDF.

Additional to the Acceleration Reduction and resistive torque (see previous paragraph), the reduction cluster also contains the Power Reduction and torque

setpoint. Hence this cluster can be seen as a set of parameters to control the iteration process.

c) Acceleration Subsystem - Power Reduction

In hybrid drivetrains not only the acceleration and resistive wheel torque define the required torque of the components that are part of the acceleration subsystem, but also the torque of the power subsystem. Indeed, due to the fact that the power subsystem is also supplying an additional torque (see “**Torque Splitter .vi**”), the required torque of the acceleration subsystem T_{req}^{AS} is the sum of the vehicle acceleration torque T_a and the resistive torque T_r minus this additional torque T_{req}^{PS} (example of a parallel hybrid drivetrain).

$$T_{req}^{AS} = T_a + T_r - T_{req}^{PS} \quad (8.10)$$

Instead of reducing the vehicle acceleration it could be sometimes better to first reduce this additional power subsystem torque with the help of a Power Reduction acting on the PDF, and this until the PDF has no effect anymore on the torque limit (e.g. PDF equals zero). If e.g. the electric motor is overloaded a PR is introduced in the model of this motor (which is part of the acceleration subsystem) and not an AR like described in the first paragraph.

d) Power Subsystem -Acceleration Reduction

Regarding that the power subsystem provides a torque corresponding to the torque setpoint, it makes no sense to reduce the vehicle acceleration (performance). One should better always reduce the Torque setpoint via PDF and PR to keep the components of the power subsystems within their boundaries.

8.3.2 AR, PR (ω) Calculation

The components have not only to operate within torque limits, but they are also not allowed to exceed their maximum speed limits.

a) Acceleration Subsystem - Acceleration Reduction

At each step of the drive cycle loop the current velocity is used as input of the drivetrain model. During the AR,PR iteration process this velocity will be kept constant (to have a constant reference). Based on the speed value ω and the required acceleration a , one can calculate what the next velocity would be when the iteration is finished. In the next speed cycle step this actual speed could be higher than the maximum allowed velocity ω_{max} (equation (8.11)).

$$\omega + T_s \cdot a > \omega_{\max} \quad (8.11)$$

When a component would exceed this maximum speed limit the required acceleration should thus be reduced to the maximum acceleration a_{\max} , as defined by equation (8.12).

$$a_{\max} = \frac{\omega_{\max} - \omega}{T_s} \quad (8.12)$$

For components being part of the acceleration subsystem a reduction of the vehicle acceleration will result automatically in a proportional reduction of the components acceleration. Equation (8.13) defines the corresponding Acceleration Reduction (T_s is the time increment of the speed cycle).

$$AR = \frac{\omega_{\max} - \omega}{T_s \cdot a} \quad (8.13)$$

The output parameter of the “**AR, PR (ω) Calculation .vi**” will not be the maximum velocity, but due to the fact that during the iteration process the velocity has to remain constant, the current speed will be taken. The maximum acceleration is the output parameter. When in a previous component another limit has already caused an Acceleration Reduction, both Acceleration Reductions will be multiplied.

b) Power Subsystem - Power Reduction

In hybrid vehicles the velocity of some components can be a function of the required torque. E.g. in a series hybrid vehicle the velocity of an engine (part of the APU) can be defined in function of the required APU output power in such a way that its corresponds to the lowest fuel consumption. Hence it is required to reduce the Power Distribution Factor to get the velocity within its speed limit.

How should one define the corresponding Power Reduction factor ?

In the power subsystem the acceleration imposes additional inertia torques. Based on the available parameters in the Reduction cluster one can calculate this inertia torque T_{inertia} (equation (8.14)).

$$T_{\text{inertia}} = T_{\text{req}} - T_{\text{sp}} \quad (8.14)$$

The maximum velocity defines a maximum acceleration (see (8.12)). The maximum allowed inertia torque is thus proportional to the maximum acceleration. The maximum corresponding torque T_{\max} can thus be calculated with equation (8.15),

with AR as defined in (8.13). At this moment the required Power Reduction can be calculated in the same way as the PR of the torque limitation (see paragraph 8.3.1b)

$$T_{\max} = (T_{req} - T_{sp}) \cdot AR + T_{sp} \quad (8.15)$$

$$PR = \frac{T_{\max} - T_{req} + T_{sp}}{T_{sp}} \cdot PR_{prev} \quad (8.8) \text{ Repeated}$$

Not in all hybrid drivetrains the reduction of the PDF or Torque setpoint, will result in a reduction of the component acceleration. E.g. when one wants to keep the engine speed within range in the case of a parallel hybrid vehicle, reducing the torque will have no effect on the velocity. In this case an acceleration reduction is required.

c) Acceleration Subsystem - Power Reduction

As opposed to the torque limitation, it makes no sense to reduce the PDF for a speed limitation of the acceleration subsystem components. Indeed the velocity of these components is only defined by the vehicle acceleration and is independent of the PDF and corresponding torque setpoint.

d) Power Subsystem - Acceleration Reduction

The only case, in which a component of the power subsystem has to impose an Acceleration Reduction, is when this component velocity depends on the vehicle velocity (e.g. “**Parallel Hybrid Vehicle .vi**”). When one has a power (see further) or torque (see higher) limitation in a component of the power subsystem, it is always with the PR that the possible value is calculated and not via the AR.. The Acceleration Reduction is calculated in an analogue way as it is done in the components of the acceleration subsystem (paragraph 8.3.2a).

8.3.3 AR, PR (P) Calculation

Most of the limits can be reduced to a power limit implementation (e.g. maximum battery current or voltage, flywheel overloaded, etc¹...). Hence this allows the conception of a uniform iteration process.

The resistive power P_r is the power corresponding to all forces acting on the vehicle exclusive acceleration force (see “**Wheels .vi**” of subchapter 10.2). The power

¹ For electric components the power limit is mainly due to the multiplication of a voltage limit and a current limit. Furthermore the two limits exist also alone. In the latter case the voltage or current limit is multiplied with the required current, respectively voltage.

setpoint P_{sp} is the power defined by the PDF. At the moment a component transforms mechanical power into electric power (or vice versa), the resistive power and power setpoint are calculated based on the speed ω and resistive torque T_r , respectively the torque setpoint T_{sp} (equation (8.16) and equation (8.17)). These transformations can be found in e.g. “**Motor .vi**” and “**Engine .vi**”.

$$P_r = T_r \cdot \omega \quad (8.16)$$

$$P_{sp} = T_{sp} \cdot \omega \quad (8.17)$$

a) Acceleration Subsystem - Acceleration Reduction

Opposed to the two previous acceleration reductions (speed and torque), it is not always possible to univocally define a resistive power P_r , due to e.g. the energy conversion from mechanical to electrical. In the different components the resistive power will be calculated in function of the efficiency (equation (8.18)).

$$P_r^o = \frac{P_r^i}{\eta} \quad (8.18)$$

With :

- P_r^i : resistive power at wheel side (W)
- P_r^o : resistive power at energy source side (W)
- η : efficiency

If the power is positive the efficiency increase the resistive power and vice versa. There is seldom a linear relation between acceleration and power, but rather a quadratic relation. When one would define the Acceleration Reduction (AR) likewise the reduction in the case of a torque limit, this could result in a too stringent reduction of the acceleration and thus in a possible speed that is lower than the maximum value corresponding with the power limit.

$$AR = \frac{P_{max} - P_r}{P_a} = \frac{P_{max} - P_r}{P_{req} - P_r} \quad (8.19)$$

With :

- P_{max} : maximum power (W)
- P_r : resistive power (W)
- P_a : acceleration power (W)
- P_{req} : required power (W)

The Acceleration Reduction (defined by equation (8.19) in the same way as the Acceleration Reduction provoked by a torque limit) must be attenuated in the case of a power limit.

When the Acceleration Reduction is positive this attenuation is implemented by extracting the n^{th} root of AR or when AR is negative by taking the n^{th} power of AR (equation (8.20)). The higher 'n', the higher the attenuation, but the slower the iteration process converges to possible value.

$$AR_{att} = \sqrt[n]{AR} \quad \vee \quad AR^n \quad (8.20)$$

With :

- AR : Acceleration Reduction
- AR_{att} : attenuated acceleration reduction
- n : attenuation factor

Each time the required power changes due to efficiency, the same influences are reflected on the resistive power of the Reduction Cluster too, to always dispose of the correct reference value for the AR calculation. When a limitation already occurred in a previous component of the drivetrain, both Power Reductions have to be multiplied to keep the correlation with the original PDF. The new possible power will be set equal to the maximum allowed value P_{max} .

b) Power Subsystem - Power Reduction

Similar to a torque limitation in the power subsystem, once a component required power reaches its maximum limit, the PDF will be reduced with the help of a Power Reduction. The reference to calculate the Power Reduction in this iteration process will be the Power setpoint P_{sp} defined via the PDF in the “**Torque Splitter .vi**” (parallel and combined hybrid vehicles) or the power setpoint defined by the PDF in the “**DC-bus controller .vi**” (series hybrid vehicles).

When the required power exceeds the maximum power P_{max} the Power Reduction will be calculated by comparing the part of the maximum power that can be assigned to the power setpoint, thus taking into account the inertia power of the rotating components, to the required power setpoint (equation (8.21)).

$$PR = \frac{P_{max} - P_{req} + P_{sp}}{P_{sp}} \quad (8.21)$$

The power setpoint P_{sp}^{pos} is the remaining part of the maximum torque that is not assigned to the inertia torque (equation (8.22)).

$$P_{sp}^{pos} = P_{max} - P_{req} + P_{sp} \quad (8.22)$$

There is no need to have an attenuation of the PR, as for the AR in the previous paragraph, due to the fact that there is a better linear relation between PDF and power. Only when the efficiency of a component changes very much (e.g. from 80% to 30%) during the iteration process an unstable iteration process can possibly occur. At this moment the user has always the possibility to attenuate the PR.

c) Acceleration Subsystem - Power Reduction

Also similar to the torque limitation in the acceleration subsystem due to a too high torque setpoint, a Power Reduction is required for a power limitation. In e.g. the series hybrid drivetrain the battery power is defined by the traction power (resistive and acceleration power) plus the power delivered by the generator (see “**DC-bus controller .vi**”). The battery is a component of the acceleration subsystem and the generator a part of the power subsystem. When the battery voltage becomes too high during regenerative braking, one can first decrease the generator power setpoint and afterwards, when the battery voltage is still too high, one can implement an AR to reduce the electric regeneration braking.

d) Power Subsystem -Acceleration Reduction

When a power limit happens in the power subsystem only the PDF will be reduced via the PR and the vehicle acceleration will never be reduced via an AR.

8.4 Some Examples

Fig. 8.4 demonstrates 6 examples of acceleration and resistive torque combinations resulting in surpassing the maximum torque.

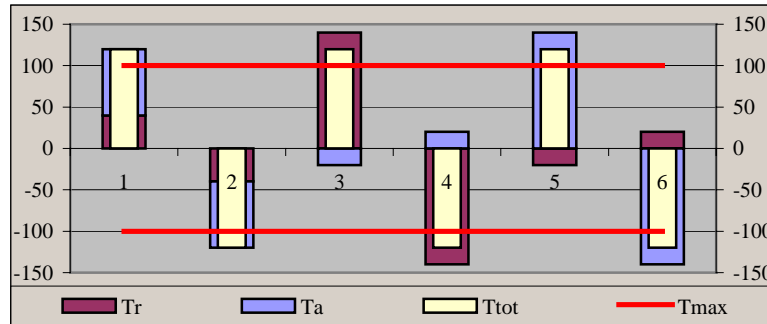


Fig. 8.4: Six examples of acceleration and resistive torque combinations

The acceleration torque can be negative or positive in function of the required acceleration, while the resistive torque sign is defined by the road inclination.

The iteration process can handle all different cases. Some real-life examples are illustrated below.

a) Electric or thermal vehicles

- An Acceleration Reduction is necessary when a motor is overloaded, an engine overspeeded, a battery current too high, etc...
- One is driving at high speed with a moderate acceleration and suddenly the battery minimum voltage limit is reached. At this moment a negative AR higher than 1 is required to decelerate the vehicle.
- One is driving at high speed with a moderate deceleration, but the battery current is not yet reversed, which means that the battery is being discharged. Suddenly the battery minimum voltage limit is reached. At this moment a positive AR higher than 1 is necessary to decelerate the vehicle more and hence recharge the battery and increase battery voltage.
- When driving at constant speed and a sudden slope occur it can be possible that the vehicle cannot deliver the required power and must decelerate (AR smaller than one).
- When the maximum power is smaller than the resistive part of the power while the vehicle is asked to accelerate, the vehicle needs to drive slower, thus a negative AR is necessary. This is the case for instance when driving with a moderate acceleration and the road inclination increases heavily.

b) Hybrid vehicles

- A Power Reduction is necessary when a flywheel is turning too fast, the required engine power is too high, the current variation in time of a Fuel Cell is too high, etc...
- If one wants to start an engine with the generator in a series hybrid vehicle a negative PR is necessary to iterate to a Power Distribution Factor corresponding to the start-up power, which should be delivered by the battery.
- When in a series hybrid vehicle the battery voltage is too high, a PR can be needed to reduce the generator charging power.
- When an engine of a parallel hybrid vehicle is operating at a rotation speed lower than the idle speed the engine cannot deliver power and a PR equals to 0 is required. At this moment the electric traction motor will deliver all power.
- In a parallel hybrid vehicle an AR can be introduced in the battery model as well as an AR can come from the engine model. When this engine rotational speed exceeds its maximum allowed value an AR is required to limit the speed of the total drivetrain.

8.5 Summary of AR, PR Calculation

All components' limits are reduced to three different cases:

- Speed limit (ω -max)
- Torque limit (T-max)
- Power limit (P-max)

Components can be part of

- Acceleration subsystem (defining the acceleration via the AR)
- Power subsystem (defining the PDF via the PR)

As described in previous chapters, not all limitations will lead to an Acceleration or Power Reduction. Next tables show the possible combination for different drivetrains.

Table 8.2: Possible AR and PR implementation for ω -max

ω -max	Acceleration subsystem	Power subsystem
Electric Vehicle	AR	
Thermal Vehicle	AR	
Series Hybrid Vehicle	AR	PR
Parallel Hybrid Vehicle	AR	AR
Combined Hybrid Vehicle	AR	PR

Table 8.3: Possible AR and PR implementation for T-max and P-max

T-max and P-max	Acceleration subsystem	Power subsystem
Electric Vehicle	AR	
Thermal Vehicle	AR	
Series Hybrid Vehicle	AR, PR	PR
Parallel Hybrid Vehicle	AR, PR	PR
Combined Hybrid Vehicle	AR, PR	PR

8.6 Iteration Order

8.6.1 1st order system

In the case of a first order system, e.g. battery electric vehicle or internal combustion vehicle, the only way to keep the operating points within limits is by controlling the acceleration. Only an AR will be used and no iteration order is required.

8.6.2 2nd order system

In a second order hybrid system different limitations can occur simultaneously, but it is not allowed to reduce the corresponding ARs or PRs at the same time. (This situation is not to be confused with the Acceleration Reduction multiplication in the situation of operating limits of succeeding components of one subsystem.) E.g. it can be possible by reducing the acceleration due to a limit of a component of the acceleration subsystem, that the power limit in the power subsystem is already solved or vice versa. When they would be implemented in the iteration process at the same time this will result in a not necessary reduction of PDF.

In some cases a limit is reached in the acceleration subsystem due to a too high PDF of the power subsystem.

An iteration order is required.

1. When a limit occurs in the acceleration subsystem it is wise to first change the Power Distribution Factor to reduce in this way the, e.g., APU power, before reducing the vehicle acceleration.
2. Once the PDF has no effect anymore on the limit in the acceleration subsystem a further reduction of the operating point can be obtained with an Acceleration Reduction. This will reduce the possible acceleration and hence the corresponding acceleration torque and power.
3. Once the vehicle acceleration is known, the acceleration of the components of the power subsystem is identified. With this acceleration corresponds a torque and power due to inertia. In the power subsystem the total required torque can exceed the maximum torque and a Power Reduction is introduced. When this PR would be implemented before the vehicle acceleration is known the PR would be calculated on the basis of an inertia power, which corresponds to an unattainable acceleration. Hence the PR would be too high.

These last two steps (2. & 3.) have to be repeated until all reduction equals one (all working points are within limits). When the first step would also be repeated it could be possible that one gets two conflicting power reductions: one from the power subsystem (e.g. decreasing PDF due to lack of engine power) and another from the acceleration subsystem (e.g. increasing the PDF due to lack of battery power). At this moment the power subsystem reduction will have priority. Repeating the two last steps is necessary because:

- The acceleration and the resistive power minus the power delivered by the power subsystem define the required acceleration subsystem power. When a limit occurs in the acceleration subsystem the acceleration will be reduced. This will define the drivetrain acceleration.

- When the power subsystem is mechanically coupled its components will have to follow the resulting acceleration (of the point above), which results in additional inertia torques. Independent from the Power Distribution Factor this inertia power is always to be delivered. Thus once the acceleration is known the operating point (inertia power included) is known and at that moment a comparison with the possible limits can be performed. These limits will introduce a power reduction. Thus less (or possibly more) power will be delivered by the power subsystem and evidently more (or possibly less) power will be delivered by the acceleration subsystem. This means that after a power reduction in the power subsystem, the operating point of the acceleration subsystem is changed. Which can lead to an acceleration subsystem limitation and corresponding acceleration reduction.
- The programme needs to start again with a new acceleration reduction until the possible acceleration is found. At its turn this defines a new power subsystem operating point. This can lead to a new power subsystem limit. Etc, etc.

It is clear that this iteration order gives priority to an optimal vehicle performance at the expense of the, e.g., APU operating point (first reducing the PDF, then the acceleration). However the user can find it more important that the APU operating point dominates on vehicle performance. E.g. operating the APU at a constant working point, even when this means slower vehicle acceleration or less regeneration of braking energy. For this reason one can select the iteration order on the front panel of the model of each hybrid vehicle: first AR then PR or first PR then AR (see subchapter 7.6).

8.6.3 3^d order system

The whole iteration process can become even more complex if one simulates complex hybrid vehicles of third order: e.g. combined hybrid drivetrains or series hybrid vehicles with three energy sources. In the case of the combined hybrid drivetrains the required torque setpoint is split up in two parts in the planetary gear (see “**Combined hybrid Vehicle .vi**” and “**Planetary Gear .vi**”). The engine will deliver one part and the generator the other, which is coupled to the battery via an inverter. Both the engine and the generator can be overloaded, resulting in two Power Reductions acting on the same PDF. If a series hybrid vehicle consists of a battery (energy buffer), a flywheel (peak power unit) and an engine (base power unit) three reductor clusters and two Power Distribution Factors (PDF₁ and PDF₂) are required. With PDF₁ the engine power is controlled and with PDF₂ the power of the flywheel (see “**Series Hybrid Vehicle .vi**” and “**DC-bus controller .vi**”). A third order system can be modelled as a system consisting in two power subsystems and one acceleration subsystem. A new iteration order has to be defined:

1. When the acceleration subsystem is overloaded the PDF₂ is first reduced via the PR of the acceleration subsystem. Hence the power of the peak

power unit (e.g. flywheel) is first adapted in function of the limitations of the components of the acceleration subsystem (e.g. the battery).

2. When the acceleration subsystem is still overloaded the PDF_1 is reduced via the same PR of the acceleration subsystem. Hence the power of the base power unit (APU) is adapted in function of the limitations of the components of the acceleration subsystem.
3. When the acceleration subsystem is still overloaded the acceleration must finally be reduced via the AR of the acceleration subsystem. Hence the power of the buffer power unit (battery) is adapted in function of the limitations of the components of the acceleration subsystem.
4. Once the vehicle acceleration is known, the operating point of the peak and base power units are defined. At this moment the possible PR of the peak power unit will first reduce, if necessary, its PDF_2 until its working point lies within boundaries.
5. Finally the PR of the base power unit is allowed to reduce, if necessary, the PDF_1 .

The whole process starts again at point 2 until all PRs and ARs equals 1.

Steps 1 and 2 are only useful when PDF_1 respectively PDF_2 are not zero. Zero means that the peak power unit, respectively the base power unit, are not delivering power.

Furthermore when AR is different from one and PR equals one (both coming from the acceleration subsystem) these first and second step can be skipped too. This means that the AR is a result of a limitation in a component of which the power is not influenced by the PDF. If a limit happens in the acceleration subsystem both PR as well as AR would be different from one. Since the power in the common subsystem is independent from the PDF, the PR in the common subsystem remains one.

In the exceptional case one wants to start the engine of a series hybrid vehicle via the generator, step 2 is skipped too. In this case the generator will introduce a PR to calculate the power required from the battery to start up the engine. Any PR coming from the battery is not allowed to change the PDF due to the fact that the engine needs to be start up in any case.

When an Acceleration Reduction needs to be introduced at a moment when the vehicle is running at constant speed the acceleration equals zero. Using (8.2) would have no effect and a small default acceleration is used to start the iteration (in the first iteration step the AR will be infinitive and will be not used).

Also when a PR is required when PDF equals zero, a default value is used to start the iteration process. These default values may only be used in the first iteration step.

In step 3 the most stringent of the Acceleration Reductions coming from the acceleration subsystem as well as from the power subsystem have to be selected. The AR can be positive, negative, higher and smaller than one. If some of the acceleration reductions are higher than one and some smaller, there is an error in the simulation model, because this is physically not possible. Indeed a vehicle needs to accelerate or it needs to decelerate, both at the same time is not possible. At that moment the programme will generate an error message alert.

a) Higher order systems

Up to now the simulation programme can process up-to third order systems. Due to the uniform approach of ARs and PRs higher order systems can be implemented in a similar way if required.

8.7 End of Iteration

The iteration process is finished when:

- All acceleration and speed reductions are almost equal to one, with one percent tolerance (between 0.99 and 1.01). This small error is allowed to fasten the iteration process, without an important influence on the final results. The user can change this value to increase accuracy, but hence he reduces simulation speed. This control is done within the “**Within range .vi**”.
- The battery voltage is not changing anymore. This voltage is used in a lot of components and can change during the iteration process. The battery voltage is calculated in the battery model after all components are successively simulated. To be sure that during the iteration all calculations are done with the same battery voltage this control is necessary.
- When the iteration process has still not found a solution after 500 iterations, an error message will appear and the iteration process as well as the simulation run is stopped. This means that there is no convergence of the iteration process.

Once these conditions are satisfied the drivetrain will be simulated for a last time. At this moment the ‘No iteration’ global is set to true. This allows tracing the final possible parameters of the different components and storing them in the “**Tracer .vi**”.

8.8 Flow Chart and Front Panel of the “Iteration Algorithm .vi”

With the help of the flow chart of Fig. 8.5 the above-described iteration methodology can be summarised. Based on the speed cycle requirements the input of the drivetrain is calculated. Within the drivetrain different ARs and PRs can be introduced to control the vehicle acceleration and powerflow. When the user has selected to first reduce the PDF and afterwards the acceleration the ‘Order’ boolean is true. When all ARs and PRs equals one, the iteration process stops.

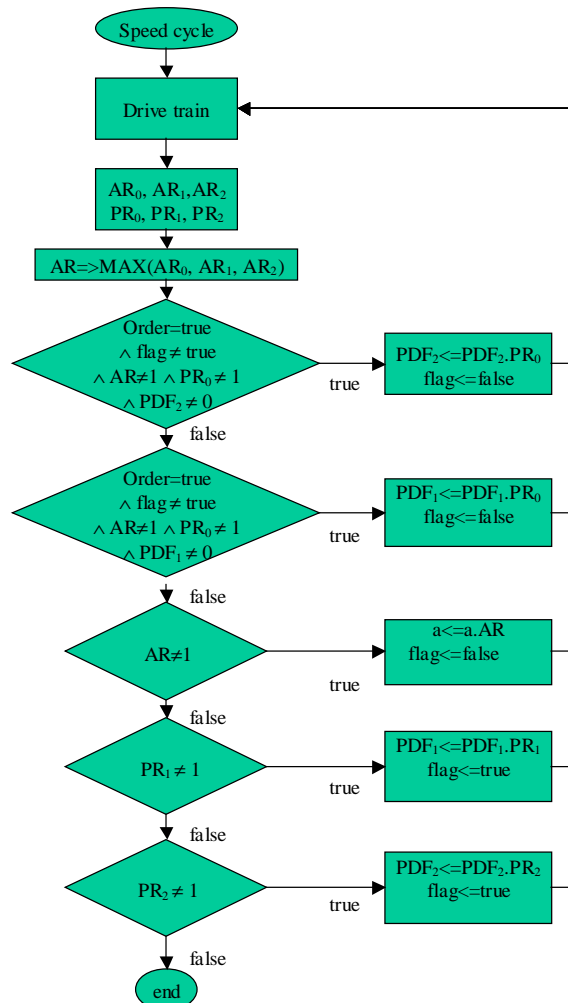


Fig. 8.5: Iteration order and end of iteration flow chart

Fig. 8.6 illustrates the front panel of the “**iteration Algorithm .vi**”. On top one can find the power control criteria or iteration order selection. Four indicators specify the position of the iteration process. In the middle one can find the required and reduced acceleration and PDF 1 and 2, as well the iteration accuracy, threshold levels and maximum number of iterations. At the bottom of the figure the three iteration clusters, which are controlling the iteration process can be found.

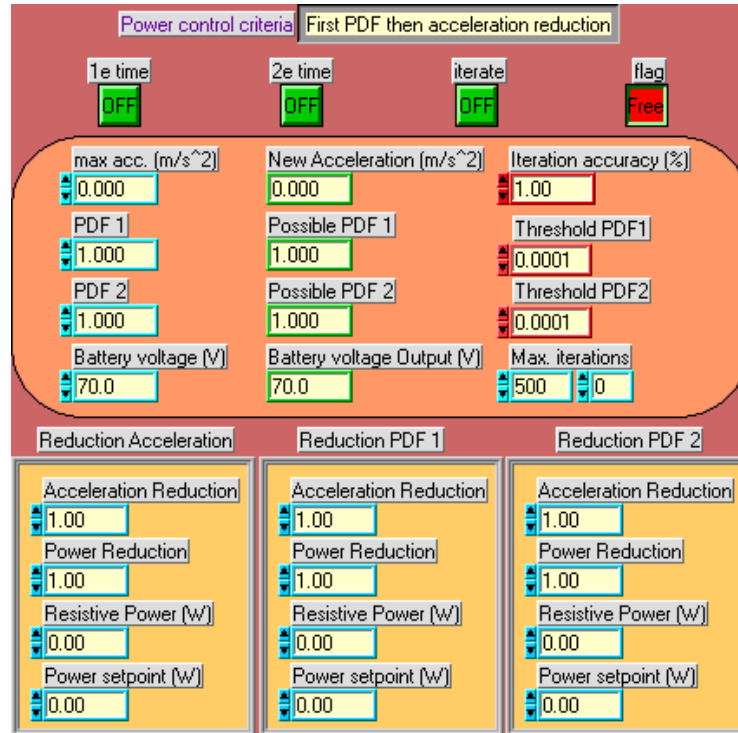


Fig. 8.6: Front panel of “Iteration Algorithm .vi”

9 POWER CONTROL DEVICES FOR HYBRID VEHICLES

In the previous chapter the iteration process is explained. In this chapter the methodology to control the powerflow with the help of the Power Distribution Factor in hybrid electric drivetrains is described. As mentioned in Part I the control strategy is inherently implemented in the model of each component. The components having a direct effect on the powerflow distribution are:

- The DC-bus controller for:
 - Series Hybrid Electric Vehicles
 - Fuel Cell Hybrid Electric Vehicles
- The Torque Splitter for:
 - Parallel Hybrid Electric Vehicles
 - Combined Hybrid Electric Vehicles
- The Planetary Gear for:
 - Combined Hybrid Electric Vehicles

9.1 DC-Bus Controller .vi

The main task of this “vi” is to control the power split up into the different ‘energy sources’ used in the “**Series Hybrid Vehicle .vi**” or the “**Fuel Cell Hybrid Vehicle .vi**”. The input is the power demand coming from the convertor.

The way the power is divided between the different energy sources can be very diverse (see Part I). At one extreme the energy source (engine-generator group) will be forced to track the total car load demand; at the other extreme the batteries will take care of all traction dynamics and the energy source will operate only at one working point corresponding to the, e.g., average power.

In the case of a series hybrid vehicle the user can select on the front panel of the DC-bus controller (see Fig. 9.2) five operating criteria for the APU.

1. In the first criterion the APU needs to deliver a constant power P_{gen} (equation (9.1)) independent from driving conditions. Mostly this corresponds with the average driving power.

$$P_{gen} = PDF_1 \cdot P_{gen}^{setpoint} \quad (9.1)$$

2. The second criterion is just opposed to the first. The APU needs to deliver the required traction power P_{req} plus an additional constant battery charging power $P_{gen}^{setpoint}$ (equation (9.2)). Even if there is no regeneration of

braking energy (see “**Inverter .vi**”), the APU will keep charging the battery during braking.

$$P_{gen} = PDF_1 \cdot (P_{req} + P_{gen}^{setpoint}) \quad (9.2)$$

3. In the third criterion the required traction power is relatively split-up between battery and APU, as illustrated with the following equation.

$$P_{gen} = PDF_1 \cdot P_{req} \quad (9.3)$$

4. The fourth criterion takes the State of Charge (SoC) of the battery into account. Hence the influence of the driving cycle is taken into account in an indirect way. When the speed cycle is a very demanding one, which means that the battery SoC is decreasing very fast, the engine power level should be enlarged to compensate this energy consumption. At the contrary, when driving a very moderate cycle, e.g. cruising at 50km/h, the engine will provide the traction power and probably it will charge the battery at the same time. At this moment the engine power level can be decreased. This is implemented in this fourth case by using (9.1) and a simple linear relation between PDF and SoC.

$$PDF_1 = a \cdot SoC + b \quad (9.4)$$

5. The last criterion is used in a battery depleting hybrid vehicle, where it is allowed to discharge the battery in function of a recommended SoC deviation ($DSoC/Dt$). If the SoC is decreasing less fast, the APU setpoint power will be forced to zero. If the SoC is decreasing within a boundary defined by the recommended SoC deviation and a ΔSoC setpoint, the APU will deliver a power corresponding its optimal (user-defined) power level. If the SoC is decreasing faster the APU will be forced to deliver the maximum power. To avoid setpoint switching at the boundaries a small hysteresis is foreseen.

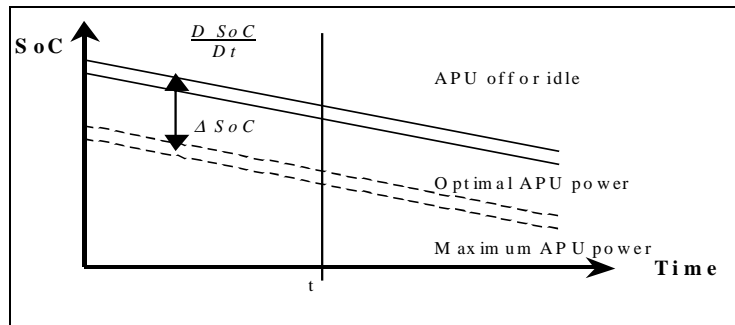


Fig. 9.1: SoC deviation APU power criterion

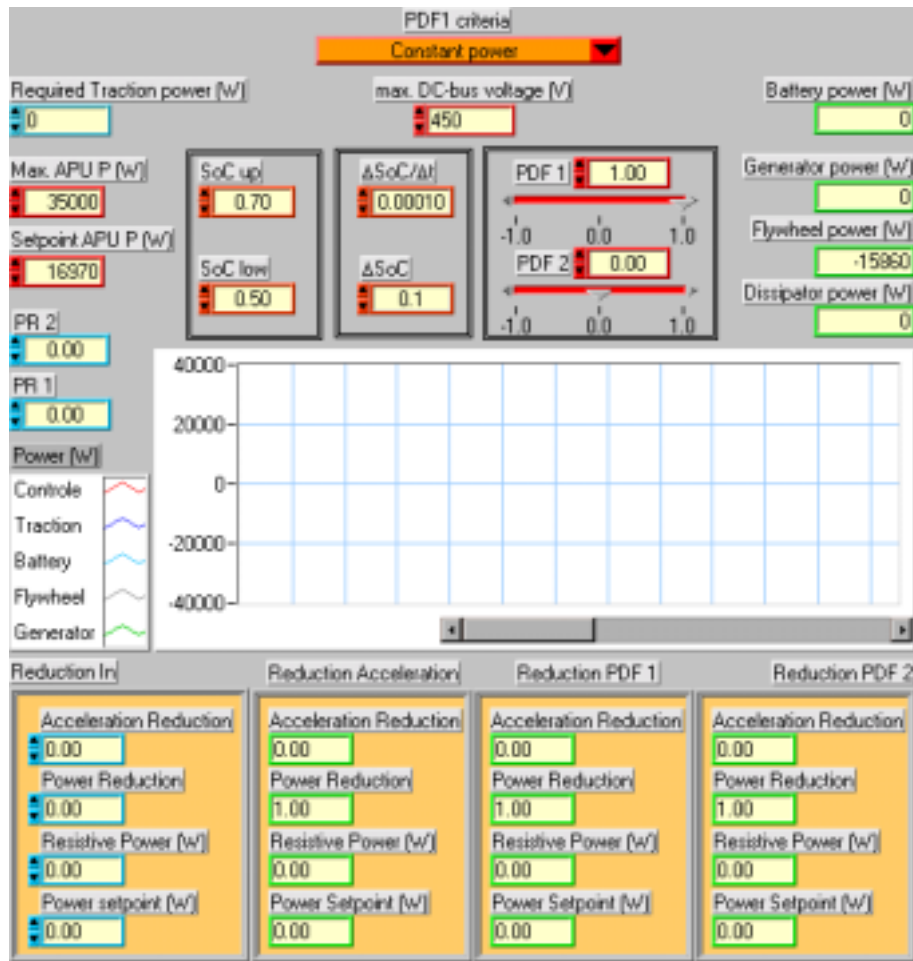


Fig. 9.2: Front panel of DC-bus controller .vi

If the APU is not able to deliver the required power the Power Distribution Factor is reduced in the “**Iteration Algorithm .vi**”, and in the next iteration step the required APU power (P_{gen}) will be smaller.

To start the internal combustion engine of an APU a start power is required (see “**Generator .vi**” of subchapter 11.6). This is also implemented with the help of the PDF and results in a negative generator power. If the generator setpoint power is zero, but the generator needs to start up, then (7.4) cannot be used. Hence a default value for the generator setpoint equal to one is used to start the iteration and to find the required start-up power. In some cases the generator is not allowed anymore to deliver power, even if it is asked to follow the inverter or traction power, e.g., the engine rotational speed is too low to deliver torque. In such a case the iteration

process will make the generator power zero via the PDF and the battery must deliver all the power.

$$PDF_{pos} = PR \cdot PDF_{req} \quad (7.4)$$

Repeated

The same operating criteria can be used to control the powerflow of a fuel cell hybrid vehicle. In that case the fuel cell will have the same role as the APU.

Some hybrids can have a power unit, such as a flywheel or super capacitor, to deliver the power peaks. The power required by this power unit P_{pu} is calculated with the help of the second Power Distribution Factor PDF_2 (equation (9.5)).

$$P_{pu} = PDF_2 (P_{req} - P_{gen}) \quad (9.5)$$

The battery must deliver the remaining power P_{bat} (equation (9.6)).

$$P_{bat} = P_{req} - P_{gen} - P_{pu} \quad (9.6)$$

If the DC-bus voltage is higher than the user defined maximum DC-bus voltage a braking resistant is engaged. This resistant will dissipate all braking power and no power flows to the battery. When the battery voltage drops back to a value lower than e.g. 95% of the maximum DC-bus voltage the braking resistant is disengaged.

9.2 Torque Splitter .vi

In parallel and combined hybrid vehicles a toothed wheel can connect an electric motor with one shaft to the wheels via the differential, and another shaft to the engine via a gearbox. In the model of this toothed wheel the shaft at wheel side will be called the input and the shafts at engine and motor side respectively output 1 and output 2. The relations between in- (ω_i) and output velocities (ω_{o1} , ω_{o2}) and accelerations are defined by a constant transmission ratio (x_1 and x_2) (see from equation (9.7) to (9.10)). The torque division between both output shafts can be controlled. Considering the speed of each shaft this results in a power split. The “**Torque Splitter .vi**” controls this power split with the help of the Power Distribution Factor. This factor defines the relative distribution of power between the two output shafts (equation (9.11) and (9.12)).

$$\omega_{o1} = x_1 \cdot \omega_i \quad (9.7)$$

$$\omega_{o2} = x_2 \cdot \omega_i \quad (9.8)$$

$$a_{o1} = x_1 \cdot a_i \quad (9.9)$$

$$a_{o2} = x_2 \cdot a_i \quad (9.10)$$

$$P_{o1} = PDF \cdot P_i \quad (9.11)$$

$$P_{o2} = (1 - PDF)P_i \quad (9.12)$$

With :

- x_1 : transmission ratio (x:1) corresponding to output 1
- x_2 : transmission ratio (x:1) corresponding to output 2
- ω_i : input velocity (rad/s)
- ω_{o1} : output shaft 1 velocity (rad/s)
- ω_{o2} : output shaft 2 velocity (rad/s)
- a_i : input acceleration (rad/s²)
- a_{o1} : output shaft 1 acceleration (rad/s²)
- a_{o2} : output shaft 2 acceleration (rad/s²)
- PDF : Power Distribution Factor
- P_i : input power (W)
- P_{o1} : output 1 power (W)
- P_{o2} : output 2 power (W)

Five different PDF criteria can be selected on the front panel of the “**Torque Splitter .vi**”:

1. *Relative torque reference*: Within the first criterion, the PDF remains constant as long as no limitations occur in other components (equation (9.13)). This means that the traction power is proportional delivered by the engine and by the electric motor (see equation (9.11) and (9.12)).

$$PDF = Ct \quad (9.13)$$

2. *Absolute torque reference*: The second criterion imposes a constant torque at one of the two output shafts (equation (9.14)). The other output shaft must deliver the remaining part of the required torque. During the simulation it can be necessary to disengage an output shaft. Hence the PDF will become zero via the PR and the output torque equals zero too. The other shaft will deliver all the required power.

$$PDF = \frac{Ct}{P_i} \quad (9.14)$$

3. *Minimum efficiency loss*: In this third one it is possible to operate the engine on its optimal working line corresponding with low fuel consumption. The transmission ratio (e.g. of output 2) and the input velocity define indeed the engine velocity. One can define the PDF to minimise the efficiency loss for the entire vehicle. In this case the PDF will be a function of input velocity and torque, equation (9.15).

$$PDF = f(\omega_i, T_i) \quad (9.15)$$

4. *In function of SoC*: This criterion takes the state of charge into account in the same way like it is done in the DC-bus controller (see subchapter 9.1): with a linear relation between PDF and SoC (equation (9.16)); a and b are constant values).

$$PDF = a \cdot SoC + b \quad (9.16)$$

5. *In function of SoC bis*: When the SoC is high the electric motor will deliver the driving power, equation (9.17). Between maximum and minimum SoC boundaries the IC engine will provide the required driving power, equation (9.18). When the SoC is low the engine will drive the wheels and moreover it will supply an additional power to charge the battery via the electric motor, equation (9.19).

$$PDF = 0 \quad \Leftarrow \quad SoC_{\max} \leq SoC \quad (9.17)$$

$$PDF = 1 \quad \Leftarrow \quad SoC_{\min} \leq SoC < SoC_{\max} \quad (9.18)$$

$$PDF = 1 + \frac{Cte}{P_i} \quad \Leftarrow \quad SoC < SoC_{\min} \quad (9.19)$$

In combined hybrid vehicles this torque splitter is connected to a planetary gear that, at its turn split up the power between an engine and a generator (see subchapter 7.8). An operating limit can appear in the engine as well as in the generator. To restrict the required power, the PDF of the torque splitter should be reduced. To be able to implement a unique iteration algorithm in all types of drivetrains, the “**Iteration Algorithm .vi**” will treat the PR coming from the engine separately from the one coming from the generator, both resulting in two different reductions of the Power Distribution Factor (named PDF₁ and PDF₂). But in the “**Torque Splitter .vi**” there

is only one PDF to control the powerflow. Hence both PDFs are multiplied to get only one outcome PDF_{eff} (equation (9.20)). This is possible because PDF₂ in the “**Combined hybrid Vehicle .vi**” is always one, except when an operating limit is attained. If at a certain moment the multiplication of both PDFs equals zero and one of them should be reduced due to an operating limit, a default value will be used to start the iteration process.

$$PDF_{eff} = PDF_1.PDF_2.PDF \quad (9.20)$$

With :

- PDF₁ : PDF from PR₁ of iteration process (engine)
- PDF₂ : PDF from PR₂ of iteration process (generator)
- PDF_{eff} : effective Power Distribution Factor

The resulting PDF is taken into account for the calculation of the output torque (T_r and T_a). The torque from output shaft 1 (engine) will be handled as a pure resistive torque. The torque of the output shaft 2 (motor) will be decreased with the same amount (equation (9.22)).

$$T_r^{o1} = \frac{T_r^i.PDF}{\eta.x_1} \quad (9.21)$$

$$T_r^{o2} = \frac{T_r^i(1 - PDF)}{\eta.x_2} \quad (9.22)$$

$$T_a^{o1} = 0 \quad (9.23)$$

$$T_a^{o2} = \frac{(T_a^i + J.a_i)}{\eta.x_2} \quad (9.24)$$

With :

- η : efficiency (%)
- T_rⁱ : input resistive torque (Nm)
- T_r^{o1} : output 1 resistive torque (Nm)
- T_r^{o2} : output 2 resistive torque (Nm)
- J : inertia seen at wheel side(kg.m²)
- T_aⁱ : input acceleration torque (Nm)
- T_a^{o1} : output 1 acceleration torque (Nm)
- T_a^{o2} : output 2 acceleration torque (Nm)

In the transmission the dominant power losses arise in the gear meshes. These losses depend on load and speed. Furthermore there are oil-churning losses of the gearwheels. The efficiency η can be defined as a function of torque, stored in an array or look-up table, or can be an empirical equation in function of the input speed and torque. If the torque is positive the efficiency increases the required torque at motor side and vice versa.



Fig. 9.3: Front panel of Torque Splitter .vi

9.3 Planetary Gear .vi



Fig. 9.4: Front panel of Planetary gear .vi

In parallel and combined hybrid vehicles there is a mechanical connection between two or more energy sources. This coupling can be implemented with a speed addition device like a planetary gear. Fig. 9.5 below shows the different elements of the planetary gear. In the middle one can find the sun wheel, on which three toothed wheels can rotate. These three wheels are connected together by the carrier. These three wheels can also rotate within the ring wheel. The fundamental torque and speed formulae illustrate the proportional torque relationship and the addition of the different wheel speeds (equation (9.25) and (9.26)) [110,155]. This equation clearly demonstrates the possibility to regulate the speed of the carrier by changing the sun speed independently of the ring speed.

$$x_{C/R} \cdot \omega_C = x_{S/R} \cdot \omega_S + \omega_R \tag{9.25}$$

$$T_C = -x_{S/R} \cdot T_S = x_{C/R} \cdot \frac{T_R}{\eta} \tag{9.26}$$

With :

- T : torque
- η : efficiency
- ω : rotational speed
- $x_{S/R}$: sun to ring transmission ratio
- $x_{C/R}$: carrier to ring transmission ratio

In the model of the combined hybrid vehicle the planetary gear set divides the carrier driving force (driven by the engine) into two forces: one that is transmitted via the ring gear to drive the wheels and the other one that drives the generator through the sun gear [110]. For any given steady-state vehicle speed, the speed of the engine can be adjusted simply by varying the speed of the generator [114]. The generator is also used to start up the engine. Next to the torque transmission equations and speed addition formulae, this simulation model also contains the tools to simulate a drivetrain power strategy corresponding to a combined hybrid vehicle.

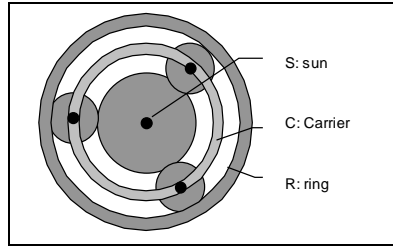


Fig. 9.5: Planetary gear

In the simulation model it is chosen to define the ring wheel, connected to the transmission going to the wheels, as an input element. The sun and carrier wheels are output variables, imposing the speed and torque respectively to the generator and the engine. The resistive T_r^C and acceleration T_a^C part of the carrier torque are respectively defined by equation (9.28) and equation (9.29) in function of the ring torque (T_r^R and T_a^R). In the same way the sun wheel torques (T_r^S and T_a^S) are defined by equation (9.34) and equation (9.35). A constant inertia J seen at input side will increase the ring acceleration torque. The efficiency is also taken into account. The efficiency can be defined like described in previous subchapter 9.1.

The ring power is given by

$$P_R = \omega_R (T_r^R + T_a^R + J \cdot a_R) \quad (9.27)$$

Equation (9.25) requires the knowledge of two of the three velocities to calculate the third one. The ring speed is known as input parameter, but the velocities of sun and carrier are still not defined. In the simulation model it is chosen to define the carrier speed in function of the carrier torque (equation (9.31)). This way it is possible to control the operation of the engine connected to the carrier (e.g. it is possible to

operate the engine on its optimal working line corresponding with low fuel consumption). Once the carrier speed is defined the sun speed can be calculated by using equation (9.36). The angular accelerations are defined in an analogue way (see equations (9.33) and (9.38)).

		<i>Sun wheel locked</i>	<i>No locking</i>	<i>Carrier wheel clocked</i>	
CARRIER		$T_r^C = x_{C/R} \cdot \frac{T_r^R}{\eta}$ (9.28) Carrier resistive torque			
		$T_a^C = x_{C/R} \frac{(T_a^R + J \cdot a_R)}{\eta}$ (9.29) Carrier acceleration torque	0		
		$\omega_C = \frac{\omega_R}{x_{C/R}}$ (9.30)	$\omega_C = f_\omega(T_a^C + T_r^C)$ (9.31) Carrier angular velocity	0	
		$a_C = \frac{a_R}{x_{C/R}}$ (9.32)	$a_C = f_a(T_a^C + T_r^C)$ (9.33) Carrier angular acceleration	0	
SUN		$T_r^S = -x_{S/R} \cdot \frac{T_r^R}{\eta}$ (9.34) Sun resistive torque			
		0	$T_a^S = -x_{S/R} \frac{(T_a^R + J \cdot a_R)}{\eta}$ (9.35) Sun acceleration torque		
		0	$\omega_S = \frac{x_{C/R} \cdot \omega_C - \omega_R}{x_{S/R}}$ (9.36) Sun angular velocity	$\omega_S = -\frac{\omega_R}{x_{S/R}}$ (9.37)	
		0	$a_S = \frac{x_{C/R} \cdot a_C - a_R}{x_{S/R}}$ (9.38) Sun angular acceleration	$a_S = -\frac{a_R}{x_{S/R}}$ (9.39)	

With (equations (9.27) up to (9.39)):

ω_R = ring angular velocity (rad/s)	ω_S = sun angular velocity (rad/s)	ω_C = carrier angular velocity (rad/s)
a_R = ring angular acceleration (rad/s ²)	a_S = sun angular acceleration (rad/s ²)	a_C = carrier angular acceleration (rad/s ²)
T_r^R = ring resistive torque (Nm)	T_r^S = sun resistive torque (Nm)	T_r^C = carrier resistive torque (Nm)
T_a^R = ring acceleration torque (Nm)	T_a^S = sun acceleration torque (Nm)	T_a^C = carrier acceleration torque (Nm)
J = inertia seen at wheel side (kg.m ²)	$x_{S/R}$ = sun to ring transmission ratio	$x_{C/R}$ = carrier to ring transmission ratio
η = efficiency (%)		

Operating the engine on its optimal working line does not necessarily results in overall low energy consumption. When a low engine power is required it might be better to disengage the engine by locking the carrier wheel. At this moment the carrier speed equals zero and the sun velocity is proportional to the ring speed. In the simulation model the carrier will be locked when the carrier power P_C (equation (9.40)) becomes lower than the minimum carrier power and also when the engine is required to deliver a negative torque.

$$P_C = \omega_C \cdot (T_r^C + T_a^C) \quad (9.40)$$

In the same way it could be interesting to lock the sun wheel when the sun power P_S (equation (9.41)) becomes smaller than the minimum sun power. When the sun is locked the carrier velocity is defined by equation (9.30). This speed equals the engine velocity and with this engine velocity corresponds an optimal engine torque. Via a PR the PDF of the Torque Splitter model will be modulated in such a way to iterate to this optimal torque. The user can select on the front panel of this simulation programme to allow locking or not (see Fig. 9.4).

$$P_S = \omega_S \cdot (T_r^S + T_a^S) \quad (9.41)$$

10 FORCE AND TORQUE CALCULATION: FROM WHEELS TO TRANSMISSION

In the previous chapter the iteration process is described as well as the powerflow control algorithms. This and the succeeding chapters will clarify the different models of the different components of the drivetrain. Each component model is composed out of basically three parts:

1. The initialisation phase: These calculations are only performed one time, the first time the model is activated. Mainly the components weight as well as data accuracy is put into a data tracer and some parameters are initialised to their start value.
2. The core programme: This part performs the actual simulation of the model.
3. No iteration: When the iteration process is finished and the vehicle acceleration and powerflow is defined, all components are simulated once again to store the calculation results and update the graph on the front panel of each component.

In this chapter the forces acting on the vehicle are described beginning with the aerodynamic force acting on the vehicle body (paragraph 10.1) and the other forces calculated in the wheel model (paragraph 10.2). This part is exactly the same for all kind of vehicles; it is the common subsystem.

10.1 Body & Weight .vi

This model contains the data necessary to calculate the main forces acting on the vehicle body. Inputs are the weight of all different components of the drivetrain to calculate the total weight. The vehicle load (luggage, passengers, etc.) is also taken into account in the total weight. The variation of weight due to fuel consumption is also considered. The user can also select to use a constant vehicle weight during the whole simulation process.

The first time the “**Body & Weight .vi**” is run, the tracer will contain default values, which are different from the real component weights. While simulating backwards through the drivetrain the weight data is gathered out of the different components of the drivetrain, with the help of the “**Tracer .vi**”. Due to the fact that within the iteration loop the programme runs at least two times through the drivetrain, one can be sure to simulate with the correct values. In the case the weight values may

change during the simulation run the average weight is calculated to use it afterwards to define some specific values in the main programme “**VSP .vi**”.

The aerodynamic drag force F_v is calculated in function of the frontal surface S , the aerodynamic drag coefficient C_x , the vehicle current speed v_{cur} , the average head wind velocity v_w and the air density ρ (equation (10.1)). The other forces acting on the vehicle are based on the wheel parameters and hence calculated within the “**Wheel .vi**” programme.

$$F_v = \frac{1}{2} \cdot \rho \cdot S \cdot C_x \left(\frac{v_{cur} + v_w}{3,6} \right)^2 \quad (10.1)$$

10.2 Wheels .vi

This model translates the linear velocity v (km/h) and vehicle acceleration a_v (m/s^2) into rotational speed ω (rad/s) and rotational acceleration a (rad/s^2) by using the wheel radius R (m)

$$a = \frac{a_v}{R} \quad (10.2)$$

$$\omega = \frac{v}{3,6 \cdot R} \quad (10.3)$$

Based on [5] the maximum acceleration a_{max} and deceleration d_{max} before wheel slip is calculated. This is a function of the static friction coefficient μ_r and the numbers of wheels that are driven by the drivetrain (equation (10.4), respectively (10.5)).

$$a_{max} = k_r \cdot g \cdot (\mu_r \cdot \cos(\alpha) - \sin(\alpha)) \quad (10.4)$$

$$d_{max} = -k_r \cdot g \cdot (\mu_r \cdot \cos(\alpha) + \sin(\alpha)) \quad (10.5)$$

With :

- a_{\max} : maximum acceleration before wheel slip (m/s^2)
- d_{\max} : maximum deceleration before wheel slip (m/s^2)
- α : road inclination ($^\circ$)
- μ_r : static friction coefficient
- k : 1 for four-wheel drive
1/2 for two-wheel drive
1/4 for one-wheel drive

In this way two or four wheel driven vehicles can be simulated. The acceleration will always be limited to these maximum values. This limitation is implemented in the sub programme “**Wheel slip .vi**”. Consequently this assures the wheels are not slipping and the required acceleration of the other drivetrain mechanical components will have an acceptable value. If the required acceleration is higher than the maximum acceleration before wheel slip, an error message will occur on the screen. These equations are depending on the road inclination α , which is the angle of the road with the horizontal. This angle is calculated based on the road slope s , which is defined in the speed cycle.

$$\alpha = \cot\left(\frac{s}{100}\right) \quad (10.6)$$

The rolling resistance consists in the dissipation of energy by the tyres. This dissipation is the result of the contact of the tyres with the road surface and the deforming of the tyre [156]. The friction resistance coefficient f_r is depending on the type of tyres, the road surface, the tyre pressure TP , the temperature and the vehicle speed v . This friction coefficient is calculated by using an empirical formula (equation (10.7), [112, **Error! Bookmark not defined.**]). The coefficients x_{fr1} and x_{fr2} can be used to take into account the type of tyres and road surface and hence to possibly calibrate the simulation model. Their default values are respectively 0.01 and 0.0095.

$$f_r = 0.005 + \left(\frac{1}{TP} \left(x_{fr1} + x_{fr2} \left(\frac{36.v}{10^3} \right)^2 \right) \right) \quad (10.7)$$

The friction or rolling resistance force F_r is calculated in function of this friction coefficient, the current total weight, the road inclination α and the gravity constant g (equation (10.8)). The climbing resistance F_c is also taken into account by using the road inclination α . The higher the road inclination the lower the friction resistance, but the higher the climbing resistance (equation (10.9)) [**Error! Bookmark not defined.**].

$$F_r = M \cdot g \cdot f_r \cdot \cos(\alpha) \quad (10.8)$$

$$F_c = M \cdot g \cdot \sin(\alpha) \quad (10.9)$$

The total resistive torque corresponds with the sum of the aerodynamic force F_v , the friction force F_r and the climbing force F_c . By multiplying by the wheel radius R , one gets the output resistive torque T_r (equation (10.10)).

$$T_r = R \cdot (F_v + F_r + F_c) \quad (10.10)$$

As described in chapter 8 the resistive torque and acceleration torque are separated because - when the vehicle is not able to follow the imposed cycle due to a lack of power - the model will have to reduce the acceleration in proportion to the missing power. So we need the acceleration torque explicitly in the other components of the drivetrain.

This acceleration torque is calculated based on the vehicle weight, wheel radius and acceleration (equation (10.11)).

$$T_a = M \cdot R \cdot a_v \quad (10.11)$$

Most references use a weight, which is increased by a rotational inertia coefficient m_f , taking into account the inertia of the rotating parts of the drivetrain. This factor moreover depends on the gear engaged, the drivetrain topology, the component losses, etc. Hence it is better to take the inertia into account within every rotating component itself, using the mechanical equations (10.12), (10.13).

$$J \cdot a = T_{in} - T_{out} \quad (10.12)$$

$$T_{tot} = T_a + T_r + J \cdot a \quad (10.13)$$

The programme calculates the additional deceleration, which the drivetrain itself is not able to deliver. Indeed, some drivetrains can regenerate the braking energy into the battery or power unit. The total amount of the braking power cannot always be regenerated. The mechanical brakes must deliver the remaining part of the required braking power, as long as the wheels of the vehicle will not slip. The brakes can be seen as a 'Anti Blocking System'. The brake torque T_b is calculated as a function of the total vehicle weight M , the wheel radius R and the difference between required and possible drivetrain deceleration (equation (10.14)).

$$T_b = T_r + M.R.(a_{req} - a_{pos}) \quad (10.14)$$

Due to braking, the pressure of the hydraulic system will drop. The correlation between brake power and pressure drop power is simulated with the pressure drop ratio i_{pd} (equation (10.15)). This pressure drop power PD (W) must be compensated with a compressor, which is implemented in the “**Auxiliary .vi**” (see subchapter 11.11). One can disengage the mechanical brake to allow the simulation of coasting and/or evaluate the regenerative braking.

$$PD = \omega.T_b.i_{pd} \quad (10.15)$$

To implement this idea in the iteration process, several accelerations are defined. The required acceleration a_{req} is defined by the speed cycle. On the other hand the possible drivetrain acceleration a_{pos} is the acceleration, the drivetrain is able to deliver. As long as the iteration loop is running, the possible drivetrain acceleration is passed through the drivetrain to allow the programme to converge to the possible acceleration of the drivetrain. If the vehicle is *accelerating*, the possible vehicle acceleration is equal to the possible drivetrain acceleration and passed through the “**Iteration Algorithm .vi**”. If the vehicle is *decelerating* ($a_{req} < 0$ or $T_{tot} < 0$), the possible vehicle acceleration equals the possible drivetrain acceleration during the iteration process. But at the end of the iteration (‘no iteration’ boolean is true), this possible vehicle acceleration will correspond with the required acceleration (when the ‘brake ON’ boolean is on), always limited to the maximum acceleration before wheel slip. This means that the mechanical brakes will deliver the part the drivetrain itself is not able to deliver. If the ‘brake ON’ boolean is off, the possible vehicle acceleration remains equal to the possible drivetrain acceleration.

Finally in the wheel module, every iteration the ARs and PRs are initialised to one and the angular speed ω , the total force acting on the wheels T and the corresponding wheel power P_w are calculated and stored into the “**Tracer .vi**”.

$$P_w = (T_r + T_a + J.a).\omega \quad (10.16)$$

The implemented formulae are valid within the following hypotheses:

- No slip between road and wheels.
- Only dry friction and no hydrodynamic forces are calculated at the wheels.
- Lift has an influence on the losses in the bearings, which are linear with speed but usually very small and are thus neglected.
- Uniform acceleration between time increments.
- No cornering resistance is taken into account.

10.3 Differential .vi

The differential provides a torque equalisation on the wheels on the same axis. It allows different speeds on both wheels, which facilitates the taking of turns. However, in this programme no road turnings and differences of wheel velocity are considered. In a first approach the differential can be regarded as a gearbox with a single gear. The operation consists in deviating the powerflow. Therefore the efficiency is lower compared to the manual gearbox [112].

The component has an inherent speed reduction x , which is taken into account while calculating the output torque, T_r^o (equation (10.19)) and T_a^o (equation (10.20)), the speed ω (equation (10.17)) and the acceleration a (equation (10.18)). The inertia J will increase the required acceleration torque T_a (equation (10.20)). The efficiency η can be defined as a function of torque, stored in an array or look-up table, or can be an empirical equation in function of the input speed and torque [**Error! Bookmark not defined.**,157]. If the torque is positive the efficiency increases the required torque at motor side and vice versa.

$$\omega_o = x.\omega_i \quad (10.17)$$

$$a_o = x.a_i \quad (10.18)$$

$$T_r^o = \frac{T_r^i}{\eta.x} \quad (10.19)$$

$$T_a^o = \frac{(T_a^i + J.a_i)}{\eta.x} \quad (10.20)$$

$$P = (T_r^o + T_a^o)\omega_o \quad (10.21)$$

With :

- x : transmission ratio (x:1)
- ω_o : velocity at motor side (rad/s)
- ω_i : velocity at wheel side (rad/s)
- a_o : acceleration at motor side (rad/s²)
- a_i : acceleration at wheel side (rad/s²)
- η : efficiency (%)
- T_r^o : resistive torque at motor side (Nm)
- T_r^i : resistive torque at wheel side (Nm)
- J : inertia seen at wheel side(kg.m²)
- T_a^o : acceleration torque at motor side (Nm)
- T_a^i : acceleration torque at wheel side (Nm)
- P : output power (W)

10.4 Gear .vi

The engine behaviour, represented by its particular torque-speed characteristic, in opposition to most electric motors, requires necessarily a transmission system adapting the engine speed and torque to the wheels. This can be realised by different ways from gearboxes up to automatic continuously changing transmission devices [112]. The gear component imposes a variable speed reduction in order to coerce the speed at engine side within the operation range. This implies switching to higher gears if the engine speed is too high.

Two different switching criteria are implemented in the simulation programme.

- a) Switching at fixed velocities seen at wheel side:
 - First to second gear switching speed (rad/s)
 - Second to third gear switching speed (rad/s)
 - Third to fourth gear switching speed (rad/s)
 - Fourth to fifth gear switching speed (rad/s)
- b) Keeping the engine speed between limits:
 - Upper engine speed limit (rad/s)
 - Lower engine speed limit (rad/s)

The first criterion consists in a gear selection based on fixed switching velocity points seen at wheel side and defined on the front panel. If the velocity becomes higher than a certain value, the gear switches to a higher level and vice versa. The ECE-15 cycle imposes switching from first to second gear at 17 km/h and from second to third gear at 34 km/h. These values can be chosen as default values.

The second criterion is a more intelligent one, choosing the gear in such a way that the engine velocity remains between fixed limits. Hence it is possible to operate the

engine in an operating area corresponding with e.g. low fuel consumption. Within an internal control loop of the gear model, the gear will switch to a higher gear if the engine speed exceeds the upper speed limit, and will switch to a lower gear when this engine speed drops down the lower speed limit. These limits can be adjusted on the front panel of the gear model (see Fig. 10.1). This results in a kind of hysteresis effect. However the engine speed can be lower than the lower speed limit when the vehicle is driving very slow (first gear is engaged) or higher than the upper speed limit when the highest gear is engaged.

The resulting transmission ratio x_i is taken into account for the calculation of the output torques, T_r^o and T_a^o , the speed ω and the acceleration a . A constant inertia J seen at wheel side will increase the required acceleration torque. This is not entirely correct since the inertia of the second part of the gearbox itself changes with the engaged gear. The error however will be small if one compares this inertia with the other inertia of the drivetrain.

In a gear transmission the biggest part of the power losses arise in the gear meshes. These losses depend on load and speed. Furthermore there are oil-churning losses of the gearwheels [157]. Backlash effects within the gears have not been considered. Similar to the differential the efficiency η can be defined as a function of torque, stored in an array or look-up table, or can be an empirical equation in function of the input speed and torque.

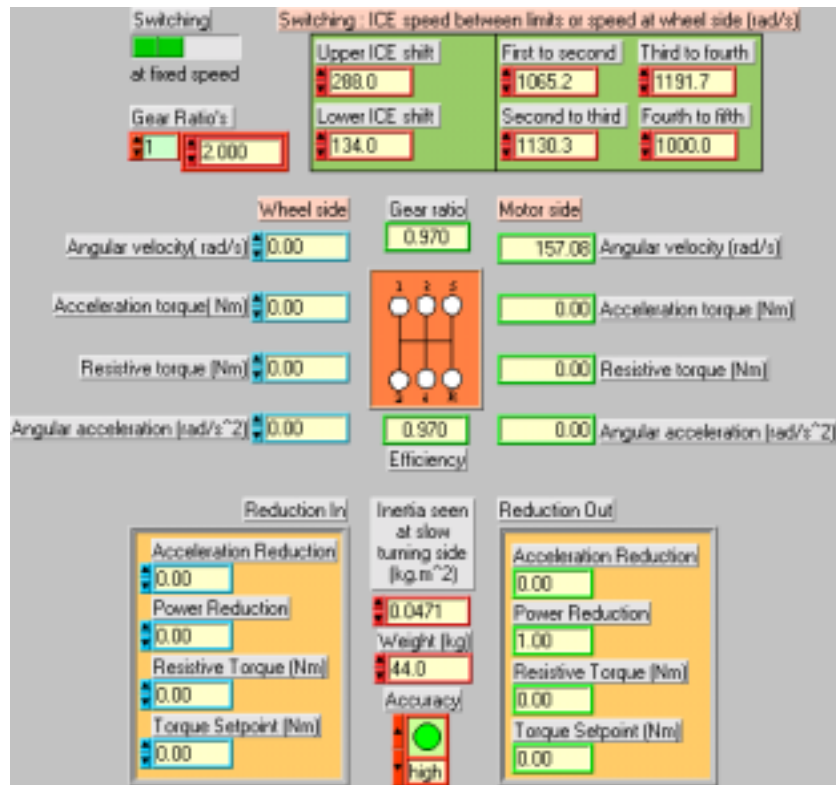


Fig. 10.1: Front panel of gear model

11 POWERFLOW TRANSFORMATION

Up-to-now most fundamental equations have been described in previous chapters: force calculation, powerflow control, iteration process, etc. The current chapter will describe all other types of components of the drivetrain that were not yet explained:

- Motor .vi
- Convertor .vi
- Battery .vi
- Charger .vi
- Generator .vi
- Clutch .vi
- Engine .vi
- Fuel Cell .vi
- Flywheel .vi
- Auxiliaries .vi

11.1 Motor .vi

This model describes the basic outlines used to simulate an electric motor. This principle can be used for different kind of electric motors: e.g. direct current series or separated excited, asynchronous motor or permanent magnet motors. The distinction between them is implemented in the subprogramme “**Motor model .vi**”, describing the specific characteristics of the motor in question.

The generic model is useful for driving and braking (positive and negative torques) but not for reverse driving. The model can also be used for the generator component of the combined hybrid vehicle (see subchapter 7.8 “**Combined hybrid Vehicle .vi**”). At that moment it must be extended to four-quadrant operation (positive and negative velocities), inclusive operating limits.

11.1.1 Working Boundaries

The generic model contains the implementation of the different operating limits. The maximum acceleration is defined by the difference between the current velocity ω and the *maximum velocity* ω_{\max} .

$$a_{\max} = \frac{\omega_{\max} - \omega}{T_s} \quad (8.12)$$

Repeated

The subprogramme “**Maximum torque .vi**” defines the *maximum motor torque*. This subprogramme contains a look-up table in function of the angular velocity (equation (11.1)). The maximum value defines the boundaries of the available motor characteristics. The maximum torque can be different for motor working or generator working (which is given by the sign of the total torque). Furthermore one can implement a maximum torque deviation. In certain drives the motor is not able to deliver a braking torque under a certain velocity. When the motor velocity is smaller than this minimum velocity before braking and the acceleration is negative, the maximum torque is set to zero. With the help of the “**AR, PR(T) Calculation .vi**” the required torque is limited to the maximum value and the corresponding AR en PR are calculated.

$$T_{\max} = f(\omega) \quad (11.1)$$

The subprogramme “**Motor model .vi**” can impose a possible second torque limitation, which can be different from the previous look-up table. When using theoretical models a theoretical torque limit can be calculated for instance. The motor model can define also *maximum current limit* (equation (11.2)). The maximum power or current of an electrical machine is related to the heat production due to losses. Hence this maximum value is a function of power or current peak duration. However within the simulation tool no this time dependency, or temperature effects are implemented. The current limit can be measured by accelerating the examined vehicle and logging the motor current with an on-road measurement system.

$$I_{\max} = f(T, \omega, U_{bat}) \quad (11.2)$$

All operating limits, different from maximum velocity and torque, are converted to power limits to simplify the iteration process. The Reduction cluster reference values, Torque setpoint T_{sp} and Resistive torque T_r , are transformed, by multiplying with the velocity ω , to Power setpoint P_{sp} and Resistive power P_r (equation (11.3) and (11.4)) for further use in succeeding component models.

$$P_r = \omega T_r \quad (11.3)$$

$$P_{sp} = \omega T_{sp} \quad (11.4)$$

11.1.2 Different Motor Models

The motor inertia J will increase the acceleration torque T_a in function of the possible acceleration. Hence the total torque T_{mot} includes the inertia torque, the

acceleration torque and the resistive torque T_r . Equation (11.6) gives the mechanical power.

$$T_{mot} = T_r + T_a + J.a \quad (11.5)$$

$$P_{mot} = \omega.T_{mot} \quad (11.6)$$

This total torque is the mechanical torque, which the motor shaft should deliver to drive the imposed speed cycle. The motor torque itself is defined by the motor own characteristics. When the motor is not able to deliver this torque, the required total torque should be decreased via the iteration process. Note that this motor torque is different from the electrical air gap torque delivered at the rotor. The torque corresponding to rotor inertia and mechanical losses should be subtracted from this electrical torque to get the motor torque. The electric torque is not used directly in this generic motor model. All losses and energy transformation are treated in the “**Motor model .vi**”, which is different for each type of motor. To calculate the electrical motor parameters different approaches are possible: empirical formulae, look-up tables, surface fitted equations based on measurements, theoretical formulae based on equivalent circuits, ... All these approaches use the angular velocity ω and the total torque T_{mot} as input parameters, as well as the battery voltage global parameter. This battery voltage is function of the battery current. In the reverse calculation the motor models is treated before the battery model. To avoid this problem a battery voltage feedback loop is implemented in the iteration algorithm. The output parameters are selected in function of the required parameters to calculate the inverter characteristics (see further).

Physically the motor working point, in terms of electrical parameters, is not completely fixed by its mechanical output: torque and speed. There are different degrees of freedom to produce a give output torque. In order to deal with a deterministic system in reverse calculation going to electrical physical input parameters from mechanical output parameters a motor control strategy is necessary [112]. This control strategy is inherent implemented in the look-up tables. This is of course a simplification of the model.

The motor and convertor are modelled as two different black boxes. However due to the close interaction they have to be treated as one black box. The most accurate way to implement a motor is by characterising a motor together with its convertor like it would be used in the electric or hybrid electric vehicle. Some examples can be found in Part III. Hence the effect of magnetic saturation, harmonic effects, flux control strategy, etc are implemented in an inherent way. If analytical relation would be used for the model all these effects should be taken into consideration. For the model the motor is supposed to be always in steady state operation, electrical transients are neglected. Furthermore no thermal aspects are considered in the model.

11.1.3 Separate excited DC-motors

In the case of a separate excited DC motor, next to the motor voltage U_{mot} (equation (11.16)) and the motor current I_{mot} (equation (11.17)), the excitation current I_{ex} and voltage U_{ex} are two additional output parameters.

The technique used in modelling the DC-motor consists in the analysis of the power equations described by the following equations [158].

$$P_{elec} = P_f + P_{ar} \quad (11.7)$$

$$P_f = R_f \cdot I_f^2 \quad (\text{field losses}) \quad (11.8)$$

$$P_{ar} = U_{ar} \cdot I_{ar} = P_{le} + P_{mi} \quad (\text{armature}) \quad (11.9)$$

$$P_{le} = U_b \cdot I_{ar} + I_{ar}^2 R_{ar} \quad (\text{electrical armature losses}) \quad (11.10)$$

$$P_{mi} = T_{inertia} \cdot \omega + P_{rot} + P_{mot} \quad (\text{mechanical}) \quad (11.11)$$

$$P_{mot} = T_{mot} \cdot \omega \quad (\text{load}) \quad (11.12)$$

$$P_{rot} = P_{fric} + P_{core} \quad (\text{rotation losses}) \quad (11.13)$$

$$P_{fric} = K_f \left(\frac{\omega}{\omega_{nom}} \right)^{ef} \quad (\text{friction losses}) \quad (11.14)$$

$$P_{core} = K_c \left(\frac{\omega}{\omega_{nom}} \right)^{ecn} i_f^{eci} \quad (\text{core losses}) \quad (11.15)$$

With :

- P_{elec} : electric motor input power (W)
- P_f : field losses (W)
- P_{ar} : armature power (W)
- I_f : field current (A)
- R_f : field resistance (Ω)
- I_{ar} : armature current (A)
- U_{ar} : armature voltage (V)

- P_{le} : electrical armature losses (W)
- P_{mi} : mechanical power (W)
- U_b : brush voltage (V)
- R_{ar} : armature resistance (Ω)
- $T_{inertia}$: inertia torque (Nm)
- ω : rotational speed (rad/s)
- P_{rot} : losses due to rotation (W)
- P_{mot} : mechanical motor output power (W)
- T_{mot} : motor torque (Nm)
- P_{fric} : friction losses (W)
- P_{core} : core losses due to eddy current and hysteresis (W)
- K_f : constant for friction losses calculation
- ef : exponent for friction losses calculation
- ω_{nom} : nominal rotational speed (rad/s)
- K_c : constant for core losses calculation
- ecn : exponent for normalised rotational speed
- eci : exponent for normalised field current
- i_f : normalised field current ($= I_f/I_{f,nom}$)

These formulas can be used to develop a theoretical model. Hence the coefficients and constants have to be defined. The formulas demonstrate also the dependency of the electrical parameters on the mechanical parameters. However the motor parameters should be identified. At the other hand, with the help of a laboratory test bench, the motor can be characterised, together with its chopper. With a best fitting algorithm, corresponding to these theoretical equations, the motor can be modelled.

11.1.4 Series excited DC-motors

In the case of a series excited DC motor the only output parameters of the “**Motor .vi**” model are the motor voltage U_{mot} (equation (11.16)) and the motor current I_{mot} (equation (11.17)) since the excitation winding is connected in series with the armature winding. Analogue to the separated excited DC-motor the current and voltage can be defined by look-up table or calculated with experimental formulae in function of the required torque T_{mot} and velocity ω and possibly the battery voltage U_{bat} . The electric motor power and motor efficiency can be expressed with equations (11.18) and (11.19).

$$U_{mot} = f(T_{mot}, \omega, U_{bat}) \quad (11.16)$$

$$I_{mot} = f(T_{mot}, \omega, U_{bat}) \quad (11.17)$$

$$P_{elec} = U_{mot} \cdot I_{mot} \quad (11.18)$$

$$\eta = \frac{P_{mot}}{P_{elec}} \quad (11.19)$$

An example of a motor characterisation based on experiments can be found in Part III.

11.1.5 Asynchronous motors

In the case of an asynchronous motor, the RMS-current and -voltage as well as the power factor ($\cos \phi$) and the fundamental frequency f are output parameters of the motor model. In the same way as for the DC-motor experimental as well as theoretical models can be developed and implemented in the software.

a) Theoretical ACM model

A user-friendly graphical interface assists the user to enter its data (Fig. 11.1). It can be difficult to get the exact parameters in the case of a theoretical model.

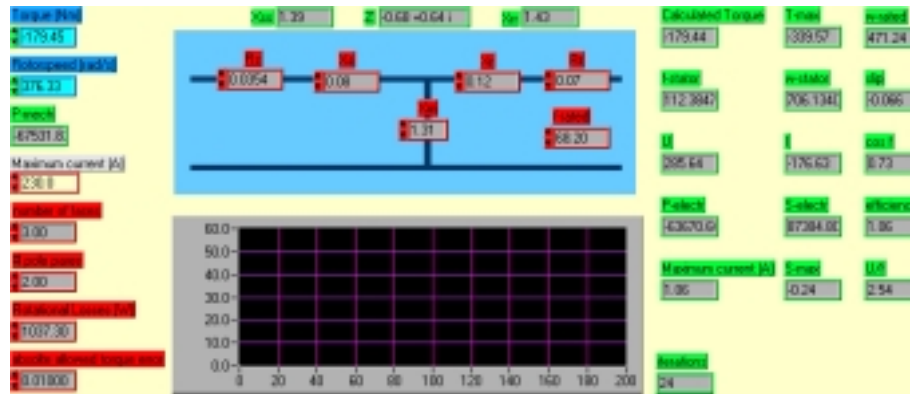


Fig. 11.1: Front panel of theoretical asynchronous motor model

The implemented theoretical model is based on a formula, which calculates the electromagnetic torque T_{em} in function of the motor slip s and the voltage U_{mot} [159,160]. The voltage is defined by the implemented control strategy. This voltage frequency relation is related to the implemented control strategy. A control strategy can optimise the motor behaviour for e.g. maximum torque or for maximum efficiency (see Part I). With an internal iterative loop the slip is found in such a way that the theoretical electromagnetic torque corresponds with the required torque input. This required torque includes the inertia torque and rotational losses.

$$T_{em} = \frac{\frac{m.p}{\omega_s} X_m^2 R_r .s.U_{mot}^2}{(R_s .R_r - s(X_{ss} .X_{rr} - X_m^2))^2 + (X_{ss} .R_r + s.R_s X_{rr})^2} \quad (11.20)$$

$$\omega_s = \frac{p.\omega}{(1-s)} \quad (11.21)$$

$$X_{ss} = \frac{f_s}{f_r} (X_m + X_s) \quad (11.22)$$

$$X_{rr} = \frac{f_s}{f_r} (X_m + X_r) \quad (11.23)$$

With :

- T_{em} : electromagnetic torque (Nm)
- m : number of phases
- p : number of pole pairs
- X_m : magnetisation reactance at pulsation $2\pi f_r$
- X_s : stator leakage reactance at pulsation $2\pi f_r$
- X_r : rotor leakage reactance at pulsation $2\pi f_r$
- X_{ss} : stator reactance
- X_{rr} : rotor reactance
- R_r : rotor resistance (Ω)
- R_s : stator resistance (Ω)
- ω : rotor speed (rad/s)
- ω_s : synchronous speed (rad/s)
- f_f : synchronous frequency (Hz)
- f_r : rated frequency (Hz)
- s : slip
- U_{mot} : motor phase voltage (V)

These equations suppose that the motor is powered by an equilibrated three phases voltage signal. All quantities (voltage, current, magnetic flux) are supposed to be sinusoidal. Voltage, current and magnetic flux harmonics are neglected. The motor is supposed to be always in steady state operation. Electrical transients are neglected. Saturation is not considered. However these parameters have their effect on the motor efficiency. To be sure taking all losses into account one should characterise the motor together with its convertor and develop statistical models.

b) Statistical ACM model

Two different approaches have been developed to implement a statistical model. A first one in which the motor shaft torque T_{mot} and voltage U_{mot} are the primary parameters describing the two dimensional statistical model. In a second model the motor shaft torque T_{mot} and rotational speed ω are the describing parameters.

As an Input/Output system the voltage and torque are independent values and the motor can be described by a function of the form [161]:

$$Y = f\{X\} \quad (11.24)$$

$$X = [U_{mot}, T_{mot}]^r \quad (11.25)$$

$$Y = [I_{mot}, P_{elec}, \omega, f] \quad (11.26)$$

A second order system would look like equation (11.27) in which the output parameter Y represents the electric motor power P_{elec} , current I_{mot} , speed ω or frequency f (the parameters $x_1..x_6$ and $y_1..y_6$ are constant coefficients).

$$Y = \frac{x_1 + x_2.U_{mot} + x_3.T_{mot} + x_4.U_{mot}^2 + x_5.T_{mot}^2 + x_6.U_{mot}.T_{mot}}{y_1 + y_2.U_{mot} + y_3.T_{mot} + y_4.U_{mot}^2 + y_5.T_{mot}^2 + y_6.U_{mot}.T_{mot}} \quad (11.27)$$

There practically exist two operating regions during the normal operation of a motor: one in which the motor voltage and frequency is used to control the speed (constant flux), and another in which the speed is controlled by the frequency (constant voltage). Hence the motor has to be described by one of the two following functions depending of the current operating point.

$$Y = f(U_{mot}, T_{mot}) \quad \text{if } U_{mot} < U_{nom} \quad (11.28)$$

$$Y = f(f, T_{mot}) \quad \text{if } U_{mot} = U_{nom} \quad (11.29)$$

To be able to use this model, the voltage and frequency need first to be defined in function of the velocity and the torque. This can be calculated on an iterative way or the voltage and frequency can be defined with a look-up table in function of the motor speed and torque. In the simulation programme the motor speed is described as a second order system in function of torque and voltage (see equation (11.30)).

$$\omega = \frac{x_1 + x_2.U_{mot} + x_3.T_{mot} + x_4.U_{mot}^2 + x_5.T_{mot}^2 + x_6.U_{mot}.T_{mot}}{y_1 + y_2.U_{mot} + y_3.T_{mot} + y_4.U_{mot}^2 + y_5.T_{mot}^2 + y_6.U_{mot}.T_{mot}} \quad (11.30)$$

This second order equation can be mathematically solved to get the voltage. Once the voltage (or frequency) is calculated all other parameters can be calculated in function of voltage and torque.

Due to the fact that it is practically not possible to take measurements for all the operating points of the torque-speed diagram, and that a model out of a curve/surface fitting process is mostly valid for the operating points inside the measurement data set, some extrapolations are necessary. Especially for the operating points between the “zero-conditions”, which corresponds to the cases $U_{\text{mot}} = 0$ and/or $T_{\text{mot}} = 0$, and the real measured points.

When the measured data has a low accuracy, the fitting can become weakly correlated to the measurements. The use of the previous approach can be simplified without affecting the total simulation accuracy. Instead of using the independent variables, voltage U_{mot} and torque T_{mot} , one can use the velocity ω and torque T_{mot} to develop a statistical model that describes the electrical output parameters: the stator voltage U_{mot} , the current I_{mot} , the active input power P , the fundamental frequency f of the stator voltage and finally the real torque that the motor is able to deliver.

Some examples of statistical models are illustrated in Part III.

11.1.6 Permanent magnet motor

Similar models can be developed for permanent magnet motors. At the moment some statistical models are available in the database.

11.2 Convertor .vi

The battery voltage and the output parameters of the motor model are used to characterise the efficiency of the convertor. This efficiency is function of the input current, power factor, DC voltage, switching frequency and transistor parameters. The switching frequency can be selected out of a look-up table in function of the fundamental motor frequency.

Basically the losses in a convertor can be devised into:

- Switching losses
- Conduction losses

Different approaches are possible.

1. An empirical approach can be based on e.g. equation (11.31) for DC-AC convertors that calculates the power loss P_{loss} in function of the

commutation frequency f_c (Hz), motor current I_{mot} per phase and the battery voltage U_{bat} (α_l is the coefficient for conduction type losses; β_l is the coefficient for commutation type losses). For the AC-DC convertor no detailed calculation is taken into account of the differences between diode and power transistor conduction losses and the dependence of their respective losses on the transistor opening time. No harmonic analysis considering the motor relevant characteristics is performed. The control electronic is supposed to be perfect.

$$P_{loss} = 3(\alpha_l \cdot I_{mot}^2 + \beta_l \cdot f_c \cdot U_{bat} | I_{mot} |) \quad [112] \quad (11.31)$$

2. An empirical approach can be based on e.g. equation (11.32) for DC-DC convertors that calculates the power loss in function of the commutation frequency f_c , motor current I_{mot} and the battery voltage U_{bat} . (α_t is the coefficient for conduction losses in the transistors, α_d is the coefficient for conduction losses in the diodes; β_l is the coefficient for commutation type losses and $R_v = U_{mot}/U_{bat}$ = voltage ratio).

$$P_{loss} = R_v \cdot \alpha_t \cdot I_{mot}^2 + (1 - R_v) \cdot \alpha_d \cdot I_{mot}^2 + \beta_l \cdot f_c \cdot U_{bat} \cdot I_{mot} \quad [112] \quad (11.32)$$

3. A statistical surface-fitting model can be based on measured data. The preference goes to the use of the losses instead of the efficiency due to the fact the convertor efficiency is mostly close to 100%. Due to measurement faults the difference between in- and output power can be within the measurement accuracy. The fault on the difference of numbers, that lies to close to each other, is smaller than the fault on the division of these numbers. The losses are a statistical function of motor current, voltage, frequency and/or battery voltage.
4. In some cases a constant value can be already an acceptable approximation, due to the fact the efficiency of most convertors is rather constant in the biggest part of the operating field.

Additional to the previous models the user is able to choose a minimum value for the power losses. The programme will always use this minimum value, even when one of the four previous approaches calculates a lower value. During the iteration process the battery voltage U_{bat} used to calculate the power loss is kept constant (it is up-dated every step of the speed cycle loop). Otherwise in exceptional cases of very low convertor power, iteration problems can occur. Indeed, suppose the motor is regenerating a small amount of power. The battery voltage defines the convertor losses, which can lead to discharging the battery instead of charging the battery with a very low power level. But due to this discharging, the battery voltage will drop and in a next iteration step the convertor losses can become smaller, even so small that the battery will be charged again. At this moment the battery voltage will rise

again and so also the convertor losses, which results in an infinitive iteration loop. By keeping the battery voltage used for calculating the convertor loss constant during the iteration process this flip-flop process is disabled, without any important influence on the overall energy consumption.

While decelerating, the braking energy can be regenerated into the battery. On the front panel of the convertor model the user can chose between different regenerative braking operation modes:

1. No regeneration of energy (maximum braking power equals zero).
2. Constant current I_{regen}^{max} regeneration, which value can be selected on the front panel (the maximum braking power is defined by equation (11.33) in function of the DC-bus or battery voltage U_{bat}).
3. Regenerating the total amount of braking power (maximum braking power equals required braking power).

The maximum braking power P_{inv}^{max} is compared with the required braking power resulting in a possible PR or AR.

$$P_{inv}^{max} = U_{bat} \cdot I_{regen}^{max} \quad (11.33)$$

Once the possible power is defined, the required battery power P_{bat} is calculated by adding the convertor power P_{inv} with the auxiliary power P_{aux} and possibly a second convertor power P_{inv2} (equation (11.34)).

$$P_{bat} = P_{inv1} + P_{inv2} + P_{aux} \quad (11.34)$$

The auxiliary power is the required power for the lights, wipers, etc. In combined hybrid vehicles a second convertor can be necessary and hence the corresponding power has to be delivered by the battery. The reduction cluster resistive power P_r (reference for AR) has to be adapted in the same way, due to the fact that these power values P_{aux} and P_{inv2} have no contribution to the acceleration power. The reduction cluster setpoint power P_{sp} (reference for PR) is not affected by the auxiliary or second convertor power.

11.3 Battery .vi

In this paragraph a model example for a lead acid battery is described. The component library contains similar models for NiCd batteries. This component contains a model to track the State of Charge SoC according to the power drawn

from the battery. The state of charge is the relative remaining capacity C_1 of the battery, expressed in percentage. Discharging during a period T_s with a current I_{bat} leads to a SoC equals:

$$SoC = 1 - \frac{I_{bat} \cdot T_s}{C_1 \cdot 3600} \quad (11.35)$$

The capacity C_5 is the numbers of Ampere-hours (Ah), which can be drawn out of the battery during five hours with a current equal to C_5 divided by five. A battery consists in a number of cells connected in series and possibly in a number these series-cells groups connected in parallel.

The effect of ambient temperature t_a (in degrees Celsius) on the capacity C_5 is taken into account with the help of an empirical formula. An example for a lead acid battery is give by equation (11.36)[162]. The influence of age, numbers of discharge/charge cycles are not taken into account. The capacity C_5 is multiplied by the number of serie-cells in parallel Nr^p to get the total battery capacity C_{tot} .

$$C_{tot} = \frac{Nr^p \cdot C_5}{1 + 0,006 \cdot (30 - t_a)} \quad (11.36)$$

This programme uses a cell-module, “**Battery cell .vi**”, that characterises the open-circuit voltage U_o and the internal resistance R_i , both dependent on the current SoC, the temperature and on discharge or charge condition (equations (11.37) and (11.38)). E.g. the internal resistance of a Lead Acid battery dependency of the SoC is due to the variation of electrolyte conductivity and of the bad conducting lead-sulphate deposited on the electrodes. The dependency on the internal resistance with the state of charge is bound to the battery type. These figures can be measured for charging as well as for discharging. Notice that the model does not take into account the possible unbalance between cells or monoblocs.

$$U_o = Nr^s \cdot f(SoC, t^\circ) \quad (11.37)$$

$$R_i = \frac{Nr^s}{Nr^p} \cdot f(SoC, t^\circ) \quad (11.38)$$

With :

- N_r^s : number of cells in series
- N_r^p : number of serie-cells in parallel
- t° : cell temperature ($^\circ\text{C}$)
- U_o : open-loop voltage (V)
- R_i : internal resistance (Ω)

The capacity of the battery changes in function of the discharge (or charge) current. The implemented model tracks the state of charge according to the power drawn from the battery. On the bases of the actual battery current I_{bat} and the time increment T_s , the variation of state of charge ΔSoC is calculated. It is primarily based on the empirical law of **Peukert** [163,164].

Peukert's equation is a formula that shows how the available capacity of a battery changes according to the rate of discharge. The capacity of a battery is expressed in Ampère-Hours (Ah), but it turns out that the simple formula of current times hours does not accurately represent the situation. Peukert found that the equation (11.39) fits better the observed behaviour of batteries.

$$C = I^k \cdot \text{Time} \quad (11.39)$$

The equation captures the fact that at higher currents, there is less available energy in the battery. C is the theoretical capacity of the battery, I is the current, Time is the total charge time, and k is the Peukert number, a constant for a given battery. A value close to 1 indicates that the battery performs well. The higher k , the more capacity is lost when the battery is discharged at high currents. The Peukert number of a battery is determined empirically and lies normally between 1.2 and 1.4 for lead acid batteries. If k would be selected equal to one, a linear relation between SoC and capacity would be assumed. Fig. 11.2 represents this equation for different values of k . It is quite remarkable that discharging at 0.1 times the nominal current increases the capacity with a factor 2 when the battery has a Peukert constant k equals 1.3.

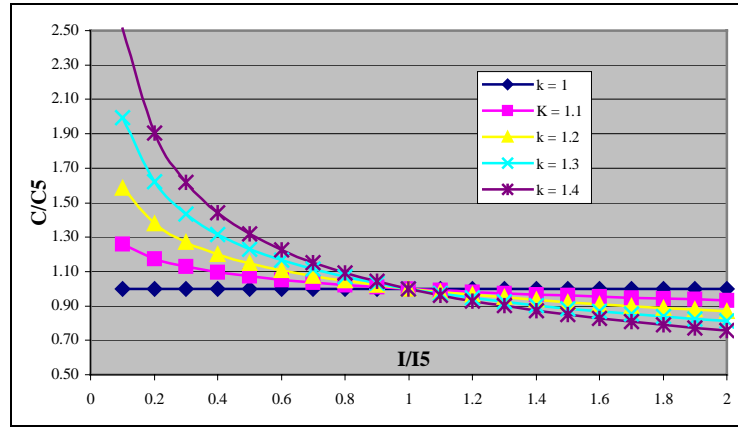


Fig. 11.2: The battery capacity versus discharge current

When the five-hour rate capacity C_5 is given the Peukert expression can be used to calculate the capacity for any give current.

$$C_I = C_5 \cdot \left(\frac{I_5}{I_{bat}} \right)^{k-1} \quad (11.40)$$

The substitution of (11.40) in (11.35) gives:

$$SoC = 1 - \frac{I_{bat} \cdot T_s}{C_5 \cdot 3600} \cdot \left(\frac{I_{bat}}{I_5} \right)^{k-1} \quad (11.41)$$

This law is transformed into (11.42) that expresses the state of charge increment ΔSoC . This equation assumes that the current I_{bat} remains constant during one step T_s of the simulated speed cycle. In this equation, C_{tot} , taking into account the temperature effect, replaces C_5 .

$$\Delta SoC = \frac{T_s}{3600} \cdot \frac{|I_{bat}|^k}{(C_{tot}/5)^{k-1} \cdot C_{tot}} \quad (11.42)$$

To be able to implement this formula the knowledge of the battery current is required. This value can be calculated based on the fundamental electric equations (11.43) and (11.44), which described the simple battery model of Fig. 11.3. Transforming these formulas gives (11.45), which defines the battery current I_{bat} in function of the required battery power P_{bat} , the internal resistance R_i and the open loop voltage U_o .

$$U_{bat} = U_o - R_i \cdot I_{bat} \quad (11.43)$$

$$P_{bat} = U_{bat} \cdot I_{bat} \quad (11.44)$$

$$I_{bat} = \frac{U_o - \sqrt{U_o^2 - 4 \cdot P_{bat} \cdot R_i}}{2 \cdot R_i} \quad (11.45)$$

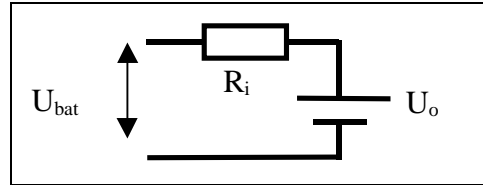


Fig. 11.3: Equivalent scheme of a simple battery model

Modelling of a battery is extremely difficult. Understanding what is going on in battery requires an in-depth research of several years. Finding the right equation to describe these phenomena is not straightforward, especially when they have to be implemented in a simulation tool. The time constant characterising the dynamic behaviour of the battery (e.g. the battery voltage) is of the same order of magnitude as the mechanical driving time constants. A dynamic battery model can thus lead to a more accurate simulation result. Different models are already proposed, but experimental data is very hard to find. Fig. 11.4 illustrates an example of a dynamic battery model for a lead acid battery [165]. Fig. 11.5 shows a possible equivalent circuit for a NiCd Battery [166]. Specific battery management and test infrastructure has recently been developed at the Vrije Universiteit Brussel to perform dynamic battery test in a well-controlled environment. With the help of powerful surface fitting algorithms, dynamic models as well as a new type of SoC-indicator are under development. Up-to-now a maximum open-loop-voltage deviation in time is implemented in the software model.

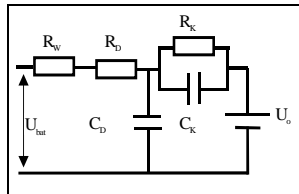


Fig. 11.4: Dynamic battery model

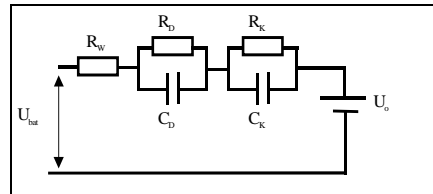


Fig. 11.5: Equivalent circuit for the NiCd Battery

With some types of batteries the electrolyte can start gassing when the battery cell voltage exceeds a certain level U_g . For lead acid batteries gassing occurs above 2.4

Volts. Whenever the voltage exceeds this value a constant charge acceptance of 80% is assumed in the simulation.

In equation (11.45) a square root is taken. If the argument of this square root is negative, it means that the battery is not able to deliver the required power P_{bat} . The maximum power that can be delivered is thus given by equation (11.46). Remark that according to equation (11.45) the battery is able to accept negative powers of any amplitude since the square root then certainly is a real value.

$$P_{\max} = \frac{U_o^2}{4.R_i} \quad (11.46)$$

When the battery cell voltage exceeds the maximum allowed voltage U_{\max}^{cell} , the battery power is limited to the corresponding maximum power $P_{\max}(U_{\max})$ (equation (11.47)). And vice versa, when the battery cell voltage drops under a minimum level U_{\min}^{cell} the corresponding maximum power $P_{\max}(U_{\min})$ is calculated with equation (11.48). Note that $P_{\max}(U_{\max})$ is always positive and $P_{\max}(U_{\min})$ always negative. The possible battery power P_{pos} is thus limited to one of these values (equations (11.49)). These voltage limits are required in real life too. Outside these limits irreversible electrochemical process will damage the battery.

$$P_{\max}(U_{\max}) = \frac{U_o - Nr^s . U_{\text{cell}}^{\max}}{R_i} . Nr^s . U_{\text{cell}}^{\max} \quad (11.47)$$

$$P_{\max}(U_{\min}) = \frac{U_o - Nr^s . U_{\text{cell}}^{\min}}{R_i} . Nr^s . U_{\text{cell}}^{\min} \quad (11.48)$$

$$P_{\text{pos}} = P_{\max}(U_{\max}) \vee P_{\max}(U_{\min}) \quad (11.49)$$

Furthermore two other operating limits are implemented: the maximum battery charge current I_{\max}^{ch} and the maximum discharge current I_{\max}^{dis} . The corresponding maximum power $P_{\max}(I_{\max})$ is calculated with equation (11.52) and equation (11.53).

$$I_{\max} = I_{\max}^{\text{ch}} \quad \text{if} \quad (I \geq 0) \quad (11.50)$$

$$I_{\max} = I_{\max}^{\text{dis}} \quad \text{if} \quad (I < 0) \quad (11.51)$$

$$P_{\max}(I_{\max}) = \frac{P_{\text{pos}}}{I_{\text{bat}}} . I_{\max} \quad \text{if} \quad (I \neq 0) \quad (11.52)$$

$$P_{\max}(I_{\max}) = U_0 \cdot I_{\max} \quad \text{if } (I = 0) \quad (11.53)$$

For each limit the appropriate AR and PR are calculated. Remark that all the operating limits (U_{\max} , U_{\min} , I_{\max}) are reduced to a kind of power limit, which simplifies the iteration process.

Finally, when all parameters are within operating boundaries, the amount of capacity charged into the battery Ah^+ and the amount discharged out of the battery Ah^- are calculated (equations (11.54) and (11.55)) as well as the new value of the state of charge (equation (11.56)). The regeneration of braking energy is expressed in the relative value defined by equation (11.57).

$$Ah_t^+ = Ah_{t-1}^+ + I \cdot T_s / 3600 \quad (11.54)$$

$$Ah_t^- = Ah_{t-1}^- + I \cdot T_s / 3600 \quad (11.55)$$

$$SoC_t = \Delta SoC + SoC_{t-1} \quad (11.56)$$

$$regen = 100 \cdot \frac{Ah^-}{Ah^+} \quad (11.57)$$

11.4 Ultra-capacitor .vi¹

The model of an ultra-capacitor can be developed in a similar way as that of the battery. The voltage U_c over the capacity C has the same roll as the openloop voltage U_0 of the battery. The capacity voltage U_c changes with the electrical charge q . The electrical charge will change in function of the cell current I_c [167].

$$U_c = \frac{q}{C} \quad (11.58)$$

$$q_{t+1} = q_t - I_{cell} \cdot T_s \quad (11.59)$$

The equivalent circuit (Fig. 11.6) is also similar to the battery model.

¹ As up-to-now there was no need to simulate an ultra-capacitor, this model is not yet implemented in the software tool.

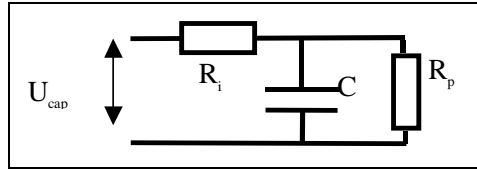


Fig. 11.6: Ultra-capacitor equivalent circuit

Several capacitors can be connected in series N_r^s and in parallel N_r^p . This result in the total capacity voltage U_{cap} and current I_{cap} (equations (11.60) and (11.61)). The internal resistance R_i is dependent on the current and temperature [112].

$$U_{cap} = N_r^s (U_c - R_i \cdot I_{cell}) \quad (11.60)$$

$$I_{cap} = N_r^p \cdot I_{cell} \quad (11.61)$$

Additionally the self-discharge of the capacitor should be taken into account with the resistance R_p [168].

This model does not take into account the possible unbalance between individual cells.

This model can be used as a black box model that is connected to the drive system via a DC/DC converter. The purpose of an ultra-capacitor is to provide the acceleration power, while the power for constant driving comes from the battery. This operation is not possible when the ultra-capacitor and battery are directly connected in parallel [169].

11.5 Charger .vi

The charger model is a multifunctional model simulating the recharging of the battery after the simulation of the drive cycle. This is the pure charging process itself, not considering the charging phase while driving the vehicle (regenerative braking, generator in series hybrid electric vehicle, etc). It can be used for an electric as well as for a hybrid vehicle. Within the simulation programme the charger is not a part of the drivetrain of the vehicle, but is a subprogramme of the main programme “**VSP .vi**” (see chapter 6).

In electric vehicles the energy is drawn from the mains. After the speed cycle simulation run the battery will be recharged starting from the current SoC of the battery (stored in the “**VSP globals .vi**”) until the SoC equals its required end value. The model for this charging algorithm uses as two subprograms: the “**Battery .vi**” (see paragraph 11.3), as describe in the previous paragraph, and the “**Charge profile .vi**”.

In hybrid vehicles the battery can be recharged from the mains as well as by means of the generator. In the latter case the model of the drivetrain is used again, but the required vehicle velocity is zero. The vehicle stands still and the APU will charge the battery.

The “**Charge profile .vi**” defines the required charging current. E.g. in the case of an I-U profile the battery will be charged with a constant current until a certain maximum voltage is reached. At this moment the current is decreased to not exceed the maximum voltage. Another example is the I-U-I-profile. Both profiles are illustrated by the following figure.

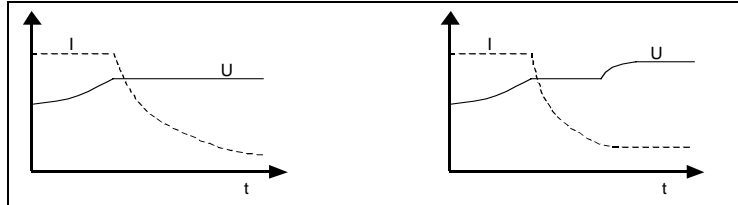


Fig. 11.7: Charge profiles: I-U (left) and I-U-I (right)

The same principles as used in the vehicle drivetrain iteration process (see chapter 8 “**Iteration Algorithm .vi**”) are used to simulate the possible battery charging, taking into account battery operating boundaries. Within a while loop a Power Distribution Factor PDF will be controlled with the help of a Power Reduction factor. Both equal one as long as the charging process keeps the battery operating points within limits. Based on the charge current I_{ch} coming from the charging profile and the battery voltage U_{bat} , the battery charge power P_{ch} is calculated (equation (11.62)).

$$P_{ch} = -I_{ch} \cdot U_{bat} \cdot PDF \quad (11.62)$$

Once the charging current and power are calculated the efficiency η of the charger can be calculated based on e.g. an empirical equation. During a certain time of the charging process battery heating can be possibly required. This option is foreseen as an additional required power $P_{heating}$. Together with the required charging power and the charger efficiency η the power drawn from the mains, the grid power P_{grid} , can be calculated (equation (11.63)).

$$P_{grid} = \frac{P_{ch}}{\eta} + P_{heating} \quad (11.63)$$

By integrating the charging power and the grid power, the energy to the battery E_{bat} (equation (11.64)) respectively the energy from the mains E_{grid} (equation (11.65)) are calculated.

$$E_{bat} = \int_{charging\ time} P_{ch} \cdot dt \quad (11.64)$$

$$E_{grid} = \int_{charging\ time} P_{grid} \cdot dt \quad (11.65)$$

The charging stops when the SoC reaches its required end value. The model allows to simulate a part of the whole charging process. Partial charging can give important differences for the energy consumption in comparison to a full charge (end charge included). Some chargers have a low efficiency during the end phase of the charging process. By simulating some short reference cycles (e.g. ECE-15) there can be only a small part of the battery capacity used. Simulating the end charge for such a short speed cycle would cause unrealistic energy consumption (in Wh/km). At the other side not simulating the end charge would give a too optimistic energy consumption for long speed cycles.

11.6 Generator .vi

The only objective of this generator model is to control the engine of an APU in a series hybrid electric drive. It is a different model, with a different purpose, than the motor model. The generator is mechanically coupled to the engine. The engine model can be used for an internal combustion vehicle as well as for the APU of a series hybrid drivetrain model. Hence the generator model has to impose the same parameters as the clutch model, namely the engine velocity ω_{ice} , the acceleration torque T_a , the resistive torque T_r , the acceleration a and the key switch. The purpose of the generator model (or engine starter motor) is to start the engine [170] and to control the velocity of the engine in function of a certain optimisation criteria.

The input parameter of the generator is the required DC-power that it has to deliver to the DC-bus. If one would use an AC-generator the same black box approach is possible, where the generator and the required rectifier are gathered in one model.

The generator model differentiates three operating modes:

1. OFF
2. Starting
3. Normal operating

The generator will switch the engine *OFF* when this is required by the basic power control algorithm defined in the e.g. “**Series Hybrid Vehicle .vi**” (see subchapter 7.6). This can only be done when the starting process is completely finished and when the user did not select to use idle mode (instead of shutting down the engine).

Once the engine is switched off and need to restart again or if it was never before engaged, it will first pass the *start-up phase* before it can deliver the required power. The corresponding starting will take a certain time, selectable by the user. This starting time T_{start} will define a required acceleration a_{start} in function of the generator initial speed ω_{ini} and the required start-up velocity ω_{start} (equation (11.66)).

$$a_{start} = \frac{(\omega_{start} - \omega_{ini})}{T_{start}} \quad (11.66)$$

The generator velocity will rise proportional to this acceleration in function of the simulation time increment (equation (11.67)).

$$\omega_{gen}^t = a_{start} T_s + \omega_{gen}^{t-1} \quad (11.67)$$

Hence the generator velocity is defined and the resistive output torque T_r can be calculated in function of the required generator DC power P_{DC} (equation (11.68)).

$$T_r = \frac{P_{DC}}{\eta \cdot \omega_{gen}^t} \quad (11.68)$$

With :

- ω_{gen}^t : generator velocity (rad/s)
- ω_{gen}^{t-1} : previous generator velocity (rad/s)
- η : generator efficiency (%)
- T_s : time increment (s)

Due to its inertia J , accelerating the generator will introduce an additional inertia torque T_a (equation (11.69)). Probably the engine will not be able to deliver these torques, due to the fact its velocity is lower than idle speed. At this moment the engine model will introduce a PR, taking into account the inertia of both generator and engine. In this way the battery will deliver the inertia power during start-up. During the first step of the speed cycle the engine will always start, except when the user has selected the initial generator velocity higher than the start up velocity. Hence it is possible to disengage all starting operations during the simulation.

$$T_a = J.a \quad (11.69)$$

Once the generator velocity is higher than the start-up velocity and the generator is not switched off, the *normal operating mode* will be active. In this mode the DC power will be limited to the maximum generator power P_{max} . The model will also impose a maximum power variation dP/dt . In this way it is possible to simulate moderate variations of the engine required power. Consequently the additional fuel

consumption due to the dynamic operation of the engine is prevented. Similar to the power variation limitation, the model will impose a given maximum velocity variation or generator acceleration a_{\max} . Hence the additional inertia torque T_a , due to too fast acceleration, can be limited.

In e.g. the Series Hybrid Vehicle the engine velocity is independent from the vehicle velocity. This makes it possible to control the generator speed in such a way to operate the engine following different criteria like (see Part I):

1. At constant speed independent from the required power.
2. At a velocity corresponding to the minimum fuel consumption of the engine in function of the required generator power.
3. At a velocity corresponding to the minimum NOx emissions (or other pollutant) of the engine in function of the required generator power.
4. At a velocity corresponding to a rule that is a compromise between fuel consumption and emission minimisation of different pollutants. (An energy optimisation does not automatically imply optimisation of the emissions.)

These criteria can be implemented with the help of a look-up table that describes the relation between generator power and generator velocity. In this way the generator velocity is defined.

The efficiency can be defined with the help of statistical surface fitting models based on measured data in function of e.g. the generator power and velocity. Comparable to the start-up mode the resistive torque T_r is calculated with equation (11.68).

The generator mechanical power is calculated with (11.70). The reduction cluster reference values, the power setpoint P_{sp} and the resistive power P_r , are transformed, by dividing by the velocity ω_{gen} , to torque setpoint T_{sp} and resistive torque T_r . Hence they can be used in the engine model when possibly an operating limit would occur.

$$P_{gen} = (T_r + T_a) \omega_{gen} \quad (11.70)$$

11.7 Clutch .vi

Internal combustion engines require a minimum shaft speed otherwise the motor will stall. Normally the driver takes care of this by playing appropriately with the clutch.

The clutch is not so easy to model as one may think. Especially the process of starting from rest or engine braking depends very much on driver behaviour. The gear shifting moments are also driver related. Therefore it is not feasible to model each possible scenario. Fortunately according to reference [112], it is not necessary for acceptable results.

The clutch model simulates additional losses due to slipping of the clutch at velocities lower than idle speed. When the engine is starting, this model will introduce a certain time during which no torque can be delivered. The model is used in the internal combustion engine as well as the parallel hybrid electric vehicle.

As long as the input velocity (at wheel side) is higher than the speed corresponding to idle engine speed and the engine is not in a starting phase, the clutch is engaged. The clutch inertia is taken into account by increasing the acceleration torque. Also the clutch efficiency is considered.

Once the input velocity drops under the idle speed ω_{idle} the clutch starts slipping. This clutch operation is simulated by the use of an elementary method. When the clutch is slipping the possible torque that can be delivered to the wheels is limited. Hence the input torque is limited to the clutch torque T_c . When the vehicle is decelerating or the engine is still starting, this maximum torque is set to zero. The engine required velocity is set to 50% higher than idle speed and the required engine torque is the clutch torque T_c divided by the clutch efficiency η and an additional slipping efficiency η_{slip} .

$$T_a^o = \frac{T_a^i + J \cdot a_i}{\eta \cdot \eta_{slip}} \quad (11.71)$$

$$T_r^o = \frac{T_r^i}{\eta \cdot \eta_{slip}} \quad (11.72)$$

With :

- J : inertia seen at wheel side(kg.m²)
- T_a^o : acceleration torque at engine side (Nm)
- T_a^i : acceleration torque at wheel side (Nm)
- η : clutch efficiency (%)
- η_{slip} : additional slip efficiency (%)

When the engine is switched off the current velocity is set to zero or one could choose to operate the engine at idle speed. When the engine is starting no power can be delivered to the wheels. Via the starter-indicator a start-up power will be demanded at the auxiliaries (see subchapter 11.11). The starting of the engine will take a certain time, selectable by the user. Similar to the generator model this

starting time T_{start} will define a required acceleration a_{start} in function of the required engine initial speed ω_{ini} (which is mostly zero) and the minimum required idle velocity ω_{idle} .

$$a_{start} = \frac{(\omega_{idle} - \omega_{ini})}{T_{start}} \quad (11.73)$$

The engine velocity will rise proportional to this acceleration in function of the simulation time increment T_s .

$$\omega_{ice}^t = a_{start} \cdot T_s + \omega_{ice}^{t-1} \quad (11.74)$$

The clutch power is given by:

$$P = (T_r^o + T_a^o) \omega_o \quad (11.75)$$

11.8 Engine .vi

The programme simulates the behaviour of an internal combustion engine independent from the kind of fuel.

The model can be used in a classical thermal vehicle or in a hybrid vehicle. On the front panel a selector switch is foreseen to define the vehicle type, because the engine can be used for traction or for power generation, which has an influence on the iteration process. If the engine velocity ω is going to exceed its maximum allowed speed ω_{max} an AR and/or PR is required in function of the type of vehicle. Indeed when the engine is used in a thermal vehicle it is in charge of the accelerating power. This means that when the engine is going to be over-speeded an AR is required to slow down the acceleration. Also in the case of a parallel hybrid vehicle the engine acceleration is likewise proportional to the vehicle velocity and an AR is required.

On the contrary when the engine is used in a series hybrid vehicle any acceleration reduction has no effect on the velocity due to the fact that the generator defines this velocity in function of the generator power. In this case a Power Reduction PR is required to decrease the generator power via the Power Distribution Factor. This is also valid in the case of a combined hybrid vehicle, where the generator modulates the engine velocity via the planetary gear.

The motor inertia J will increase the acceleration torque T_a in function of the possible acceleration. The engine is also in charge of the auxiliary alternator power

P_{alt} (see paragraph 11.11 “**Auxiliaries .vi**”). This power shall increase the resistive torque T_r . This results in a total engine torque T_{ice} defined by the following equation.

$$T_{ice} = T_r + \frac{P_{alt}}{\omega_{ice}} + T_a + J.a \quad (11.76)$$

Internal combustion engines require a minimum shaft speed. This is implemented in the clutch or in the control algorithm of the hybrid vehicle (in paragraphs 11.6“**Generator .vi**” or 9.3 “**Planetary Gear .vi**”).

If the engine is running, with the engine velocity higher than idle speed and the resistive torque different from zero, then the engine is in normal operating mode (see further down). If not, the engine can be in off-mode with the ‘key switch’ and all output parameters are zero. If the key switch is on, with the engine velocity strictly lower than idle speed, then the engine is starting.

The user can select a start-up penalty. This start-up penalty has to be measured and can be imported as a cluster of correction factors for each type of emission and for the fuel consumption. This can be done for different engine start-up temperature. Hence the additional fuel consumption and emissions can be taken into account at start-up. If the user prefers not to use this feature or the data is not available, the idle emissions and consumption are used during this start-up phase. Further it is possible that the key switch being ON, the engine speed equals the idle speed, but the required resistive torque is zero. E.g. in the case of a Series Hybrid Vehicle, when the generator for instance imposes to operate the engine at idle mode (instead of a complete shutdown), the engine speed will be equal to idle speed and the resistive torque equals zero. At this moment the corresponding fuel consumption and emissions will be calculated. As long as the engine is not in normal operating mode the maximum engine torque is zero.

In normal operating mode the maximum torque is defined in a look-up table in function of the angular velocity and the total torque. With the help of the “**AR, PR(T) Calculation .vi**” (see paragraph 8.3.1) the required torque is limited to the maximum value and the corresponding AR en PR are calculated, to allow the iteration loop to converge to the maximum possible corresponding working point. For more details see chapter 7.

Table 11.1: Possible AR en PR implementation for engine operating limits

	ω -max	T-max
ICV	AR	AR
PHV	AR	PR
SHV	PR	PR
CHV	PR	PR

Once the possible engine torque is known the emissions (in g/s) and fuel consumption (in L/s) can be calculated on the basis of iso-emission and consumption curves (in g/kWh). Out of the possible speed and torque the emissions are calculated using bilinear interpolation of the discretised iso-emission curves, which are entered in several arrays. These curves or maps are describing the static behaviour of an internal combustion engine. This works when transients are negligible. However if transients are large the interpolated results may be wrong with several orders of magnitude [171].

If the engine torque is negative - the engine is slightly braking the drivetrain - a small constant fuel consumption and emission are assumed

The engine will produce additional emissions when the engine is cold. A cold/hot emission ratio can be introduced, which is a function of ambient temperature and trip length [172,173,154]. On the front panel the user can select if the motor operates in a warm mode or cold mode. In the case of a cold engine an additional penalty is implemented based on an empirical model, which describes emissions and fuel consumption correction factor in function of the ambient temperature and fuel type [172].

The mechanical power P_{ice} of the engine shaft (equation (11.77)) as well as the power of the consumed fuel P_{fuel} (equation (11.80)) is calculated. The last one is a function of the fuel density D and fuel specific energy E_{fuel} . The efficiency is calculated and the fuel content F is reduced by the fuel consumption (equation (11.81)). The fuel mass M_f is proportionally decreased (equation (11.82)). A small gadget is added allowing the user to see the engine operating point moving in the torque-speed-operating plane. The emissions are multiplied by the simulation time increment and stored in the parameter tracer for further use in the main programme (“VSP .vi”).

$$P_{ice} = \omega_{ice} \cdot T_{ice} \quad (11.77)$$

$$fc = fc(\omega_{ice}, T_{ice}, t_a^o) \quad (11.78)$$

$$Cons = \frac{fc}{1000 \cdot D} \quad (11.79)$$

$$P_{fuel} = Cons \cdot E_{fuel} \cdot 10^6 \quad (11.80)$$

$$F_t = F_{t-1} - Cons \cdot T_s \quad (11.81)$$

$$M_f = F_t \cdot D \quad (11.82)$$

With :

- T_{ice} : total engine torque (Nm)
- T_r : resistive torque (Nm)
- P_{alt} : alternator power (W)
- T_a : acceleration torque (Nm)
- ω_{ice} : angular velocity (rad/s)
- P_{ice} : mechanical shaft power (W)
- t_a° : ambient temperature ($^\circ\text{C}$)
- fc : fuel consumption (g/s)
- D : fuel density (kg/L)
- $Cons$: fuel consumption (L/s)
- E_{fuel} : specific energy (MJ/L)
- P_{fuel} : fuel power (W)
- F_t : fuel content (L)
- F_{t-1} : previous fuel content (L)
- T_s : simulation time increment (s)
- M_f : mass of remaining fuel (kg)

If engine data corresponding to an engine with a certain required size is not available, an engine can be selected out of the database and its characteristics can be scaled down (or up) by the help of a scaling factor.

The functional model of a *turbine* is similar to that of an engine. There are characteristic maps, which contain the specific properties of a turbine. Due to the fact that a turbine is driving the APU of a series hybrid vehicle and operates during most of the time in one working point, the turbine simulation can be easier than simulating an engine. For this working point one point of the different maps like specific consumption, CO, NO_x, CO₂, HC, smoke particle emissions can be considered [112].

Nevertheless the engine model considers cold operation and start-up penalties it is still a rather simple model. Several other parameters, not taken into account up-to-now, can influence the fuel consumption and emissions.

The model does not consider any time delay associated with fuel transport or torque production. The model does not simulate cranking or associated emissions. No transients of any kind are included. Mean value torque model is used, corresponding to the average torque over the engine cycle.

Recent investigations carried out in the frame of the German and Swiss emission factor programme have shown that it is necessary to take into account the influence of altitude when determining pollutant emissions for the vehicle concepts investigated in cases where a major proportion of the mileage is on roads at a high elevation [154].

In the case of conventional spark-ignition and diesel vehicles, the emission behaviour generally deteriorates within a service interval. In the case of catalyst vehicles an unavoidable deterioration in the degree of conversion by the catalyst (due to thermal ageing and contamination) leads to an increase in emission with increasing mileage. Defects, setting errors and lack of maintenance are superimposed, in practical operation, on the physically determined reduction in the degree of conversion by the catalyst. Consequently the implemented look-up tables describe the engine behaviour corresponding to the age of the characterised engine.

Hydrocarbon emissions from motor vehicles arise from two major sources, exhaust emissions and evaporative losses through the vehicle's fuel system (storage tank, carburettor or injection system, fuel pipes). Evaporative emissions occur as a result of fuel volatility combined with the variation of the ambient temperature during a 24-hour period or the temperature changes of the vehicle's fuel system that occur over a normal driving procedure.

In general there are four types of evaporative losses:

1. Filling losses. These losses occur when the vehicle's fuel tank is filled and the contents of saturated vapours are displaced and usually vented to the atmosphere. The filling losses are usually attributed to the fuel handling chain and not to the vehicle emissions. Consequently they are considered in subchapter 6.4, describing the fuel refinery.
2. Diurnal breathing losses. These losses are the result of the night-day temperature cycle, causing the contents of the fuel tank to contract and expand, pushing saturated vapour out on expansion.
3. Hot soak losses. These occur when a vehicle is switched off after operation and the equalisation of the temperatures leads to the evaporation of the fuel in certain parts of the engine. Hot soak losses and diurnal losses constitute the main part of evaporative losses. In newer vehicles, vapour traps (carbon canisters) installed on the vehicle should largely capture these losses.
4. Running losses. These evaporative losses occur during the operation of the vehicle. Running losses are the least documented source of evaporative emissions. On modern cars, equipped with carbon canisters, the canister should capture any running losses but there are reports, which show that running losses would occur nevertheless. On vehicles without carbon canisters, running losses should be regarded as a reality [154].

The model could be further improved by taken into account certain high-emission events. Such high-emission events occur during phases of extreme high acceleration and during gear changes. The duration of such an event is usually only a few seconds, but the emissions level might reach many (even up to 20 000) times the level

of emissions during normal operation. This is especially true for modern petrol vehicles with closed-loop catalytic converters [174].

11.9 Fuel Cell .vi

The fuel cell model is once again a typical black box approach. This made it possible to develop in the first instance one simplified model containing the fuel cell stack, the dc-dc convertor, the reformer and the auxiliary system [175]. The disadvantage of the chosen model is that the fuel cell itself cannot be connected parallel to a battery pack, to study the influence of e.g. power distribution between battery and fuel cell based on their proper voltage characteristics. A convertor controlling the powerflow will always be in-between in the implemented simulation model.

Furthermore temperature and pressure effects are not included in the model, due to lack of sufficient data. A higher stack temperature or lighter pressure will lead to a lower voltage level. The starting process of some fuel cells can be very long and can give important additional energy consumption and emissions. This starting state is as well not included. The model is based on experimental data found for an Alkaline Fuel Cell (AFC), as well as for a Proton Exchange Membrane fuel cell (PEM) [176]. An analogous approach can be carry out for other fuel cell types.

The dc-dc convertor adapts the fuel cell voltage level to the DC-bus voltage or battery voltage. It is modelled by a simple efficiency value (see (11.83)). The fuel cell can only deliver a positive power. If the fuel cell power P_{fc} is negative the maximum power level is set to zero.

$$P_{fc} = \frac{P_{FC}}{\eta_{conv}} \quad (11.83)$$

The power required for the fuel cell auxiliaries P_{aux} (pump, compressor, controller) is calculated based on experimental data in function of the required fuel cell power (see equation (11.84)).

$$P_{aux} = a + b.P_{fc} + c.P_{fc}^2 \quad [176] \quad (11.84)$$

$$P_{ref} = \frac{P_{fc}}{\eta_{ref}} \quad (11.85)$$

$$P_{stack} = P_{fc} + P_{aux} + P_{ref} \quad (11.86)$$

With :

- P_{FC} : convertor power to DC-bus (W)
- η_{conv} : convertor efficiency (%)
- P_{fc} : fuel cell power (W)
- a, b, c, : constant empirical values
- P_{aux} : auxiliary power (W)
- η_{ref} : reformer efficiency loss (%)
- P_{ref} : reformer power (W)
- P_{stack} : fuel cell stack power (W)

The power required for the Reformer P_{ref} is also taken into account proportional to the delivered power (equation (11.85)). The sum of these power components results in the total required stack power P_{stack} (equation (11.86)). If this stack power exceeds the maximum allowed stack power P_{max} , the iteration process will decrease the fuel cell power P_{FC} .

The fuel cell stack consists of different modules connected in serie. Each module is a combination of a number of individual cells in serie and different rows of serie-cells are connected in parallel. The required power for each cell P_{cell} can be calculated by dividing the stack power by the total number of cells. This is not totally correct due to the possible unbalance between cells. Based on experimental data the cell current I_{cell} can be computed in function of this cell power [176]. The Fuel Cell is mainly acting as a resistance. A fuel cell is characterised by a certain dynamic behaviour. The current cannot change infinitively fast. The larger the cell surface the faster the current can change. The simulation model shall check the maximum current variation and if necessary it will reduce the required fuel cell power. If the fuel cell is used in a hybrid drivetrain its power will be modulated by the Power Distribution Factor via the PR. If the fuel cell is used in an electric drivetrain without a battery, the fuel cell required power can only be reduced via the Acceleration Reduction factor acting on the acceleration of the vehicle.

The Fuel Consumption (fc) is calculated in function of the current Law of Faraday, which gives the relation between the reactant consumption and the produced current: one gram equivalent weight of matter is electrochemically altered at each electrode for 96489 Coulomb of electricity passed through the electrolyte. Two gram of hydrogen H_2 produces 192978 Ampère-seconds (As) or 53.61 Ampère-hours (Ah). The elimination (purge) of impurities is taken into account with a correction factor (e.g. 1.012 in equation (11.87)) [176]. The fuel consumption corresponds with a certain fuel power content in function of the density D (kg/m³) and the specific energy E_{H_2} (equation (11.89)).

$$fc = 1.012 \cdot \frac{I_{\text{cell}} \cdot 22,4(\text{L/mol})}{2.96489(\text{As})} \quad (11.87)$$

$$Cons = Nr_{\text{cells}} \cdot fc \quad (11.88)$$

$$P_{\text{fuel}} = Cons \cdot E_{H_2} \cdot D \cdot 10^6 \quad (11.89)$$

$$F_t = F_{t-1} - T_s \cdot Cons \quad (11.90)$$

With :

- I_{cell} : cell current (A)
- fc : fuel consumption per cell (L/s)
- $Cons$: fuel consumption of the whole stack (L/s)
- Nr_{cells} : number of cells
- D : Fuel density (kg/m³)
- E_{H_2} : specific energy (MJ/kg)
- P_{fuel} : fuel power (W)
- F_t : fuel content (L)
- F_{t-1} : previous fuel content (L)
- T_s : simulation time increment (s)

The overall transformation efficiency, from fuel power P_{fuel} to delivered DC power P_{FC} including reformer and auxiliaries, is calculated. The emissions are calculated proportional to the fuel consumption [177]. This is a very simplified approach that only gives an indication of the order of magnitude of the emissions. Additional data has to be available for the extension of the model. This model is an unpretentious model, but due to the black box approach it can easily be completed as soon as more experimental data are available.

11.10 Flywheel .vi

This model simulates the behaviour of a flywheel and its convertor. This flywheel-convertor group is connected to the “**DC-bus controller .vi**” of the “**Series Hybrid Vehicle .vi**” or it can replace the “**Battery .vi**” of a “**Battery electric Vehicle .vi**”. In the case of the series hybrid vehicle it acts like a generator and its power is modulated via a Power Distribution Factor. In the case of the electric vehicle it is in charge of the traction power and when an operation limit occurs the vehicle acceleration will be reduced.

As long as the key switch of the flywheel is OFF the flywheel is not able to deliver power, even if requested by the drivetrain. If the key switch is on, the required flywheel-converter power P_{req} will be divided by the converter efficiency η (including converter losses and all flywheel losses except the friction moment). This required power is compared with the maximum power P_{max} that the flywheel can deliver. The flywheel current rotational velocity ω_{fw} , the maximum acceleration a_{max} , flywheel inertia J and the maximum torque T_{max} define this maximum power.

$$P_{max} = \omega_{fw} \cdot \max(T_{max}, J \cdot a_{max}) \quad (11.91)$$

The flywheel velocity must be kept above a certain minimum speed ω_{min} , otherwise the flywheel is not able to deliver power and below a maximum velocity ω_{max} otherwise it can be damaged. The “**FW-limits .vi**” subprogramme will control if the flywheel velocity remains within limits. If this is not the case the maximum power is set to zero.

The maximum velocity defines the maximum energy content of the flywheel E_{max} , which corresponds with a State of Energy (SoE) equal to one (equation (11.92)). To have no confusion with the battery model, in the flywheel model a state of energy is used instead of a state of charge.

$$E_{max} = \frac{\omega_{max}^2 \cdot J}{2 \cdot 3600} \quad (11.92)$$

Even if the flywheel is not delivering power, its energy content E_{cons} will decrease due to the friction moment T_{fr} . In function of the simulation time increment T_s the energy consumption E_{cons} is computed with equation (11.93).

$$E_{cons} = \frac{T_s}{3600} \cdot \left(T_{fr} \cdot \omega_{fw} + \frac{P_{fw}}{\eta} \right) \quad (11.93)$$

The flywheel energy will decrease or increase in function of the sign of the flywheel power P_{fw} (equation (11.94)).

$$E_{fw}^t = E_{fw}^{t-1} - E_{cons} \quad (11.94)$$

The corresponding flywheel state of energy and angular velocity can be calculated according to respectively (11.95) and (11.96).

$$SoE = \frac{E'_{fw}}{E_{max}} \tag{11.95}$$

$$\omega_{fw} = \sqrt{\frac{E'_{fw} \cdot 3600 \cdot 2}{J}} \tag{11.96}$$

With :

- E_{fw}^t : flywheel energy (Wh)
- E_{fw}^{t-1} : previous flywheel energy (Wh)
- ω_{fw} : velocity (rad/s)
- J : inertia ($kg \cdot m^2$)

11.11 Auxiliaries .vi

Some vehicles can be equipped with that many auxiliaries (e.g. servo-actuators, hydraulic transmission, air-conditioning, etc.), that their energy consumption can no longer be neglected. Reference [178] indicates that 30% of the energy consumption of their examined diesel-electric bus was due to the power consumption of the auxiliaries.

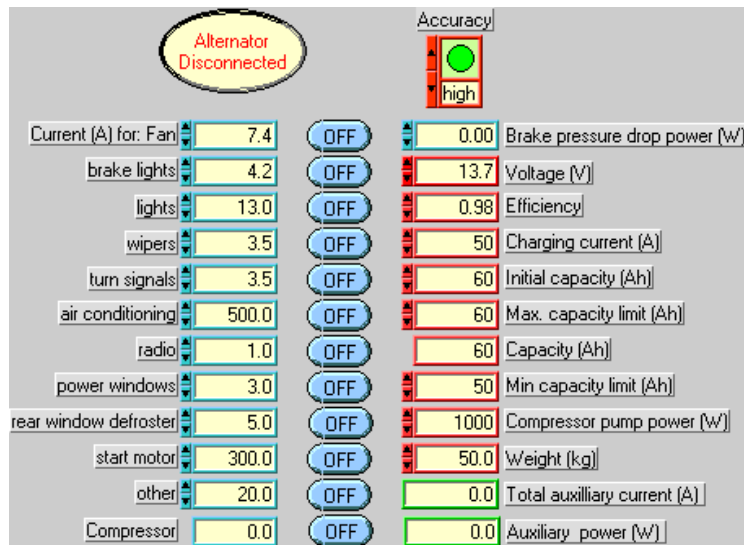


Fig. 11.8: Front panel of the Auxiliary .vi

An auxiliary battery is used as energy buffer. To recharge the battery power is usually drawn mechanically from the shaft by an electric alternator. In the case of an electric vehicle this battery is recharged via a DC/DC convertor.

The auxiliary circuit model allows the user to engage some 12V (or 24V) components by selecting the corresponding ON/OFF button on the front panel (e.g. fan, rear window defroster, lights, wipers, turn signals, air conditioning, radio, power windows, etc.), as illustrated with the figure below.

When an internal combustion engine must be started with a starter motor, the boolean switch ‘start motor’ will be switched on and the auxiliary battery will be discharged. During braking, the brake lights are switched on and when the brake pressure level becomes to low, the compressor will be activated, which results in an additional auxiliary consumption.

The subprogram “**compressor .vi**” contains the model for electric and hybrid electric vehicles, which calculates the pressure level of the brakes p . In traditional vehicle this brake pressure is assured via a vacuum pump. In any case the brake pressure should be kept on level, which requires an additional power.

If this level becomes lower than a pressure lowest limit, the compressor pump will be activated until the pressure upper limit is reached. This results in a power P_p and current consumption I_c , which is delivered by the auxiliary battery. The compressor efficiency η_c parameter reflects the losses between the power required from the auxiliary battery and the power necessary to build up the pressure. In function of the auxiliary battery voltage U_{aux} the current I_c of the motor driving the compressor is calculated (equation (11.97)). In function of the pump power P_p , brake power P_b and the pressure ratio coefficient i_p the pressure drop is calculated (equation (11.98)). At the start of the simulation the compressor is switched on and an initial pressure level of 90% is assumed.

$$I_c = \frac{P_p}{\eta_c \cdot U_{aux}} \quad (11.97)$$

$$p_t = p_{t-1} \cdot i_p \cdot (P_b + P_p) T_s \quad (11.98)$$

The programme will calculate the total current I_{tot} and corresponding power, consumed by all auxiliary components.

The auxiliary battery will be recharged with a constant current I_{ch} at the moment a minimum battery capacity is attained. The battery is charged until a maximum capacity level (equation (11.99)). The equation describes a very simple linear model for a battery, but is more than sufficient for the modelling of the auxiliary extra power consumption.

$$C_t^{aux} = C_{t-1}^{aux} + \frac{T_s}{3600} \cdot (I_{ch} - I_{tot}) \quad (11.99)$$

The charging is only allowed when the starter motor is switched off (during the start phase of an internal combustion engine, the engine is assumed not to deliver power).

The corresponding required alternator or DC/DC power is calculated with equation (11.100). A constant efficiency is assumed.

$$P_{aux} = \frac{U_{aux} \cdot I_{ch}}{\eta} \quad (11.100)$$

The DC/DC or alternator can be disengaged to allow a simulation without taking into account this auxiliary consumption.

PART III
EXPERIMENTS, RESULTS AND
COMPARATIVE ASSESSMENTS

12 INTRODUCTION TO PART III

Accurate and validated data describing the characteristics of the drivetrain components is the power of a simulation programme. Reliable data is very important, as well as the ‘coverage’. The latter requires that the data describe the characteristics covering the whole working field of the components. When data is available, but only for a few working points, it will be difficult to have good simulation results.

Due to the use of the simulation tool in different research projects, the software could be debugged and the programme structure could be made flexible allowing different kinds of input data. Furthermore a good test protocol has been developed. The laboratory of Electrical Engineering Department of the VUB disposes of measurement equipment to characterise electrical and mechanical components, as well as entire vehicles.

This third part describes briefly the measurement equipment as well as the different types of measurements that can be performed. Furthermore the manipulation of the measured data to useful input figures for the simulation is explained. Different examples of the database are illustrated. Additionally a calibration and validation of the simulation programme is performed as well as a parameter sensitivity analysis.

This third part also illustrates several simulation results of different drivetrains, powerflow control strategies of hybrid concepts as well as comparisons of the energy consumption and emissions of different vehicles.

13 MEASUREMENT EQUIPMENT

The components database is developed based on own measurements and information found in literature. Following measurement equipment and test benches were available to characterise the components and vehicles and to validate the simulation results:

- An “on road” measurement tool to evaluate the drivetrain of electric or hybrid vehicles (only DC).
- A second “on road” measurement tool able to measure AC and DC signals.
- A roll bench to assess passenger cars.
- Laboratory equipment to characterise the components of an electric drivetrain individually (Foucault brakes, electric loads, analogue and digital measurement devices, torque transducers, etc.).

The laboratory of electrical engineering is equipped with mainly electrical and mechanical measurement tools. When fuel consumption- and emission characterisation were required other laboratories¹ have offered their help.

13.1 Measurement System Requirements

An on-road measurement system has to be modular, easy to extend, user-friendly and able to measure different type of quantities like e.g. alternating and direct current and voltage, torque, velocity, frequency and power. The system has to be capable to evaluate bicycles as well as urban buses. The system should be very flexible since the amplitude of the quantities that has to be measured, can strongly vary in function of the tested vehicle. To have a sufficient accuracy (required for measuring losses and characterising efficiencies) the system had to be modular. This modularity requires the possibility to use different measurement traducers, with different measurement range. A ‘Plug and Play’ based system is preferred.

A mobile data-acquisition system has some specific requirements concerning the use in vehicles on road. In the first place it has an independent supply (e.g. a 12 V battery). The system is very compact and easy to install in the vehicle, without permanent damage to the vehicle and without endangering the safety of the driver and passengers. It is robust and should withstand shocks and vibrations. All mechanical as well as electrical connections are realised in a reliable way.

Since the measurement will be accomplished in a possible ‘electrical dirty environment’, the measurement transducers may not be disturbed by the

¹ The department of mechanical engineering of the V.U.B. and the Royal Military School of Belgium

electromagnetic interference of e.g. inverters and chargers. Appropriate filtering and isolation is necessary.

Both on-road measurement systems of the VUB fulfil these requirements. The systems are able to perform four different types of measurement campaigns:

- Acceleration tests: this requires a sampling frequency of maximum 50 Hz.
- Drive cycle test: can be performed at 1 Hz.
- Battery charging test: every three minutes the average of e.g. 10 measuring points should be taken and this over a period of at least 8 hours (in function of the charge characteristic).
- Laboratory test: requires high accuracy and a sampling frequency of some 100 kHz if e.g. PWM-signals are to be measured.

Most of the parameters that are to be measured are DC quantities. Conventional AC equipment is designed to measure commercial 50 Hz AC signals. Such equipment is not appropriate to measure the power of a PWM inverter having a high switching speed. The inverter frequencies vary from 0.01 Hz to 600 Hz, with superposed modulation frequencies [179]. Another solution consists in first measuring the time signals at a high sampling frequency and processing the measurement to calculate true RMS values afterwards. If the power is calculated out of these time signals the voltage and current are measured at exactly the same time (sample and hold device required). The measurements are synchronised before sampling.

13.2 Measuring Points on Roll Bench and Laboratory Test Bench

Fig. 13.1 shows the different measurement points in the case of a series hybrid vehicle. Measurements can be performed on an existing drivetrain or on individual components. In the first case the drivetrain can be evaluated on-road or on a roll bench. The on-road measurements give results of the energy consumption and component behaviour in real life conditions. The characterisation on the roll bench allows the selection of different operating points by the appropriate choice of the load of the rolls. The roll bench (see Fig. 13.2) is equipped with an electromagnetic brake. It can also be driven by a separately excited DC-motor; this allows imposing speed and torque, either positive or negative. This is necessary to simulate real road conditions and speed cycles on the roll bench. With the help of a PLC-driven system it is possible to simulate predefined speed cycles. Unfortunately, the size of the roll bench is not sufficient to characterise all kind of vehicles. It is originally designed to test passenger cars simulating the ECE-15 cycle, which has a top speed of 50 km/h [180]. Additionally to speed cycles, the roll bench is also used to characterise the entire vehicle as well as to qualify drivetrain components by imposing different constant speed and torque values at the wheels of the vehicle. In

this way one can measure e.g. the losses of the different components if their in- and outputs are accessible.

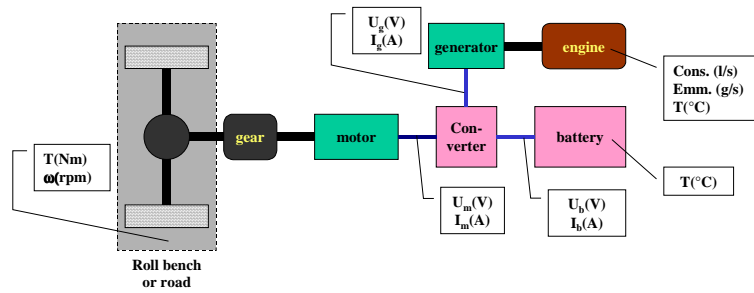


Fig. 13.1: Series hybrid drivetrain characterisation



Fig. 13.2: Roll bench

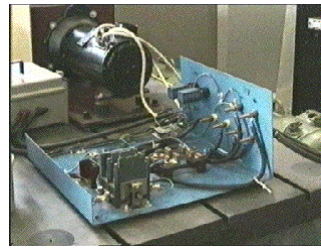


Fig. 13.3: Laboratory test bench

However it is not always possible to have access to all parts of the drivetrain (e.g. the output shaft of the motor). In most circumstances the battery and converter can be characterised separately but the motor must be characterised together with the transmission. In the case of some series hybrid vehicles the APU can be measured when the vehicle is not driving with off-board diagnostic tools. This is when the APU operates independently from driving conditions.

Components can also be characterised on a laboratory test bench (see Fig. 13.3). Hence e.g. the motor can be connected to a load and the converter to a DC supply, replacing the battery (see Fig. 13.4). All possible operating points can be selected with the help of the load and supply. The corresponding losses can be characterised.

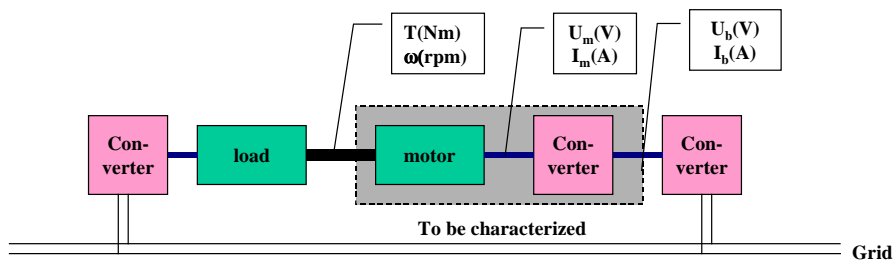


Fig. 13.4: Component characterisation

13.3 “ON ROAD” Measurement Equipment

13.3.1 First Measurement System (only DC)

The first on-road measurement system [181,182,183] is based on a compact 16 channels data-acquisition system. The datalogger has the following characteristics:

- ANERMA-UPC 1 CARD
- 16 analogue channels
- Input range: -5 V to + 5 V (bipolar mode) or 4-20mA
- Micro-controller: buffer 64 Kbytes
- Maximum sampling rate: 10 Hz for each channel

Fig. 13.5 illustrates the principal outline of the measurement system.

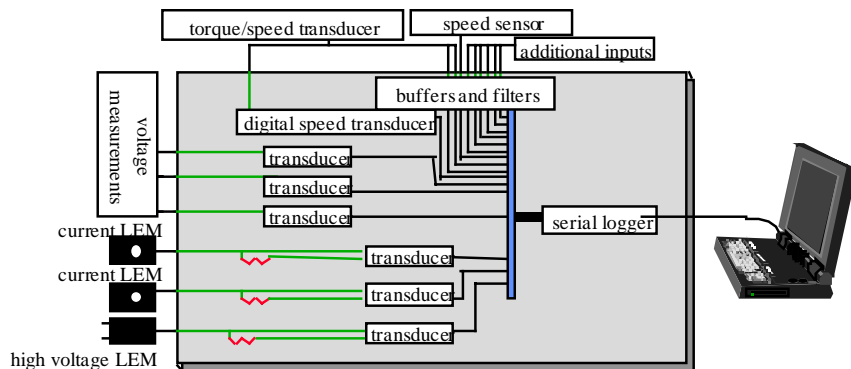


Fig. 13.5: Principal outline of the measurement system

The vehicle speed (max. 200 km/h) is measured with a DATRON DLS sensor. The speed sensor is based on a correlation optical method with spatial-frequency filtering [184]. This technology is used by most of the major institutes in charge of testing and evaluating vehicles. It has a high accuracy (higher than 0,1 %), it is robust and very easy to install on the vehicle (see Fig. 13.6).

Torque and speed can be qualified with the help of the torque transducer of the roll bench. The power from the mains (up to 380 V / 10 A / 50 Hz) can also be determined with the data-acquisition.

Three channels can measure voltages up to 300 V, one up to 800 V and two channels are designed to measure currents of maximum 600 A. For the current and the voltage measurement Hall-effect transducers are used (LEM LT1000S, LV800, LT300 and LT100). Voltages, currents and digital speed measurements are converted into load-independent output signals by ABB-GTU transducers with

linear characteristics. Voltages can also be measured directly with ABB transducers. These transducers allow a minimum re-cabling of the drivetrain on board of the vehicle. It does not influence the normal operation of the drivetrain. The transducers provide filtering and galvanic isolation of the signals. All the signal conditioning, multiplexing, and digitalisation equipment is put into a portable 19"-rack (Fig. 13.7). The rack is small and meets the needs that are demanded for such a device (electric and electromagnetic isolation, proof against external shocks).

A 24 V NiMH-battery inside the rack provides the supply of all electronics and auxiliary devices, except for the speed sensor that has its own external 12 V maintenance-free Pb-battery.



Fig. 13.6: Speed measurement



Fig. 13.7: On road DC-measuring system

The data-acquisition system is controlled by a Laptop. The measurement software is written in LabVIEW™. The data are stored as ASCII-files, which makes it easy to use them afterwards in other programmes (e.g. spreadsheet programmes). During the measurement, the Laptop shows the test results in real time. Fig. 13.7 illustrates the measurement system installed in an electric van.

This data-acquisition system allows characterising electric and hybrid electric vehicles (only electric and mechanical parameters). However it cannot be easily extended if needed. Furthermore only measurements of DC-signals can be carried-out.

13.3.2 AC and DC Measurement System

On the bases of the first on road measurement system a second more powerful and flexible system was designed (see Fig. 13.8) [185]. It is mainly based on equipment from National Instruments.

On one side a portable Pentium PC with a PCMCIA card slot is used. The DAQcard-AI-16E-4 is from the E-series technology from National Instruments and gives up to 500 kS/s, 12-bit performance on 16 single-ended analogue inputs. The

card feature analogue and digital triggering capability, as well as two 24-bit, 20 Mhz counter/timers and 8 digital I/O lines [186].

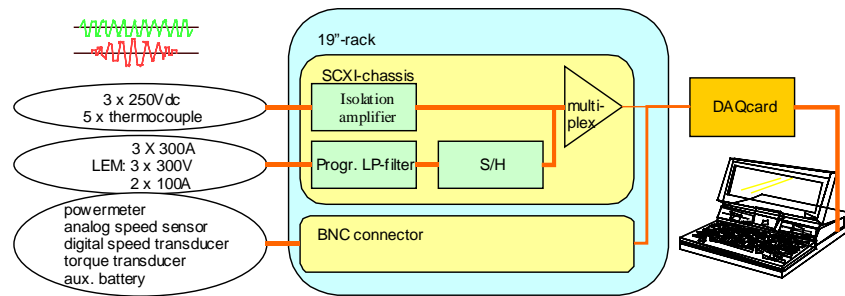


Fig. 13.8: Principle outline of the second measurement system

The PCMCIA data-acquisition card is connected to a 4 slot SCXI-rack. This rack stands for a modular plug and play system. Currently it contains [186]:

- An SCXI-1141 8 channel programmable elliptic lowpass filter (from 10 to 25 kHz) module of which each channel has a differential instrumentation amplifier with software-programmable gains. The eight-order elliptic lowpass filter provides a very sharp “brick wall” response with a rolloff of 135 dB/octave. An external clock input and output are also provided. The SCXI-1141 is connected in series with the SCXI-1140.
- An SCXI-1140 8 channel simultaneous sampling differential amplifier allowing sampling at the same time and multiplexing the measurement to one channel.
- An SCXI-1120 8 channel isolation amplifier that has 250 Vrms working isolation, selectable gains up to 1000. The SCXI-1120 with configurable lowpass filters of 4 Hz and 10 kHz on each channel, is ideal for amplification and isolation of DC millivolt sources, volt sources, 0 to 20 mA, 4 to 20 mA and thermocouples. It has a scanning rate of 333 kS/s.

The software is programmed in LabVIEW and NI-daq. The user interface allows selecting the different channels, changing the scales and offsets, calibration of the probes, visualisation in real time of the measured data and of course storing the measurements on the hard disk. An important part of the software contains the algorithm to calculate the AC-power [187]. It is based on the “quasi-synchronous power-calculating algorithm”.

On the other side different sensors are connected to the cards of the SCXI-rack. Current and voltage Hall-effect transducers can be plugged on (LEM LT300S, LT100S, LT1000, LV800 and LV300). An additional BNC connector with 8 differential analogue and 8 digital channels, allowing the connection of different laboratory equipment, is put in a 19”-rack together with the SCXI-chassis (see Fig. 13.9). RC-filters and voltage dividers are installed to have appropriate measurements. The vehicle speed is measured with a DATRON DLS sensor. To

the BNC terminal accessory additional laboratory equipment with analogue output can be connected, such as a digital power meter (mainly used to measure the grid power during charging the battery) or a torque and speed transducer (of the roll bench).



Fig. 13.9: On road AC and DC-measuring system

14 THE COMPONENT LIBRARY

The data of the Vehicle Simulation Programme are gathered in three different ways:

- Measured in the VUB laboratory
- Obtained from partners in national and European research projects
- Out of literature

These data can have different forms:

- Graphs, maps
- Theoretical formulae and equivalent circuits
- Computed data tables
- Measured data tables

Data coming from the literature are usually incomplete and their accuracy is often unknown. When receiving data from partners of research programmes, the description of the used measurement equipment and the data accuracy have to be identified. Self-measured data are figures that can be very well validated. These measurement campaigns are very time consuming.

Based on a number of laboratory and on-road measurements, models have been developed for different types of electric and hybrid vehicles. As described in Part I most components are characterised by measuring a grid of static working points, covering the whole operating area (see Fig. 14.1). Additionally the operating boundaries are measured, with the help of the bench tests or by maximum accelerating the considered vehicle.

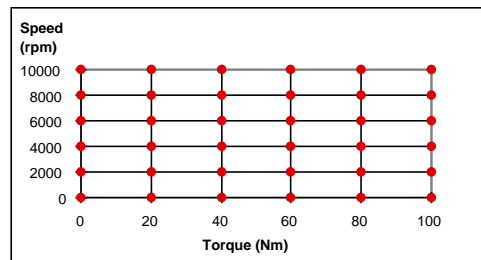


Fig. 14.1: Step-by-step working procedure, covering the whole operating range

Once the data are measured they have to be transformed to a format that is adequate for the simulation programme. Most data are stored in look-up tables or remodelled to statistical formulae. The latter has the advantage to require less computer memory, but formulae can only be used when there is a good correlation with the measurements. Finding a good fitting requires a good understanding of the working behaviour of the component. In some cases the operation grid is split-up into several operation areas with different statistical fittings.

It is not the purpose to describe the whole database of the software programme, but to illustrate the data handling approach and the different data structures possible in the software tool.

14.1 Examples

The characterisation of the electric motor of the Elcat-van has been carried out together with its chopper [188]. The full torque- and speed range is covered.

To have an idea of which kind of statistical equation best describes the motor efficiency, one has to examine the relation between the motor losses with the torque T and speed ω parameters. The following model was selected to estimate the motor efficiency η_{mot} :

$$\eta_{mot} = a.T_{mot}^2 + b.T_{mot} + c.\omega_{mot}^2 + d.\omega_{mot} + e \quad (14.1)$$

In which a, b, c, d and e are coefficients to be determined.

Using about 160 measured working points of the motor, the next coefficients were deduced, with a correlation coefficient of 84 %, which is reasonable:

- $a = -5,067e-5$
- $b = 1,764e-3$
- $c = -8,090e-8$
- $d = 3,598e-4$
- $e = 4,274e-1$

Instead of using this statistical equation one can also prefer to use a look-up table based on the measurements. Table 14.1 illustrates an example of motor efficiency (%) defined by horizontally the motor speed (rpm) and vertically the motor torque (Nm).

Table 14.1: Example of look-up table

	200	400	600	800	1000	1200	1400	1600	1800	2000	2200	2400	2600	2800	3000	3200	3400	3600	3800	4000
0	50	56	61	66	71	74	77	80	81	82	83	82	82	80	78	75	72	67	63	57
10	51	57	63	68	72	76	79	81	83	84	84	84	83	81	79	76	73	69		
20	51	57	63	68	72	76	79	81	83	84	84	84	83	82	79	77				
30	50	57	62	67	71	75	78	80	82	83	83	83	82	81						
40	49	55	60	65	70	73	76	79	80	81	82	81	81							
50	46	52	58	62	67	70	73	76	77	78	79	79								
60	42	48	54	59	63	67	70	72	74	75	75									
70	37	43	49	54	58	62	65	67	69											

In the example a basic model is used to calculate the motor current I_{mot} in function of the motor torque T_{mot} based on the experimental results. A series excited DC motor would figure a quadratic relation between current and torque. The tested motor saturates already at very low torques and from thereon the torque-current relation is linear.

The following relations hold for the Elcat motor, with a correlation of 99 %:

$$T_{mot} \geq 15 Nm \quad I_{mot} = a + b.T_{mot} \quad (14.2)$$

$$T_{mot} < 15 Nm \quad I_{mot} = \sqrt{c.T_{mot}} \quad (14.3)$$

With :

$$\bullet a = 40,82$$

$$\bullet b = 3,546$$

$$\bullet c = 484,0$$

A small difference between this motor current model and the reality will have a insignificant impact on the total energy consumption of the vehicle (see subchapter 15.3 Parameter Sensitivity, below).

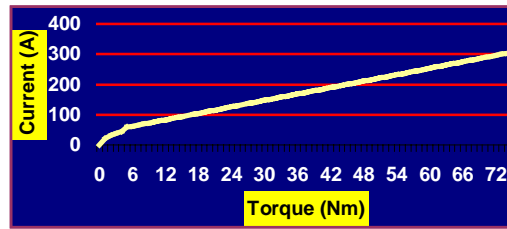


Fig. 14.2: Motor current model

The total electric power is calculated using the motor efficiency, the torque and the speed. Based on motor power and current the motor voltage U_{mot} is calculated. If this voltage exceeds the maximum admissible motor voltage or battery voltage, an AR is introduced.

Based on the same measurement campaign, useful data about the choppers efficiency was gathered. The efficiency is listed in the complete motor voltage-current plane. An empirical statistical model with a high correlation with the measurements (99% and 94%), was extracted, giving the following result:

$$U_{mot} < 20V \quad \eta = a_1.I + b_1.U + c_1.I^2 + d_1.U^2 + e_1.U.I + f_1 \quad (14.4)$$

$$U_{mot} \geq 20V \quad \eta = a_2.I + b_2.U + c_2.I^2 + d_2.U^2 + e_2.U.I + f_2 \quad (14.5)$$

With:

	a	b	c	d	e	f
1	-3,190E-05	5,688E-02	-1,075E-18	-1,605E-03	2,568E-06	4,123E-01
2	4,643E-05	3,225E-03	-1,024E-18	-2,128E-05	-1,656E-06	8,634E-01

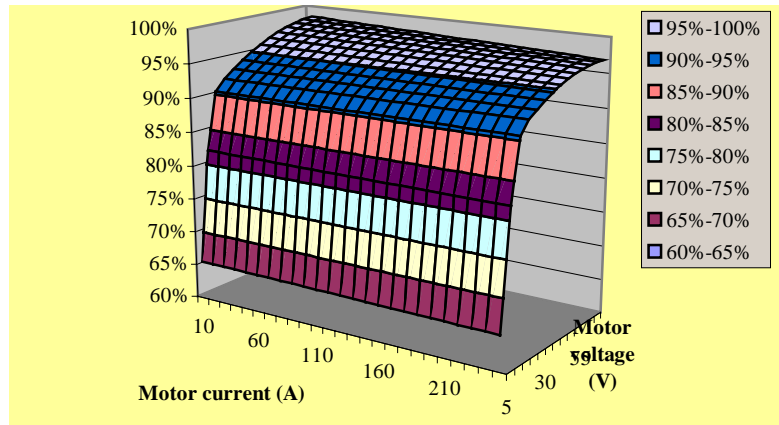


Fig. 14.3: Chopper efficiency model

14.2 Database

Up to now 19 different drivetrains are implemented into the database. They can be divided in several subcategories:

A first group contains models based on an **experimental drivetrain** set-up [113]. The characterised components are used to simulate different drivetrain topologies, with the same body and chassis as of a 2,7 ton van. The electric traction motor is a 30 kW asynchronous motor and the 1900 cc / 68 kW diesel engine can be used to drive the vehicle or to drive the 65 kW alternator and rectifier of the APU. The battery is a 310,8 V / 60 Ah NiCd battery. Additional models of fuel cells and flywheels [175] are added to enlarge the possible drivetrain topologies. Hence following models are established (see Part II chapter 7):

- V1. diesel van, comparable with the Citroën Jumper (1,7 ton);
- V2. battery electric drivetrain;
- V3. flywheel drivetrain;
- V4. fuel cell electric drivetrain;
- V5. diesel-electric van;
- V6. series hybrid electric drivetrain;
- V7. parallel hybrid electric drivetrain;
- V8. combined hybrid electric drivetrain;
- V9. fuel cell hybrid electric drivetrain;

Furthermore models of existing vehicles are developed for electric, series hybrid as well as internal combustion vehicles:

- V10. The **PGE-TM** is a first-generation (1979) basic electric car with a robust body, a 14 kW¹ separated excited DC motor and a 96 V / 180 Ah lead acid battery. It has a total static weight of 1,6 ton.
- V11. The **Panda Elettra**, a second-generation (1990) electric passenger 2 seat car, has a 9,2 kW series excited DC motor and a 96 V / 180 Ah lead acid battery. Its mass is 1,25 ton.
- V12. The **Peugeot electric 106** is a third-generation (1994) 4 seat passenger car, with an 11 kW separated excited DC motor and a 120 V / 100 Ah NiCd battery, with a total weight of 1,14 ton.
- V13. The **Elcat** electric van is a 1,32 ton vehicle and is derived from the Subaru E10. A 13 kW series excited DC motor fed, via a chopper, by a 72 V / 250 Ah lead acid battery, powers the vehicle.
- V14. The **Peugeot Scootelec** is a 110 kg two-wheeler equipped with a DC separated excited motor of 1,5 KW and a 18 V / 100 Ah NiCd battery.
- V15. In the framework of an oncoming European research project **PRAZE** [189] some preliminary simulations were carried out for a 115 kg scooter with permanent magnet brushless wheel motors and a 36 V / 76 Ah NiZn battery.
- V16. The **Citroën AX** is a small passenger car with a 954 cm³ / 32,5 kW gasoline engine. It has a total static weight of 0,8 ton.
- V17. The **Mitsubishi Galant** has a 3 L / 16 valves gasoline engine with electronic injection and 3-way catalyst. It has a total static weight of 1,4 ton.
- V18. The **ALTRA CNG series hybrid** 16-ton city bus is powered by a 105 kW asynchronous motor powers. The energy is provided by a 600 V / 100 Ah lead acid battery and a 30 kW permanent magnet generator driven by a 2500 cm³ spark ignition compressed natural gas engine.
- V19. The **Luxbus** is another series hybrid city bus, with a total static weight of 9,3 ton. The battery pack consists in two parallel 58 Ah packs. Each pack consists in 26 lead acid 12 V blocks connected in series. The vehicle is driven by two 105 kW (peak power) asynchronous motors, with a combining gear system. A 2 L gasoline engine with electronic injection and catalyst powers a permanent magnet generator.

¹ All electrical power values are continuous and not maximum values.

15 SOFTWARE VALIDATION

Calculating the final error in a complex system like a simulation programme requires the development of a second simulation programme. Indeed, one cannot define one single error value of a component model, since the errors differ from working point to working point and are not constant during the simulation. E.g. the efficiency map for an electric motor is more accurate at the nominal working point than at low speeds. Furthermore the powerflow in the drivetrain can be very complex, especially in hybrid vehicles. This increases the complexity to calculate the simulation error.

However a vehicle simulation programme is in the first place a programme to compare different drivelines and strategies. One is interested in comparing results and strategies, where parameters like fuel consumption and battery state of charge are important parameters. The absolute value of these parameters is mostly of less importance [190].

In order to evaluate the software tool different approaches are worked out. First the different errors are described. This is followed by a sensitivity analysis allowing to define how sensitive the output results are to changes of the software parameters. Finally, the simulation results are compared with measured data. This correlation process gives a good idea of the validation of the simulation results.

15.1 Error Analysis

The input data for the simulation models are based on measured data. This introduces *measuring errors*. The measured data are processed to forms that can be used as input values for the simulation models. This data processing at its turn results in errors. When for example the DC motor efficiency is calculated based on the measurement of torque T , velocity ω , current I and voltage U ; the error on the efficiency can be calculated as follows:

$$\eta = \frac{T \cdot \omega}{U \cdot I} \quad (15.1)$$

$$\frac{\Delta \eta}{\eta} = \frac{\Delta T}{T} + \frac{\Delta \omega}{\omega} + \frac{\Delta U}{U} + \frac{\Delta I}{I} \quad (15.2)$$

If all measured values are measured with an accuracy of 0,5 %, the error on the efficiency will be maximum 2 %. The *data error* can be reduced in the case of a

random error by measuring several times the same working point. For this reason statistical fitting of the measured data increases the accuracy of the component data.

Next to the component data error, a second kind of error is introduced: the *modelling error*. The modelling error is a result of the approximation of the reality by mathematical equations. Hence some influences are disregarded. In the simulation tool only a few temperature effects are implemented. However several environmental conditions (temperature, air pressure, etc) will have their impact on the behaviour of a component. Neither are the transient phenomena considered. Additionally, the effect of ageing (e.g. battery capacity) will introduce differences between the current component behaviour and the original data maps. When using look-up tables the interpolation process will introduce errors that can also be classified as modelling errors. The hypotheses of the component modelling can all be found in Part II.

Due to truncation and rounding processes of the software, supplementary errors are introduced, which can be classified as *calculation errors*. Furthermore, as a result of calculations in the modelling, an input error is propagated through the model. The calculated output contains this propagated error. Reference [190] stated that, if one has an error of 0.7% of the total tractive resistance, the error on the gear input power can vary from almost 7% to more than 8%, taking into account the data errors in function of the vehicle operating point. Such an error can propagate further through the driveline resulting in e.g. an error of more than 10 % of the actual fuel consumption (in l/s).

At the end of the driveline (battery, fuel, etc) one gets a final error that can be used to define the accuracy of the simulation. As already mentioned before, to really have a more or less exact idea of this final error one should write a new parallel simulation program to calculate the error in every working point of the simulation and implement the appropriate error analysis equations on the component models [190].

15.2 Simulation Time vs. Accuracy

Factors such as drive cycle time, number of components contained within a vehicle layout, complexity of the hybrid control algorithm and number of parameters to be stored or visualised during the simulation run, affect the overall time taken to run a single simulation. Also hardware resources such as processor speed, available memory, hard disk access time, influences the simulation time [142]. With a 550 MHz Pentium III processor the fastest simulation is about 400 times faster than the simulated drive cycle. If all parameters are visualised and stored and a complex iteration process is required the simulation time would be about 20 times the simulated drive cycle.

The user can increase simulation accuracy by reducing the time increment. However this will reduce the simulation speed as is illustrated in the next figure. Simulations were performed by modelling an electric vehicle driving a standard ECE drive cycle. Using different time increments ranging from 0.01 to 10 seconds, successive simulations were run. The error on the battery SoC related to simulation processing time was monitored for each simulation run. This process time monitoring is one of the practical aspects of the programme language LabVIEW™.

Fig. 15.1 illustrates that the relative error on the battery state of charge converge to a definitive value, showing a good indication of stability within the modelling routines. To calculate this relative SoC error the value at a time increment of 0.01 s is chosen as the reference. The graph also shows how the processing time increases significantly when a simulation uses a small time increment. A time increment, lower than 0,1 s, influence the accuracy not much. However, while simulating the ECE cycle, time increments larger than 1 s will lead to high SoC deviations.

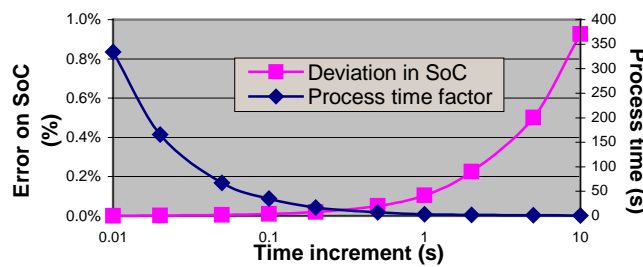


Fig. 15.1: Effect of time increment on simulation accuracy

15.3 Parameter Sensitivity

A sensitivity analysis of the key parameters of the simulated model illustrates how sensitive the output (e.g. energy consumption) is to changes in the input parameters. This allows a side-by-side comparison of the input parameters in order to focus on technology areas that are important to the final fuel economy [192]. This sensitivity analysis gives also important information on the required accuracy of the input parameters. The higher the sensitivity, the more important it is to have accurate values.

Fig. 15.2 illustrates the relative deviation of the energy consumption when important input parameters are enlarged with 10%. Simulations are performed for an electric van (V2), an electric passenger car (V12) and an internal combustion engine van (V1). Taking the original parameters as a reference, the weight, aerodynamic drag coefficient C_x , the wheel radius and tyre pressure are successively increased with 10%, while the gear efficiency is reduced with 10% ($\eta \Rightarrow \eta * 90\%$).

Due to the fact that the effect of the parameter deviations on the energy consumption is also depending on the speed cycle, three different cycles are simulated: the ECE-15, a Dutch Urban Bus cycle (DUB) and constant driving at 90 km/h (see subchapter 6.2).

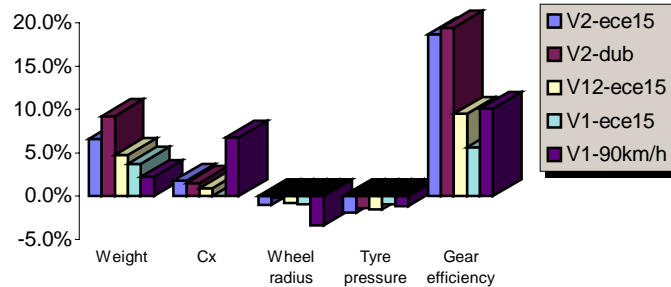


Fig. 15.2: Output deviation in function of 10% deviation of input parameters

One can clearly notice that the total vehicle weight has an important influence on fuel or energy consumption. The more important the dynamic characteristic of the reference cycle (V2-dub), the higher this impact. Among other elements this impact of the speed cycle on the energy consumption is due to the effect of regenerative braking, which is highly related to the kinetic energy of the vehicle.

The higher the top and average speed of the drive cycle, the higher the impact of the aerodynamic drag coefficient on the energy consumption. This is expected since the aerodynamic drag is quadratic related to the vehicle speed.

Changing the wheel radius influences the operating points of the rest of the drivetrain. While increasing the wheel radius with 10 %, the rotational velocity will decrease and the wheel torque will rise. The effect when driving a city cycle (ECE-15 or DUB) is very moderate (less than 1 %). In the case of the constant speed cycle, the engine will continuously operate in another working point than the reference vehicle. This results, in the example, in a decrease of fuel consumption with 3 %, but the opposite result could also be obtained, because it is related to another operating point of the engine, while the engine still needs to deliver the same driving output power.

The higher the tyre pressure, the lower the friction resistance coefficient (see subchapter 10.2) and hence the lower the energy consumption. In the case of the electric van, driving an ECE-15 cycle, an increase of 10% of tyre pressure results in a decrease of almost 2 % of the energy consumption.

The highest influence on the energy consumption can be found when decreasing the efficiency of a drivetrain component. In the given example the gear efficiency is reduced with 10 %, which results in an augmentation of 6 to 19 % in energy consumption. Due to the important influence of regenerative braking on the energy

consumption, the effect of efficiency variation is much higher in the case of electric drives compared with internal combustion vehicles, in which braking energy is never regenerated. The difference is also remarkable between the electric van (V2) and the electric passenger car (V12) due to the fact that the van can regenerate a relative higher amount of braking energy and moreover the van has a higher weight and hence a higher vehicle inertia.

When comparing on-road measured data with simulation results, one must be aware that some parameters can influence the measurements. The effect of wind and road inclination is difficult to measure [190], but they are always present and will influence the comparison. E.g. when there is a very small slope of 0.1% of the road, the electricity and fuel consumption can rise from 1 to more than 4%. Also a moderate head wind of 5 km/h increases the aerodynamic drag force and hence the energy consumption can rise from 2 to 7%. Fig. 15.3 illustrates this parameter sensitivity.

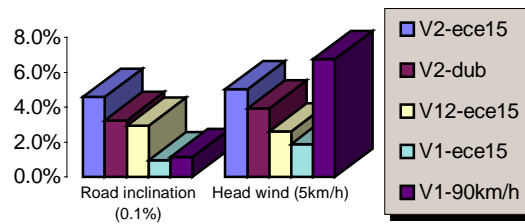


Fig. 15.3: Output deviation in function of head wind and road inclination

To evaluate the motor current model of the example in subchapter 14.1, one can increase the motor current, based on the statistical model, with 10%. Hence the input parameters to calculate the chopper efficiency will change, which are in our example the motor current and voltage. Since the motor voltage is calculated from motor efficiency and motor current, this voltage will decrease with increasing motor current. The global energy consumption however, will only change with 0.7% when the motor current is enlarged with 10%. This example illustrates that it is not really necessary to have very high accurate statistical models of some of the intermediate parameters to have a good idea of the global energy consumption. On the other hand the efficiency models have to be very accurate.

This sensitivity analysis also shows clearly the importance of the accuracy of some essential simulation parameters. Especially vehicle weight and component efficiency have a major impact on the fuel and electricity consumption. Additionally the effect of the road inclination and head wind on the energy consumption is remarkable. Other parameter deviations, like motor current, have less impact on the total energy consumption.

15.4 Calibration and Validation

Even when a detailed description of the components is available, some parameters will always be estimated. A calibration is thus recommended. By comparing measured data with simulated data, some parameters like C_x , tyre friction coefficient, etc can be fine-tuned.

To verify the models, measurements on road were carried out and compared with the simulation results.

Usually comparing ICE vehicles is more difficult than electric vehicles. While comparing simulation results with measured data there will always be a difference due to drivers behaviour. The simulation tool will change gear following a certain criteria, but a driver will do this in a more arbitrary way. Furthermore instantaneous fuel consumption cannot be a true replicate because the simulation model cannot take into account the erratic pedal motion.

15.4.1 Speed Cycles

The ECE-cycle is performed on road with an electric passenger car. Since the real speed can differ from the theoretical ECE speed, the speed is measured during driving and used as input file for VSP. Hence the same cycle is simulated as the one driven on road. The comparison of both simulated and measured parameters demonstrates a good correlation (see Table 15.1 [191]). The relative error is less than 5%. One can also compare the real driven speed cycle with the theoretical ECE-cycle. This demonstrates that the on road driven cycle energy consumption corresponds close to the theoretical ECE-15 cycle.

Table 15.1: Speed cycle: simulation vs. measurements

	Measured	Simulation	ECE-15
Ah discharged	1.52	1.46	1.53
Ah charged	0.19	0.18	0.19
Tot Ah	1.33	1.28	1.34
% recuperation	12.35	12.20	12.71

Similar results are found by comparing other vehicles and other drive cycles measured on road.

15.4.2 Acceleration Test

One of the most difficult experiments to simulate is an acceleration test. Contrary to a comparison based on a pre-defined speed cycle, one is not performing a straightforward step-by-step calculation, but for each point the simulation has to

iterate towards the possible working point. A little error in the beginning can, due to integration, result in a large deviation at the end of the simulation.

In the next graph (Fig. 15.4) one can find the measured speed while maximum accelerating the electrical vehicle, compared with the simulation results. The boundaries of the motor are the maximum speed and torque. This motor was current controlled. A current limit (as a function of the revolutions per minute) is introduced too. Simulated values are marked with ‘-s’ and measured values with ‘-m’.

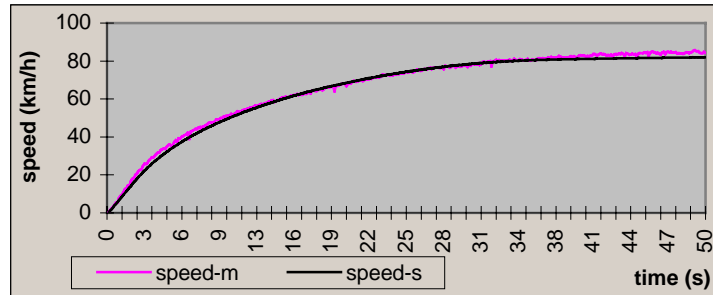


Fig. 15.4: Acceleration simulation vs. measurement

The good correlation between the measurement and the simulation demonstrates the performance of the iteration algorithm. An average deviation of 2% is found.

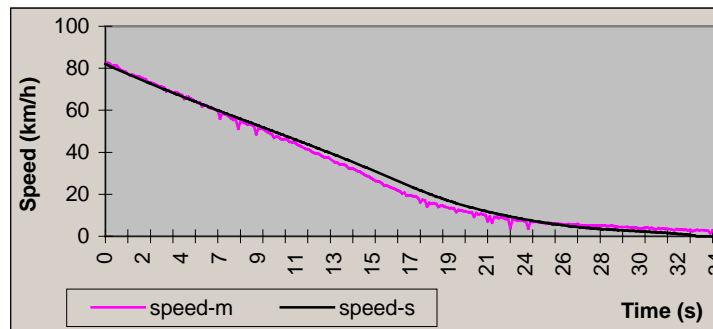


Fig. 15.5: Deceleration simulation vs. measurement

In Fig. 15.5 one can see the deceleration test. During this test only regenerative braking by the motor was performed, without using any mechanical brakes.

The graph of Fig. 15.6 compares the motor current and voltage for the acceleration and deceleration test.

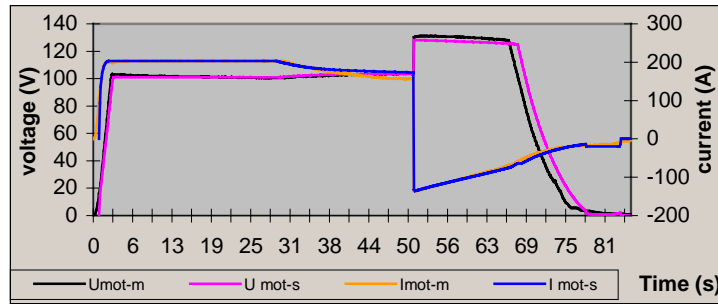


Fig. 15.6: Motor current and voltage comparison

The little deviation in current can be explained by a possible minor wind and road inclination during the on-road measurement.

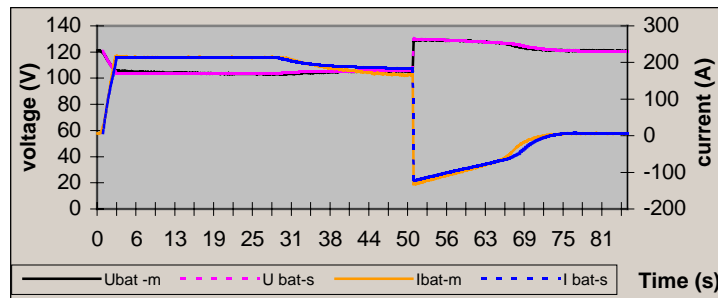


Fig. 15.7: Battery voltage and current

The graph of Fig. 15.7 demonstrates, for the same acceleration test, the variations in current and voltage of the battery.

15.5 Software Validation Conclusions

Although it is almost impossible to calculate an exact error on the simulation results, the simulation can be well-validated by comparing the simulation results with measured data. Taking into account the error on the measurement as well as the error provoked by the simulation programme, it can be stated that the correlation is very good. It can be stated that the end-results have an error of less than 5 %.

Additionally, based on a sensitivity analysis the most critical parameters can be identified, indicating how the end results will change due to an error on the input parameters.

16 SIMULATION RESULTS

The following discussed cases illustrate the ability of the simulation programme to evaluate different drivetrain control algorithms.

16.1 Engine Start-up, Clutch and Gear Shifting

Fig. 16.1 illustrates the simulation results of an acceleration test of a small passenger car with internal combustion engine. The first seconds the starter motor brings the engine velocity above idle speed. Afterwards the clutch starts slipping and the vehicle accelerates. The maximum motor torque defines the maximum acceleration. Once the differential speed exceeds 80 rad/s, the gear shifts to second gear. At 180 and 220 rad/s it shifts further to third and fourth gear. In this example the gearshifts at fixed differential velocities.

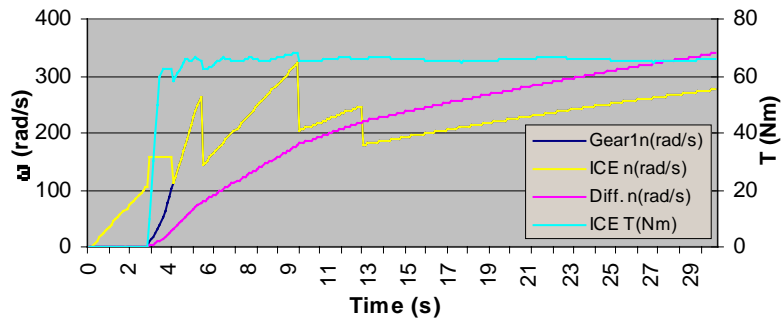


Fig. 16.1: ICV – Gearshifts at fixed differential speed

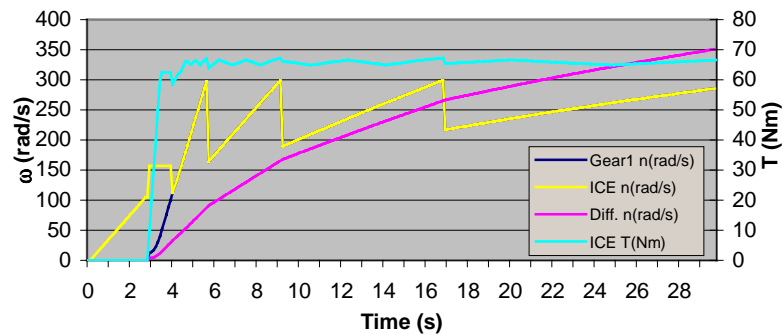


Fig. 16.2: ICV – Gearshifts keeping the ICE within speed limits

Gearshifts can also be controlled by keeping the engine speed between limits (see subchapter 10.4). In the example above (Fig. 16.2) the engine speed will be kept between 150 and 300 rad/s. On the graph one can clearly notice the 300 rad/s upper limit. In a deceleration test one could see the lower limit. Other gearshift moments result in another maximum vehicle acceleration as well as fuel consumption.

If the engine is part of the APU of a series hybrid electric vehicle, it is started up with the help of the generator. Fig. 16.3 shows the first part of the ECE cycle.

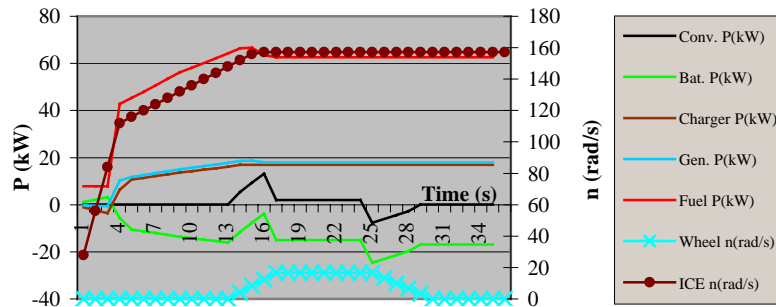


Fig. 16.3: SHEV – Engine start

Before the APU can deliver power the engine velocity is brought above idle speed (the first 4 seconds). The battery delivers the required power (battery power (green line) is positive) via the charger (this is the converter connected to the generator). This power corresponds in the model with the inertia of the APU. The start-up acceleration is defined by the start-up time and the required idle speed. Once the engine velocity exceeds the idle speed, the engine will further accelerate to the required operating setpoint. The generator control process defines this acceleration. After 17 seconds the APU delivers a constant power.

16.2 Electric & Internal Combustion Vehicle

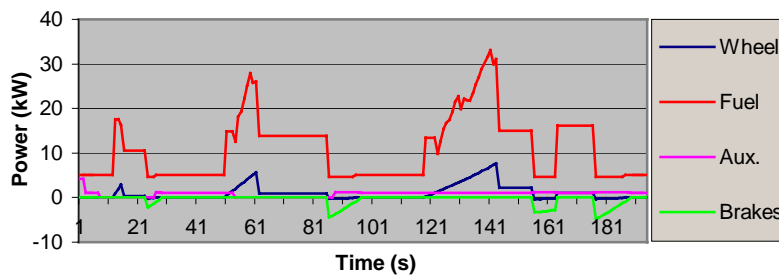


Fig. 16.4: ICV – ECE – Power

Fig. 16.4 shows the power of some components of an internal combustion passenger car performing an ECE drive cycle. The auxiliary power necessary to start-up the engine can be seen at the left side of the graph. At stand still the engine requires idle consumption and during braking all braking power is provided by the mechanical brakes.

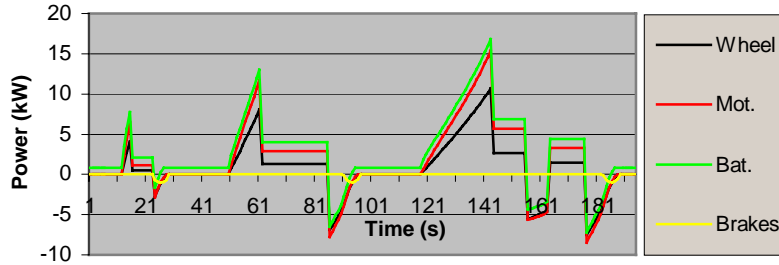


Fig. 16.5: BEV – ECE – Power

In the case of the electric vehicle the braking power is mostly regenerated into the battery (see Fig. 16.5). Only at very low velocity the electric motor is not able to brake further and the mechanical brakes will take over the deceleration process. Neither idle consumption nor gear shifting can be noticed on this graph. However in comparison with Fig. 16.4 the corresponding power levels (e.g. the wheel power) are higher due to the fact that the electric vehicle is somewhat heavier than the internal combustion vehicle.

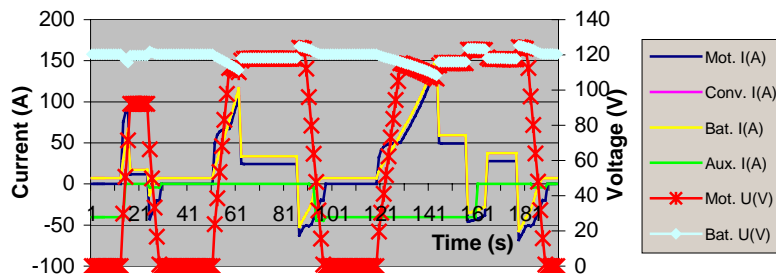


Fig. 16.6: BEV – ECE – Current and voltage

Fig. 16.6 demonstrates the behaviour of the currents and voltages. One can partially recognise the speed profile of the ECE cycle in the motor voltage. However the motor voltage is limited to somewhat less than the battery voltage. The auxiliary current is needed for the compressor, which provides the brake pressure.

16.3 Series Hybrid Vehicle

Some power control strategies are illustrated in this chapter for a series hybrid vehicle. Following assumptions are made:

- The vehicle is driving the ECE cycle.
- The APU consists of a generator connected to a diesel engine.
- The additionally a flywheel can be engaged as peak power unit.
- The maximum acceleration of the generator is set to 4 rad/s^2 .
- The maximum APU-power deviation is set to 10 kW/s .

Fig. 16.7 represents an example of a SHEV in which the APU delivers a constant power of 24 kW to the DC-bus. This power corresponds to the highest fuel efficiency. However the APU is oversized allowing the simulation of different power strategies. Hence this constant power of 24 kW in this example does not correspond to the average driving power. A high CHR is sometimes used to be able to charge the battery when not driving in electric mode (urban areas).

Once again the start-up process can be noticed, where after the APU delivers the constant power. The battery is recharged with a power corresponding to this APU power minus the required driving power. During braking the brake power will charge the battery too. After 90 seconds the battery current reaches its maximum allowed value. The iteration algorithm will reduce the APU power to keep the battery current within limits.

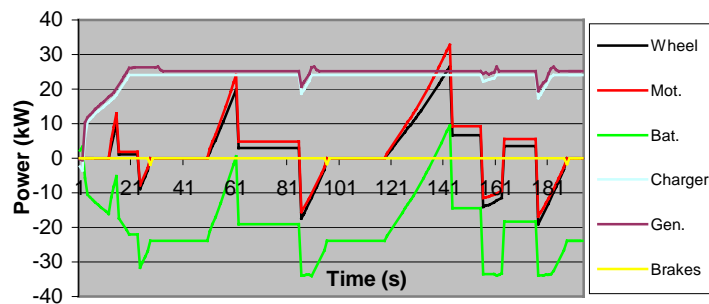


Fig. 16.7: SHEV – ECE – Maximum regeneration – Power

As described in subchapter 8.6 the user can choose the iteration order. Hence he can select to reduce the maximum motor braking power, instead of decreasing the APU power, in the case of a battery power limit. At this moment less power is regenerated during braking and the mechanical brakes will be in charge of the remaining braking power. This strategy is illustrated in Fig. 16.8.

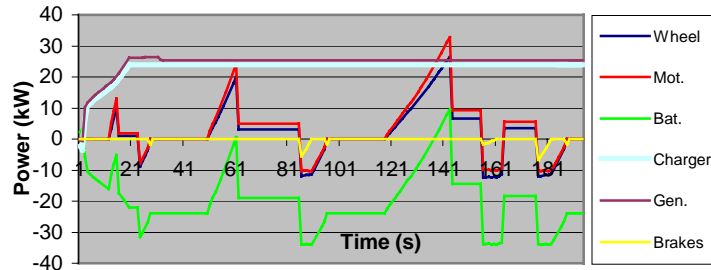


Fig. 16.8: SHEV – ECE – Less regeneration – Power

Another power strategy consists in charging the battery at a constant power (e.g. 7 kW). The APU is in charge of the traction power as well as this charging power. During braking, additional to the constant charging power, the brake energy is also regenerated into the battery. Fig. 16.9 illustrates this strategy.

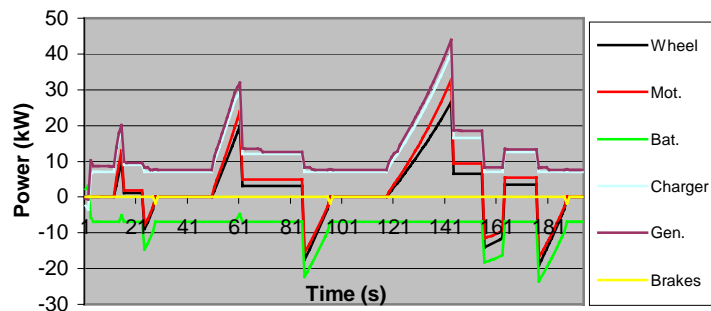


Fig. 16.9: SHEV – ECE – Constant battery charging – Power

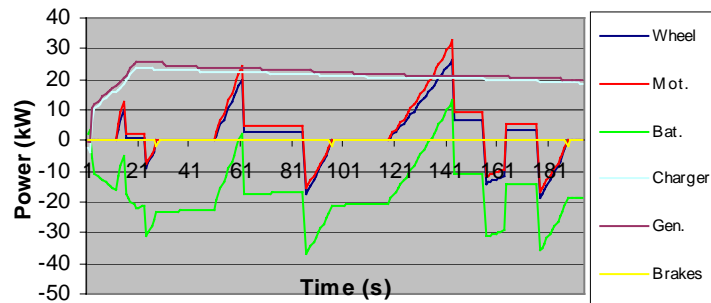


Fig. 16.10: SHEV – ECE – APU power in function of SoC – Power

To take into account the battery discharge rate, the power of the APU can be selected in function of the SoC. Fig. 16.10 illustrates an example in which the APU will deliver full power (in the example 24 kW) when the SoC is lower than 50 %.

Above 70 % the APU will be disengaged. Between both SoC levels the APU power is a linear relation of the SoC. In this example the start SoC is chosen at 50% and the battery capacity is selected very small to see the evolution of the APU power within a short simulation time.

Fig. 16.11 shows a model in which the APU delivers 30 % of the required instantaneous driving power, except during braking. At this moment all braking power is regenerated into the battery and the APU is switched off.

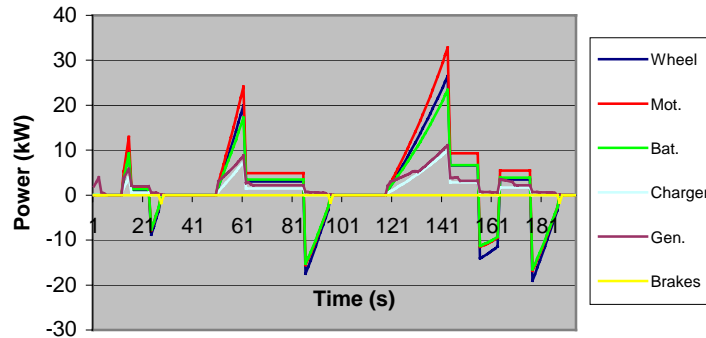


Fig. 16.11: SHEV –ECE – Relative power distribution – Power

In a following example, Fig. 16.12, the SHEV is equipped with a flywheel and the APU delivers 7 kW continuously. The flywheel (P.U. or Power Unit) provides all peak powers. When the flywheel reaches its maximum deliverable power, the battery will deliver the lack of traction power. This example is a good demonstration of the iteration process.

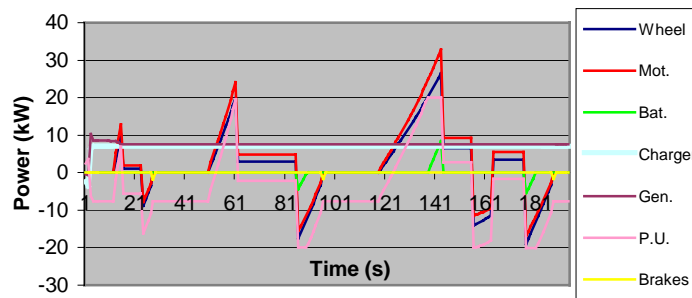


Fig. 16.12: SHEV – ECE – With flywheel. – Power

The last example illustrates the “thermostat” SHEV. Several succeeding ECE cycles are simulated. The SoC is monitored. Above 80 % the APU is switched off in the example, until the SoC drops under 70 %.

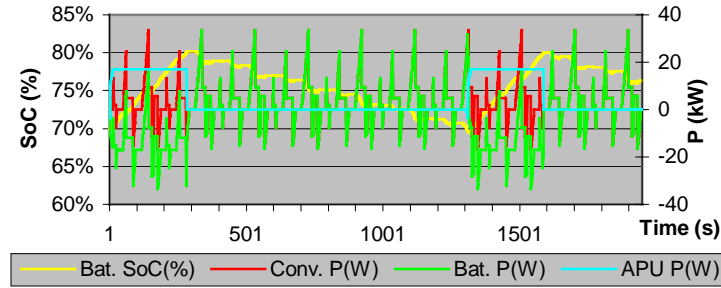


Fig. 16.13: SoC in thermostat SHEV

16.4 Parallel Hybrid Vehicle

To clarify the Parallel hybrid Electric drivetrain the following example illustrates the power strategy based on following hypothesis:

- When driving slower than 10 km/h the drivetrain is in electric mode only.
- Above 10 km/h the vehicle is in hybrid mode.
- If one engine or motor is not able to deliver the power the other one will be in charge of the lacking power.
- The motor charges the batteries by regenerative braking.
- Gearshifts are selected to keep the engine in an efficient operating area.
- The simulation starts with an initial battery SoC of 60 %.

Fig. 16.14 is a simulation result of an ECE cycle. When the SoC is lower than 50 % the engine delivers all required traction power. Above 70 % all traction power is delivered by the electric motor (Mot-mech). In this graph the engine (Gear-ICE) delivers about 55 % of the required driving power (Wheel). If the speed cycle is much longer, the dependency of the engine power on the SoC is better demonstrated.

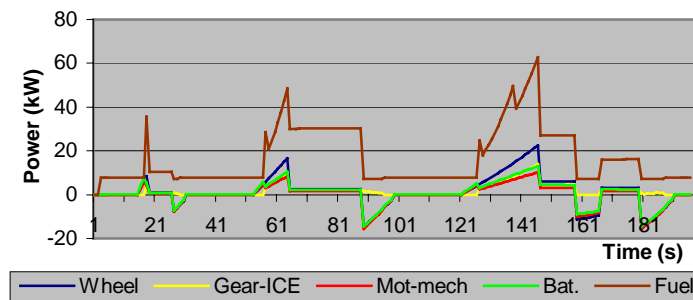


Fig. 16.14: PHEV – ECE – P_{ICE} in function of SoC – Power

Fig. 16.15 shows the same PHEV driving at constant speed. The SoC drops from 57 % to 50 %. The contribution of the engine to the driving power increases, while the electric motor and battery have to deliver a reduced amount of power.

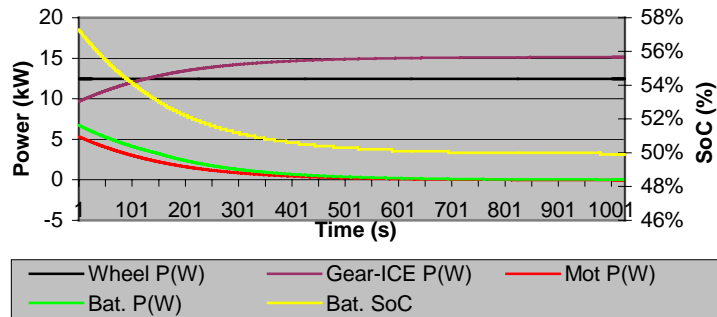


Fig. 16.15: PHEV –Acceleration – P_{ICE} in function of SoC (2) – Power

In the following strategy the engine is in charge of all driving power (if the vehicle’s speed is higher than 10 km/h and the vehicle is not braking). Fig. 16.16 below demonstrates this *electric-assist* strategy. In this case the engine is able to deliver all driving power.

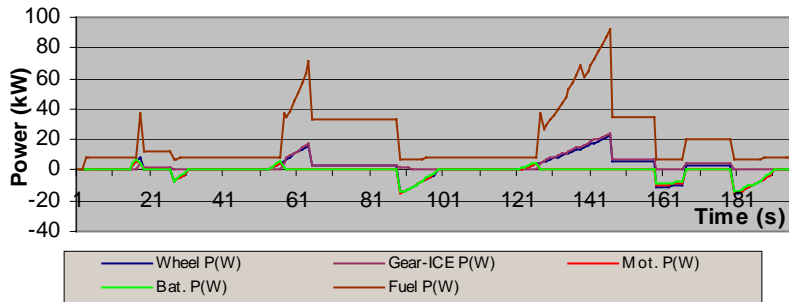


Fig. 16.16: PHEV – ECE – Electric-assist – Power

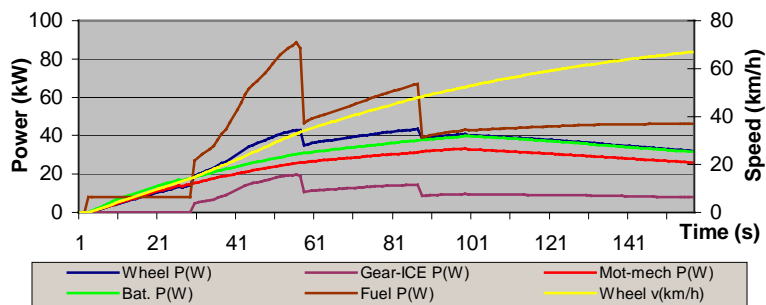


Fig. 16.17: PHEV – Acceleration test – Electric-assist – Power

In Fig. 16.17 an acceleration test is simulated. In this case the engine delivers its maximum power. Additionally the electric motor will deliver the lacking part of the driving power. In this maximum acceleration test this corresponds with the maximum motor power. Hence the acceleration is defined by engine and motor power together.

16.5 Combined Hybrid Vehicle

The characteristics of the combined hybrid drivetrain are explained in subchapter 3.4. Some drivetrain power strategies are demonstrated with the help of the simulation programme.

a) Constant working point

One could consider keeping the torque and speed value of the engine constant, corresponding with its lowest consumption. Hence the drivetrain is controlled like it is generally done in a series hybrid vehicle (see subchapter 3.4.3).

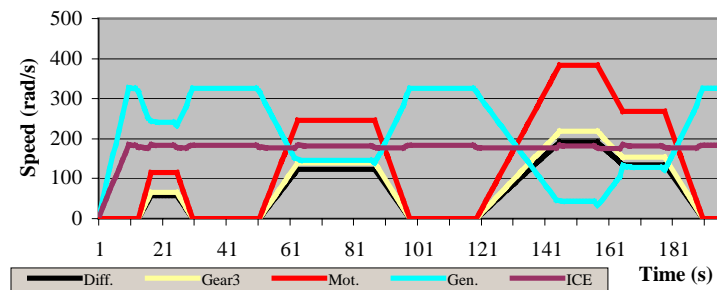


Fig. 16.18: CHEV – ECE – Constant working point – Speed

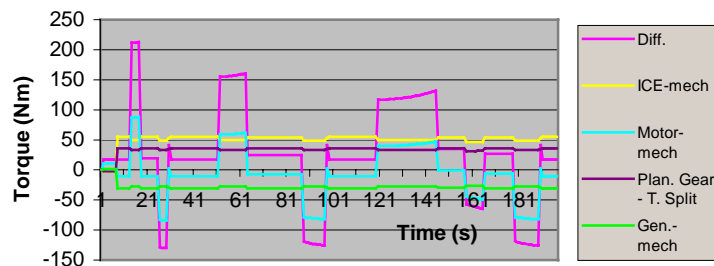


Fig. 16.19: CHEV – ECE – Constant working point – Torque

Fig. 16.18 illustrates the different velocities of some of the components. When vehicle speed increases, the generator velocity is decreased to keep the engine speed constant.

In Fig. 16.19 the torque values are displayed. Due to the inertia of the planetary gear and the engine, the resulting engine torque shows a minor fluctuation.

Fig. 16.20 shows the corresponding power levels. At stand still all engine power flows via the generator into the battery. During the first seconds of the acceleration phase, a part of the engine power goes to the wheels. The remaining engine power flows through the generator. A fraction of this generator power is used by the electric motor, another part still charges the battery.

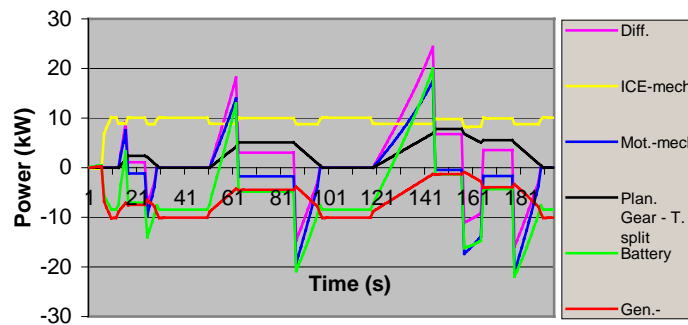


Fig. 16.20: CHEV – ECE – Constant working point – Power

At a certain time, additional battery power is required to accelerate the vehicle further on. This is due to the fact that the higher the vehicle speed the higher the required driving power on one hand and the lower the generator power on the other hand.

If in this example the vehicle would exceed 55 km/h, the generator power is inverted and hence battery power flows through the generator as well as through the electric motor. In this mode, engine, generator and electric motor drive the wheels.

b) Overall power loss minimalisation

Fig. 16.21 shows the simulation result in which the Torque Splitter imposes a torque at the planetary gear corresponding to the minimum overall drivetrain losses. This covers the total efficiency loss for all vehicle components (power to battery and wheels compared to engine power).

During braking no torque goes to the planetary gear and all braking energy is regenerated via the motor to the battery. The engine is engaged only above a certain

level (at lower values the engine efficiency is very bad) and the generator is locked at low required power (all engine power flows directly to the differential).

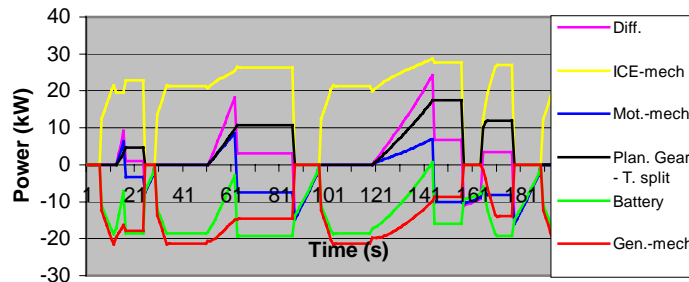


Fig. 16.21: CHEV – ECE – Minimum losses – Power

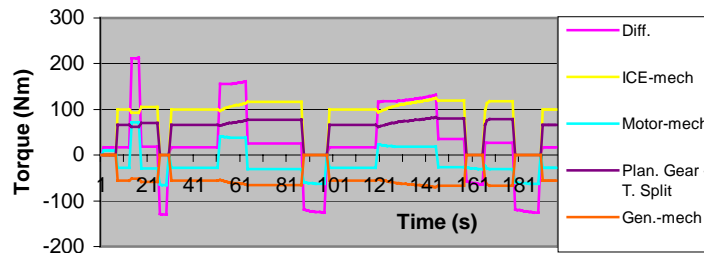


Fig. 16.22: CHEV – ECE – Minimum losses – Torque

c) relative torque distribution

In the last example the power distribution in the complex hybrid drivetrain is simulated following a relative distribution of traction torque between planetary gear and motor.

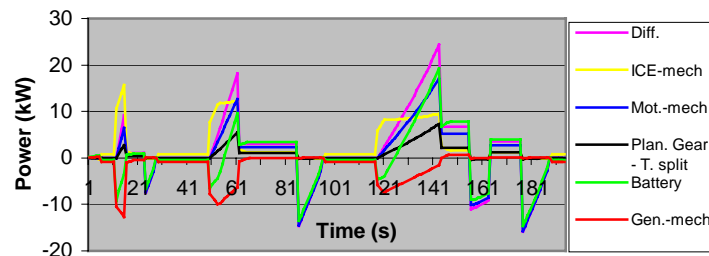


Fig. 16.23: CHEV – ECE – Relative power distribution – Power

Fig. 16.23 illustrates the simulation results of the drivetrain performing an ECE-cycle. The required driving torque is proportionally split-up: 30% is delivered by

the planetary gear and 70% by the motor. Fig. 16.23 shows the corresponding power flow. Fig. 16.24 displays the torques developed by the different components.

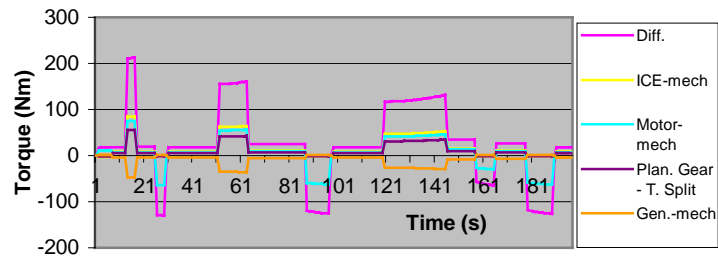


Fig. 16.24: CHEV – ECE – Relative power distribution – Torque

17 COMPARISON

This chapter gives an objective approach to compare different kinds of vehicles (electric, hybrid and internal combustion vehicles) on the level of:

- Acceleration performance
- Energy consumption
- Direct and background emissions

To have an accurate comparison of vehicles, it is necessary to eliminate external influence factors like wind, rain, driver's behaviour, etc. Simulation programmes, which can simulate exactly the same speed cycles for two different kinds of vehicles, can do this.

17.1 Hypothesis

The simulation results are based on the following hypotheses:

a) Segmentation

It is not possible to assess and conduct evaluations on one type of vehicle and utilisation pattern representing all together the different segments of the automobile population. In this chapter comparisons will be performed for the segment of the small passenger car and the segment of the medium sized delivery van.

The vehicles, which will be compared with VSP are an internal combustion Citroën AX and an electric Peugeot 106, both very similar and commercial available vehicles of the same class.

Additionally, to compare different hybrid drivetrain topologies and power strategies a fictive body and chassis of a 2,7 ton van is chosen. The different drivetrain topologies are described in chapter 7. The drivetrain is composed out of industrial components [113]. The drivetrains are based on an asynchronous motor, a NiCd battery and a diesel engine. The size of the engine is such to allow simulating different power strategies in PHEV as well as in SHEV.

One must be very careful in making conclusions. The components mentioned above were not optimised for the application and no optimisation of component vehicle integration was carried out. Connecting different industrial or vehicle components one to another doesn't result automatically in an optimised vehicle drivetrain. Furthermore, the results depend on the chosen reference cycle. Other cycles can give slightly different results.

b) Reference drive cycle

The energy consumption and emissions are not only depending on the drivetrain topology, but the simulated drive cycle will have an important impact on the end-results. Five different cycles are compared:

- Constant speed cycle.
- Standardised ECE-15 cycle and EUDC.
- On-road measured ‘Dutch Urban Bus’ and ‘Line 71’ cycle.

The characteristics of these cycles can be found in subchapter 6.2.

c) Zero net variation of SoC

To be able to compare the results of the different control strategies in hybrid vehicles, there should not be any variation of the battery state of charge at the end of the drive cycle or simulation run.

$$\int_0^T SoC(t) dt = 0 \quad (17.1)$$

This constraint can be taken into account by choosing:

- the moment the APU is engaged during the drive cycle;
- the power setpoint of the APU (if allowed);
- the limits of thermostat hybrid strategy (if applicable);
- a complementary charge of the battery at the end of the cycle;
- different start values of the SoC.

The latter approach consists in running two (or more) reference cycles back-to-back from high SoC and from low SoC, causing a decrease and an increase in battery SoC, respectively. A simple linear interpolation can be used to predict the fuel economy estimated for the vehicle if the battery had no net change in SoC [192].

All methodologies have their drawbacks due to the fact that the APU has an influence on the drive performance. E.g. at the moment the APU is engaged and the vehicle needs to brake heavily, the APU power needs to be decreased or the regenerative braking needs to be reduced. If the vehicle is driving the same speed cycle in pure electric mode, more braking energy can be regenerated. A repetitive simulation of the reference cycle reduces this small error.

d) Background emissions

It is true that electric motors are completely emission-free themselves; to make a valid comparison in emissions between electric and thermal vehicles, one should however take into account the emissions generated by electricity production. The background emissions corresponding to electricity production and fuel refinery used to perform the comparison are based on data representing the European average and

the ‘worst’ and ‘best’ environmental-friendly European country (see subchapters 6.3 and 6.4).

17.2 Internal Combustion Vehicles

Three different internal combustion vehicles are evaluated over 5 speed cycles. The first is a small gasoline vehicle (V16), the second is a medium family gasoline car (V17) and the third is a diesel light duty van (V1). A detailed description of these vehicles can be found in subchapter 14.2. The influence of the speed cycle and gear shifting is demonstrated in Fig. 17.1. The index between brackets stands for:

- (a) Gear shifting at fixed vehicle speed
- (b) Gear shifting to keep engine speed between limits

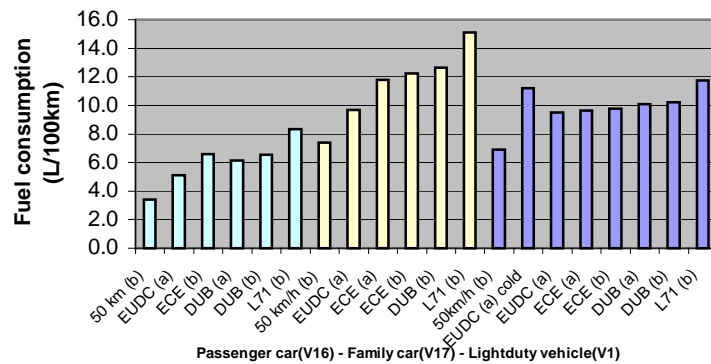


Fig. 17.1. Comparison of fuel consumption

Driving at constant speed gives the lowest fuel consumption, as could be expected. The higher the speed cycle dynamics, the higher the fuel consumption. The standard test cycles (ECE and EUDC) give lower fuel consumptions than the hilly on-road measured cycle (L71). Compared to the constant speed cycle, the supplementary fuel consumption, when driving the L71 cycle vary from 170 %, in the case of the diesel van, to 250 % for the gasoline passenger car.

The influence of gear shifting moments can also be observed in the figure. In one simulation result the consequence of a cold engine is simulated, resulting in 18% higher fuel consumption.

17.3 Battery Electric Vehicles

The effect of reference vehicle, speed cycle and start value of the battery SoC on the electricity consumption of electric vehicles is evaluated in the following figures.

Fig. 17.2 shows the important reduction of energy consumption (at the grid) during the last twenty years. One of the first generation electric vehicles (V10) driving an ECE cycle had an energy consumption of more than 550 Wh/km. The current electric passenger cars (V12) have an energy consumption of somewhat higher than 200 Wh/km, due to, among others, lighter vehicle weight and lower component power losses.

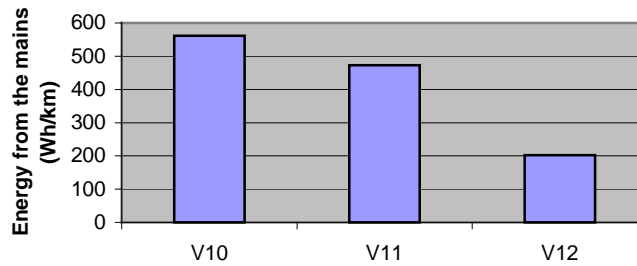


Fig. 17.2: Evolution in energy consumption of battery electric vehicles

Fig. 17.3 demonstrates the influence of the speed cycle as well as the start value of the battery SoC. The later describes the impact of the battery end-charge on the energy consumption.

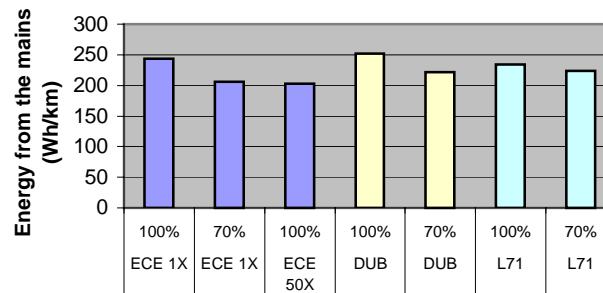


Fig. 17.3: Energy consumption in function of drive cycle and SoC start value (V12)

If one would drive the ECE cycle, which only covers 1,016 km in 195 seconds and recharge the battery to 100 %, the energy consumption is high due to the fact that only a small amount of battery capacity is consumed and the charge efficiency of the end charge is unfavourable. If the same cycle is simulated starting at a SoC of 70 %

and recharging the battery afterwards to the same SoC, the energy consumption is much lower. The same result can be noticed if this short ECE cycle is simulated 50 times, corresponding to 50,8 km, before recharging the battery back to 100 %.

The influence of speed cycle dynamics is less important than in the case of the internal combustion vehicle. However, if the same distance is driven in the same time as for the ECE cycle, but at constant speed, one can notice a significant reduction in energy consumption as illustrated in Fig. 17.4.

This reduction is even higher for an electric light duty van (V1) compared to a small passenger car (V12).

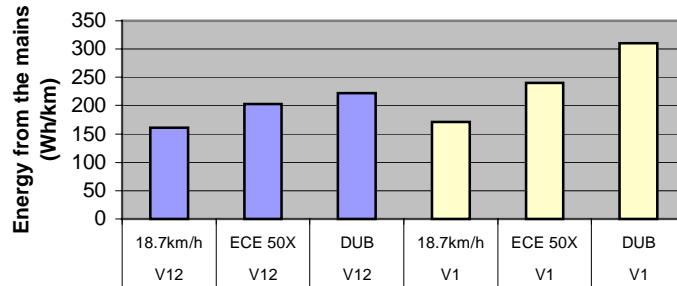


Fig. 17.4: Energy consumption of an electric passenger car and electric van

The primary energy consumption depends on the electricity production plant efficiency. Fig. 17.5 compares the primary energy consumption for an electric car consuming 211 Wh/km at the mains. In this graph SGC and CHP stands for two state of the art gas turbines as described in subchapter 6.3. No losses are taken into account for the renewable energy sources.

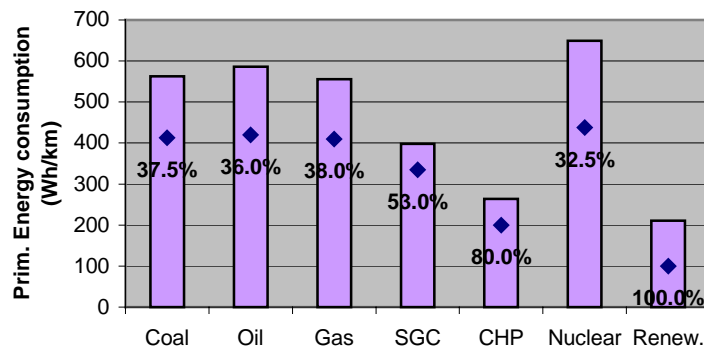


Fig. 17.5: Primary energy consumption in function of electricity production plant

Commonly the primary energy consumption is calculated in function of the average production mix of these different power plants in a considered country. The large diversity of different emission levels is illustrated in Table 17.1 and Fig. 17.6.

Table 17.1: Background emissions of EV driving ECE cycle

	CO ₂ g/km	CO g/km	HC g/km	NO _x g/km	SO ₂ g/km	PM g/km
European average	96,9	0,016	0,017	0,248	0,566	0,030
Belgium	71,7	0,013	0,009	0,220	0,406	0,021
Denmark	195,7	0,033	0,019	0,617	0,694	0,048
Norway	1,3	0,000	0,000	0,002	0,003	0,000

In countries where almost no fossil fuels are used to produce the electricity, like Norway, the emissions are extremely low.

Fig. 17.6 reveals noticeably the important impact of the considered European countries on the background emissions.

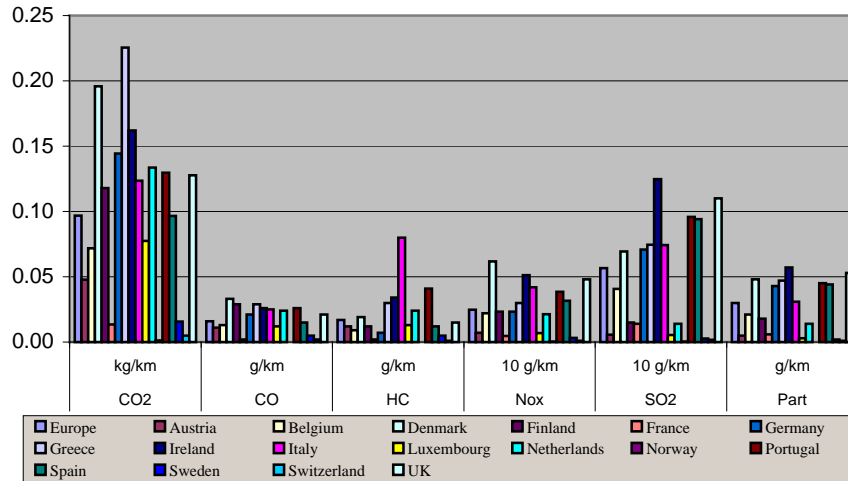


Fig. 17.6: Background emissions of EV driving ECE cycle

17.4 Hybrid Electric Vehicles

In comparison with electric or ICE vehicles, it is more difficult to compare energy consumption of hybrid vehicles due to the fact that the net state of charge deviation over the speed cycle must be zero.

The reference vehicle is a 2,7 ton hybrid van driving the DUB cycle. The drivetrain has the same components as the electric van (V2) and diesel van (V1) in previous chapters.

In the case of hybrid vehicles, a strategy has to be defined for putting the battery charging/discharging efficiency in competition with the engine efficiency.

17.4.1 Series Hybrid Vehicle

Different power control strategies (see subchapter 3.4.1) can be evaluated for the series hybrid electric van (V6). Table 17.2 summaries the different selected setpoints.

In the first four examples the APU needs to deliver a constant power (see 'APU setpoint') at a constant velocity (see 'ICE speed setpoint'). In examples 5 and 6 the APU delivers the required driving power as well as an additional battery charging power. At this moment the engine operating point will not be constant. In case 5 the engine operating velocity is chosen in function of the required APU power corresponding to the minimum fuel consumption line. In case 6 the engine speed is kept constant and the torque will change in function of the required APU power. Examples 7 and 8 represent a power control strategy taking into account the SoC of the battery.

Table 17.2: Simulated power strategies for a SHEV

	APU setpoint	ICE speed setpoint	APU on time	CHR	Remarks
1	24 kW	2100rpm	23%	217%	AR-PR
2	24 kW	2100rpm	23%	217%	PR-AR
3	17 kW	1500 rpm	30%	217%	
4	6 kW	2100 rpm	87%	54%	
5	P _{trac} + 15 kW	Consumption	24%	217%	35 kW max
6	P _{trac} + 15 kW	2100 rpm	24%	217%	35 kW max
7	P=P(SoC)	2100 rpm	DUBc 5X	54%	24kW@50% - 0kW@70%
8	P=P(SoC)	1500 rpm	DUBc 5X	54%	17kW@50% - 0kW@70%

By using the engine of a diesel van for the APU, this APU will be oversized. This can be noticed in Table 17.2 from the Combustion Hybridisation Rate (CHR). The

time the APU is engaged during the cycle is chosen in such a way that there is not any net variation of SoC ('APU on-time').

In case 1 the APU is operated at constant power corresponding to the maximum engine efficiency. Due to the oversized engine and taking into account the previous constraint, the APU is engaged during a rather short period of the simulated cycle. Only 23 % of the cycle the APU is engaged, as indicated in Table 17.2. In cases 4, 7 and 8 the engine is scaled down to have a lower CHR and a longer 'APU-on time'.

Fig. 17.7 shows the fuel consumption and Fig. 17.8 the NO_x emissions of different power control strategies.

In case 1 the priority is give to the performance of the vehicle and hence the AR is calculated before the PR. This means that if the battery charging power for example is too high, the regenerative braking will be reduced before the APU power. In the second example the APU power is decreased when a battery limit occurs. Due to the higher regenerative braking in this second case, the fuel consumption is better than in the first case, as illustrated in Fig. 17.7.

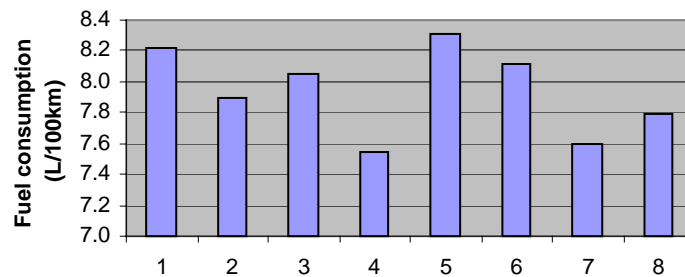


Fig. 17.7: Comparison of fuel consumption of different power control strategies in SHEV

Low fuel consumption does not automatically mean optimal emissions. In case 3 the APU setpoint corresponds to the NO_x minimum of the engine map. In this example the fuel consumption is slightly increased compared to case 2, but the NO_x emissions are decreased by more than 40 %.

By downscaling the engine and hence using a lower CHR (case 4 compared to case 2) the fuel consumption reduces due to the fact the APU power is more directly used for driving than for recharging the battery. A very low CHR however results in smaller electric mode driving range.

In cases 5 and 6 another power strategy is simulated: the APU needs to follow the required driving power. The APU power is limited to 35 kW in these examples to keep the engine in a good operating area and in case 5 the engine speed is defined in

function of the required power following the minimum consumption line. However due to the dynamic operating of the engine, the fuel consumption increases compared to case 2. If the engine speed is kept constant and the engine torque follows the speed cycle dynamics (case 6), this augmentation is somewhat lower.

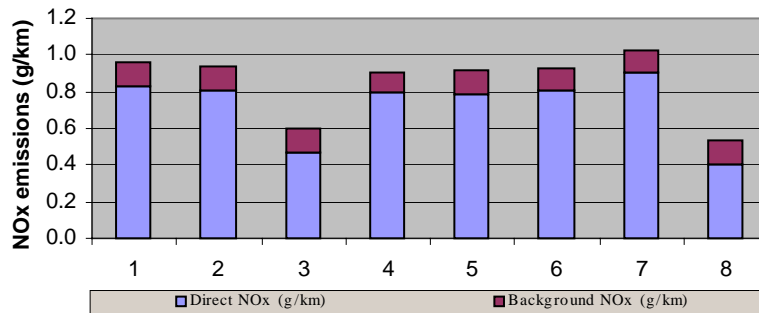


Fig. 17.8: Comparison of NOx emissions for the different power control strategies in SHEV

The last two cases illustrate a strategy in which the SoC defines the APU power. When the SoC equals 50 %, the APU delivers 24 kW and when the SoC exceeds 70 %, the APU is disengaged as in case 7.

Fig. 17.9 shows several simulation results for fuel consumption and NOx emissions using different start values of the SoC. The horizontal axis illustrates the deviation between the start and end-value of the SoC, the left vertical axis the corresponding fuel consumption and the right vertical axis the direct and background NOx emissions.

Using a linear interpolation, the fuel consumption and emissions corresponding to no net SoC deviation can be calculated. The same calculation is performed in case 8, where the ICE speed setpoint corresponds to a lower NOx emission.

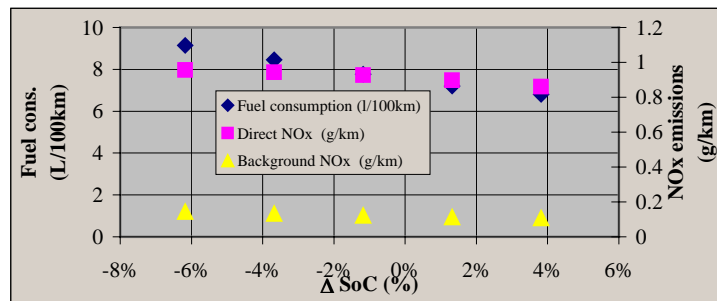


Fig. 17.9: Fuel consumption and NOx emissions for different SoC start values (case 7)

17.4.2 Parallel Hybrid Vehicle

Six different power control strategies are compared for the parallel hybrid drivetrain topology, as summarised in Table 17.3. Fig. 17.10 illustrates the simulation results. In contrast to the SHEV, no scaling is carried out and the Combustion Hybridisation Rate (CHR) equals 68 %.

Table 17.3: Simulated power strategies for a PHEV

	APU setpoint	Min. vehicle speed	APU on time	Remarks
1	$T_{\text{gear}} = T_{\text{trac}}$	0 km/h	76%	No idle
2	$T_{\text{gear}} = T_{\text{trac}}$	10 km/h	77%	No idle
3	$T_{\text{gear}} = T_{\text{trac}}$	10 km/h	77%	
4	$T_{\text{gear}} = 220 \text{ Nm}$	10 km/h	39%	
5	$T_{\text{gear}} = 220 \text{ Nm}$	10 km/h	75%	50% ICE
5	$T = T(\text{SoC})$	10 km/h	DUB 5X	$T_{\text{trac}}@70\% - 0\text{Nm}@50\%$

In the first case the engine will deliver the required driving forces. The battery will regenerate the braking energy and will drive the vehicle in the electric mode part of the speed cycle. In the second case the engine is engaged when the vehicle speed exceeds 10 km/h. Hence the engine does not need to operate at low velocities, which results in a reduction of the fuel consumption with more than 20 %. Additional consumption due to frequent starting the engine is yet not taken into account. However this can considerably increase the fuel consumption.

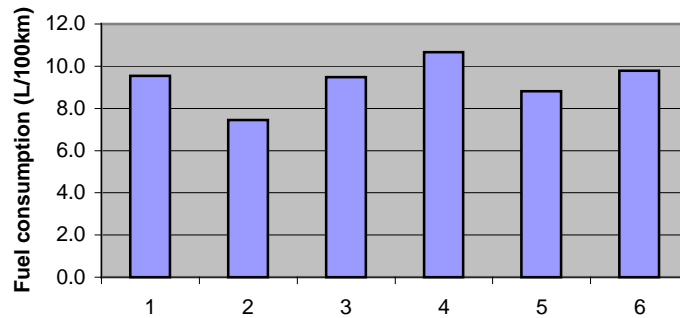


Fig. 17.10: Comparison of fuel consumption for different power control strategies in PHEV

Case 3 differs from case 2 in the fact that, when the engine is disengaged, it works in idle mode. Obviously this gives higher fuel consumption.

In example 4 the engine torque is kept constant and the battery is in charge of the speed cycle dynamics. However, due to the mechanical coupling of engine and wheels, the engine speed is not constant. Although the engine torque corresponds with a low fuel consumption operating line of the engine map, this does not give

good fuel economy. This is somewhat better (see case 5), if the engine is scaled down with a factor 2 and the CHR is decreased to 52 %.

Also case 6, where the battery SoC defines the engine torque setpoint, gives no interesting fuel consumption. However this strategy can be required, if a small battery capacity is used.

17.4.3 Combined Hybrid Vehicle

Three different power control algorithms, as described in subchapter 3.4.3, are compared in 8 different examples. Table 17.4 summarise the simulation setpoints.

Table 17.4: Simulated power strategies for a CHEV

	APU setpoint	Min. vehicle speed	APU on time	Remarks
1	$T_{\text{mot}} = 30 \% T_{\text{trac}}$	0 km/h	44%	
2	$T_{\text{mot}} = 30 \% T_{\text{trac}}$	10 km/h	69%	
3	$T_{\text{mot}} = 30 \% T_{\text{trac}}$	10 km/h	69%	lock
4	$T_{\text{ICE}} = \text{Cte}$	0 km/h	60%	50 % ICE
5	$T_{\text{ICE}} = \text{Cte}$	0 km/h	85%	50 % ICE + lock
6	min. losses	0 km/h	35%	lock
7	min. losses	10 km/h	75%	lock
8	min. losses	10 km/h	97%	70 % ICE + lock

The first three cases demonstrate an algorithm in which the required traction torque is proportionally split-up between the electric motor and the planetary gear. In the planetary gear this torque condition is divided between engine and generator in such a way that the engine torque-speed relation matches up with the minimum fuel consumption line.

In the second case the vehicle operates in pure electric mode at vehicle speeds below 10 km/h. This improves the fuel economy. Fig. 17.11 shows the simulation results.

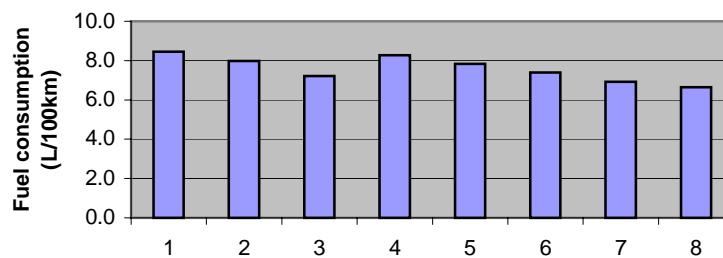


Fig. 17.11: Comparison of fuel consumption of different power control strategies in CHEV

When the engine load is very low, its efficiency is bad. In the third example the engine is locked when the requested engine power is too low, which results in a lower overall fuel consumption.

Cases 4 and 5 demonstrate an algorithm where the planetary gear torque and engine torque are kept constant. The motor will be in charge of all vehicle dynamics. In this way the engine is operated as it is done in a series hybrid vehicle. To have a better hybridisation rate the engine is scaled down. Although the engine is operated at its working point corresponding to the highest efficiency, the overall fuel consumption is not optimal. This is due to the fact that the power delivered by the engine sometimes passes, in function of the speed cycle requirements, through the generator and the motor before reaching the wheels. Locking the engine during vehicle braking (case 5) improves to some extent the fuel economy since more braking energy can be regenerated.

A last strategy consists in splitting-up the power in such a way that the powerflow in the drivetrain corresponds to the minimum overall drivetrain losses. By disengaging the engine at vehicle speed lower than 10 km/h (case 7) and scaling down the engine (case 8) a further decrease in fuel consumption is obtained.

17.5 Comparison of Drivetrain Topologies

The different drivetrain topologies, discussed in previous chapters as well as other examples, will be compared.

17.5.1 Energy Consumption

The simulation results are based on:

- Driving five times the Dutch Urban Bus cycle.
- A fictive 2,7 ton light duty van.
- No component integration work or drivetrain component optimisation.
- End-charge of electric drivetrain included.

Fig. 17.12 shows the results of the total primary energy consumption, including fuel preparation and electricity production. The diesel van (ICV) is used as the reference vehicle. The diesel-electric drivetrain (DEV) has a 19 % higher fuel consumption. This could be expected: the diesel engine needs to deliver all traction dynamics since there is no battery. Due to multiple energy-conversion the diesel-electric yields higher losses than a conventional diesel van.

In our example the three types of hybrid drivetrain topologies, series (SHEV), parallel (PHEV) and combined (CHEV), give similar results: the fuel consumption is reduced by more than 40 %. However, as demonstrated in previous chapters, a

good chosen drivetrain power strategy is required to reach these low consumption values. The optimal strategy is selected to perform this comparison. Among the three hybrid electric topologies the combined hybrid gives the lowest fuel consumption: almost half of the diesel reference.

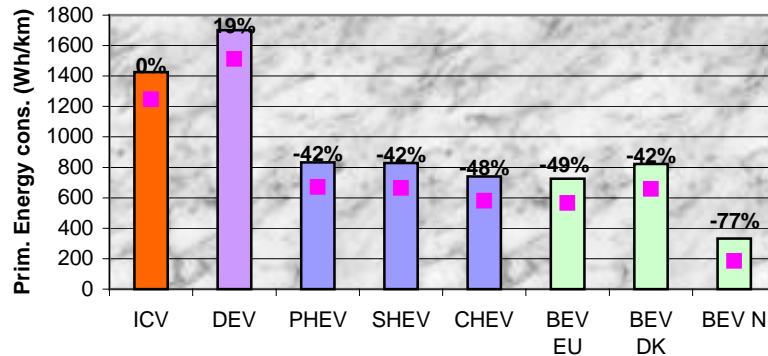


Fig. 17.12: Global comparison of primary energy consumption

A similar energy consumption-savings can be attained with the battery electric drivetrain. The primary energy consumption is closely related to the electricity production. In Fig. 17.12 the European average production mix, the ‘worst’ European country and the ‘best’ are illustrated. In the cases of solar, wind or hydraulic power stations no electricity production losses are taken into account, because they use renewable energy sources. For a ‘European’ electric car (BEV-EU) the energy saving is 49 %. When the battery of this vehicle would be charged in Denmark (BEV-DK) the primary energy consumption is 42 % less than for the diesel van. In Norway energy consumption reduction goes up to 77 %.

These results are based on fictive vehicles with the same total static weight. However, after component integration there will be a significant difference in weight between the different drivetrain topologies. Hybrid vehicles have more components. On the other hand their size and weight will be smaller: the engine of a SHEV does not need to be as large as in a ICV and the battery of a CHEV can be chosen compact than the one of an BEV.

To have an idea of the impact of the total vehicle weight Fig. 17.12 is extended with the results of the same drivetrains with a reduced mass: 1,7 ton instead of 2,7. The upper horizontal axis gives the simulated vehicle and its corresponding static weight. The lower horizontal axis gives the reduction of the primary energy consumption each time in comparison with the ICV references vehicle of respectively 1,7 and 2,7 ton (the two first cases).

The fuel consumption or electricity consumption at the grid is illustrated in Fig. 17.13 with “consumption” and the “production” of fuel or electricity is calculated as

described in subchapters 6.3 and 6.4 and is taken into account to determine the total primary energy consumption

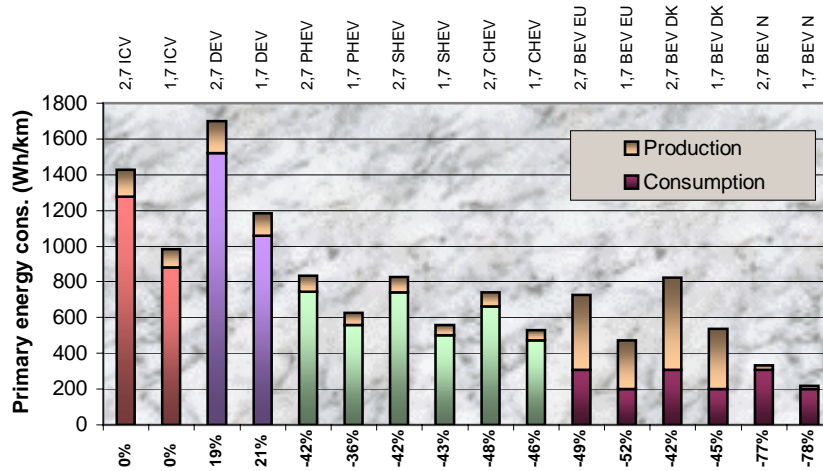


Fig. 17.13: Global comparison of primary energy consumption of a 1,7 and a 2,7 light duty van with different drivetrain topologies

17.5.2 NOx and CO-emissions

An excellent fuel economy does not automatically stands for favourable emission levels. Especially in the hybrid configuration, the engine operating point can be selected in function of low fuel consumption, but possibly at high emissions levels.

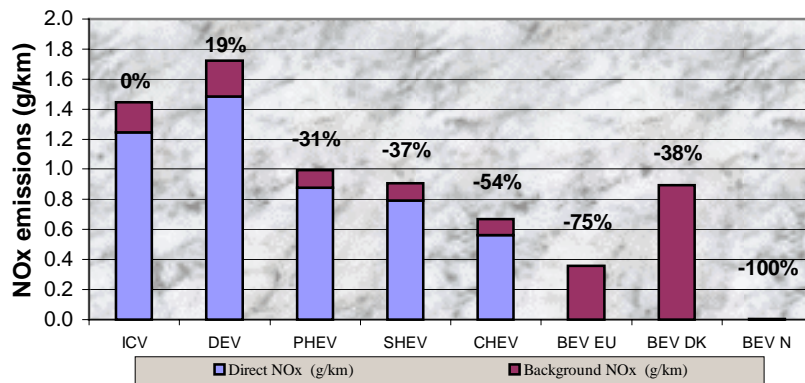


Fig. 17.14: Global comparison of NOx-emissions

Fig. 17.14 demonstrates the NO_x-emissions for the same vehicle topologies as in §17.5.1. In Fig. 17.15 the CO-emissions are illustrated. Remark that the absolute emission results cannot necessarily be generalised, because they are valid for the considered components used in the light duty van. However the relative comparison is very useful as an indication of the potential emission reduction of hybrid and electric vehicles.

Once again the diesel-electric drivetrain give an increases of NO_x-emissions with 19 % and CO-emissions with 79 % compared to the ICV.

The simulated PHEV decreases NO_x-emissions with 31 % and CO-emissions with 49 %. The SHEV reduces NO_x with 37 % and CO with 81 % and the CHEV respectively 54 % and 74 %. These results show that the hybrid electric vehicles not only have the outlook to reduce fuel consumption, but at the level of emissions they have even a higher reduction prospective.

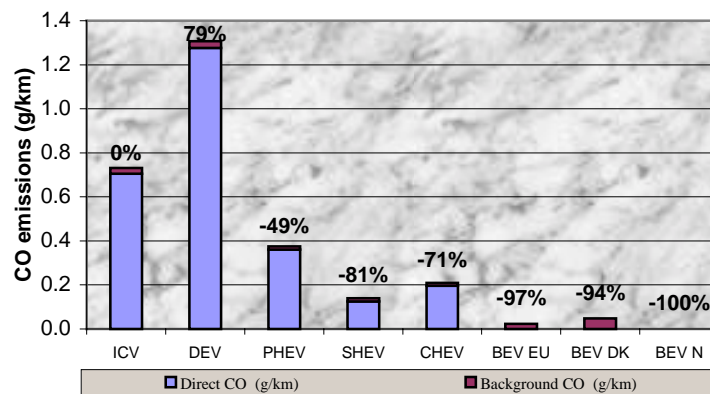


Fig. 17.15: Global comparison of CO emissions

The composition of the power production park is particularly decisive to the evaluation of emissions of battery electric vehicles. The NO_x-emissions can be reduced from 38 % to almost 100 % and the CO-emissions by more than 94 %. However if one would compare the SO₂-emissions it would not be in favour of electric vehicles. This is due to the use of sulphurous coal in power stations. It should however be stated that the sulphur dioxide emissions from power stations are likely to reduce significantly in the future, due to the use of advanced fuel gas treatment systems and to changes in the production mix.

17.5.3 Acceleration Performance

With the help of the simulation programme the different drivetrains are compared on the bases of an acceleration test. Fig. 17.16 illustrates the results. The results are

function of the maximum power characteristics of the considered components and cannot be generalised.

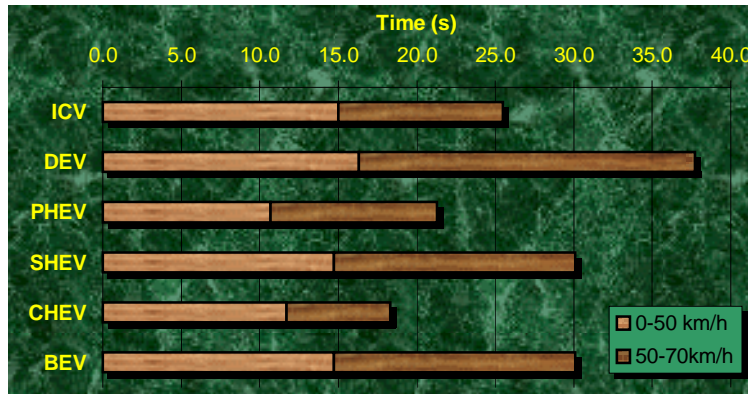


Fig. 17.16: Acceleration comparison

The BEV and SHEV have the same acceleration performance since their acceleration power is limited by the maximum operation of the electric traction motor.

The DEV should have the same speeding up time, but the generator and engine power limit the acceleration, since there is no battery.

The PHEV has an improved acceleration performance due to the fact that the engine as well as the motor contributes to the acceleration torque.

Although the engine in the CHEV is scaled down with 70 % compared to the ICV and PHEV, the CHEV has the fastest acceleration. To clarify this result it is necessary to have a closer look at the power distribution in this complex drivetrain.

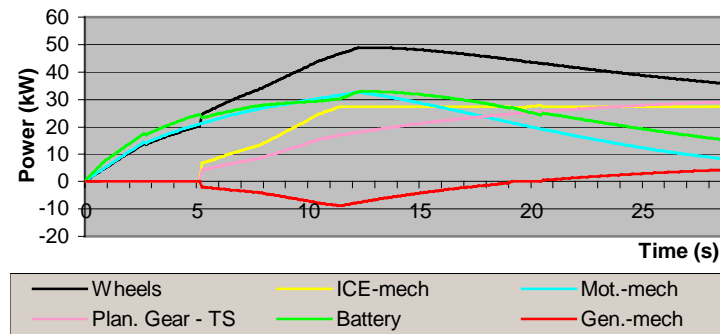


Fig. 17.17: Power in CHEV – acceleration test

As can be seen in Fig. 17.17, the first seconds (vehicle speed is inferior to 10 km/h) the CHEV operates in electric mode. Subsequently the engine contributes to the acceleration power in function of the overall minimum loss criteria. Between 5 and 20 seconds the main part of the engine power flows directly via the planetary gear to the wheels. The remaining engine power goes through the generator and via the motor, to drive the wheels as well. After 20 seconds the generator power is inverted. The battery power is split-up between generator and traction motor and both electric drives (motor and generator) as well as the engine contribute to the acceleration wheel power.

17.6 Comparison of Commercial Passenger Cars

The previous results were based on a fictive vehicle with different drivetrain topologies. It is interesting to validate these results on the bases of commercial passenger cars. A small gasoline passenger car (V16) is weighed against a small battery electric passenger vehicle (V12).

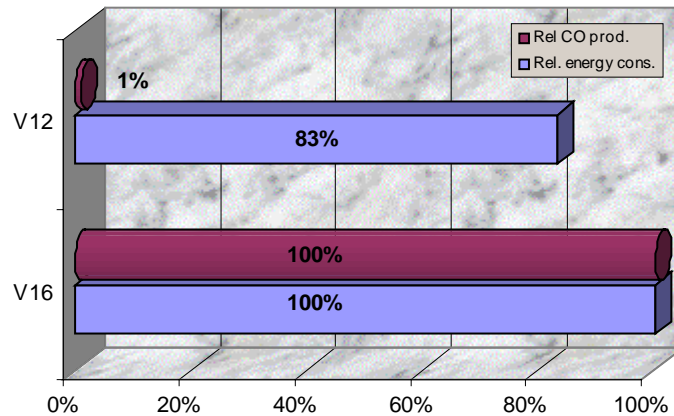


Fig. 17.18: Primary energy comparison of an electric (V12) and an ICE (V16) passenger car

The energy reduction is less spectacular as subchapter 17.5, mainly due to the fact that in this previous chapter all vehicles were supposed to have the same total static weight. In Fig. 17.18 the electric vehicle has a total static mass of 1140 kg compared to the gasoline car that has a weight of 800 kg. The electric car consumes 17 % less primary energy than the gasoline car.

However the CO reduction, by using an electric car of which the battery is charged in 'Europe', is 99 % lower compared to the gasoline reference vehicle.

Fig. 17.19 presents the simulation results of an acceleration test.

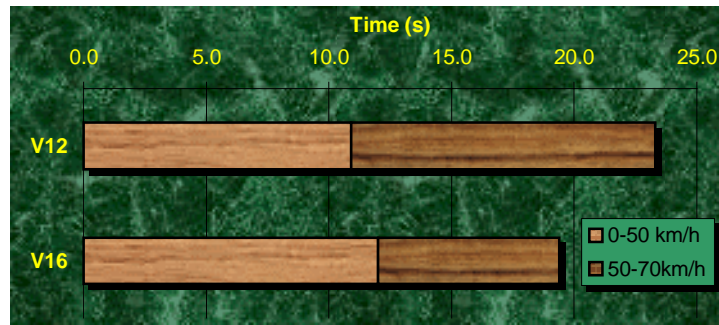


Fig. 17.19: Acceleration of electric (V12) and ICE (V16) passenger car

Even so, the electric vehicle is heavier, its acceleration to 50 km/h is faster than for the gasoline vehicle. The electric drive has a high starting torque at stand still and does not need gear shifting and clutch slipping, as is required for the gasoline vehicle.

However when further accelerating the vehicle to 70 km/h the gasoline vehicle accelerate faster. This is due to the diminution of the electric motor torque due to flux weakening.

PART IV CONCLUSIONS

18 CONCLUSIONS

18.1 Overview of The Research

18.1.1 Overview of Part I

The first part gives an overview of the state of the art of electric and hybrid electric vehicle technology including:

Electric and hybrid electric vehicles drivetrain layout.

Infrastructures, market incentives and environmental aspects.

Summary of the technical aspects of traction motor, convertor, battery and charger.

Description of the different hybrid drivetrain topologies as well as of the power control algorithms of hybrid electric vehicles.

The fundamental calculation algorithms, the component modelling, language environment and accessibility levels.

18.1.2 Overview of Part II

This second more technical part describes the models of the different subprogrammes of the simulation software.

The main programme and related subprogrammes (electricity production, speed cycle definition, etc.).

The implemented drivetrains of the different vehicles.

The specification of the iteration algorithm, defining, the maximum vehicle acceleration performance and controlling the power management of the different subsystems.

The mechanical and electric power control devices for hybrid electric vehicles. In these subprogrammes the different hybrid drivetrain control strategies are mainly implemented.

The description of the components related to the forces acting on the vehicle body and wheels and the mechanical transmission.

The drivetrain components, figuring as powerflow transformation, are described from the transmission to the energy source(s).

18.1.3 Overview of Part III

The third part elucidates the simulation results, including:

A brief description of the measurement equipment, on-road and in laboratory.

The data handling as well as the database.

The calibration and validation of the simulation programme as well as a sensitivity analysis illustrating how sensitive the output is to changes in the input parameters.

The possibilities of the simulation programme are illustrated with several simulation results. Different vehicles as well as different powerflow control strategies of hybrid electric vehicles are compared.

18.2 General Achievements

Within the framework of this PhD research the next most important achievements are realised:

- A state-of-the-art overview is outlined of the different concepts, components, and power management strategies of battery, fuel cell and hybrid electric vehicles.
- A vehicle simulation programme VSP is developed.
 - VSP enables the simulation of battery, fuel cell and hybrid electric, as well as internal combustion vehicles.
 - VSP is a powerful tool to develop new concepts and compare drivetrains and power management strategies. It has the ability to compare multiple simulations on both second by second as well as on fuel economy, emissions and acceleration performance.
 - VSP can predict vehicle range and acceleration.
 - VSP can simulate regulated driving cycles. Real world driving patterns can be performed to get an accurate assessment of the impact of real world energy consumption. Additionally it has the ability to simulate mountainous drive cycles.
 - VSP has an interactive graphical interface and is flexible in use.
 - VSP is useful for a wide variety of users with different expertise, like: engineers, transport operators and suppliers, energy utilities and decision-makers. But mainly it is an engineering tool to evaluate different drivetrains and to optimize power management in hybrid vehicles in particular.

- VSP has a flexible database structure, integrated in the component models, allowing an easy implementation of different kind of component data in the form of look-up tables, maps, theoretical equations, and empirical formulae; this all in function of the available data.
 - VSP has an in-depth worked out programme modularity in which almost all parameters are only accessible in the module of the component itself.
 - VSP has a unique iteration algorithm dedicated for the flexible implantation of different kind of hybrid drivetrain topologies and powerflow management algorithms taking into account the component operating boundaries or desired operating conditions. This iteration algorithm, the core of the programme, is based on two control parameters: a Power Distribution factor (PDF) and the vehicle acceleration (\dot{a}). The first defines the power division in the hybrid drivetrains taking into account the proper characteristics of each component. Via a feedback loop this PDF can be modified in function of the component capabilities via the Power Reduction (PR). Within the same loop the maximum vehicle acceleration is controlled with the help of the Acceleration Reduction (AR).
 - The iteration algorithm is also able to simulate driving downhill at constant speed. This is a very difficult situation, because the algorithm is essentially based on the reduction of the acceleration. When one needs to drive at constant speed the acceleration is zero. However the algorithm is able to find the power splitting up between regenerative braking and pneumatic braking.
 - VSP contains scaling possibilities and “zero-delta state of charge” routines.
- Based on experimental results, different components have been modelled, calibrated and validated. It can be stated that the end-results have an error of less than 5 %.
 - A comparative assessment is achieved for the real environmental impact of different traction systems (case study). The comparison is realized at the level of:
 - consumption (fuel and electricity);
 - emissions (CO₂, HC, NO_x, CO, particles, etc.);
 - performances (acceleration, range, maximum slope, etc.).

18.3 Concluding Comparative Assessment of Energy Consumptions and Emissions

To finally conclude this research exertion a comparative assessment of battery electric, hybrid electric and internal combustion vehicles is reviewed. What are the decisive factors affecting the energy consumptions and exhaust emissions? What are the potential benefits of battery and hybrid electric vehicles?

Defining a good drivetrain power strategy is a very complex task. The combination of different characteristics of different components in different drivetrain topologies makes it necessary to use a good simulation tool.

Based on a case study of a fictive body and chassis of a light duty van fitted out with different types of drivetrains some important results can be established as described hereafter.

18.3.1 *General Hybrid Power Management Optimization Criteria*

Use a high efficient battery with a high power density.

Use an efficient engine with a broad operating area with low fuel consumption.

Compromise between battery charging/discharging losses and fuel economy evaluated to the engine operating point.

Compromise between energy consumption, exhaust emissions and acceleration performance.

The possibility of driving in pure electric mode in certain parts of the drive cycle (city centres) is one of the most important benefits of hybrid vehicles.

A good strategy consists in, considering the previous statements:

- The choice of a good hybridisation rate.
- The choice of only electric mode at low vehicle speed.
- Limiting engine-working area.

The most important factors influencing the energy consumption of vehicles are:

- total weight;
- component efficiency;
- speed profile.

The impact of these parameters is different from one drivetrain type to another (see subchapter 15.3).

18.3.2 Parallel Hybrid Electric Vehicles Conclusions

a) PHEV benefits

No idling:

PROFIT: 15 to 20 % reduced fuel consumption.

Possibility of regenerative braking:

PROFIT: up to 30 to 40 % reduced energy consumption possible if the battery allows it.

Direct connection of engine to the transmission:

PROFIT: less energy conversions.

b) PHEV power management

Operate engine only in its most efficient working area:

- Above 10km/h the engine may deliver all driving power.
- An automatic gear should keep the engine between efficient operating limits.
- When braking or stand still the engine is switched off.

The electric motor is used when driving slower than 10km/h, while braking and for high accelerations.

c) PHEV market segment

This PHEV benefits makes the PHEV useful for the family or higher class vehicle segment while mainly driving on highway and long distances.

18.3.3 Series Hybrid Electric Vehicles Conclusions

a) SHEV benefits

Similar to the PHEV benefits from the no idling and regeneration capabilities.

Possibility of choosing constant engine operating point:

PROFIT: 30 % (diesel) engine energy efficiency instead of 15 to 20 % in ICV.

b) SHEV power management

The size, weight and operating of the engine of a SHEV should be chosen in such a way that its most efficient working point corresponds with the average driving power (in city traffic) of the considered vehicle.

Continuous operating the APU at this most efficient operating point will result in the lowest vehicle fuel consumption, especially when an efficient battery with a high power density is used.

If necessary the APU power can be reduced during braking to benefit from maximum energy regeneration.

c) SHEV market segment

The SHEV is an interesting solution for driving in urban areas with passenger cars, light duty vehicles (with e.g. range extender) as well as with heavy (urban) busses (e.g. battery non-depleting type).

18.3.4 Combined Hybrid Electric Vehicles Conclusions

a) CHEV benefits

The CHEV combines both benefits from the PHEV as from the SHEV:

- High engine operating efficiency.
- Direct connection of engine to the transmission.

b) CHEV power management

Manifold power path are possible in this complex hybrid drive train. An optimisation function should define the power distribution between electric motor and planetary gear (ICE) to minimize overall drivetrain losses.

The generator speed should be chosen to optimize, via the planetary gear, the engine speed in function of the required engine torque.

Lock the engine at low requested load (e.g. vehicle speed lower than 10 km/h), during braking (maximum regeneration of braking energy via the electric motor).

c) CHEV market segment

The CHEV is an interesting solution for the intermediate car population segment that frequently is used in town but also as a commuter car, with a good road performance and is often the main or only family car.

18.3.5 Electric Vehicles Conclusions

It can be stated that for Europe as a whole, the electric vehicle is an ideal means to reduce air pollution.

The electric vehicle has a beneficial effect at two levels:

- On one hand, it is totally emission-free at the place of use.
- On the other hand the emissions caused by the generation of electricity for electric vehicles are significantly lower than the emissions caused by internal-combustion engine vehicles.

Even if electric vehicles are at this moment much heavier than conventional vehicles the global energy consumption in real traffic conditions is in the advantage of electric vehicles. The benefit is strongly depending on the type of electricity production plant. Decentralised production based on wind-, solar- and static fuel cell plants could be a revolutionary approach.

The acceleration from standstill in the slow speed region is higher for electric vehicles.

This demonstrates that electric vehicles are ideal city vehicles due to their environmentally friendliness and good performance.

18.3.6 General Comparison

One of the manifold figures and graphs of the case study described in chapter 17 is redraw illustrating the primary energy consumption of different types of drivetrains with a total static weight ranging from 1,7 to 2,7 ton.

In Fig. 18.1 the blue-yellow line represents the Internal Combustion Vehicle (ICV) reference energy consumption. The top of the purple stroke corresponds with the energy consumption of this vehicle with a total weight of 2,7 ton and the bottom with 1,7 ton.

This reference is compared with the Diesel-Electric (DEV), the Parallel Hybrid Electric (PHEV), Series Hybrid Electric (SHEV), Combined Hybrid Electric (CHEV) and Battery Electric Vehicle (BEV). The latter is charged in Europe (EU), Denmark (DK) and Norway (N).

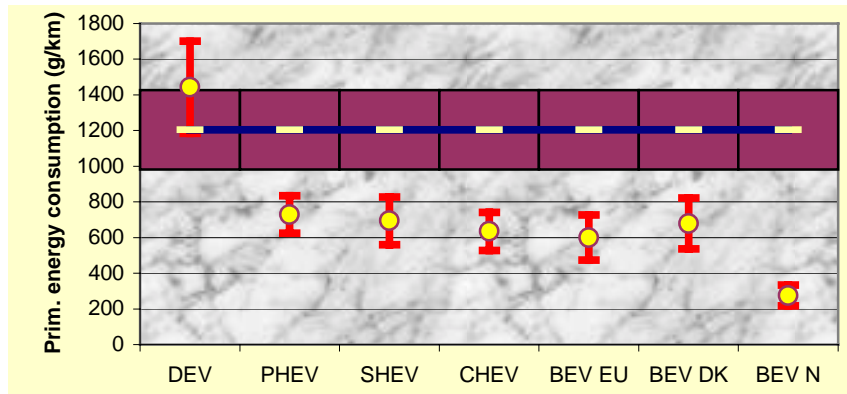


Fig. 18.1: Primary energy consumption of different types of drivetrains with a total static weight ranging from 1,7 to 2,7 ton

The results give a confident indication of the potential energy reduction of battery and hybrid electric vehicles.

In general the case study indicates the possibility to reduce energy consumption, when using hybrid or battery electric vehicles, with more than 40 % in comparison with conventional thermal vehicles.

The comparison between the hybrid vehicles shows a benefit for the combined hybrid. However the choice of the power management strategy is more decisive for the energy consumption than the drivetrain topology itself. This later should be chosen in function of the market segment, cost, etc.

The battery electric vehicle gives similar results as for the hybrid vehicles. However the power generation efficiency influences these results very much.

On the contrary the diesel-electric drivetrain demonstrates a potential of very bad energy balance.

The potential reduction of emissions by the use of hybrid and especially battery electric vehicles is even higher than the energy reduction potential, as illustrated with the following figures.

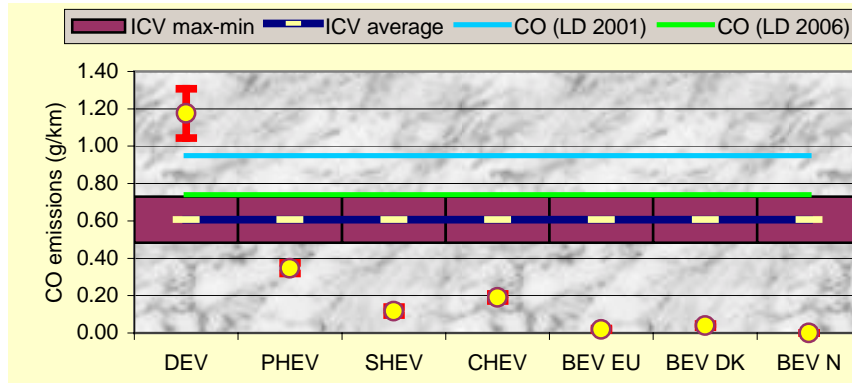


Fig. 18.2: CO emissions of different types of drivetrains with a total static weight ranging from 1,7 to 2,7 ton

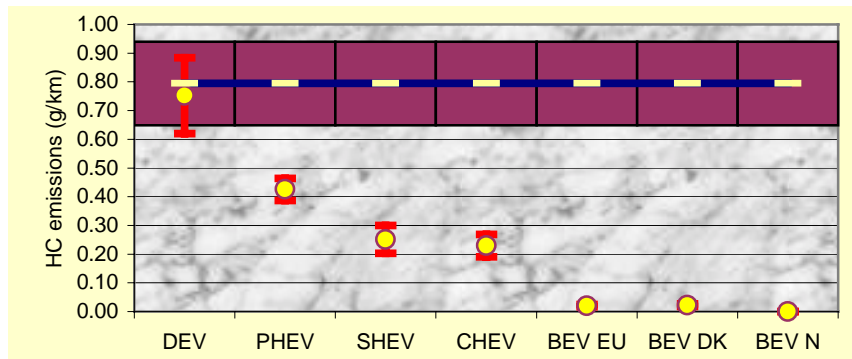


Fig. 18.3: HC emissions of different types of drivetrains with a total static weight ranging from 1,7 to 2,7 ton

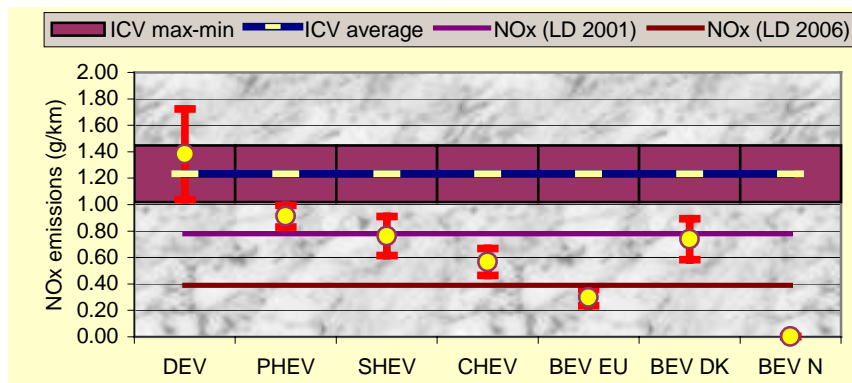


Fig. 18.4: NOx emissions of different types of drivetrains with a total static weight ranging from 1,7 to 2,7 ton

Curriculum vitae

Joeri Van Mierlo is born on April 28th, 1969 in Vilvoorde, Belgium.

He attended the Koninklijk Atheneum Laken from 1981 to 1987. In 1987 he started his studies in electro-mechanical engineering at the Vrije Universiteit Brussel, V.U.B., and graduated in 1992. His graduation project was devoted to the development of PLC-controlled roll-bench for the evaluation of electric vehicles [180].

After his civil duties he started in 1994 as a research assistant at the department of electrical engineering of the V.U.B. He was in charge of several national and international research projects mainly regarding the test and evaluation of electric and hybrid electric vehicles [120,145,158,177,193,194,195]. He assisted many students with their graduation projects. He made several scientific publications on national and international conferences as first author [183,191,158,196,197,198,199,200,201,202,203,204,205] and as second author [206,207,208,209,210], as well as some publications for the general public [211,212,213,214].

He was engaged in different boards of the V.U.B. as well as in several demonstration and PR projects of CITELEC and AVERE, European scientific association hosted by the University on the bases of contracts.

References

- [1] P. Van den Bossche, G. Maggetto
“RECENT TECHNOLOGICAL DEVELOPMENT OF ELECTRIC AND HYBRID ROAD VEHICLES”
Conference, Incontro Municipale Veicoli Elettrici Città di Torino, Torino, Italy, 1994
- [2] S. T. Mc Broom
“DEVELOPMENT OF A HYBRID VEHICLE PERFORMANCE EMISSIONS AND EFFICIENCY MODEL”
Final report, IR&D project 03-9788, Southwest Research Institute, June 1995
- [3] G. Maggetto, H. Kahlen
“ELECTRIC AND HYBRID VEHICLES”
Proceedings EPE-97, Norwegian University of Science and Technology, Norway, 1997
- [4] J.A. Gregoire
“50 ANS D’AUTOMOBILE. 2. LA VOITURE ÉLECTRIQUE”
ISBN 2-08-010751-8, 1981
- [5] H. Bauer
“AUTOMOTIVE HANDBOOK”
4th edition, SAE, Warrendaele, PA, USA, ISBN 1-56091-918-3, 1996
- [6] G. Stirano, A. Roggero, P.Garella
“HYBRID BUS WITH WHEEL HUB MOTORS”
AVERE contract P-039 of the EDS study, “Advanced electric drive systems for buses, vans and passenger cars to reduce pollution (EDS)”, funded by the Commission of the European Communities, December 1992.
- [7] J. Beretta
“NEW CLASSIFICATION ON ELECTRIC-THERMAL HYBRID VEHICLES”
proceedings EVS-15, Brussels, Belgium, 1-3 October 1998
- [8] CEN prEN 13447
Comité Européen de Normalisation , 1989
- [9] “RECOMMENDED PRACTICE FOR MEASURING THE EXHAUST EMISSIONS AND FUEL ECONOMY OF HYBRID-ELECTRIC VEHICLES”
SAE J1711, September 1998

- [10] G. Maggetto , P. Van den Bossche , J. Van Mierlo , C. Lecho
“ELEKTRISCHE EN HYBRIDE VOERTUIGEN IN VLAANDEREN:
EEN MILIEUVRIENDELIJK ALTERNATIEF VOOR HET
STADSVERKEER”
Info text of the demonstration “Ronde van Vlaanderen voor elektrische
voertuigen”, CITELEC, Brussels, Belgium 1997
- [11] “BEST AVAILABLE ENERGY TECHNOLOGIES FOR OUR
ENVIRONMENT”
Commission of the European Community, DGXVII, Thermie
- [12] <http://www.mira.co.uk/app/>
Advanced Powertrain Projects, Motor Industry Research Association
(MIRA), Nuneaton, England
- [13] V. Vandeweerd
“MILIEU- EN NATUURRAPPORT VLAANDEREN: THEMA’S
MIRA-T 1999”
Vlaamse Milieu Maatschappij, VMM, Erembodegem, Belgium, April
1999
- [14] I. De Vlieger
“LUCHTVERONTREINIGENDE EMISSIES DOOR HET VERKEER”
AMINAL contract 931095V00, Min. Vlaamse Gemeenschap, Brussel,
Belgium, December 1993
- [15] M. Van den Heede
“IMPACT VAN MILIEUPOLLUENTEN OP DE MENS:
BELANGRIJKE POLLUENTEN DIE EEN RISICO KUNNEN
VORMEN VOOR DE MENSELIJKE GEZONDHEID”
Energie & Milieu, March-April 1996
- [16] S. Bostaji
“SIMULATION DE LA CONSOMMATION DE CARBURANT D'UNE
AUTOMOBILE EN RELATION AVEC LES CONDITIONS DE
CIRCULATION”
Thesis, Promotor Prof. B. Leduc, ULB, Brussels, Belgium, 1992
- [17] C.A. Lewis
“FUEL AND ENERGY PRODUCTION EMISSION FACTORS”
MEET project, deliverable no20, EC Contract No. ST-96-SC.204,
ETSU, Didcot, UK, June 97
- [18] B. Eliasson
“EMISSIONS AND THE GLOBAL ENVIRONMENT – STATISTICS
AND SCENARIO’S3
PUBLICATION, ABB Corporation Research Center, Switzerland, 1994”
- [19] <http://www.epe.be/epe/tcui.2.2.html>
EPE, European partners for the environment, Woluwe, Belgium

- [20] J-P. Heirman
“MINA-PLAN 2 HET VLAAMS MILIEUBELEIDPLAN 1997-2001”
AMINAL, Ministerie van de Vlaamse Gemeenschap, Brussels, Belgium,
1997
- [21] “AVERTING THE THREE OUTRIDERS OF THE TRANSPORT
APOCALYPSE: ROAD ACCIDENTS, AIR AND NOISE
POLLUTION”
<http://www.who.int/inf-pr-1998/en/pr98-57.html>
Press Release, WHO/57, 31 July 1998
- [22] F. Fabre, A. Klose, G. Somer
“COST 302 - TECHNICAL AND ECONOMIC CONDITIONS FOR
THE USE OF ELECTRIC ROAD VEHICLES”
Cost 302 project, European Commission, Brussels, Belgium, 1987
- [23] G. Maggetto, P. Van den Bossche, H. Van Muylem
“EDS, ADVANCED ELECTRIC DRIVE SYSTEMS FOR BUSES,
VANS AND PASSENGER CARS TO REDUCE POLLUTION”
European Commission and AVERE, Brussels, Belgium, 1992
- [24] L’association Charentaise de promotion des véhicules électriques
“OPÉRATION ÉNERGIE SÉDUCTION”
Final report, Thermie, European Commission, Brussels, Belgium,
October 1994
- [25] B. Harbolla
“ANALYSIS OF HYBRID DRIVE SYSTEMS WITH NEW ELECTRIC
COMPONENTS – MORPHOLOGY, EVALUATION AND
OPTIMISATION”
AVERE contract P-030 of the EDS study, “Advanced electric drive
systems for buses, vans and passenger cars to reduce pollution (EDS)”,
AVERE, Brussels, Belgium, December 1992
- [26] M. André
“DRIVING STATISTICS FOR THE ASSESSMENT OF POLLUTANT
EMISSIONS FROM ROAD TRANSPORT”
MEET project, deliverable no15, EC Contract No. ST-96-SC.204,
INRETS, Bron, France, February 1999
- [27] <http://www.arb.ca.gov/msprog/levprog/levii/overview.htm>
Proposed Changes to the LEV Program, California Air Resources Board
(ARB), Sacramento, CA 95814, USA
- [28] D. Naunin
“CONCEPTS AND MODELS FOR THE INTRODUCTION OF
BATTERY CHARGING STATIONS FOR ELECTRIC VEHICLES IN
CENTRES OF BIG CITIES”
AVERE contract P-002 of the EDS study, “Advanced electric drive
systems for buses, vans and passenger cars to reduce pollution (EDS)”,
AVERE, Brussels, Belgium, December 1992

- [29] R. Holslag
“BESCHRIJVING VAN HET WITKARSYSTEEM”
Thesis, T.H. Delft, The Netherlands, 1976
- [30] C.A.Bleijs, E.Bénéjam
“RESULTS OF THE EXPERIMENTAL SELF SERVICE ELECTRIC
CAR SYSTEM PRAXITELE”
Proceedings EVS-15, EPE, AVERE, Brussels, Belgium, October 1998
- [31] J. Couturier
“LISELEC: A PUBLIC INDIVIDUAL TRANSPORT SYSTEM”
Proceedings EVS-15, EPE, Brussels, Belgium, October 1998
- [32] C. Bleys
“IMPROVING CITY LIVING WITH ELECTRIC TRANSPORT”
Proceedings Nordisk Miljöbil 99, Helsinki, Finland, 8-9 September 1999
- [33] P. Van den Bossche
“ELECTRIC VEHICLE DELIVERY POST”
<http://www.citelec.org/EVDpost/default.htm>
Project supported under Thermie (TR140/97), 30 June 1999
- [34] CEN prEN 1821-2
Comité Européen de Normalisation , 1997
- [35] “INSTALLATION AND MAINTENANCE MANUAL”
Curtis PMC, Dublin, Ireland
- [36] H. Kahlen, W.-D. Weigel
“COMPARING MEASUREMENTS ON VARIOUS ELECTRIC
DRIVES FOR AN EXPERIMENTAL CAR”
Proceedings EVS-3, EVAA, Washington D.C., USA, February 1974
- [37] J. Rödig
“APPLICATION OF THE SMART BATTERY DRIVE SYSTEM FOR
ELECTRIC ROAD VEHICLES”
AVERE contract P-021 of the EDS study, “Advanced electric drive
systems for buses, vans and passenger cars to reduce pollution (EDS)”,
AVERE, Brussels, Belgium, December 1992
- [38] E. Lajoie-Mazenc, D. Prtmarty
“EUROPEAN MARKET OF AC-ADJUSTABLE SPEED DRIVES”
EPE association, Brussels, Belgium, 1993
- [39] N. Kazutoshi
“COMPARISON STUDY BETWEEN INDUCTION MOTOR AND
PERMANENT MAGNET SYNCHRONOUS MOTOR FOR ELECTRIC
VEHICLE APPLICATION”
Proceedings EVS-13, EVAAP, Osaka, Japan, 13-16 October 1996

-
- [40] E. Grecksch, K. Lamm, U. Winter
“STATUS OF DRIVETRAIN DEVELOPMENTS FOR ELECTRICAL VEHICLES”
Siemens AG, Würzburg, Germany
- [41] C.C. Chan
“A HIGH PERFORMANCE SWITCHED RELUCTANCE MOTOR DRIVE FOR P-STAR EV PROJECT”
Proceedings EVS-13, EVAAP, Osaka, Japan, 13-16 October 1996
- [42] C.C. Chan
“FUZZY VARIABLE STRUCTURE CONTROL OF SWITCHED RELUCTANCE MOTOR DRIVE FOR EV’S”
Proceedings EVS-13, EVAAP, Osaka, Japan, 13-16 October 1996
- [43] N.F. Ilinski, M.G. Bitchkov
“SWITCHED RELUCTANCE DRIVE FOR ELECTRIC LIGHT EVS”
Proceedings EVS-16, EVAAP, Beijing, China, October 1999
- [44] Y. Sugii.
“APPLICABILITY OF VARIOUS MOTORS TO ELECTRIC VEHICLES(EV)”
Proceedings EVS-13, EVAAP, Osaka, Japan, 13-16 October 1996
- [45] J. F. Lutz, B. R. Patel
“PERFORMANCE COMPARISON OF A 100 KW BRUSHLESS PM AND INDUCTION MOTOR SYSTEM”
Proceedings of EVS-14, EVAA, Orlando, Florida, USA, 15-17 December 1997
- [46] C.C. Chan
“A NOVEL BRUSHLESS PM HYBRID MOTOR WITH A CLAW-TYPE ROTOR TOPOLOGY FOR ELECTRIC VEHICLES”,
Proceedings EVS-13, Osaka, Japan, 13-16 October 1996
- [47] S. Henneberger, R. Belmans
“DESIGN AND DEVELOPMENT OF A PERMANENT MAGNET SYNCHRONOUS MOTOR FOR A HYBRID ELECTRIC VEHICLE DRIVE”
PhD-thesis, Katholieke Universiteit Leuven, Belgium, 1999
- [48] S. Eriksson
“DRIVE SYSTEMS WITH PERMANENT MAGNET SYNCHRONOUS MOTORS”
ABB Automation and drives
- [49] Y. Hirohisa
“AC DRIVE SYSTEM FOR ELECTRIC VEHICLES”
Proceedings EVS-13, EVAAP, Osaka, Japan, 13-16 October 1996

- [50] J. Angelis, H. Scherf, F. Walkowiak
"COMPACT DRIVE SYSTEM FOR ELECTRIC VEHICLES READY FOR SERIES PRODUCTION"
Proceedings EVS-7, AVERE, Versailles, France, June 1984
- [51] M. Giussani, E. Durelli, A. Bobbio, G. Mantovani
"LOW EMISSION URBAN HYBRID VEHICLE"
AVERE contract P-033 of the EDS study, "Advanced electric drive systems for buses, vans and passenger cars to reduce pollution (EDS)", AVERE, Brussels, Belgium, December 1992
- [52] J.L. Van Eck, H. Abdul Sater, P. Mathys, L. Vanbever, PH. Lataire
"ELABORATION DE STRATEGIES DE COMMANDES ADAPTEES AUX VEHUCULES ELECTRIQUES MUS PAR MOTEURS A COURANT ALTERNATIF"
AVERE contract P-004 of the EDS study, "Advanced electric drive systems for buses, vans and passenger cars to reduce pollution (EDS)", AVERE, Brussels, Belgium, December 1992
- [53] H. Kahlen
"TECHNOLOGICAL STEPS IN THE ELECTRIC VEHICLE DRIVETRAIN DEVELOPMENT"
Proceedings EVT-95, Paris, France, 13 - 15 November 1995
- [54] R. Vittorio
"DEVELOPMENT OF A NEW HIGH PERFORMANCE INDUCTION MOTOR DRIVETRAIN FOR EUROPEAN CITY-CAR FOR NEAR TERM PRODUCTION"
Proceedings EVS-13, Osaka, Japan, 13-16 October 1996
- [55] M. Kouki
"FAST ROTOR FLUX CONTROL OF VECTOR CONTROLLED INDUCTION MOTOR OPERATING AT MAXIMUM EFFICIENCY FOR ELECTRIC VEHICLES"
Proceedings EVS-13, EVAAP, Osaka, Japan, 13-16 October 1996
- [56] Y. Kenji
"AN EFFICIENCY MAXIMIZING INDUCTION MOTOR DRIVE SYSTEM FOR TRANSMISSIONLESS ELECTRIC VEHICLE"
Proceedings EVS-13, EVAAP, Osaka, Japan, 13-16 October 1996
- [57] A. M. Nasser
"COMPARISON OF INDUCTION, PM, AND SR MOTOR TECHNOLOGIES"
Proceedings EVS-16, EVAAP, Beijing, China, October 1999
- [58] H. Bausch
"ROAD VEHICLE WITH FULL ELECTRIC GEAR"
Proceedings EVS-10, EVAAP, Hong Kong, China, 3-5 December 1990

- [59] C.C. Chan
“DEVELOPMENT OF PHASE-DECOUPLING PERMANENT
MAGNET MOTOR DRIVES FOR THE PROPULSION SYSTEM OF
ELECTRIC VEHICLES”
Proceedings EVS-13, EVAAP, Osaka, Japan, 13-16 October 1996
- [60] K. Hisao, M. Tetsuya
“DEVELOPMENT OF MOTOR FOR ELECTRIC VEHICLES”
Proceedings EVS-13, EVAAP, Osaka, Japan, 13-16 October 1996
- [61] Y. S. Kouetsu Fujita Takao
“NEW CONTROL METHODS FOR HIGH PERFORMANCE PM
MOTOR DRIVE SYSTEMS”
Proceedings of EVS-14, EVAA, Orlando, Florida, USA, December 1997
- [62] B. Koretz, J. R. Goldstein, Y. Harats, M. Y. Korall
“A HIGH-POWER, MECHANICALLY RECHARGEABLE ZINC-AIR
BATTERY SYSTEM FOR ELECTRIC VEHICLES”
ISATA, Florence, 1992
- [63] J. Helling, H. Schreck, B. Gira
“HYBRID DRIVE WITH FLYWHEEL COMPONENT FOR
ECONOMIC AND DYNAMIC OPERATION”
Proceedings EVS-3, EVAA, Washington D.C., USA, 1974
- [64] H Kahlen
“ENERGY AND POWER FROM SUPERCAPACITORS AND
ELECTROCHEMICAL SOURCES”
Proceedings EVS-16, EVAAP, Beijing, China, October 1999
- [65] “TESTING OF BATTERIES FOR ELECTRIC ROADS VEHICLES”
Committee draft, IEC TC 21/458/CD
- [66] P. Mauracher, W. Geuer
“COMPARISON AND EVALUATION OF NICKEL-CADMIUM,
ZINC-BROMINE, SODIUM-SULPHUR, SODIUM-
NICKELCHLORIDE AND LEAD-ACID BATTERIES”
AVERE contract P-044 of the EDS study, “Advanced electric drive
systems for buses, vans and passenger cars to reduce pollution (EDS)”,
AVERE, Brussels, Belgium, December 1992
- [67] <http://www.aver.org/>
AVERE, Brussels, Belgium,
- [68] Ed. Van Geel
“BATTERIJEN IN DE INDUSTRIE”
Chloride Belgium, Mortsels Belgium
- [69] D.A. J. Rand, R. Woods, R.M. Dell
“BATTERIES FOR ELECTRIC VEHICLES”
1998

- [70] H. Quadflieg, J. Brosthaus, S. Weber, R. Kober
“ELECTRIC VEHICLES CHANGE FOR ENVIRONMENT AND QUALITY OF LIFE?”
Thermie action, DGXVII, TUV Rheinland, Köln, Germany
- [71] G. Jones
“A REPORT ON THE STATUS OF THE DEVELOPMENT OF THE VANADIUM REDOX FLOW BATTERY FOR MOBILE APPLICATIONS”
Unisearch, July 1997
- [72] L. d’Ussel, G. Chagnon, J.P. Schultze
“ADAPTING THE EV BATTERY TECHNOLOGY TO NEW HYBRID VEHICLE REQUIREMENTS”
Proceedings EVS-16, EVAAP, Beijing, China, October 1999
- [73] Ch. St-Pierre, R. Rouillard
“LITHIUM POLYMER BATTERY FOR ELECTRIC VEHICLE AND HYBRID ELECTRIC VEHICLE APPLICATIONS”
Proceedings EVS-16, EVAAP, Beijing, China, October 1999
- [74] J. A. Zaun
“NICKEL BATTERIES DO NOT HAVE “MEMORY””
http://www.paranoia.com/~filipg/HTML/FAQ/BODY/F_NiCd_Memory.html
- [75] “POSITIVE CONTACT”
Brochure SAFT, Romainville, France
- [76] P. Gifford, V. Hellmann, J. Adams
“DEVELOPMENT OF ADVANCED OVONIC NICKEL METAL HYDRIDE BATTERIES FOR ELECTRIC AND HYBRID VEHICLES – A STATUS UP-DATE”
Proceedings EVS-15, AVERE, Brussels, Belgium, October 1998
- [77] C. Madery, J-L Liska
“SAFT NICKEL-METAL HYDRIDE BATTERY IN PRODUCTION”
Proceedings EVS-15, AVERE, Brussels, Belgium, October 1998
- [78] M. Meeus, Y. Gravenstein
“NON-FERROUS METALS MAKE ELECTRIC VEHICLES MOVE”
Proceedings EVS-15, AVERE, Brussels, Belgium, October 1998
- [79] K. Soo-Whan
“DEVELOPMENT OF HIGH PERFORMANCE NICKEL METAL HYDRIDE BATTERIES FOR ELECTRIC VEHICLES”
Proceedings EVS-16, EVAAP, Beijing, China, October 1999
- [80] M. Klein
“BIPOLAR NICKEL-METAL HYDRIDE BATTERY”
Proceedings EVS-16, EVAAP, Beijing, China, October 1999

-
- [81] P. Van den Bossche, G. Maggetto
“SAFETY CHARACTERISTICS OF ELECTRIC VEHICLES IN CITY TRAFFIC”
CITELEC, Brussels, Belgium, October 1993
- [82] J. W Sheard
“FUTURE OF THE VANADIUM REDOX BATTERY IN ELECTRIC VEHICLES”
Proceedings EVS-15, AVERE, Brussels, Belgium, October 1998
- [83] T. Brohm, M.Maul,E.Meissner
ADVANCED LITHIUM-ION BATTERIES FOR ELECTRIC VEHICLES”
Proceedings EVS-15, AVERE, Brussels, Belgium, October 1998
- [84] C. Létourneau
“PROGRESS IN LITHIUM POLYMER BATTERY SYSTEMS FOR ELECTRIC VEHICLES”
Proceedings EVS-15, AVERE, Brussels, Belgium, October 1998
- [85] I. Yonezu, T. Maeda, Y. Chikano, K. Ookita
“DEVELOPMENT OF 250 WH CLASS LITHIUM SECONDARY BATTERIES WITH A GRAPHITE-COKE HYBRID CARBON NEGATIVE ELECTRODE AND A $\text{LiNi}_{1-x}\text{Co}_x\text{O}_2$ POSITIVE ELECTRODE”
Proceedings EVS-15, AVERE, Brussels, Belgium, October 1998
- [86] C. St-Pierre
“LITHIUM POLYMER BATTERY FOR ELECTRIC VEHICLE AND HYBRID ELECTRIC VEHICLE APPLICATIONS”
Proceedings EVS-16, Beijing, China, October 1999
- [87] W. J. Weydanz
“THE GAIA LITHIUM POLYMER BATTERY TECHNOLOGY IN VIEW OF A TRACTION APPLICATION”
Proceedings of Nordisk Miljöbil 99, Helsinki, Finland, 8-9 September 1999
- [88] H. Horie
“DEVELOPMENT OF A HIGH-POWER LITHIUM-ION BATTERY FOR PARALLEL HEVS”
Proceedings EVS-16, EVAAP, Beijing, China, October 1999
- [89] F. Brucchi
“ULTRACAPACITOR TESTS FOR EV APPLICATIONS: INTRODUCTION OF NEW EQUALISATION COEFFICIENTS”
Proceedings EVS-16, EVAAP, Beijing, China, October 1999
- [90] <http://www.hev.doe.gov/components/ultra.html>
Department of Energy (DOE) Hybrid Vehicle Propulsion Program Online Resource Center brought by the National Renewable Energy Laboratory (NREL)

- [91] <http://www.hev.doe.gov/components/flywheels.html>
Department of Energy (DOE) Hybrid Vehicle Propulsion Program On-line Resource Center brought by the National Renewable Energy Laboratory (NREL)
- [92] F.J.M. Thoolen
“DEVELOPMENT OF AN ADVANCED HIGH SPEED FLYWHEEL ENERGY STORAGE SYSTEM”
PhD thesis, Technische Universiteit Eindhoven, The Netherlands, December 1993
- [93] R. Wurster
“PEM FUEL CELLS IN STATIONARY AND MOBILE APPLICATIONS: INFRASTRUCTURE REQUIREMENTS, ENVIRONMENTAL BENEFITS, EFFICIENCY ADVANTAGES AND ECONOMICAL IMPLICATIONS”
<http://www.hydrogen.org/>
Ludwig-Bölkow-Systemtechnik GmbH, Ottobrunn, Germany
- [94] H. Vandenborre
“TECHNICAL AND ECONOMICAL COMPARISON BETWEEN A CONVENTIONAL TROLLEY BUS SYSTEM AND A BUS SYSTEM BASED ON ELECTROLYTIC HYDROGEN”
AVERE contract P-016 of the EDS study, “Advanced electric drive systems for buses, vans and passenger cars to reduce pollution (EDS)”, AVERE, Brussels, Belgium, December 1992
- [95] R. L. Hodkinson
“ADVANCED FUEL CELL CONTROL SYSTEM”
Proceedings EVS-15, AVERE, Brussels, Belgium, October 1998
- [96] H. Van den Broeck
“FUEL CELLS AND REFORMERS”
AVERE contract P-001 of the EDS study, “Advanced electric drive systems for buses, vans and passenger cars to reduce pollution (EDS)”, AVERE, Brussels, Belgium, December 1992
- [97] K. Dircks
“RECENT ADVANCES IN FUEL CELLS FOR TRANSPORTATION APPLICATION”
Proceedings EVS-15, AVERE, Brussels, Belgium, October 1998
- [98] M. Juhala, P. Sainio, M. Melin
“FUEL CELL TECHNOLOGY. STATE-OF-THE-ART”
Proceedings of Nordisk Miljöbil 99, Helsinki, Finland, 8-9 September 1999

-
- [99] G. Maggetto
“SYNTHESIS REPORT FOLLOWING A SYSTEM ANALYSIS
STUDY ON ADVANCED ELECTRIC DRIVE SYSTEMS FOR
BUSES, VANS AND PASSENGER CARS TO REDUCE POLLUTION
(EDS)”
EC contract TEAE-CT88-0001, Vrije Universiteit Brussel, Belgium,
December 1992
- [100] M. Friedman
“CONDUCTIVE CHARGING COMMERCIALIZATION”
Proceedings of EVS-14, EVAA, Orlando, Florida, USA, 15-17 December
1997
- [101] P. Griffith, G. Gleason
“DEMONSTRATION OF 300-KW RAPID CHARGER IN TRANSIT
BUS APPLICATION”
Proceedings of EVS-14, EVAA, Orlando, Florida, USA, 15-17 December
1997
- [102] H. Van Muylem, Ph. Lataire
“ANALYSIS OF DISTRIBUTION, TRAINING AND INFORMATION
INFRASTRUCTURES WHICH ARE REQUIRED FOR THE USE OF
ELECTRIC AND HYBRID CARS IN TOWN TRAFFIC”
AVERE contract P-018 of the EDS study, “Advanced electric drive
systems for buses, vans and passenger cars to reduce pollution (EDS)”,
AVERE, Brussels, Belgium, December 1992
- [103] E. Vanderelst, G. Maggetto
“THE INDUCTIVE CHARGER: AN OPPORTUNITY FOR
AUTOMATIC ENERGY DISTRIBUTION FOR EV'S”
BRITE/EURAM 2 project, TAUT CT92 0006, DG XII, Vrije Universiteit
Brussel, Belgium, 1995
- [104] G. Maggetto
“EVIAC: FULLY AUTOMATIC INDUCTIVE CHARGING SYSTEMS,
REQUIRING NO DRIVER INTERVENTION, FOR ELECTRIC
VEHICLES”
Brite-Euram project, BE-CT97-0205, Vrije Universiteit Brussel, Belgium
- [105] M. Squilbin, J. Wauters
“STUDIE VAN HET ELEKTRICITEITSNET TE BRUSSEL EN
EVALUATIE VAN DE IMPACT VAN HET INVOEREN VAN
ELEKTRISCHE VOERTUIGEN”
Thesis, Vrije Universiteit Brussel, Belgium, 1993
- [106] “ENERGIE- EN MILIEU-ASPECTEN VAN ELEKTRISCHE
VOERTUIGEN”
nv Samenwerkende elektriciteits-productiebedrijf, SEP, The Netherlands

- [107] P. Van den Bossche
“INFRASTRUCTUUR, MARKT, BELEID”
Proceedings “Elektrische voertuigen symposia: EVS-13 en EVS-14: synthese”, KBVE, Brussels, Belgium, February 1998
- [108] B. Harbolla, G. Maggetto, P. Van den Bossche, H. Van Muylem
“ANALYSIS OF HYBRID DRIVE SYSTEMS WITH NEW ELECTRIC COMPONENTS - MORPHOLOGY, EVALUATION AND OPTIMISATION”
P-030 out of summary report “Advanced electric drive systems for buses, vans and passengers cars to reduce pollution”, EDS study, AVERE, Brussels, Belgium, December 1992
- [109] M. Van Overmeire, R.E. Jonckheere
“KINEMATIKA EN DYNAMICA VAN DE WERKTUIGEN. 2E BOEKDEEL : BASISKURSUS”
Course, Vrije Universiteit Brussel, Belgium
- [110] S. Sasaki
“TOYOTA'S NEWLY DEVELOPED ELECTRIC-GASOLINE ENGINE HYBRID POWERTRAIN SYSTEM”
Proceedings of EVS-14, EVAA, Orlando, Florida, USA, December 1997
- [111] C. N. Spentzas, I. Alkazali
“CONTRIBUTION TO THE DEVELOPMENT OF AN ELECTRONIC DIFFERENTIAL FOR ELECTRIC VEHICLES”
Proceedings EVS-13, EVAAP, Osaka, Japan, 13-16 October 1996
- [112] J. Swann
“REDUCED ENERGY CONSUMPTION AND ENVIRONMENTAL IMPACT FROM ROAD VEHICLES THROUGH THE DEVELOPMENT AND IMPLEMENTATION OF SIMULATION TOOLS”
Technical Report TR3 of WP3 Systems modelling, Fleets Energy Programme, JOULE (JOE3960031), Motor Industry Research Association Ltd, Nuneaton – Warwickshire, UK, 1998
- [113] L. Pelkmans
“HYBRIDE ELEKTRISCHE DRIJFLIJN VOOR VOERTUIGEN: ADDENDUM”
Final report of IWT research (930231a), Vlaamse Instelling voor Technologisch Onderzoek, Mol, Belgium, December 1998
- [114] D. Hermance, S. Sasaki
“HYBRID ELECTRIC VEHICLES TAKE TO THE STREETS”
IEEE Spectrum, November, 1998.

-
- [115] M. Lehna
“THE AUDI DUO A HYBRID CONCEPT READY FOR PRODUCTION”
Proceedings of EVS-14, EVAA, Orlando, Florida, USA, 15-17 December 1997
- [116] U. Winter
“THE DRIVETRAIN OF THE AUDI DUO III”
Proceedings of EVS-14, EVAA, Orlando, Florida, USA, 15-17 December 1997
- [117] <http://www.hondainsight.com/environment.html>
Honda, USA
- [118] J. Swann
“REDUCED ENERGY CONSUMPTION AND ENVIRONMENTAL IMPACT FROM ROAD VEHICLES THROUGH THE DEVELOPMENT AND IMPLEMENTATION OF SIMULATION TOOLS”
Technical Report TR3 of WP4 Optimisation, Fleets Energy Programme, JOULE (JOE3960031), Motor Industry Research Association Ltd, Nuneaton – Warwickshire, UK, 1998
- [119] Abthoff, P. Antony, Krämer, J. Seiler
“THE MERCEDES-BENZ C-CLASS SERIES HYBRID”
Proceedings of EVS-14, EVAA, Orlando, Florida, USA, 15-17 December 1997
- [120] “DEVELOPMENT AND ON-ROAD TESTING OF A NATURAL GAS-ELECTRIC HYBRID CITY BUS PROTOTYPE WITH EXTRA LOW EMISSIONS”
Final report, contract CEC N TAUT CT92 0007, ALTRA, TNO, CITELEC, Brussels, Belgium, April 1997
- [121] <http://www.hev.doe.gov/components/energman.html>
Department of Energy (DOE) Hybrid Vehicle Propulsion Program Online Resource Center brought by the National Renewable Energy Laboratory (NREL)
- [122] Peter Van den Bossche
“POWER SOURCES FOR HYBRID BUSES: COMPARATIVE EVALUATION OF THE STATE OF THE ART”
Journal of Power Sources 80, 213-216, 1999
- [123] K.E. Bailey
“DYNAMIC MODEL AND COORDINATED CONTROL SYSTEM FOR A HYBRID ELECTRIC VEHICLE”,
Proceedings of EVS-14, EVAA, Orlando, Florida, USA, 15-17 December 1997

- [124] J. Seiler
"HYBRID VEHICLE OPERATING STRATEGIES"
Proceedings of EVS-15, AVERE, Brussels, Belgium, October 1998
- [125] K. B. Wipke
"USING AN ADVANCED VEHICLE SIMULATOR (ADVISOR) TO
GUIDE HYBRID VEHICLE PROPULSION SYSTEM
DEVELOPMENT"
National renewable Energy Laboratory (NREL), Golden, CO, USA
- [126] "PARALLEL ELECTRIC ASSIST CONTROL STRATEGY"
http://www.ctts.nrel.gov/analysis/advisor_doc/Parallel.htm
Center for Transportation Technologies and Systems, National renewable
Energy Laboratory (NREL), Golden, CO, USA
- [127] B. Jeanneret
"NEW HYBRID CONCEPT SIMULATION TOOLS, EVALUATION
ON THE TOYOTA PRIUS CAR"
Proceedings of EVS-16, Beijing, China, 12-16 October 1999
- [128] <http://www.hev.doe.gov/components/energman.html#consumer>
Department of Energy (DOE) Hybrid Vehicle Propulsion Program On-
line Resource Center brought by the National Renewable Energy
Laboratory (NREL)
- [129] T. Walter
"SIMULATION PROGRAM FOR ELECTRIC AND HYBRID
VEHICLES- PROGRAMME"
EC contract JOU2-CT92-200, University of Kaiserslautern, Germany,
1993
- [130] J. Van Mierlo, J-L. Maggetto, F. Van Haelst, H. Van Muylem
"TRANSPARENT SIMULATION FOR ELECTRIC AND HYBRID
VEHICLES"
Final Report, JOULE 2 CT92-0200, Vrije Universiteit Brussel, 1993
- [131] E. Rullière, E. Toutain, J.P. Yonnet
"A SIMULATION PROGRAM FOR MULTI ENERGY SOURCES
ELECTRIC VEHICLES"
Proceedings of EVS-14, EVAA, Orlando, Florida, USA, 15-17 December
1997
- [132] "SIMPLEV, SIMULATION OF ELECTRIC AND HYBRID
VEHICLES"
<http://ev.inel.gov/simplev/desc.html>
Idaho National Engineering and Environmental Laboratory, Idaho Falls,
ID 83415, USA
- [133] <http://www-ee.eng.hawaii.edu/>
Department of Electrical Engineering at the University of Hawaii,
Honolulu, HI 96822 USA

-
- [134] <http://eve.ev.hawaii.edu/Simulation/HEVST/about.html>
University of Hawaii, Honolulu, HI 96822 USA
- [135] <http://eve.ev.hawaii.edu/ndc2.html>
University of Hawaii, Honolulu, HI 96822 USA
- [136] <http://www.swri.edu/>
Southwest Research Institute, Detroit, USA
- [137] “DEVELOPMENT OF A HYBRID VEHICLE PERFORMANCE EMISSIONS AND EFFICIENCY MODEL”
Final report, SwRI IR&D project 03-9788, Southwest Research Institute, Detroit, USA June 1995
- [138] <http://www.swri.org/3pubs/brochure/d03/elhybveh/elhybveh.htm>
Southwest Research Institute, Detroit, USA,
- [139] http://www.ctts.nrel.gov/analysis/advisor_doc/advisor_ch1.htm
Center for Transportation Technologies and Systems, National Renewable Energy Laboratory (NREL), Golden, CO, USA,
- [140] K. Wipke
“ADVISOR 2.0: A SECOND-GENERATION ADVANCED VEHICLE SIMULATOR FOR SYSTEM ANALYSIS”
NREL, Golden, USA
- [141] J. Swann
“REDUCED ENERGY CONSUMPTION AND ENVIRONMENTAL IMPACT FROM ROAD VEHICLES THROUGH THE DEVELOPMENT AND IMPLEMENTATION OF SIMULATION TOOLS”
Summary Report SR4 of WP5 Quality, Fleets Energy Programme, JOULE (JOE3960031), Fleets Energy Programme, JOULE 95 Motor Industry Research Association Ltd, Nuneaton – Warwickshire, UK, 1998
- [142] R. Noons, J. Swann, A. Green
“THE USE OF SIMULATION SOFTWARE TO ASSES ADVANCED POWER TRAINS AND NEW TECHNOLOGY VEHICLES”
Proceedings of EVS-15, AVERE, Brussels, Belgium, October 1998
- [143] J. Swann
“POSITIONING EV’S IN THE MARKETPLACE”
Proceedings of EVS-14, EVAA, Orlando, Florida, USA, 15-17 December 1997
- [144] User Manual, LabVIEW™
National Instruments™, edition January 1998

- [145] J. Van Mierlo
“HYBRIDE ELEKTRISCHE DRIJFLIJN VOOR VOERTUIGEN: ADDENDUM”
Second year report of IWT research (930231a), “Hybride elektrische (brandstofcel) drijflijn voor voertuigen”, Vrije Universiteit Brussel, Belgium, May 1996
- [146] P. Mauracher
“SYSTEM-OPTIMIZATION OF THE DRIVETRAIN OF ELECTRIC VEHICLES TO REDUCE THE ENERGY CONSUMPTION”
Proceedings EVS-13, Osaka, Japan, 13-16 October 1996
- [147] J.W. Biermann
“INNOVATIVE MODULAR COMPUTER PROGRAM FOR CALCULATION OF VEHICLE – LONGITUDINAL DYNAMICS”,
Conference on vehicle dynamics and power train engineering, EAEC N°91066, Strasbourg, France, June 1991
- [148] J. Swann
“REDUCED ENERGY CONSUMPTION AND ENVIRONMENTAL IMPACT FROM ROAD VEHICLES THROUGH THE DEVELOPMENT AND IMPLEMENTATION OF SIMULATION TOOLS”
Summary Report SR3 of WP5 Modelling, Fleets Energy Programme, JOULE (JOE3960031), Fleets Energy Programme, JOULE 95 Motor Industry Research Association Ltd, Nuneaton – Warwickshire, UK, 1998
- [149] “VÉHICULES ROUTIERS À PROPULSIONS ÉLECTRIQUE – PERFORMANCES ROUTIÈRES – MESURAGE DES PERFORMANCES ÉNERGÉTIQUES – PARTIE 1: VÉHICULES ÉLECTRIQUES PURS.”
prEN 1986-1, Comité Européen de Normalisation, Brussels, 1996
- [150] V. Blick
“SIMULATION OF ELECTRIC VEHICLES IN THE LABORATORY FOR THE EVALUATION OF BATTERY PACKS”
Bitrode Limited, Battery charging and testing equipment, Dursley, England,
- [151] ISO/TC 22/SC21
Mechanical Engineering Laboratory, Ibaraki, Japan
- [152] C.J.T. van de Weijer
“URBAN BUS DRIVING CYCLE”
Proceedings 4th International EAEC conference on “Vehicle and Traffic Systems Technology”, Strasbourg, France, 16-18 June 1993
- [153] B. Sporckmann
“COMPARISON OF EMISSIONS FROM COMBUSTION ENGINE AND EUROPEAN ELECTRIC VEHICLES”
Proceedings EVS-12, EVAA, California, USA, 1994

-
- [154] M. Keller, P. de Haan
“INTERMODAL COMPARISONS OF ATMOSPHERIC POLLUTANT EMISSIONS”
MEET project, deliverable no24, EC Contract No. ST-96-SC.204,
INFRAS, Berne, Switzerland, October 1998
- [155] A. Eiraku
“AN APPLICATION OF HARDWARE IN THE LOOP SIMULATION TO HYBRID ELECTRIC VEHICLE”
Proceedings of EVS-15, Brussels, Belgium, October 1998
- [156] J. Sneyers
“DE INVLOED VAN DE WEGBEDEKKING OP HET BRANDSTOFVERBRUIK VAN VOERTUIGEN”
Energy & Milieu, nr4, WEL, Antwerp, Belgium, July - August 1994
- [157] A. Hedman
“TRANSMISSIONS AND VEHICLE SIMULATION MODELS FOR ELECTRIC HYBRID VEHICLE.”
Machine and vehicle Design, Chalmers University of Technology,
Göteborg, Sweden
- [158] T. Walter
“TRANSPARENT SIMULATION PROGRAM FOR ELECTRIC AND HYBRID VEHICLES – MODELS AND COMPONENTS”
EC contract JOU2-CT92-200, University of Kaiserslautern, Germany,
December 1993
- [159] G. Maggetto
“ELEKTRISCHE ENERGIEOMVORMING EN ELEKTRISCHE MACHINES”
Course, Vrije Universiteit Brussels, Belgium
- [160] S. W. Director
“ANALYSIS OF ELECTRIC MACHINERY”
McGraw-Hill international editions, Singapore, ISBN 0-07-035436-7,
1987
- [161] K. Beya, J. Van Mierlo, G. Maggetto
“AC-MOTORS MEASUREMENTS BASED STATIC MODELS FOR ELECTRIC VEHICLE SIMULATION PROGRAMS”
Proceedings EPE 97, Norwegian University of Science and Technology,
Trondheim, Norway, 8-10 September 1997
- [162] “LEAD ACID TRACTION BATTERIES FOR ROAD VEHICLE AND INDUSTRIAL TRUCK APPLICATIONS”
IEC 254-1, November 1994

- [163] L.A.M. Van Dongen
“ENERGETISCHE OPTIMALISATIE VAN AANDRIJFSYSTEMEN
VOOR ELEKTRISCHE VOERTUIGEN”
Thesis, Technische Hogeschool Eindhoven, The Netherlands, March
1983
- [164] C.C. Chan, E.W.C. Lo, Shen Weixiang
“AN OVERVIEW OF BATTERY TECHNOLOGY IN ELECTRIC
VEHICLE”
Proceedings EVS-16, EVAAP, Beijing, China, October 1999
- [165] H. Kahlen, B. Hauck
“LEISTUNG UND LEISTUNGSDICHTE VON
TRAKTIONSBATTERIES”
Elektrische Bahnen 90, Germany, December 1992
- [166] U. Zoelch, D. Schroeder
“COMPARISON OF ELECTRIC DRIVES FOR A HYBRID VEHICLE”
Proceedings EPE-95, European Power Electronics and Drives
Association, Sevilla, Spain, 1995
- [167] P. Chapoulie, S. Astier
“MODELING OF AN ELECTRIC VEHICLE INCLUDING
ULTRACAPACITOR WITH SABER”
Proceedings of EVS-15, AVERE, Brussels, Belgium, October 1998
- [168] F. Brucchie
“ULTRA-CAPACITOR TEST FOR EV APPLICATIONS:
INTRODUCTION OF NEW EQUALISATION COEFFICIENTS”
Proceedings EVS-16, EVAAP, Beijing, China, October 1999
- [169] H. Kahlen
“ENERGY AND POWER FROM SUPERCAPACITORS AND
ELECTROCHEMICAL SOURCES”
Proceedings EVS-16, EVAAP, Beijing, China, October 1999
- [170] L. Stridsberg
“DUAL ELECTRIC MOTOR HYBRID POWERTRAIN”
Proceedings of EVS-15, AVERE, Brussels, Belgium, October 1998
- [171] M. Hemmingsson
“MINIMIZATION OF ENERGY LOSSES IN HYBRID ELECTRIC
VEHICLES, THEORY AND PRACTICE”
Proceedings EVS-16, EVAAP, Beijing, China, October 1999
- [172] “CADASTRE DES EMISSIONS GASEUSES”
Final report contract IBGE nr. 139, Institut Bruxellois pour la gestion de
l’environnement, STRATEC, Brussels, Belgium, February 1994

-
- [173] E. Sérié, R. Joumard
“MODELLING OF COLD START EMISSIONS FOR ROAD VEHICLES”
Report LEN 9731, INRETS, Bron, France, December 1997
- [174] “METHODOLOGY FOR CALCULATING TRANSPORT EMISSIONS AND ENERGY CONSUMPTION - RESEARCH FOR SUSTAINABLE MOBILITY”
MEET-project partnership, Transport research fourth framework programme, DG VII, Commission of the European Communities, Luxembourg, 1999
- [175] A. Vannerum
“STUDIE VAN DE NIEUWSTE TECHNOLOGISCHE ONTWIKKELINGEN BIJ ELEKTRISCHE VOERTUIGEN (BRANDSTOFCELLEN, Vliegwielen, SUPER-CONDENSATOREN) A.D.H.V. SIMULATIEMODELLEN”
Thesis, Vrije Universiteit Brussel, Belgium, 94-95
- [176] H. Van den Broeck, G. Maggetto
“FUEL CELLS AND REFORMERS”
EDS summary rapport, “Advanced electric drive systems for buses, vans and passenger cars to reduce pollution”, AVERE, Belgium, December 1992
- [177] A. Collys
“ECONOMISCHE EN ENERGETISCHE VERGELIJKING VAN ALTERNATIEVE ENERGIEBRONNEN VOOR ELEKTRISCHE EN HYBRIDE VOERTUIGEN”
Final report, Contract Nr. 95 - Ministerie van Economische zaken, Vrije Universiteit Brussel, Belgium, July 1997
- [178] K. Niemann
“LOW EMISSION BUS DRIVES”
Proceedings of Nordisk Miljöbil 99, Helsinki, Finland, 8-9 September 1999
- [179] K. Kawakami
“DEVELOPMENT OF A NEW MEASUREMENT PROCEDURE AND TEST SYSTEM FOR ELECTRIC VEHICLES”
Proceedings EVS-16, EVAAP, Beijing, China, October 1999
- [180] J. Van Mierlo
“ENERGETISCHE EN DYNAMISCHE STUDIE VAN TESTINFRASTRUKTUUR VOOR ELEKTRISCHE VOERTUIGEN”
Thesis, Vrije Universiteit Brussel, Belgium, June 1992

- [181] W. Deloof, M. De Smedt
“ONTWIKKELEN VAN MODELLEN VOOR DE COMPONENTEN VAN ELEKTRISCHE VOERTUIGEN AAN DE HAND VAN EEN ‘ON-ROAD’ MEETSISTEEM EN IMPLEMENTATIE IN EEN SOFTWAREPAKKET”
Thesis Vrije Universiteit Brussel, Belgium, June 1995
- [182] J. Vermout
“ON-ROAD MEETKAMPAGNES OP ELEKTRISCHE EN HYBRIDE VOERTUIGEN”
Thesis, Vrije Universiteit Brussel, Belgium, June 1996
- [183] W. Deloof, J. Van Mierlo, G. Maggetto
“ON-ROAD MEASURING AND TESTING PROCEDURES FOR ELECTRIC VEHICLES”
Proceedings EVS-14, EVAA, Orlando, Florida, USA, 15-17 December 1997
- [184] “DATRON – LM –SENSOR”
Operation manual, Datron messtechnik GmbH, Germany
- [185] J.J. Sarrato Martinez
“DATA-ACQUISITION MEASUREMENT SYSTEM FOR ELECTRIC VEHICLES”
Thesis, Vrije Universiteit Brussel, Belgium, 1998-1999
- [186] “MEASUREMENT AND AUTOMATION”
Catalogue, National Instruments, 1999
- [187] W. Li
“QUASI-SYNCHRONOUS ALGORITHM AND POWER MEASUREMENT FOR PWM INVERTERS”
Thesis, Vrije Universiteit Brussel, Belgium, June 1997
- [188] F. Van Haelst
“VSP5.3 COMPONENT LIBRARY”
Internal document, Vrije Universiteit Brussel, Belgium, December 1994
- [189] P. Schwarzenberger
“PERSONAL ZERO EMISSION TRANSPORT FOR THE CITY OF THE FUTURE (PRAZE)”
Approved project proposal of the 5th Framework Programme of the European Commission, PML Flightlink, Bordon, UK, 1999
- [190] J. Swann
“REDUCED ENERGY CONSUMPTION AND ENVIRONMENTAL IMPACT FROM ROAD VEHICLES THROUGH THE DEVELOPMENT AND IMPLEMENTATION OF SIMULATION TOOLS”
Technical Report TR6 of WP6 Vehicle simulation, Fleets Energy Programme, JOULE (JOE3960031), Motor Industry Research Association Ltd, Nuneaton – Warwickshire, UK, 1998

-
- [191] J. Van Mierlo, G. Maggetto
“MULTIPLE PURPOSE SIMULATION PROGRAMME FOR ELECTRIC AND HYBRID VEHICLES: SIMULATION VS. EXPERIMENTAL RESULTS”
Proceedings EVS-13, EVAAP, Osaka, Japan, 13-16 October 1996
- [192] K. B. Wipke
“AN ADVANCED VEHICLE SIMULATOR (ADVISOR) TO GUIDE HYBRID VEHICLE PROPULSION SYSTEM DEVELOPMENT”
<http://www.hev.doe.gov/components/simulation/nesea.pdf>
National renewable Energy Laboratory (NREL), Golden, CO, USA, 1996
- [193] J. Van Mierlo
"QUANTITY OF COPPER IN ELECTRIC AND HYBRID VEHICLES AND THE POTENTIAL MARKET IN FUNCTION OF DIFFERENT PENETRATION SCENARIO'S"
Project funded by the International Copper Association. Ltd, Vrije Universiteit Brussel, Belgium, June 1998
- [194] J. Van Mierlo, F. Van Haelst
“EVOLUTIE VAN DE TECHNOLOGIE VAN DE TRANSPORTMIDDELEN (O.A. WEGVOERTUIGEN) EN VAN DE BIJHORENDE INFRASTRUCTUUR, GERICHT OP VEILIGHEID, EFFICIËNTIE EN MILIEU-ONTLASTING”
Project funded by the Brussels Capital Region, Vrije Universiteit Brussel, Belgium, February 1995
- [195] J. Van Mierlo
“RATIONEEL ENERGIEVERBRUIK OMTRENT DE AANWENDING VAN ELEKTRISCHE EN HYBRIDE VOERTUIGEN”
Project funded by the Brussels Capital Region, Vrije Universiteit Brussel, Belgium, May 1998
- [196] J. Van Mierlo
“SIMULATION TECHNIQUES FOR EVALUATION OF EV'S & HV'S DRIVE TRAINS”
Presentation for the BEST-PK 2nd Summer Course 'Electric and Hybrid Vehicles in Cities', Vrije Universiteit Brussel, Belgium, September 1995
- [197] J. Van Mierlo, G. Maggetto
“VEHICLE SIMULATION PROGRAMME”
Proceedings Autotech, I-Mech-E, Birmingham, U.K., November 1995
- [198] J. Van Mierlo, G. Maggetto
“MODULAR SIMULATION PROGRAMME FOR ELECTRIC AND HYBRID VEHICLES”
Proceedings EVT-95, Paris, France, November 1995

- [199] J. Van Mierlo, G. Maggetto
"HOW TO COMPARE AND EVALUATE ELECTRIC AND THERMAL VEHICLES?"
Proceedings EPE-97, Norwegian University of Science and Technology, Trondheim, Norway, September 1997
- [200] J. Van Mierlo, W. Deloof, G. Maggetto
"DEVELOPMENT OF A SOFTWARE TOOL TO EVALUATE THE ENERGETIC AND ENVIRONMENTAL IMPACT OF ELECTRIC AND HYBRID VEHICLES IN BRUSSELS"
Proceedings EVS-14, Orlando, Florida, USA, December 1997
- [201] J. Van Mierlo
"OVERZICHT AANDRIJFSYSTEMEN IN ELEKTRISCHE VOERTUIGEN UIT EVS-13 EN 14"
Presentation for the KBVE, Electrabel, Mechelen, Belgium, February 1998 and VUB, Brussels, June 1998
- [202] J. Van Mierlo
"SYSTÈME D'ENTRAÎNEMENT, SYNTHÈSE D'EVS-13 ET 14"
Presentation for the SRBE, Electrabel, Luik, Belgium, March 1998
- [203] J. Van Mierlo, B. Kamba Bimbi, G. Maggetto, S. Van Haute, S. Henneberger, R. Belmans
"THE DESIGN OF A PERMANENT MAGNET MOTOR FOR A HYBRID VEHICLE WITH HELP OF DIFFERENT SOFTWARE TOOLS."
Proceedings EVS-15, AVERE, Brussel, Belgium, October 1998
- [204] J. Van Mierlo, B. Kamba Bimbi, G. Maggetto
"COMPARISON OF DIFFERENT POWER FLOW CONTROL ALGORITHMS IN HYBRID VEHICLES."
Proceedings EVS-15, AVERE, Brussel, Belgium, October 1998
- [205] J. Van Mierlo, G. Maggetto
"SIMULATION OF A COMPLEX PARALLEL-SERIES HYBRID DRIVE TRAIN"
Proceedings EVS-16, EVAAP, Beijing, China, October 1999
- [206] K.B. Beya, J. Van Mierlo, G. Maggetto
"AC MOTOR'S MEASUREMENTS BASED STATIC MODELS FOR ELECTRIC VEHICLES SIMULATION PROGRAMS."
Proceedings EPE-97, Norwegian University of Science and Technology, Trondheim, Norway, September 1997
- [207] W. Deloof, J. Van Mierlo, G. Maggetto
"ON-ROAD MEASURING AND TESTING PROCEDURES FOR ELECTRIC VEHICLES"
Proceedings EVS-14, EVAA, Orlando, Florida USA, December 1997

-
- [208] B. Kamba Bimbi, J. Van Mierlo, G. Maggetto
"ACCURATE POWER MEASUREMENT SYSTEM FOR EV'S AC MOTORS."
Proceedings EVS-15, Brussel, Belgium, October 1998
- [209] G. Maggetto, W. Deloof, P. Van den Bossche, J. Van Mierlo
"ELECTRIC AND HYBRID VEHICLES DEMONSTRATION PROGRAMMES IN EUROPEAN CITIES"
Proceedings EVS-16, Beijing, China, October 1999
- [210] W. Deloof, J. Van Mierlo, G. Maggetto
"MODULAR SIMULATION OF ENVIRONMENTAL, ENERGY AND MOBILITY ASPECTS OF TRAFFIC POLICIES"
Proceedings EVS-16, EVAAP, Beijing, China, October 1999
- [211] G. Maggetto, P. Van den Bossche, J. Van Mierlo
"ELEKTRISCHE EN HYBRIDE VOERTUIGEN IN BELGIË: EEN MILIEUVRIENDELIJK ALTERNATIEF VOOR HET STADSVERKEER" (F, N, E)
Press text, International Motor show Brussels, January 1996 and press text for the "Ronde Van Vlaanderen voor Elektrische voertuigen", "Ronde van Brussel" en "Force Electrique en Wallonie", CITELEC, Brussels, Belgium, February 1997
- [212] J. Van Mierlo
"ELEKTRISCHE VOERTUIGEN"
Publication "Briefing", OSB-VUB, Brussels, Belgium, February 1997
- [213] G. Maggetto, P. Van den Bossche, J. Van Mierlo
"VEHÍCULOS ELÉTRICOS E HÍBRIDOS, UNA ALTERNATIVA RESPETUOSA CON EL MEDIO AMBIENTE PARA EL TRÁFICO URBANO"
Translated article, "Energia" 2/97 nr1, Spain, 1997
- [214] G. Maggetto, P. Van den Bossche, J. Van Mierlo, C. Lecho
"ELEKTRISCHE EN HYBRIDE VOERTUIGEN IN VLAANDEREN"
Publication "Energie & Milieu" nr 2, year 13, WEL, Antwerp, Belgium, March 1997